Immobilization and application of catalysts on magnetic carbon coated metal nanoparticles

Dissertation

Zur Erlangung des Doktorgrades

Dr. rer. nat.

an der Fakultät für Chemie und Pharmazie

der Universität Regensburg

vorgelegt von

Sebastian Wittmann

aus Ergoldsbach

Regensburg 2012

Die Arbeit wurde angeleitet von: Prof. Dr. O. Reiser

Promotionsgesuch eingereicht am: 23.01.2012

Promotionskolloquium am: 08.02.2012

Prüfungsausschuss:

Vorsitz:	Prof. Dr. Manfred Scheer
1. Gutachter:	Prof. Dr. Oliver Reiser
2. Gutachter:	Priv. Doz. Dr. Kirsten Zeitler
3. Prüfer:	Prof. Dr. Henri Brunner

Der experimentelle Teil der vorliegenden Arbeit wurde in der Zeit von Oktober 2008 bis Dezember 2011 unter der Leitung von Prof. Oliver Reiser am Institut für Organische Chemie der Universität Regensburg sowie von Januar 2011 bis Mai 2011 unter der Leitung von Prof. Michael Krische an der University of Texas at Austin angefertigt.

Herrn Prof. Oliver Reiser möchte ich herzlich für die Überlassung des äußerst interessanten Themas, die anregenden Diskussionen und seine stete Unterstützung während der Durchführung dieser Arbeit danken.

Meiner Familie

Table of Contents

Abbreviations

abs	absolute
AC	activated carbon
Ar	aryl
atm	atmosphere
ATR	attenuated total reflection
AzaBOX	azabis(oxazoline)
BAIB	(diacetoxyiodo)benzene
Bn	benzyl
bmim	butylmethylimidazolium
Boc	*tert*-butyloxycarbonyl
BOX	bis(oxazoline)
Bz	benzoyl
C_2mim	1-ethyl-3-methylimidazolium
cat	catalytic
Cbz	carboxybenzyloxy
CI	chemical ionization (MS)
CNT	carbon nanotube
COD	1,5-cyclooctadiene
CuAAC	copper-catalyzed azide/alkyne cycloaddition
d	days
DCM	dichloromethane
DIPEA	*N*,*N*-di*iso*propylethylamine
DMF	dimethyl formamide
DMSO	dimethylsulfoxide
dr	diastereomeric ratio
EDTA	ethylenediamintetra-acetatic acid
ee	enantiomeric excess
EE	ethyl acetate
EI	electron impact (MS)
ent	enantiomer
eq.	equivalent
ESI	electrospray ionization (MS)
Et	ethyl
EtOH	ethanol
GC	gas chromatography
h	hour(s)
HPLC	high performance liquid chromatography
HRMS	high resolution mass spectrometry
^{i}Pr	*iso*-propyl
IR	infrared spectroscopy
L	ligand
LAH	lithium aluminum hydride
M	metal
Me	methyl
MeCN	acetonitrile
MeOH	methanol
MeOPEG	polyethylene glycol monomethyl ether
min	minute
MS	mass spectrometry
MWNT	multi wall carbon nanotube
^{n}Bu	*n*-butyl
n-BuLi	*n*-butyl lithium
nd	not determined
ndb	norbornadiene
NHC	*N*-heterocyclic carbene
NMR	nuclear magnetic resonance
NP	nanoparticle
^{n}Pr	*n*-propyl
OAc	acetate
OTf	triflate
p-	*para*
PE	hexanes
Ph	phenyl
ppm	part per million
PS	polystyrene
quant.	quantitative

R	arbitrary rest
r.t.	room temperature
rac	racemic
ROMP	ring opening metathesis polymerization
sat.	saturated
SWNT	single wall carbon nanotube
T	temperature
^{t}Bu	*tert*-butyl
^{t}BuOH	*tert*-butanol
TEM	transmission electron microscopy
TEMPO	2,2,6,6- tetramethyl-piperidine-1-oxyl
Tf	trifluormethanesulfonate
THF	tetrahydrofurane
TLC	thin layer chromatography
TMS	trimethylsilyl
TOF	turnover frequency
TON	turnover number
X	arbitrary anion

A. Introduction

1. Molecular catalysts immobilized on carbon materials

In times of high prices for raw materials, willful tightening of resources as instrument of trade policy and not least increased environmental requirements, the recycling of catalysts becomes a matter of priority. One approach to address this issue is the immobilization of catalysts onto solid supports like organic polymers, nanoparticles or porous inorganic materials in order to recycle the catalyst.[1] Since the discovery of graphene in 1961[2] and new allotropic forms of carbon like single wall carbon nanotubes (CNT),[3] fullerenes[4] and uniform porous carbon[5] a renewed interest in carbon materials has formed. Catalysis is one of the most important applications of carbon materials because they offer some advantages over the aforementioned conventional supports. Their high surface area (> 1000 m^2/g),[6] extreme thermal stability[7] and the tailorable shape and surface properties predestines them as supports for catalysts. Most of the applications aim for carbon materials as a support for metallic nanoparticles, particularly palladium on charcoal.[8] Nevertheless, in the last decade, because of their unique properties, a rising interest grew into the immobilization of molecular catalysts onto carbon supports.[9]

1.1 Methods for the functionalization of carbon surfaces

The mostly aromatic surface of carbon materials like graphene and CNTs allows multiple ways for immobilizing catalysts.[10] The most obvious way is to use functional groups, mainly oxygen groups, on defect sites of carbon materials (Figure 1). The nature and density of these functional groups can be controlled to some extent during the synthesis. Another way for covalent attachment is to functionalize the surface and construct an anchoring point for substrates. The most significant advantage of covalent linkage is the low probability of leaching from metal complexes anchored in this way to carbon supports.

But it is also possible to use the intrinsic properties of carbon materials to immobilize catalysts by physical adsorption to the surface.[11] In this case one can take advantage of the weak adsorption forces and design a catch and release system. This means that the catalyst is performing during the reaction in a homogeneous way, but afterwards is caught back by the support.[12]

1.1.1 Covalent functionalization of carbon materials

Most carbon materials have depending on their synthesis various functional groups, in particular hydroxyl and carboxyl, at their surface. The amount of these groups can be further modified by different methods. The concentration of various oxygen groups can be easily increased by oxidation using molecular oxygen, ozone, HNO_3, NaOCl, H_2O_2, $KMnO_4$, OsO_4 or K_2CrO_4 to name only a few. Depending on the oxidant used carbon surfaces can be tailored to selectively increase the amount of specific groups like phenols in a controlled manner.[10b, 13]

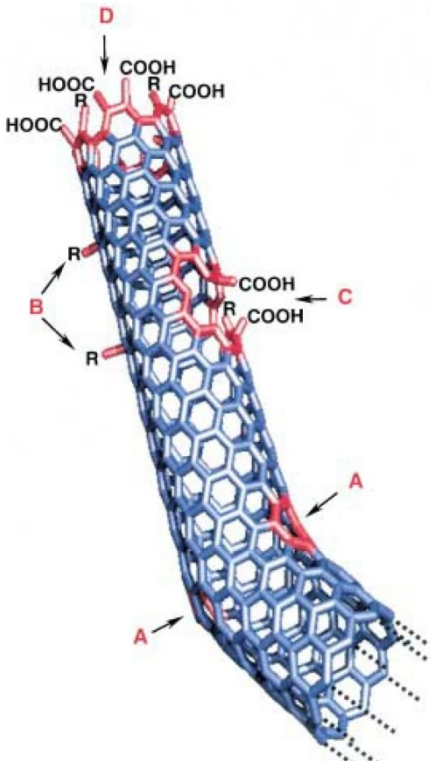

Figure 1: Representation of typical defect sites in SWNT: A: five and seven membered ring sizes in the crook; B: sp^3-hybridized defects (R= H and OH); C: broken up framework due to oxidative modification; D: open end of the nanotubes, terminated by –COOH groups. Other groups like NO_2, OH, H and =O are also possible. Reproduced with permission from reference [14]. Copyright 2002 Wiley-VCH.

Because of the high chemical stability and relatively few defect sites the functionalization of graphene sheets or CNTs requires more sophisticated techniques. In Scheme 1 some frequently used methods like fluorination,[15] diazotation[16] and cycloaddition[17] reactions are depicted.

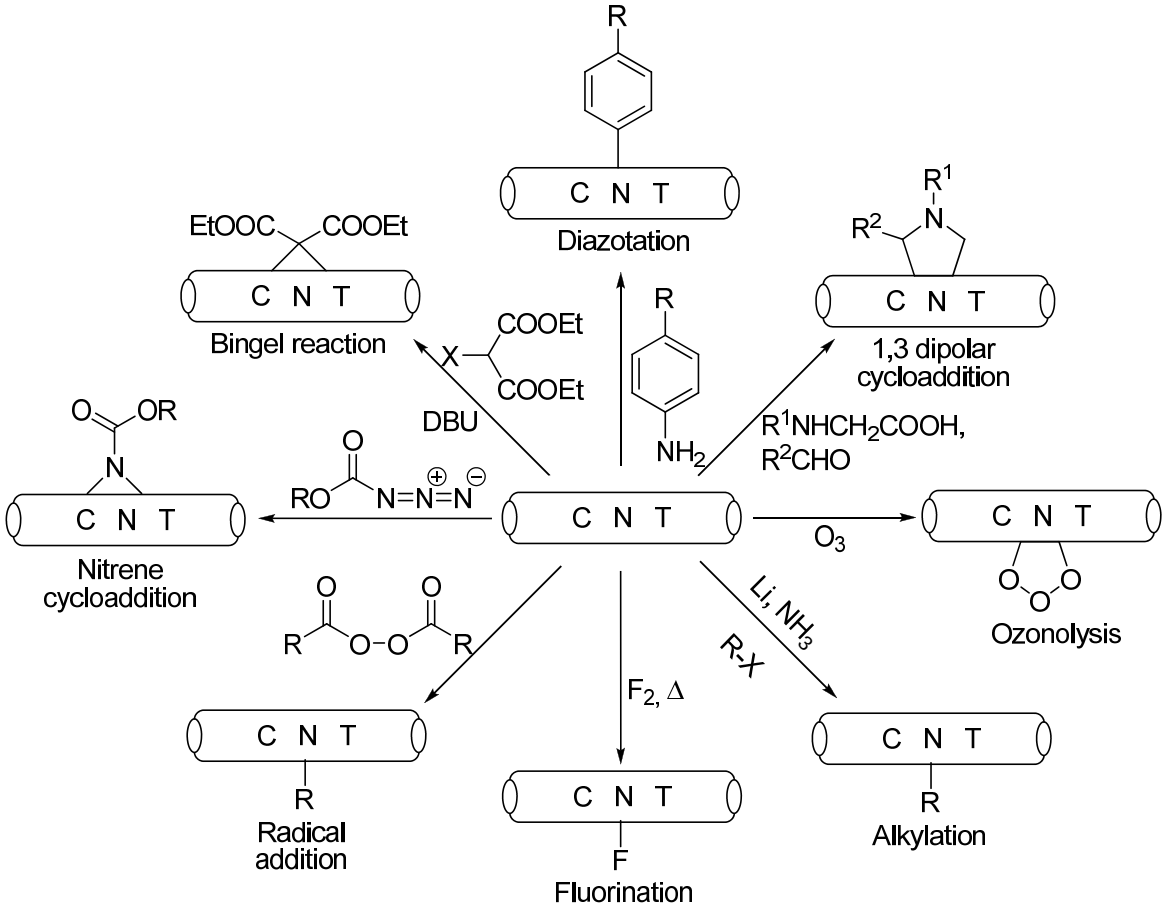

Scheme 1: Methods used for the covalent functionalization of CNT.

1.1.2 Noncovalent functionalization of carbon materials

The noncovalent interactions between molecules and carbon materials mainly comprise of hydrophobic effects, π-π bonds, hydrogen bonds and electrostatic interactions.[11, 18] These forces have been used to functionalize different carbon surfaces like AC, graphite and CNTs.[19] Direct π-π bonding can occur between extended π-systems like polyaromatic hydrocarbons or metal complexes with π-delocalization such as porphyrines and unspoilt carbon materials. Thus, catalysts can either be attached by their intrinsic π-system or by an attached linker with a suitable moiety. Due to the facile preparation of the catalyst

composite materials and the aforementioned possibility of a “catch and release” system this methodology seems to be quite advantageous.

1.2 Immobilization of catalysts

1.2.1 Rhodium catalysts immobilized on carbon materials

This first application of CNTs as carriers for an immobilized molecular catalyst was the hydroformylation of propene with a supported Rh-phosphine catalyst.[6b] In their study compared Zhang et al. a nanotube support with SiO_2, carbon molecular sieves, active carbon and a polymer support. The Rh complex $[HRh(CO)(PPh_3)_3]$ was immobilized by a incipient wetness technique. Hydroformylation of propene to butyraldehyde with the aforementioned Rh modified different supports revealed that the CNT-supported catalyst showed the highest activity (TOF = 0.12 s^{-1}) and excellent regioselectivity (14/1). To gain further information where the catalyst is immobilized, an ends unopened CNT was used as support. In this case the catalyst can only be located at the exterior of the tube. Performing the same hydroformylation reaction resulted in a TOF of only 0.06 s^{-1} and a regioselectivity of 6/1. The authors concluded that the high activity and regioselectivity can be assigned to a confinement effect in the interior of the CNT.

A similar report of a covalently bound molecular catalyst on CNTs was the attachment of Wilkinson`s catalyst with the aid of carboxylic acid groups.[20]

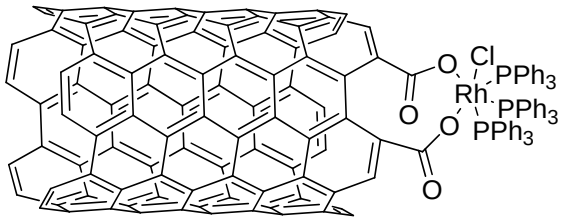

1

Figure 2: Wilkinsons catalyst covalently bound on a oxidized CNT.

The derived complex 1 was used in the hydrogenation of cyclohexene. After three days a conversion of about 30% could be observed.

Another method for the immobilization is particularly interesting for cationic complexes. These complexes form a covalent bond to a hydroxyl group on the surface of activated carbon or CNTs (Figure 3, 2).[21] Barnard et al. demonstrated this methodology by anchoring different cationic rhodium complexes with the general formula $[Rh(nbd)(diphosphine)]^+BF_4^-$ (diphosphine = dppb, S-Bophoz, Skewphos and Xylyl-Phanephos) onto activated carbon surfaces.[22] The loadings obtained differed significantly. Basic carbon supports like Acticarbone 2S (activated with steam at high temperatures resulting in a pH value of 9-11) with negatively charged donor groups on the surface gave the best results with a Rh content up to 0.52% (w/w). The immobilized complexes were applied in the asymmetric hydrogenation of dimethyl itaconate and methyl acetamidoacrylate. The results showed a distinct increase in enantioselectivity compared to the homogeneous counterpart when the catalysts are anchored on the carbon supports (91% and 82% respectively for S-Bophoz). Even recycling of the system [Rh(nbd)(Skewphos)]/AC was possible, retaining the same enantioselectivity and activity of the fist run. In addition no leaching of the catalyst was observed by ICP measurement.

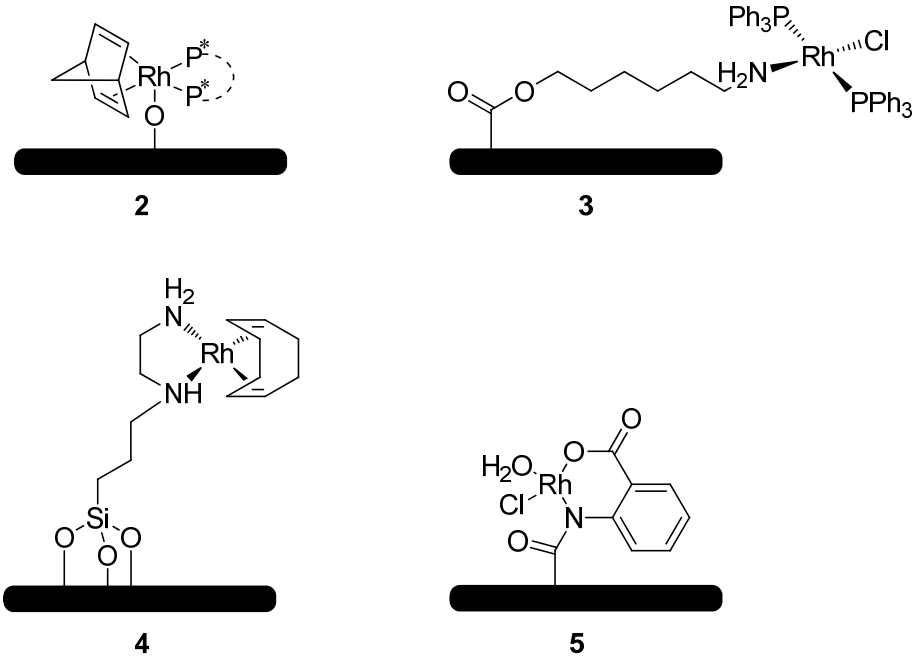

Figure 3: Different rhodium catalysts immobilized on carbon surfaces.

Román-Martínez et al. chose a different strategy to immobilize a rhodium diphosphine catalyst onto activated carbon.[23] After a moderately successful attempt to attach $[Rh(\mu\text{-}Cl)(cod)]_2$ by electrostatic interactions, the authors decided to attach the catalyst via a covalent linker.[24] The carboxylic acid groups on the surface of the activated carbon material

were activated with $SOCl_2$ and subsequently reacted with linker 6 or the preformed complex 7 respectively (Scheme 2). The hybrid catalyst 8 obtained from the latter procedure proved to be highly active in the hydroformylation of 1-octene (to nonanal and 2-methyloctanal) in four consecutive runs. The same approach is also applicable to carbon nanofibers. In this manner Konigsberger and coworkers were able to attach anthranilic acid as a ligand for $RhCl_3$ (Figure 3, 5).[25]

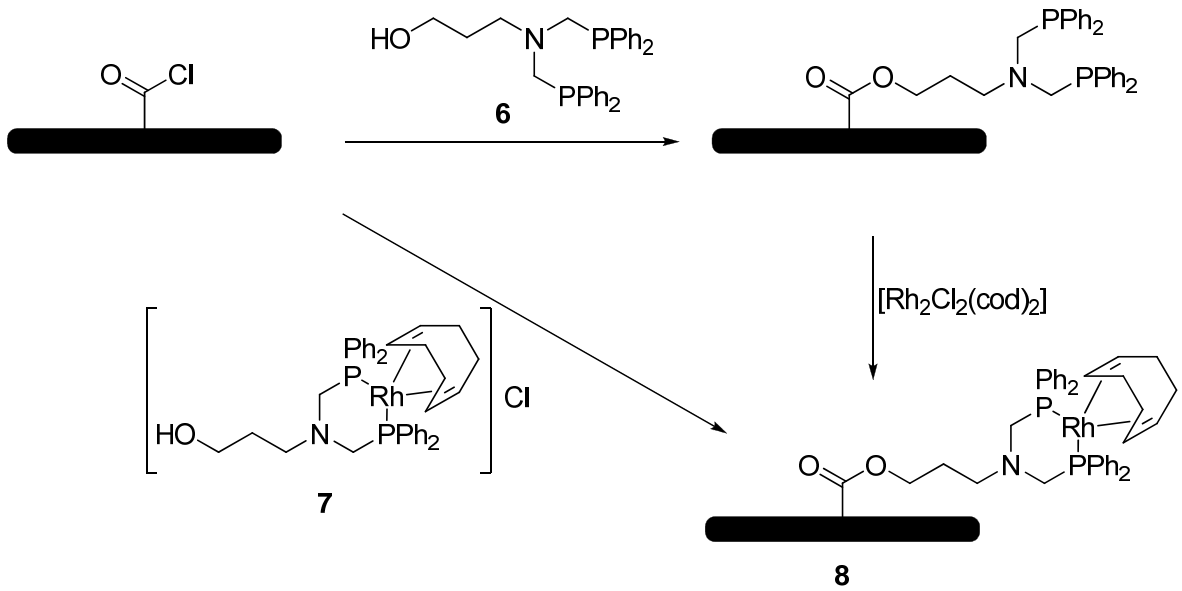

Scheme 2: Synthesis of the Rhodium complex 8 by two different routes.

Following a similar strategy Román-Martínez et al. immobilized Wilkinson`s catalyst on activated carbon and MWNT.[26] By activating the carboxylic acid groups on the surface of both supports with $SOCl_2$ they were able to construct a tethered amine anchor. These materials were reacted with [$RhCl(PPh_3)$] to give rise to catalyst 3 (Figure 3). A maximum Rhodium loading of 0.52% (w/w) (corresponding to 0.05 mmol/g Rh per g of catalyst) could be obtained. The activity of the catalysts was tested in the hydrogenation of cyclohexene. The catalyst on activated carbon showed an activity similar to the homogenous Wilkinson catalyst (TOF = 0.13 s^{-1}, TON = 1404 and TOF = 0.12 s^{-1}, TON = 1296 respectively). The MWNT anchored catalyst however, performed noticeably better (TOF = 0.33 s^{-1}, TON = 3564). The authors rationalized this finding with a confinement effect like in a nano-reactor.[6b, 27] XPS studies before and after a catalytic run revealed that the catalyst constitution has not changed significantly. Thus, the catalyst retained almost the same activity in a second run.

Another method for the installation of an anchor on the surface of carbon materials was presented also by Román-Martínez et al.[27a, 28] By reacting different carbon supports with a diamine Rhodium catalyst tethered to a trimethoxysilane group a covalent linkage between the silicon group and phenol like groups on the surface of the carbon materials was created (Figure 3, 4).[29] The catalytic activity of the resulting catalysts was tested in the model hydrogenation of cyclohexene and carvone. Among the different catalysts those prepared from CNTs and nanofibers were most active (TOF = 4.44 s^{-1} for CNT with inner diameter of 7 nm), even more active as the homogeneous catalyst itself (TOF = 0.08 s^{-1}). At least five consecutive runs could be performed with no measureable leaching of the catalyst.

1.2.2 Salen complexes immobilized on carbon materials

The use of different carbon materials for the immobilization of chiral salen-metal complexes has attracted a lot of recent interest. For these complexes four different immobilization modes have been proposed. Firstly, the covalent attachment via reaction of a hydroxyl group in the ligand backbone with a surface carboxy group (Figure 4, 9),[30] secondly, anchoring of the catalyst by an covalent linker (Figure 4, 10),[31] thirdly, the apical complexation of the Mn^{III} center with oxygen groups on the surface (Figure 4, 11)[21b, 32] and last the adsorption by $\pi-\pi$ interactions of the ligand`s extended π-system with the undecorated surface of the support (Figure 4, 12). In 2003, Freire et al. immobilized two Manganese salene catalysts via different routes.[30] A hydroxy functionalized Mn(III)salen complex was attached to AC and to its air and acid oxidized counterparts (Figure 4, 9). The unfunctionalized analogous complex was adsorbed onto the supports by impregnation. The catalysts were tested in the epoxidation of styrene with iodosylbenzene as oxidant. All heterogeneous complexes showed a slightly lower activity compared to their homogenous counterpart (maximum 42% and 56% respectively), but exhibited the same selectivity toward the styrene oxide (81 - 89% and 89% respectively). Only the acid oxidized support with the most acid groups on the surface performed inferior. This is most probably attributable to the ring opening of the epoxide product by the carboxylic acid groups. Recycling studies revealed that the covalently attached catalyst showed the same activity in a second run, but the adsorbed

unfunctionalized complex showed a sharp decrease in the activity, indicating a pronounced leaching.

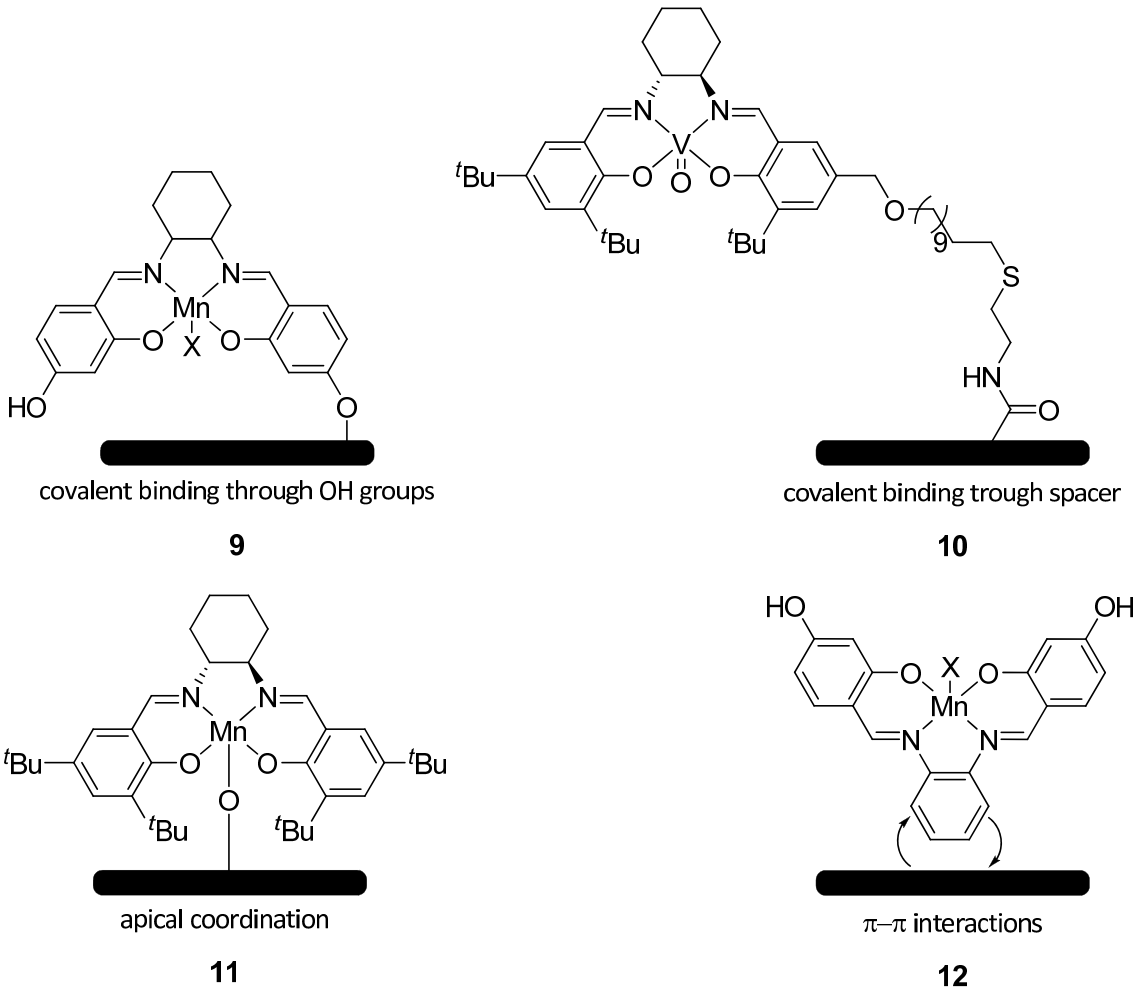

Figure 4: Different strategies to immobilize salen complexes on carbon supports.

García et al. used mercapto functionalized spacers to construct an anchor on different supports (silica, SWNT, AC and ionic liquids).[31] In the case of SWNTs and AC, 2-mercaptoethylamine was reacted with acid chloride groups on the surface of the material (Figure 4, 10). The covalent linkage between the anchor and the catalyst was then achieved by a radical initiated thiol-ene coupling of the mercapto group to a double bond tethered to the catalyst.[33] The resulting hybrid catalysts 10 were tested in the cyanosilylation of benzaldehyde. Both carbon anchored catalysts exhibited equal or higher TOF values (maximum of 3.75 h^{-1}) than the homogeneous catalyst. However, both were lacking a good asymmetric induction compared to the other supports used in the study.

1.2.3 Iron-phthalocyanine complexes

Iron–phthalocyanine (FePc) complexes are widely used for the oxidation of alkanes. For this purpose these complexes were adsorbed on carbon black by an impregnation method.[34] Carbon black turned out to be a suitable support for iron–phthalocyanine complexes used for the oxidation of alkanes with TBHP. The increased hydrophobicity of the support surface, compared to zeolite Y, promoted the adsorption behavior of the alkane. The same trend was observed when a FePc catalyst was impregnated onto carbon black supports with varying oxygen content, making the surface either hydrophilic or hydrophobic.[34b] As observed before the oxidation of cyclohexene benefited from a hydrophobic surface, whereas the decomposition of hydrogen peroxide performed best on hydrophilic carbon black with high oxygen content. Interestingly a certain amount of surface oxygen groups has to be present, otherwise the adsorption of the oxidant TBHP is prevented.[34c]

1.2.4 Catalysts immobilized on carbon coated magnetic nanoparticles

Apart from the sole carbon materials also hybrid materials with new properties are attractive materials as catalyst supports. Recently Grass et al. reported a method for coating different metal nanoparticles with graphene like layers to give rise to large amounts (>30 g/h) of magnetic carbon coated nanoparticles.[35] The surface of these particles exhibits similar properties like other carbon materials and therefore, is amenable for covalent functionalization by diazonium chemistry. Furthermore the thermal and chemical stability is remarkable.[36] Reiser and Stark et al. anchored the stable nitroxyl radical TEMPO, used as a organocatalyst in the chemoselective oxidation of alcohols, via click chemistry onto benzylazide tagged Co@C nanoparticles.[37] The hybrid material 13 promoted several benzylic and aliphatic alcohols to the corresponding aldehydes and proved to be active for 14 runs without significant loss in activity. Surprisingly, the harsh oxidative conditions (alkaline chlorine bleach) did not affect the morphology or magnetization of the particles, most probably due to the high stability of the carbon coating. The pronounced magnetic properties of the particles qualify them not only for batch reactions, but also the application in continuous flow systems is thinkable. The azabis(oxazoline)copper complex tagged Co@C particles 14 were tested in the asymmetric resolution of racemic 1,2-diphenylethane-1,2-diol

and gave, in a continuous setup with the particles fixed in a magnetic field, excellent yields and selectivities.[38]

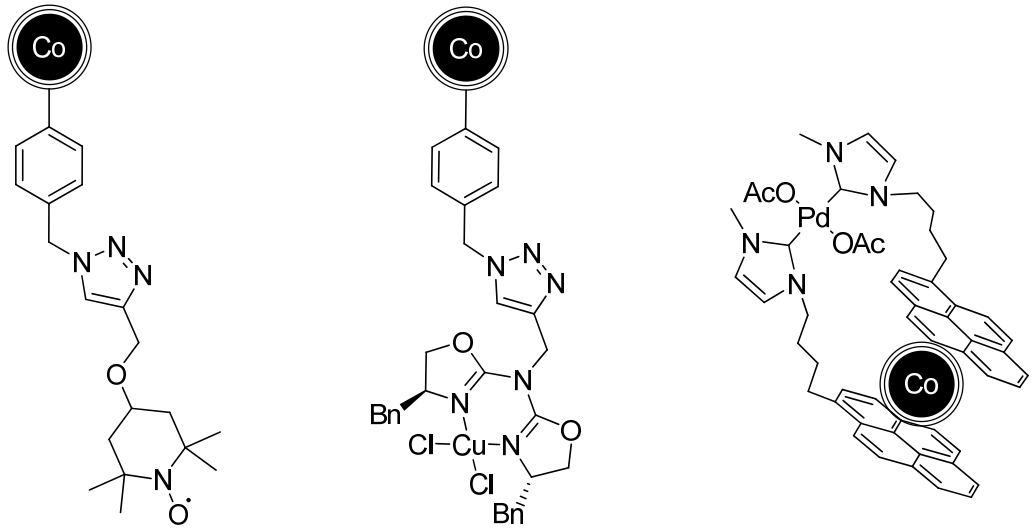

13 **14** **15**

Figure 5: Catalysts anchored on carbon coated cobalt nanoparticles.

But also the intrinsic properties of the carbon shell could be used as a tool to fix the catalyst 15 onto the surface by π-π interactions. In the next section this feature of carbon materials is highlighted in detail.

1.2.5 Noncovalent immobilization of catalysts

The first application of a noncovalently, by π-π interactions, anchored molecular catalyst was the decoration of SWNTs with a ROMP polymer.[39] For this purpose the SWNTs were functionalized with the pyrene tagged catalyst 16 in DCM. Polymerization of norbornene resulted in a 5-20 nm thick polymer coating of the SWNTs. Longer reaction times led to a decrease in the thickness most probably due to the decreased ability of the pyrenyl group to anchor the growing polymer effectively to the nanotube.

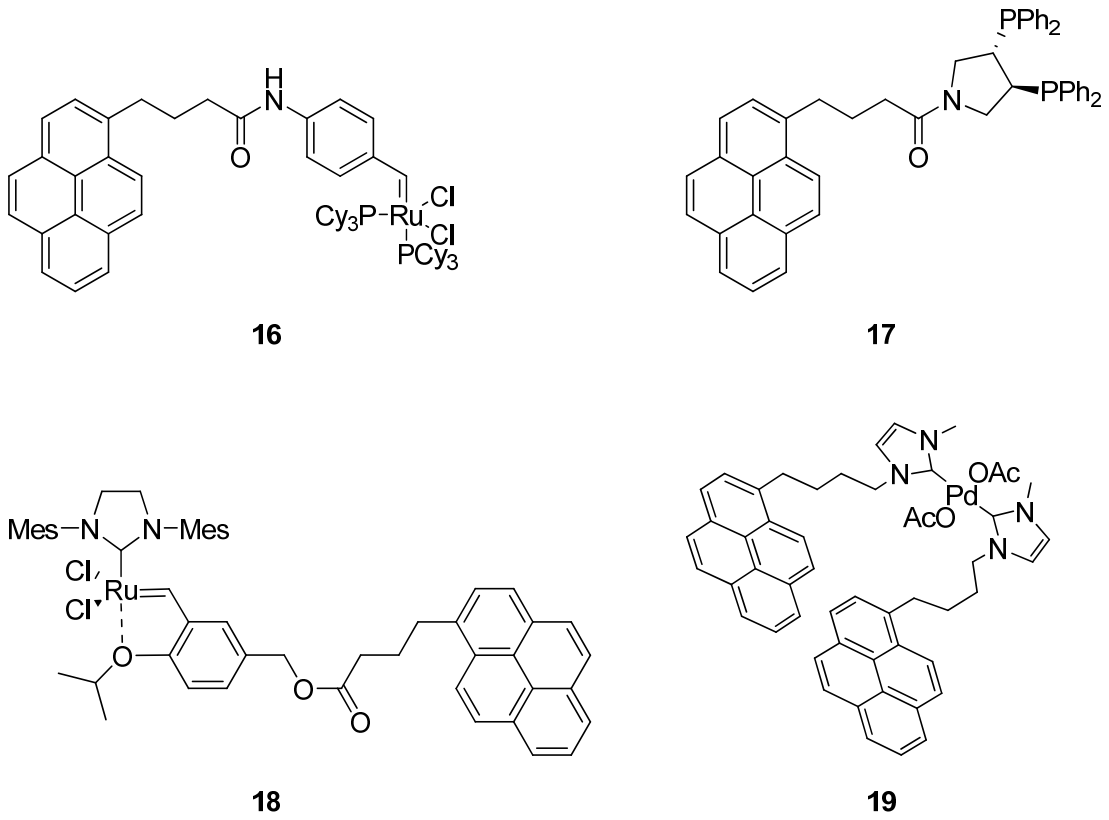

Figure 6: Different ligands used for the noncovalent immobilization onto carbon supports.

Not only CNTs can be used as a support for noncovalent functionalization. Salinas-Martìnez de Lecea et al. showed in a preliminary study with the goal to immobilize a Rh complex, that natphtoic acid is amenable to be grafted immobilized on different carbon materials.[40] All tested materials were able to adsorb naphtoic acid. However, adsorption isotherms in MeOH showed differences in the adsorption ability between different supports. Additional oxygen groups on the surface lead to a significantly lower amount of adsorbed material. This can be explained with the fact that oxygen groups make the carbon surface less electron rich and by the inhibition of the binding of naphtoic acid to the aromatic surface by sterical interactions.[41]

In 2008, Zhou et al. reported that the pyrene tagged ligand 17 in combination with $Rh(cod)_2BF_4$ shows a solvent dependent adsorption behavior on CNTs.[42] Several solvents were examined by UV measurements to determine their influence on the adsorption properties of the catalyst system. DCM was found to give the lowest value (50%). In contrast, 97% of the catalyst was adsorbed on the CNTs in EtOAc. Due to this fact the hydrogenation of α-dehydroamino esters 20 was performed with ligand 17@CNT and $Rh(cod)_2BF_4$ in DCM in a homogeneous manner (Scheme 3). In all cases the reaction reached full conversion

within two hours and resulted in enantioselectivities of 92-96%. After the reaction the catalyst was recovered by evaporating the DCM and forcing the catalyst back onto the nanotubes with EtOAc. Subsequently, the nanotubes were separated by filtration. By repeating this procedure, nine consecutive cycles were performed with only a moderate decrease in activity and remaining high selectivity.

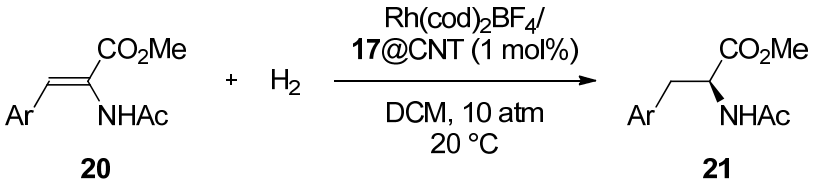

20 **21**

Scheme 3: Asymmetric hydrogenation of α-dehydroamino esters with the nanotube supported ligand 17@CNT.

Wang et al. carried the previous methodology further and immobilized the pyrene tagged catalyst 18 on CNTs by noncovalent π–π interactions.[43] Different solvents were tested to determine their ability to fix the catalyst at ambient temperature on the nanotubes, but releasing it at higher temperature. In the most organic solvents like DCM or toluene the catalyst desorbed immediately from the surface, only acetone and EtOAc were found to be suitable for this purpose. The concept was nicely demonstrated by releasing the metathesis catalyst 18 at 35 °C from the CNTs and capturing it back at ambient temperature. In this manner different metathesis reactions were carried out in a homogeneous manner and the catalyst was recovered after the reaction as a nanotube composite by simple filtration. The catalyst could be recovered up to eight times with a pronounced loss of activity after the sixth run.

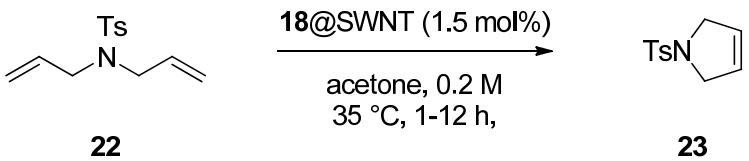

22 **23**

Scheme 4: Ring closing metathesis catalyzed by 18@SWNT.

In 2010 Reiser et al. aimed to overcome the disadvantage of the commonly required filtration step in the catalyst recovery procedure.[44] By using the magnetic carbon coated

cobalt nanoparticles 24 they were able to noncovalently immobilize the palladium complex 19, used for the hydroxycarbonylation of aryl halides in water, via pyrene tags. The desorption of the pyrene moieties could be thermally triggered to release the homogeneous calalyst at 100 °C. After the reaction the catalyst was re-adsorbed back onto the particles while cooling down to ambient temperature. The adsorbed complex 15 could then simply be recovered by magnetic decantation and was recycled 16 times.

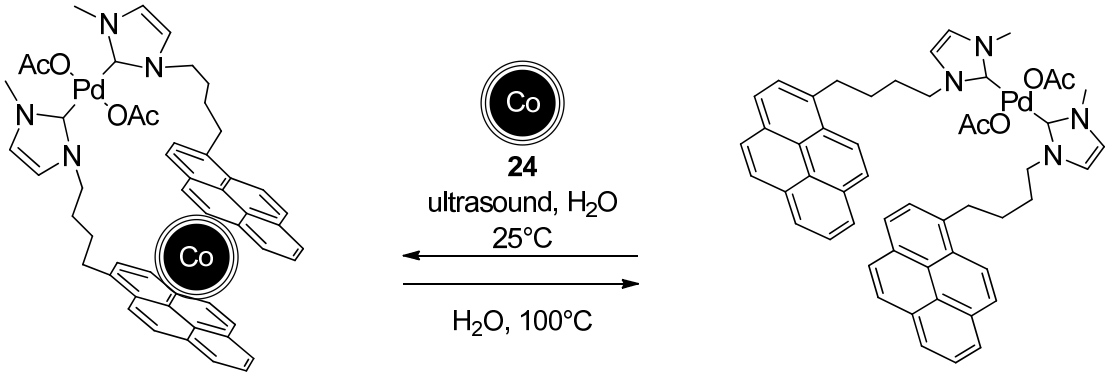

Scheme 5: Temperature triggered desorption behavior of 15 immobilized on graphene coated cobalt nanoparticles.

One property that was not exploited for immobilized catalysts until 2010 was the intrinsic conductivity of CNTs. Goldsmith et al. could show that pyrene-pendant transition metal complexes adsorb specifically onto the surface of SWNTs in the presence of other electrode materials.[45] Furthermore an efficient electronic communication between the SWNTs and the metal complex could be proven. Atero et al. utilized this concept in the hydrogen production through the reduction of water with the nickel catalysts 25a-b, immobilized on MWNTs.[46] Compared to commercial palladium nanoparticles on carbon black and a covalently anchored analogue the immobilized nickel catalysts showed higher activity and stability. Sun et al. used the complex 26, immobilized on a MWNT coated ITO electrode, for the electrochemical oxidation of water.[47] The authors claimed that the immobilized complex 26 was the most efficient molecular system for the electrocatalytic oxidation of water synthesized so far.

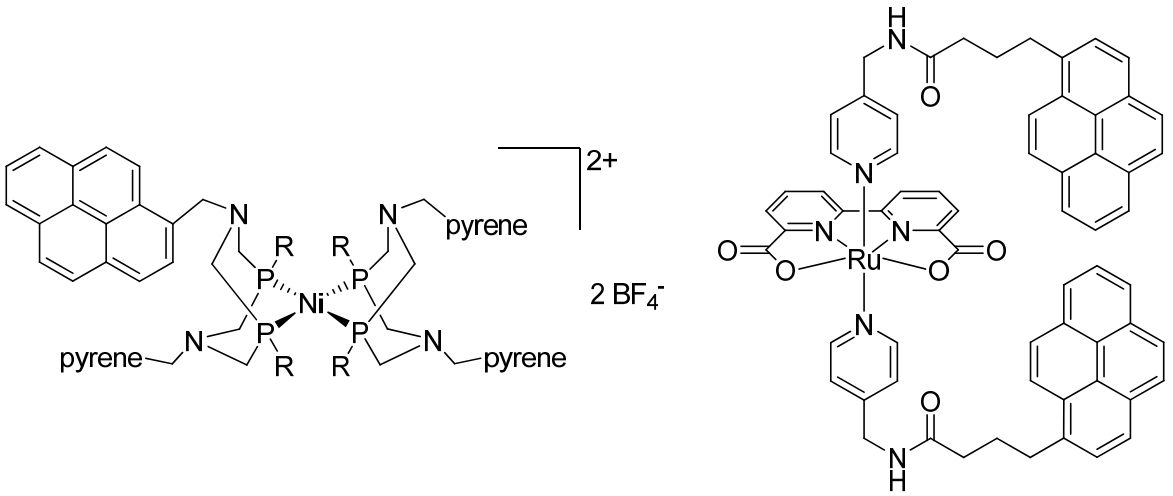

25a: R = Ph
25b: R = Cy

26

Figure 7: Catalysts used for electrochemical reduction or oxidation of water.

Although the immobilization of molecular catalysts onto carbon materials is a fairly unexploited topic, novel innovative materials like carbon coated magnetic nanoparticles and new production methods for uniform carbon materials will give this area a boost. Also new effective functionalization methods will relieve the conventional impregnation methods and allow a more targeted way of immobilizing catalysts.

2. References

[1] (a) J. A. Gladysz, *Chem. Rev.* 2002, *102*, 3215-3216; (b) J. Lu, P. H. Toy, *Chem. Rev.* 2009, *109*, 815-838; (c) M. Benaglia, A. Puglisi, F. Cozzi, *Chem. Rev.* 2003, *103*, 3401-3430; (d) D. E. Bergbreiter, J. Tian, C. Hongfa, *Chem. Rev.* 2009, *109*, 530-582; (e) V. Polshettiwar, R. Luque, A. Fihri, H. Zhu, M. Bouhrara, J.-M. Basset, *Chem. Rev.* 2011, *111*, 3036-3075; (f) S. Shylesh, V. Schünemann, W. R. Thiel, *Angew. Chem.* 2010, *122*, 3504-3537; (g) S. Shylesh, V. Schünemann, W. R. Thiel, *Angew. Chem. Int. Ed.* 2010, *49*, 3428-3459; (h) A. Schätz, O. Reiser, W. J. Stark, *Chem.-Eur. J.* 2010, *16*, 8950-8967.

[2] H. P. Boehm, A. Clauss, G. O. Fischer, U. Hofmann, *Z. Anorg. Allg. Chem.* 1962, *316*, 119-127.

[3] (a) S. Iijima, *Nature* 1991, *354*, 56-58; (b) M. Monthioux, V. L. Kuznetsov, *Carbon* 2006, *44*, 1621-1623.

[4] A. Hirsch, M. Brettreich, in *Fullerenes: Chemistry and Reactions*, Wiley-VCH Verlag GmbH & Co. KGaA, 2005.

[5] (a) J. Lee, J. Kim, T. Hyeon, *Adv. Mater.* 2006, *18*, 2073-2094; (b) J. Lee, S. Han, T. Hyeon, *J. Mater. Chem.* 2004, *14*, 478-486; (c) Y. Wu, B. Yang, B. Zong, H. Sun, Z. Shen, Y. Feng, *J. Mater. Chem.* 2004, *14*, 469-477.

[6] (a) A. Peigney, C. Laurent, E. Flahaut, R. R. Bacsa, A. Rousset, *Carbon* 2001, *39*, 507-514; (b) Y. Zhang, H.-B. Zhang, G.-D. Lin, P. Chen, Y.-Z. Yuan, K. R. Tsai, *Appl. Catal., A* 1999, *187*, 213-224.

[7] G. E. Begtrup, K. G. Ray, B. M. Kessler, T. D. Yuzvinsky, H. Garcia, A. Zettl, *physica status solidi (b)* 2007, *244*, 3960-3963.

[8] A. Fihri, M. Bouhrara, B. Nekoueishahraki, J.-M. Basset, V. Polshettiwar, *Chem. Soc. Rev.* 2011, *40*, 5181-5203.

[9] C. Freire, A. R. Silva, in *Carbon Materials for Catalysis*, John Wiley & Sons, Inc., 2008, pp. 267-307.

[10] (a) P. Serp, M. Corrias, P. Kalck, *Appl. Catal., A* 2003, *253*, 337-358; (b) N. Karousis, N. Tagmatarchis, D. Tasis, *Chem. Rev.* 2010, *110*, 5366-5397.

[11] K. Yang, B. Xing, *Chem. Rev.* 2010, *110*, 5989-6008.

[12] (a) B. W. T. Gruijters, M. A. C. Broeren, F. L. van Delft, R. P. Sijbesma, P. H. H. Hermkens, F. P. J. T. Rutjes, *Org. Lett.* 2006, *8*, 3163-3166; (b) J. I. García, C. I. Herrerías, B. López-Sánchez, J. A. Mayoral, O. Reiser, *Adv. Synth. Catal.* 2011, n/a-n/a; (c) S.-W. Chen, J. H. Kim, C. E. Song, S.-g. Lee, *Org. Lett.* 2007, *9*, 3845-3848; (d) S.-W. Chen, J. H. Kim, H. Shin, S.-g. Lee, *Org. Biomol. Chem.* 2008, *6*, 2676-2678; (e) Z. Wang, G. Chen, K. Ding, *Chem. Rev.* 2008, *109*, 322-359; (f) J. I. García, B. López-Sánchez, J. A. Mayoral, *Org. Lett.* 2008, *10*, 4995-4998; (g) A. Cornejo, J. M. Fraile, J. I. García, M. J. Gil, V. Martínez-Merino, J. A. Mayoral, *Tetrahedron* 2005, *61*, 12107-12110; (h) D.-W. Kim, S.-G. Lim, C.-H. Jun, *Org. Lett.* 2006, *8*, 2937-2940; (i) L. Shi, X. Wang, C. A. Sandoval, M. Li, Q. Qi, Z. Li, K. Ding, *Angew. Chem.* 2006, *118*, 4214-4218; (j) L. Shi, X. Wang, C. A. Sandoval, M. Li, Q. Qi, Z. Li, K. Ding, *Angew. Chem. Int. Ed.* 2006, *45*, 4108-4112; (k) J. Zhang, J. K. Lee, Y. Wu, R. W. Murray, *Nano Lett.* 2003, *3*, 403-407.

[13] D. Tasis, N. Tagmatarchis, A. Bianco, M. Prato, *Chem. Rev.* 2006, *106*, 1105-1136.

[14] (a) A. Hirsch, *Angew. Chem. Int. Ed.* 2002, *41*, 1853-1859; (b) A. Hirsch, *Angew. Chem.* 2002, *114*, 1933-1939.

[15] V. N. Khabashesku, W. E. Billups, J. L. Margrave, *Acc. Chem. Res.* 2002, *35*, 1087-1095.

[16] H. Li, F. Cheng, A. M. Duft, A. Adronov, *J. Am. Chem. Soc.* 2005, *127*, 14518-14524.
[17] (a) M. Holzinger, J. Abraham, P. Whelan, R. Graupner, L. Ley, F. Hennrich, M. Kappes, A. Hirsch, *J. Am. Chem. Soc.* 2003, *125*, 8566-8580; (b) V. Georgakilas, K. Kordatos, M. Prato, D. M. Guldi, M. Holzinger, A. Hirsch, *J. Am. Chem. Soc.* 2002, *124*, 760-761; (c) F. G. Brunetti, M. A. Herrero, J. d. M. Muñoz, S. Giordani, A. Díaz-Ortiz, S. Filippone, G. Ruaro, M. Meneghetti, M. Prato, E. Vázquez, *J. Am. Chem. Soc.* 2007, *129*, 14580-14581.
[18] D. A. Britz, A. N. Khlobystov, *Chem. Soc. Rev.* 2006, *35*, 637-659.
[19] (a) D. Baskaran, J. W. Mays, X. P. Zhang, M. S. Bratcher, *J. Am. Chem. Soc.* 2005, *127*, 6916-6917; (b) Y.-L. Zhao, J. F. Stoddart, *Acc. Chem. Res.* 2009, *42*, 1161-1171; (c) M. Á. Herranz, C. Ehli, S. Campidelli, M. Gutiérrez, G. L. Hug, K. Ohkubo, S. Fukuzumi, M. Prato, N. Martín, D. M. Guldi, *J. Am. Chem. Soc.* 2007, *130*, 66-73; (d) N. Nakashima, Y. Tomonari, H. Murakami, *Chem. Lett.* 2002, *31*, 638-639; (e) Q. Su, S. Pang, V. Alijani, C. Li, X. Feng, K. Müllen, *Adv. Mater.* 2009, *21*, 3191-3195; (f) P. Wu, X. Chen, N. Hu, U. C. Tam, O. Blixt, A. Zettl, C. R. Bertozzi, *Angew. Chem.* 2008, *120*, 5100-5103; (g) P. Wu, X. Chen, N. Hu, U. C. Tam, O. Blixt, A. Zettl, C. R. Bertozzi, *Angew. Chem. Int. Ed.* 2008, *47*, 5022-5025; (h) G. M. A. Rahman, D. M. Guldi, S. Campidelli, M. Prato, *J. Mater. Chem.* 2006, *16*, 62-65; (i) X. Wang, Y. Liu, W. Qiu, D. Zhu, *J. Mater. Chem.* 2002, *12*, 1636-1639.
[20] S. Banerjee, S. S. Wong, *J. Am. Chem. Soc.* 2002, *124*, 8940-8948.
[21] (a) R. L. Augustine, S. K. Tanielyan, N. Mahata, Y. Gao, A. Zsigmond, H. Yang, *Appl. Catal., A* 2003, *256*, 69-76; (b) A. R. Silva, C. Freire, B. de Castro, *Carbon* 2004, *42*, 3027-3030.
[22] C. F. J. Barnard, J. Rouzaud, S. H. Stevenson, *Org. Process Res. Dev.* 2005, *9*, 164-167.
[23] M. C. Román-Martínez, J. A. Díaz-Auñón, C. Salinas-Martínez de Lecea, H. Alper, *J. Mol. Catal. A: Chem.* 2004, *213*, 177-182.
[24] J. A. Díaz-Auñón, M. C. Román-Martínez, C. Salinas-Martínez de Lecea, *J. Mol. Catal. A: Chem.* 2001, *170*, 81-93.
[25] T. G. Ros, A. J. van Dillen, J. W. Geus, D. C. Koningsberger, *Chem.-Eur. J.* 2002, *8*, 2868-2878.
[26] M. Pérez-Cadenas, L. J. Lemus-Yegres, M. C. Román-Martínez, C. Salinas-Martínez de Lecea, *Appl. Catal., A* 2011, *402*, 132-138.
[27] (a) L. J. Lemus-Yegres, M. C. Román-Martínez, I. Such-Basáñez, C. Salinas-Martínez de Lecea, *Microporous Mesoporous Mater.* 2008, *109*, 305-316; (b) S. Pariente, P. Trens, F. Fajula, F. Di Renzo, N. Tanchoux, *Appl. Catal., A* 2006, *307*, 51-57.
[28] (a) L. Lemus-Yegres, I. Such-Basáñez, C. S.-M. de Lecea, P. Serp, M. C. Román-Martínez, *Carbon* 2006, *44*, 605-608; (b) L. J. Lemus-Yegres, M. Pérez-Cadenas, M. C. Román-Martínez, C. S.-M. de Lecea, *Microporous Mesoporous Mater.* 2011, *139*, 164-172.
[29] L. J. Lemus-Yegres, I. Such-Basáñez, M. C. Román-Martínez, C. S.-M. de Lecea, *Appl. Catal., A* 2007, *331*, 26-33.
[30] (a) A. R. Silva, J. Vital, J. L. Figueiredo, C. Freire, B. de Castro, *New J. Chem.* 2003, *27*, 1511-1517; (b) A. Rosa Silva, J. Luís Figueiredo, C. Freire, B. de Castro, *Microporous Mesoporous Mater.* 2004, *68*, 83-89; (c) M. Cardoso, A. R. Silva, B. d. Castro, C. Freire, *Appl. Catal., A* 2005, *285*, 110-118.
[31] C. Baleizão, B. Gigante, H. García, A. Corma, *Tetrahedron* 2004, *60*, 10461-10468.
[32] F. Maia, N. Mahata, B. Jarrais, A. R. Silva, M. F. R. Pereira, C. Freire, J. L. Figueiredo, *J. Mol. Catal. A: Chem.* 2009, *305*, 135-141.

[33] (a) A. Dondoni, *Angew. Chem. Int. Ed.* 2008, *47*, 8995-8997; (b) A. Dondoni, *Angew. Chem.* 2008, *120*, 9133-9135.

[34] (a) R. F. Parton, P. E. Neys, P. A. Jacobs, R. C. Sosa, P. G. Rouxhet, *J. Catal.* 1996, *164*, 341-346; (b) R. C. Sosa, R. F. Parton, P. E. Neys, O. Lardinois, P. A. Jacobs, P. G. Rouxhet, *J. Mol. Catal. A: Chem.* 1996, *110*, 141-151; (c) A. Valente, C. Palma, I. M. Fonseca, A. M. Ramos, J. Vital, *Carbon* 2003, *41*, 2793-2803; (d) F. Thibault-Starzyk, M. Van Puymbroeck, R. F. Parton, P. A. Jacobs, *J. Mol. Catal. A: Chem.* 1996, *109*, 75-79.

[35] (a) R. N. Grass, E. K. Athanassiou, W. J. Stark, *Angew. Chem.* 2007, *119*, 4996-4999; (b) R. N. Grass, E. K. Athanassiou, W. J. Stark, *Angew. Chem. Int. Ed.* 2007, *46*, 4909-4912; (c) I. K. Herrmann, R. N. Grass, D. Mazunin, W. J. Stark, *Chem. Mater.* 2009, *21*, 3275-3281.

[36] (a) F. M. Koehler, M. Rossier, M. Waelle, E. K. Athanassiou, L. K. Limbach, R. N. Grass, D. Gunther, W. J. Stark, *Chem. Commun.* 2009, 4862-4864; (b) M. Rossier, F. M. Koehler, E. K. Athanassiou, R. N. Grass, B. Aeschlimann, D. Gunther, W. J. Stark, *J. Mater. Chem.* 2009, *19*, 8239-8243.

[37] A. Schätz, R. N. Grass, W. J. Stark, O. Reiser, *Chem.-Eur. J.* 2008, *14*, 8262-8266.

[38] A. Schätz, R. N. Grass, Q. Kainz, W. J. Stark, O. Reiser, *Chem. Mater.* 2009, *22*, 305-310.

[39] F. J. Gomez, R. J. Chen, D. Wang, R. M. Waymouth, H. Dai, *Chem. Commun.* 2003, 190-191.

[40] I. Such-Basáñez, M. C. Román-Martínez, C. Salinas-Martínez de Lecea, *Carbon* 2004, *42*, 1357-1361.

[41] D. M. Nevskaia, A. Santianes, V. Muñoz, A. Guerrero-Ruíz, *Carbon* 1999, *37*, 1065-1074.

[42] L. Xing, J.-H. Xie, Y.-S. Chen, L.-X. Wang, Q.-L. Zhou, *Adv. Synth. Catal.* 2008, *350*, 1013-1016.

[43] G. Liu, B. Wu, J. Zhang, X. Wang, M. Shao, J. Wang, *Inorg. Chem.* 2009, *48*, 2383-2390.

[44] (a) S. Wittmann, A. Schätz, R. N. Grass, W. J. Stark, O. Reiser, *Angew. Chem. Int. Ed.* 2010, *49*, 1867-1870; (b) S. Wittmann, A. Schätz, R. N. Grass, W. J. Stark, O. Reiser, *Angew. Chem.* 2010, *122*, 1911-1914.

[45] E. W. McQueen, J. I. Goldsmith, *J. Am. Chem. Soc.* 2009, *131*, 17554-17556.

[46] (a) P. D. Tran, A. Le Goff, J. Heidkamp, B. Jousselme, N. Guillet, S. Palacin, H. Dau, M. Fontecave, V. Artero, *Angew. Chem.* 2011, *123*, 1407-1410; (b) P. D. Tran, A. Le Goff, J. Heidkamp, B. Jousselme, N. Guillet, S. Palacin, H. Dau, M. Fontecave, V. Artero, *Angew. Chem. Int. Ed.* 2011, *50*, 1371-1374.

[47] (a) F. Li, B. Zhang, X. Li, Y. Jiang, L. Chen, Y. Li, L. Sun, *Angew. Chem.* 2011, doi: 10.1002/ange.201105044; (b) F. Li, B. Zhang, X. Li, Y. Jiang, L. Chen, Y. Li, L. Sun, *Angew. Chem. Int. Ed.* 2011, doi: 10.1002/anie.201105044.

B. Mainpart

1. Synthesis of carbon coated metal nanoparticles

The majority of the magnetic nanoparticles used today as support for catalysts consist of magnetite (Fe_3O_4). These particles are mostly coated with a layer of a carboxylic acid, a dopamine derivative or with a shell of silica to protect the core from further oxidation.[48] The facile synthesis and handling makes these particles attractive. But taking the relatively low saturation magnetization of metal oxides compared to their pure metal counterparts into account, the use of the latter would be more desirable, especially when polymer coatings are considered to improve the loading (Table 1). A higher saturation magnetization makes the recycling of nanoparticles more efficient and facilitates their handling. By adding more mass to the particle`s surface, caused by a protective coating or a polymer to increase the loading, the saturation magnetization per gram decreases. Generally, values exceeding 10 emu/g are necessary to recover the particles in a convenient and quantitative way from complex mixtures.

Table 1: Comparison of the saturation magnetization (emu/g) of different metals and metal oxides in varying compositions.[49]

core material	bulk	nanoparticles with protective coating	nanoparticles with polymer coating
Fe	220	140-178[50]	33[51]
Co	161	105-180[50]	33-78[51]
Fe_3O_4	93[52]	30-92[53]	4[54]
Fe_2O_3	80	45-75	2[55]

One of the major problems in the synthesis of nanoparticles with pure metal cores is to protect the metal core from oxidation. This can either be done by coating the particles cores with a layer of its own metal oxide during a controlled oxidation step[56] or with a shell of an

inorganic material in order to exclude oxygen. For this purpose silica,[48e, 57] precious metals, such as Ag and Au[58] and carbon[59] are better suited than organic compounds.[60] Under these aforementioned materials, carbon shows by far the highest degree of chemical and thermal stability. Despite the outstanding properties, syntheses delivering uniform and pure metal nanoparticles coated with carbon in sufficient amount are scarce. The few reports concentrate on chemical vapor deposition,[61] calcination,[59a, 62] detonation,[63] solution phase[64] and reducing flame spray techniques.[35]

Another process for the decoration of metal cores with a shell of carbon is the decomposition of suitable precursors at elevated temperatures. These high temperatures can be produced by a microwave induced sparking process. Hwang et al. published 2008 a procedure where they used small pieces of silicon as the source of the sparking process and ferrocene as a precursor.[65] During the reaction, violent sparking occurred which created microwave plasma wherein temperatures of about 1600 °C were reached readily. This plasma could be retained for about 15 seconds. Afterwards, the microwave triggered itself due to overheating protection. Under these conditions high-energy atoms, clusters and subsequently "carbon-metal-alloy" nanoparticles were formed, in which the contained carbon atoms segregated and formed defined graphene shells upon cooling. This mechanism is known as the "carbon-dissolution" model.

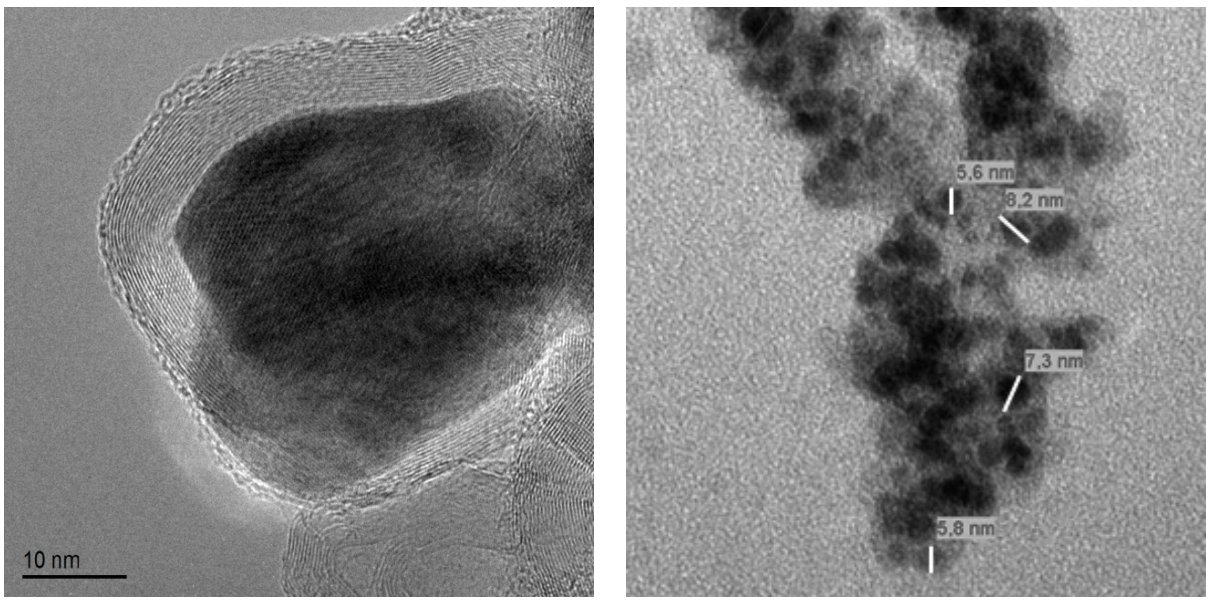

Figure 8: TEM images of carbon coated iron nanoparticles originating from a microwave arcing process. Single layers of the carbon coating can be seen on the left image.

After cooling, the formed nanoparticles could be easily collected by an external magnet. Washing with acetone and dissolution of unprotected particles in *aqua regia* for 30 minutes furnished carbon coated iron nanoparticles. About 33 wt% of the black powder was lost during this process.

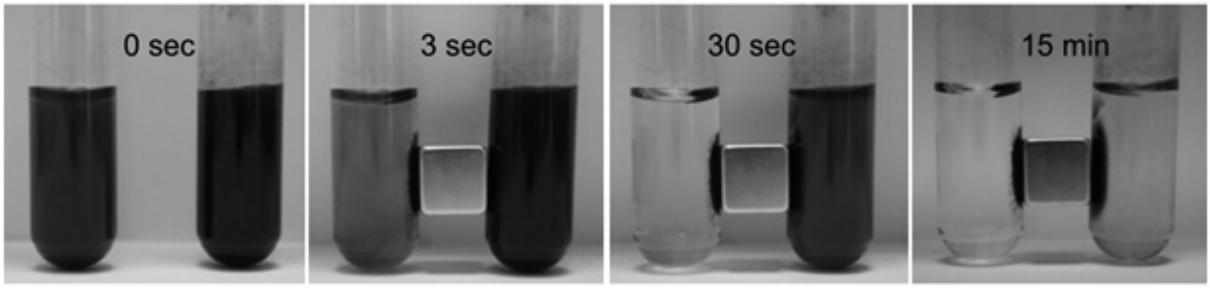

Figure 9: Comparison of Co@C 24 (left, synthesized by reducing flame spray pyrolysis) and microwave synthesized Fe@C (right) particles (Taken with permission from reference [66]).

This observation indicates a quite high amount of uncoated or not completely coated particles and carbon debris, respectively. TEM analysis revealed that the particles have an average diameter of 10 nm and are coated with several graphitic shells consisting of 4-20 graphene layers (Figure 8). The saturation magnetization of the Fe@C nanoparticles as a function of the external magnetic field was determined to be 35 emu/g, which is 16% of the value for bulk iron. The ferromagnetic nature and the low saturation magnetization value are related to the relatively small size of the particles and to the weight dilution by the high number of graphene shells (up to 77 wt% carbon).

All the so far mentioned attempts to synthesize carbon coated metal nanoparticles suffer from irregular particles or coating and limited scalability of the production process.

1.1 Carbon coated metal nanoparticles by reducing flame spray synthesis

Stark et al. applied the metal(II) complex of 2-ethylhexanoate as a precursor for the synthesis of carbon coated cobalt[35a, 35b] or iron[35c] nanoparticles 24 and 27 in a continuous reducing flame spray apparatus. In comparison to the aforementioned methods, this procedure exhibits the advantage of high scalability (>30 g/h).

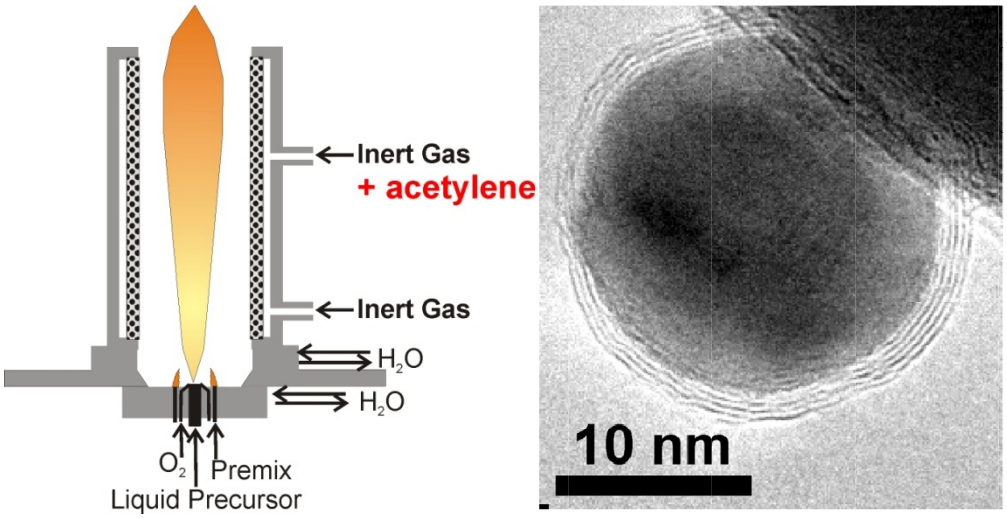

Figure 10: Schematic layout of the device for carbon coated metal nanoparticles synthesis (left). TEM image of a single Fe@C nanoparticle with visible single carbon layers on the surface (right).

By dispersion in an oxygen jet, a spray is formed, which is ignited in a premixed flame (Figure 10, left). This mixture would combust in air to H_2O, CO_2 and the corresponding metal oxide, which can be prevented by operating the process in a nitrogen filled glovebox under oxygen limitation. Due to the reducing conditions, CO and H_2 were formed and the metal precursor was reduced to the metal nanoparticles. The addition of acetylene through the side walls of the reactor led to the deposition of multiple carbon layers on the surface of the nanoparticles.

24 **27**

Figure 11: Schematic drawing of the nanoparticles 24 and 27.

The resulting carbon coated metal nanoparticles containing a cobalt core had an average diameter of about 50 nm and a saturation magnetization of 158 emu/g, which is close to bulk cobalt. In the case of an iron core, it is possible to produce the whole palette of iron based core materials, ranging from iron oxide (Fe_3O_4) to pristine iron (Fe) and iron carbide (Fe_3C). The different compositions could be specifically synthesized by limiting the oxygen content during the synthesis. In Figure 12 a SEM and TEM micrograph (A and B) and the size distribution (C) of carbon coated cementite particles can be seen. The size distribution deduced from the TEM pictures shows that the particles are moderately polydisperse.

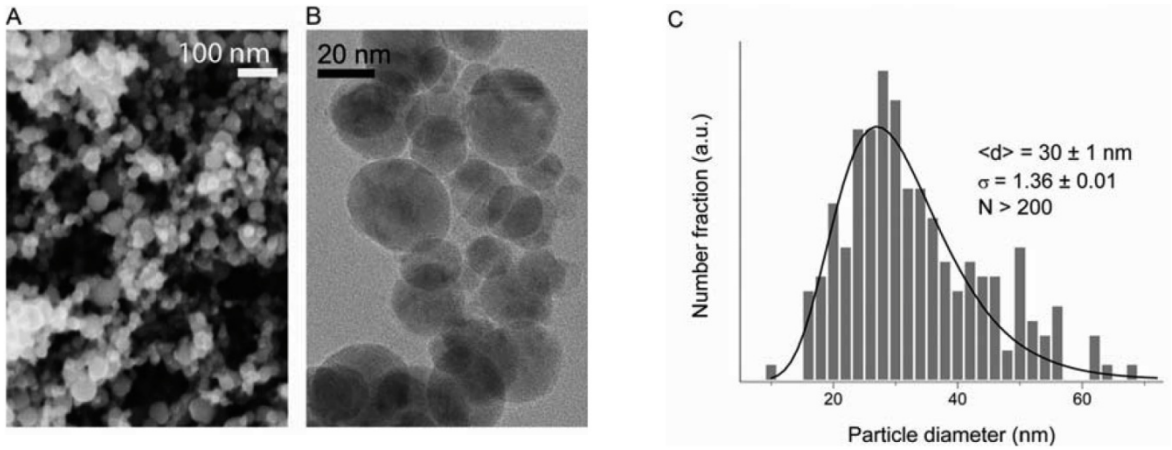

Figure 12: (A) SEM and (B) TEM images of carbon-coated cementite nanomagnets and (C) particle size distribution. Reproduced with permission from reference [35c]. Copyright 2009 American Chemical Society.

2. Surface modification of graphene and related materials

2.1 Covalent modification

Stark et al. reported two methods for the modification of 24[35a, 35b] and later also for 27[35c] nanoparticles. Their methodology uses the decomposition of *in situ* formed diazonium salts to aryl radicals followed by the addition to the carbon surface (Scheme 6).[67]

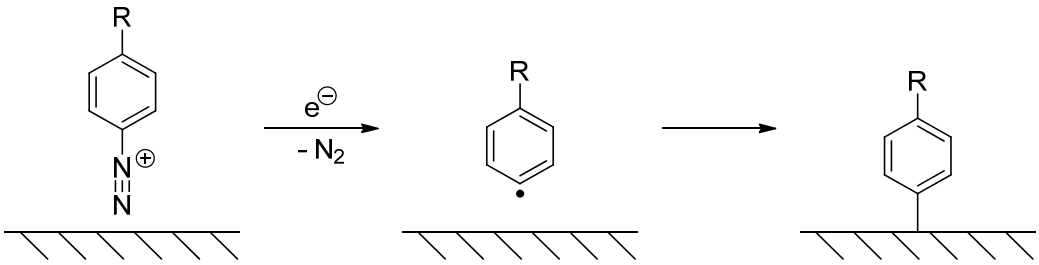

Scheme 6: Covalent modification of carbon surfaces by diazonium salt reduction.

For the covalent attachment of organic molecules onto the carbon coated nanomagnets, this methodology seems to be particularly interesting since the commonly used protocols for functionalization of such surfaces involve harsh conditions. Considering the high reactivity of the diazonium salt, this methodology is limited to simple aniline derivatives. Hence, the aryl moiety can only act as a linker to attach more complex molecules to the surface. Based on work of Stark et al.[35], Reiser et al.[37-38] established a process for the attachment of molecules, in particular molecular catalysts, on the surface of the nanomagnets 24 (Scheme 7). Functionalization of the nanoparticle surface with a benzylalcohol group furnished 29 and a subsequent modified Mitsunobu reaction gave rise to the azide tagged particles 30. These particles act as an universal precursor to attach terminal alkyne functionalized molecules, especially catalysts, by a copper(I) catalyzed click reaction.

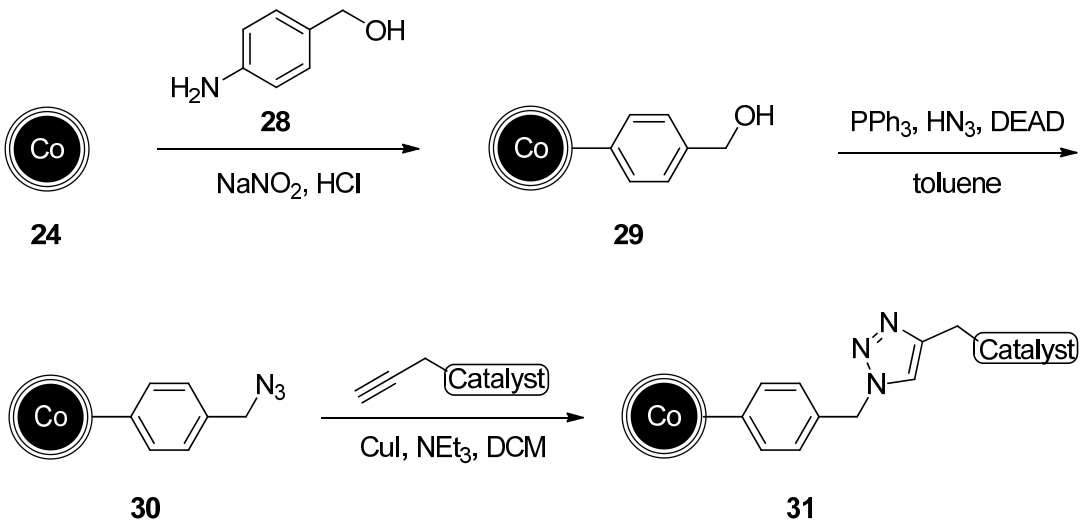

Scheme 7: Grafting of an *in situ* formed diazonium compound onto carbon coated metal nanoparticles and subsequent functionalization of the hybrid material by Mitsunobu reaction and click chemistry.

All steps involve the dispersion of the nanoparticles by sonication to prevent their aggregation. The typical loading obtained by this method was determined to be approximately 0.1 mmol/g. This value was assessed by means of elemental microanalysis and hydrolysis of an attached nitrophenol moiety followed by UV-measurement. Based on these steps, the immobilized catalyst materials 13 and 14 (Part A, Figure 5) were prepared and successfully tested in various reactions.

2.2 Polymer coated Co@C and Fe@C nanoparticles

The major drawback of the above mentioned Co@C and Fe@C nanoparticles is their relative low loading (about 0.1 mmol/g) compared to polymeric supports (> 0.6 mmol/g). Due to the high saturation magnetization (M_s > 158 emu/g), coating of the particles with a polymer shell is possible, albeit the saturation magnetization decreases as a result of the additional mass. Hence, coating of the commonly used magnetite particles results in materials with poor magnetic properties.[68] Schätz and Stark et al. used the precursor 32 to polymerize a thermo responsive poly *N-iso*propylacrylamide (PNIPAM) hybrid polymer giving rise to 35 which was used for the immobilization of a Pd-phosphine complex.[51a] The resulting hybrid catalyst material 36 was tested in Suzuki-Miyaura cross-coupling reactions.

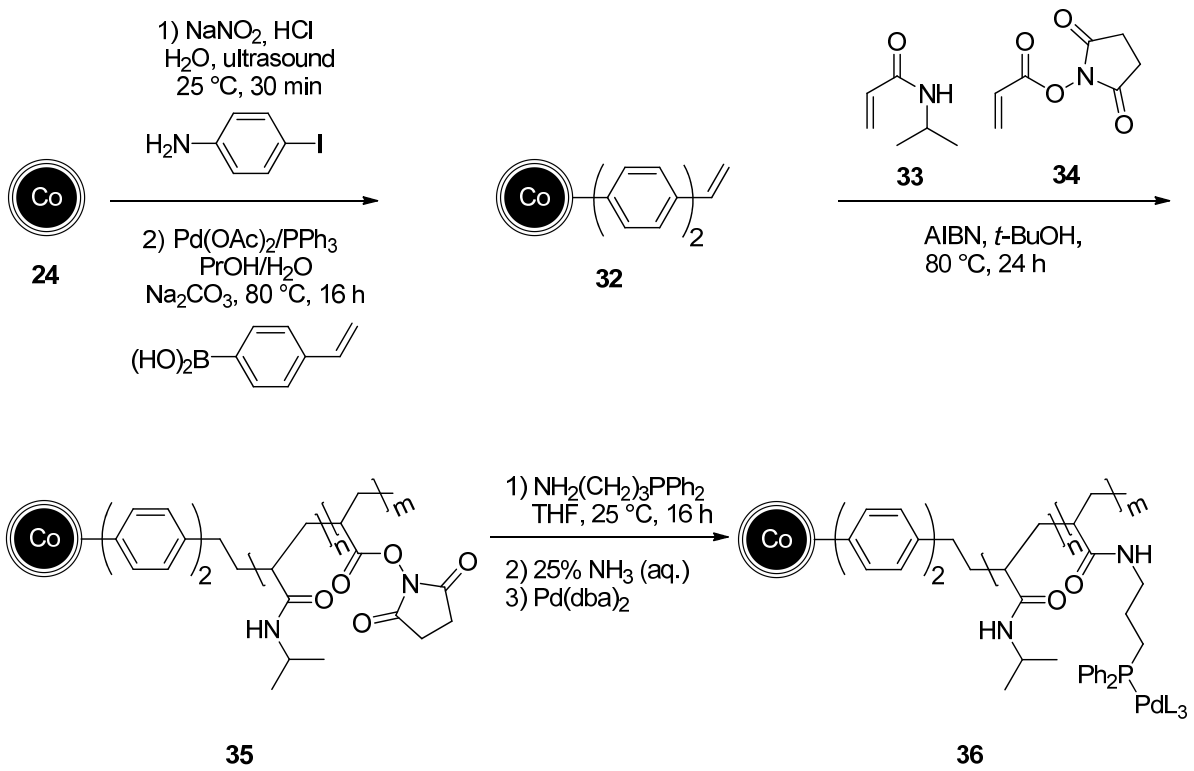

Scheme 8: Immobilization of a palladium phosphine complex onto Co@C particles coated with a thermo responsive PNIPAM shell.

The thermoresponsive PNIPAM shell facilitated a temperature dependent self separation of the catalyst composite in a biphasic water/toluene mixture (Scheme 9). At elevated temperature, the particles catalyzed the Suzuki-Miyaura cross-coupling reaction in the organic phase. However, at ambient temperature the nanobeads underwent a phase

switching and allowed simple recovery of the catalyst due to the still high saturation magnetization of 78 emu/g.

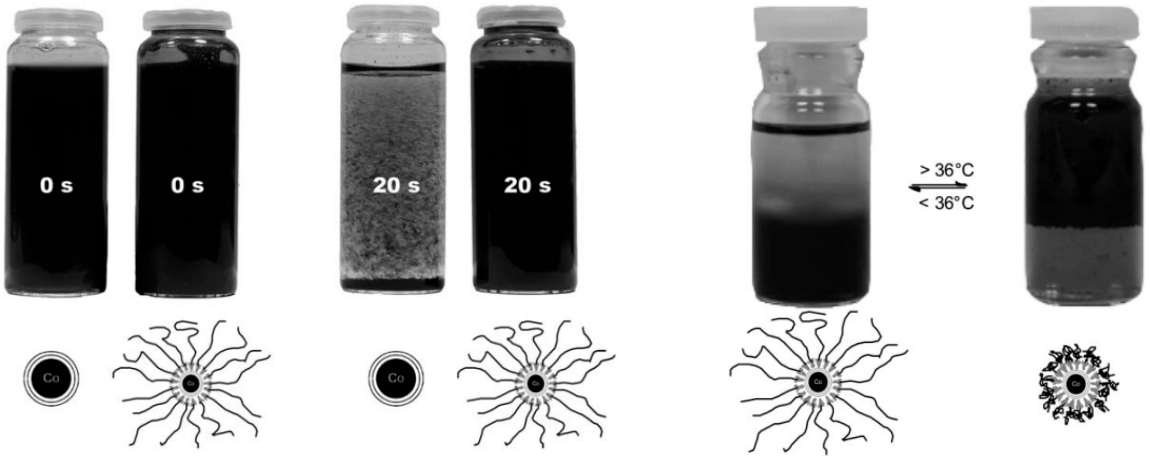

Scheme 9: Thermoresponsive polymer coated Co@C nanoparticles form stable suspensions (left) and undergo temperature dependent phase switches (right).[51a] - Reproduced with permission of The Royal Society of Chemistry.

By radical polymerization of precursor 32 with polyvinylbenzylchloride, chlorine loadings of about 3.7 mmol/g can be obtained (Scheme 10).[51b] The highly loaded particles 37 exhibit a saturation magnetization of 33 emu/g, a value typical for uncoated magnetite particles with a considerably lower loading. Furthermore 37 provides high stability against acids and the possibility for covalent attachment of various molecules by simple substitution reactions.

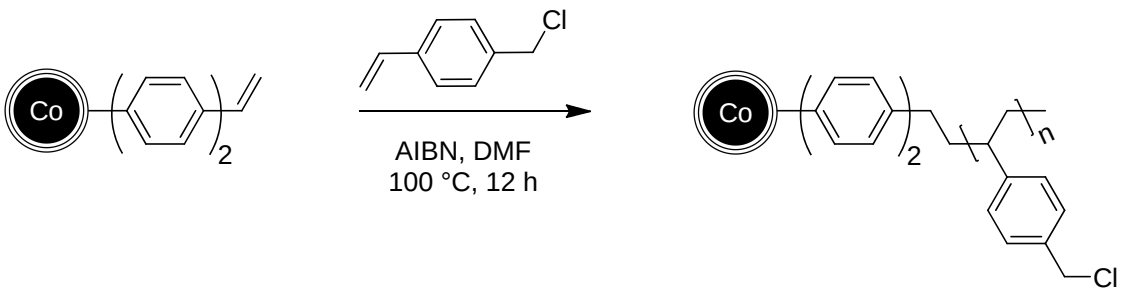

32 **37**

Scheme 10: Synthesis of 37 by radical polymerization of 4-vinylbenzylchloride at the surface of vinyl tagged magnetic particles 32.

Nitrogen adsorption at 77 K yielded a Brunauer-Emmet-Teller (BET) surface area of 1.7 m^2/g for 37. This value is lower than for the sole Co@C nanoparticles (20.5 m^2/g), which is caused by the formation of agglomerates. This feature was also evidenced by TEM measurements (Figure 13, pictures b-d).

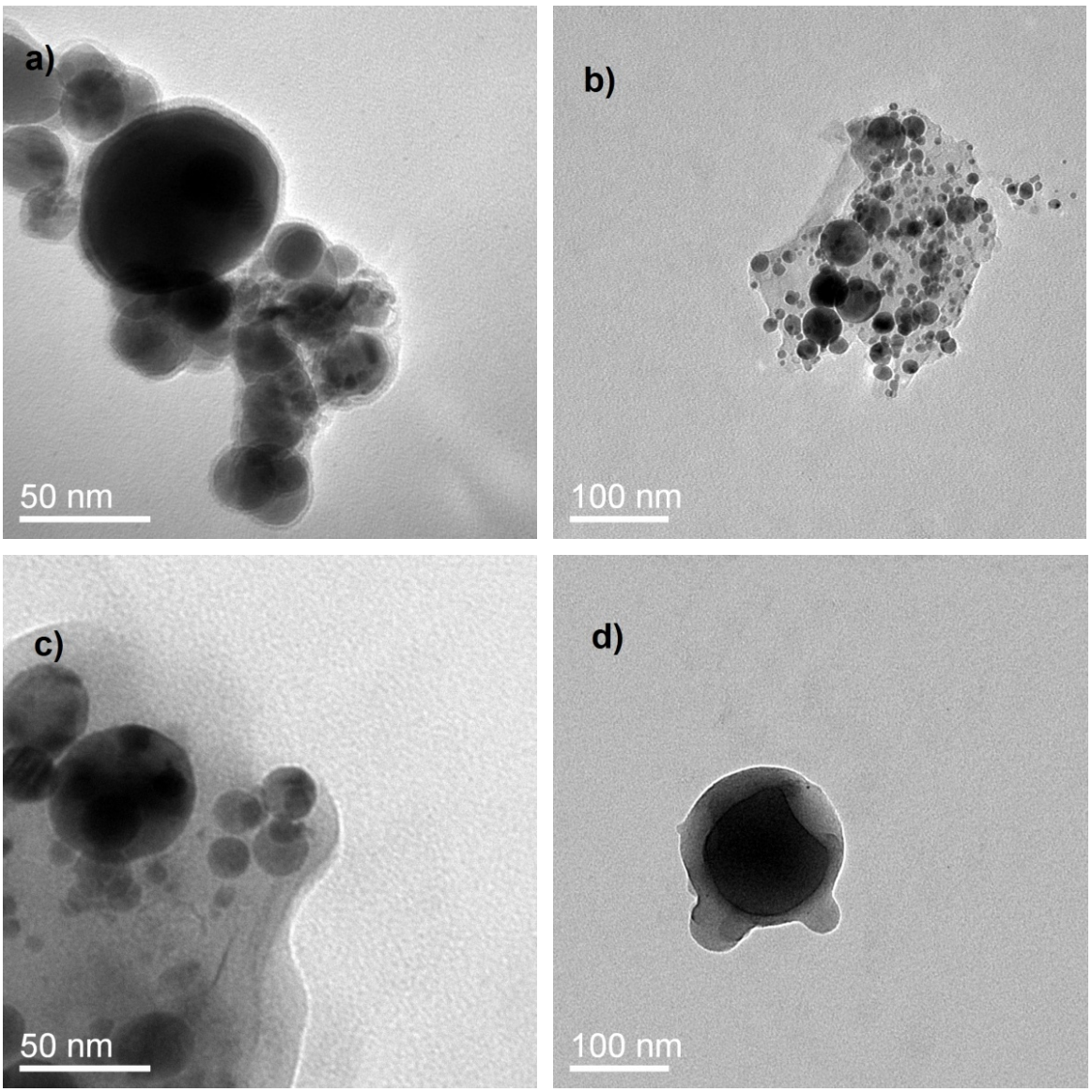

Figure 13: TEM Pictures of Co@C nanoparticles 24 (a) and polymer coated Co@C nanoparticles 37 (b-d). Reproduced with permission from reference [51b]. Copyright 2011 Wiley-VCH.

2.3 Noncovalent modification

Since the discovery of new carbon allotropes like CNTs[3] and fullerenes,[69] these materials have attracted attention for new applications like catalyst supports, optical devices and biomedical use, to name only a few.[70] The potentially high surface area of up to 3000 m^2/g predestines them as adsorbents.[71] Adsorption of substances by absorbents can be described by two aspects: the adsorption capacity and the affinity of the adsorbent. The capacity is limited by the surface area, while the affinity is dependent on the strength of attractive forces between adsorbate and adsorbent.[11] The Polanyi theory describes these two aspects for both gas and aqueous phase adsorption in the best way. The sum of attractive forces involving the adsorbate, solvent and adsorbent is responsible for the solute adsorption by sorbents such as CNTs and activated carbon. The surface of carbon coated nanoparticles has proven to be very similar to the aforementioned materials. Hence, it can be assumed that the Polanyi theory can be applied in this case as well. Five possible interactions have been observed in terms of adsorption on CNTs: hydrophobic effects, π-π bonds, hydrogen bonds and covalent and electrostatic interactions. Their overall contribution to the adsorption strength of organic molecules to CNTs depends on the properties of both partners.

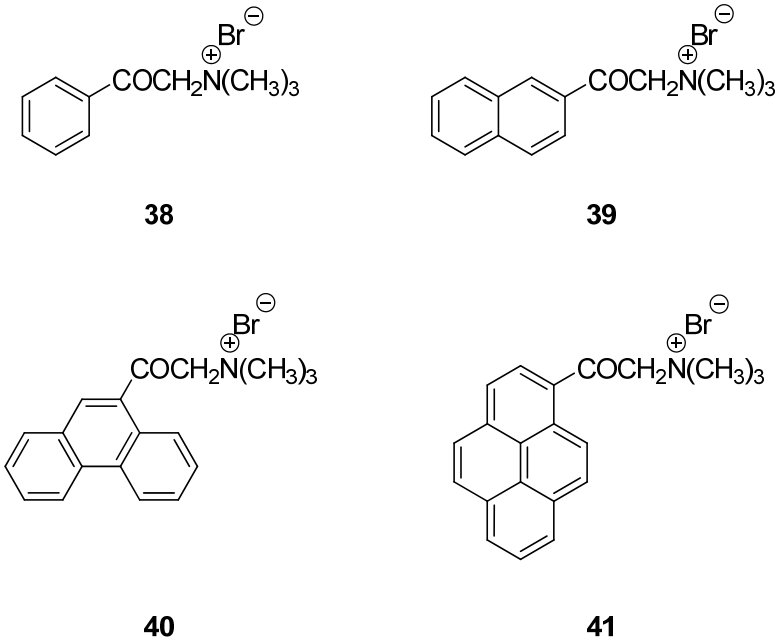

Figure 14: Differently substituted quaternary ammonium salts for the dispersion of CNTs in aqueous media.

Within the last years, many approaches were carried out to solubilize or disperse CNTs and graphene in aqueous solvent systems.[10b, 13, 72] Condensed aromatic derivatives functionalized with hydrophilic moieties have proven to be quite efficient for this task. Nakashima and coworkers used various quaternary ammonium salts fused to aromatic and polyaromatic moieties to disperse CNTs in water (Figure 14). [19d, 73] The ammonium amphiphiles carrying a phenyl or naphtyl group (38 and 39) were not able to disperse CNTs efficiently. However, phenantryl and pyrenyl groups (40 and 41) acted as good solubilizers.

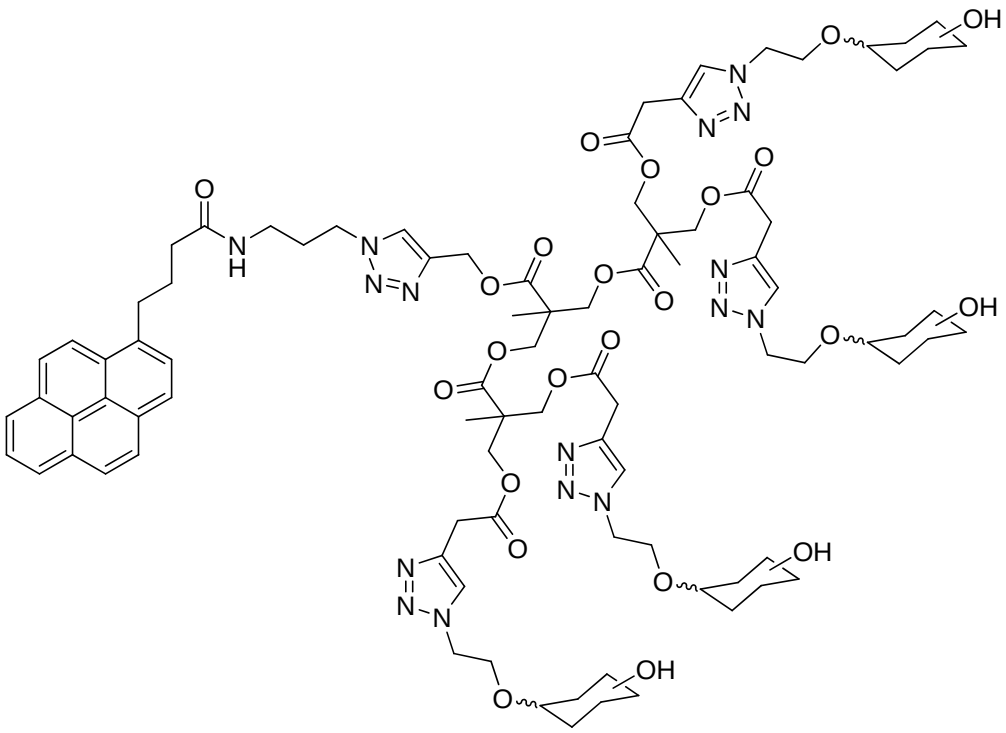

42

Figure 15: Second generation glycodendrimer used as a biocompatible coating to solubilize SWNTs for homogeneous biological applications.

Bertozzi et al. could demonstrate that 42 stabilizes SWNTs in aqueous media for periods longer than 3 months.[19f, 19g] The solubilized SWNTs could be applied as homogenous solution in various biological assays to determine their cytotoxicity. Thus, indicating that the noncovalent forces between the pyrene core and SWNTs are strong enough to fix also complex molecules to the carbon surface in aqueous media as well.

3. Noncovalent immobilization of catalysts on Co@C and Fe@C nanoparticles

3.1 Noncovalent immobilization of catalysts on Co@C nanoparticles

As already depicted in chapter A.I.1.2.5, Zhou and Wang demonstrated the ability of CNTs to act as efficient support materials for pyrene tagged catalysts. We envisioned that the Co@C particles 24 could bind pyrene units akin to CNTs to their surface in polar solvents and possibly release them at higher temperatures.[74] To test the feasibility of this catch-release concept, the nitrophenyl pyrene derivative 45 was synthesized (Scheme 11), allowing the facile quantification of the adsorption of 45 on Co@C nanoparticles by simply measuring the absorption of the nitrophenyl anion 47 after basic hydrolysis of 46 by UV/Vis measurements (Figure 16).

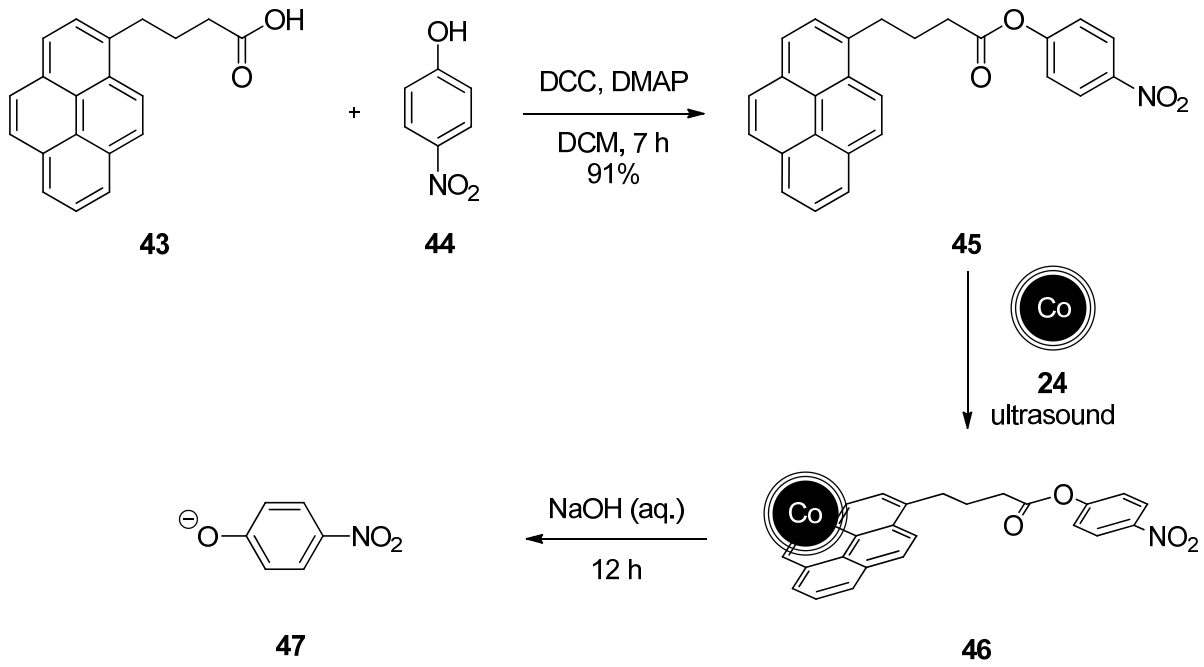

Scheme 11: Synthesis and hydrolysis of the immobilized nitrophenyl tagged pyrene derivative 45.

In order to immobilize 45 on the carbon coated Co@C nanobeads 24, an excess of 45 and the particles were dispersed in water by sonication (Scheme 11). After multiple washing steps with water the loading was assessed after basic hydrolysis (1M NaOH (aq.), 12 h) by means of UV/Vis spectroscopy.[75] Measurement of the concentration of 47 against a

likewise hydrolyzed standard solution of 45 gave a loading of 0.2 mmol/g, a value almost twice as high as obtained by covalent modification of the Co@C nanoparticles (Figure 16).[37]

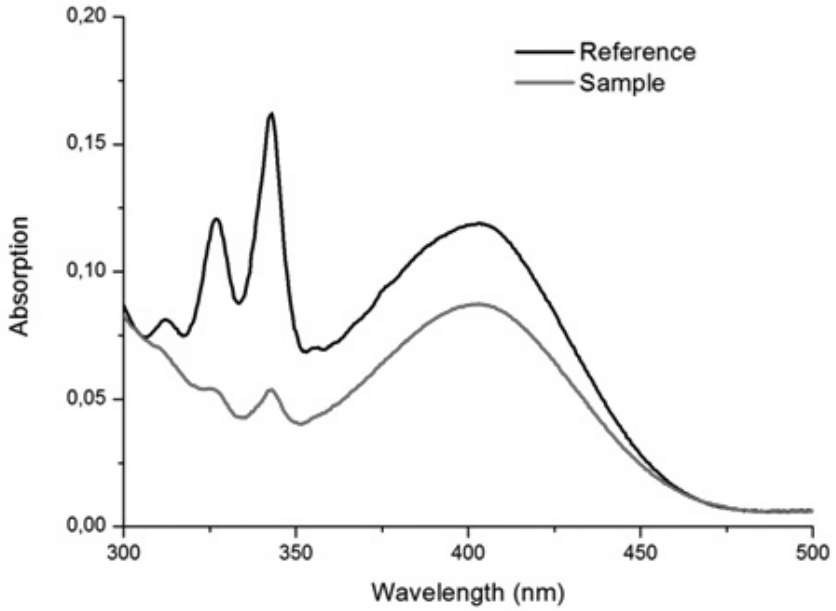

Figure 16: UV/Vis spectra of reference 45 after basic hydrolysis and nitrophenolate cleaved from 46 in water. Signals at 400 nm are assigned to the nitrophenolate. Signals below 350 nm correspond to the pyrene unit.

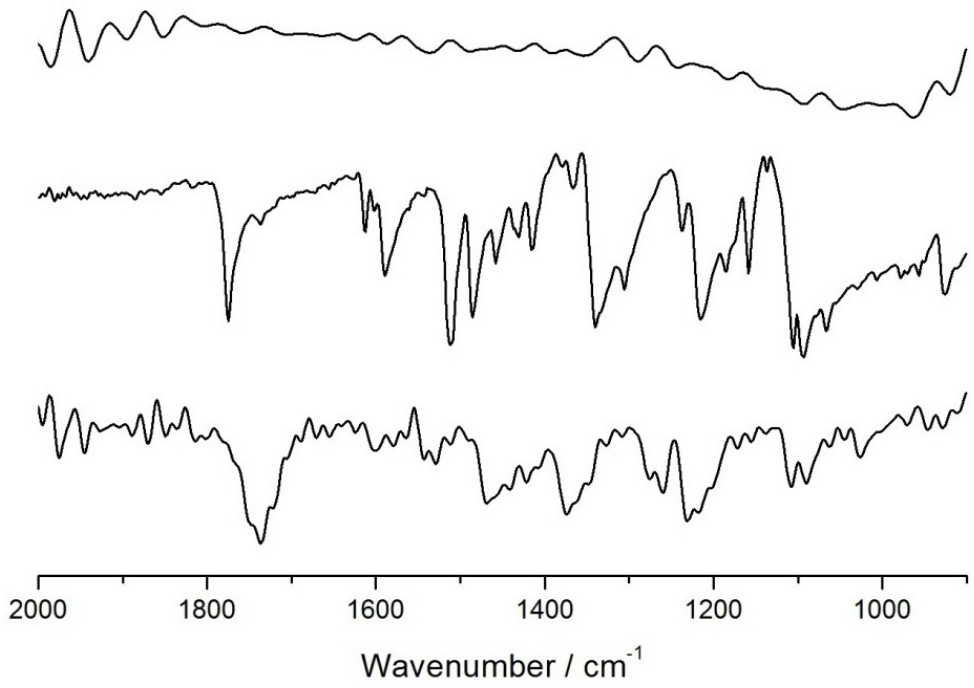

Figure 17: ATR-IR spectra of unfunctionalized particles 24 (top), 45 (center) and functionalized particles 46 (bottom).

The functionalization is also pursuable by means of IR spectroscopy (Figure 17). To estimate the desorption behavior of 45 from the surface of Co@C nanoparticles at elevated temperatures, the nanoparticles 46 were filtered through a sinter funnel with hot water which resulted in desorption of 49% of the nitrophenyl moieties (Figure 18, red curve). Alternatively, repeated magnetic decantation of an aqueous hot supernatant solution from the nanocomposite 46 was performed. The procedure resulted in desorption of 60% after four times and 76% after eight times (Figure 18, blue and green curve). The same treatment at ambient temperature caused no desorption.

These results show the strong temperature dependence of π-π stacking interactions between pyrene units and the aromatic graphene-like layers of the nanoparticles. Thus, the noncovalent immobilization of 45 is reversible under the appropriate reaction conditions.

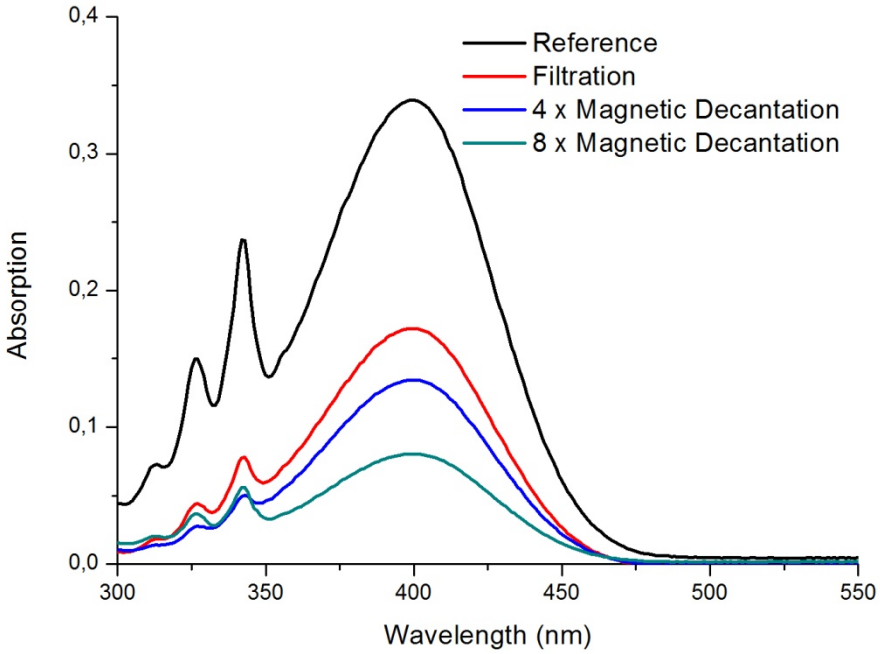

Figure 18: Desorption experiments by treating 46 with boiling water followed by filtration or repeated magnetic decantation.

3.2 Immobilization of an NHC-palladium catalyst on Co@C nanoparticles

Encouraged by the aforementioned results catalysts were searched which could be easily attached to pyrene moieties and that are sufficiently stable for catalysis in aqueous solutions.[76] Palladium complexes have received much interest as powerful catalysts in cross coupling reactions of aryl halides[77] with great industrial potential. One of the most stable ligand classes for this purpose are *N*-heterocyclic carbenes (NHCs).[78] Since the pioneering work of Döring,[79] Wanzlick[80] and Öfele,[81] carbenes have been recognized as a unique type of reactive species. Although NHCs have been stabilized as mercury complexes already by Wanzlick[82] in 1970, it took thirty years until the first free NHC was isolated. For a long time isolation of carbenes seemed to be impossible, until Arduengo et al.[83] showed the remarkable stability of the singlet carbene 48. With this discovery also in the field of catalysis a new interest in NHCs as ligands for transition metals raised. The first application of a NHC ligand in a catalytic reaction was performed by Herrmann using the catalyst 49 in crosscoupling reactions.[78, 84] Enders,[85] Grubbs[86] and others showed since then many applications of NHCs in catalysis.[87]

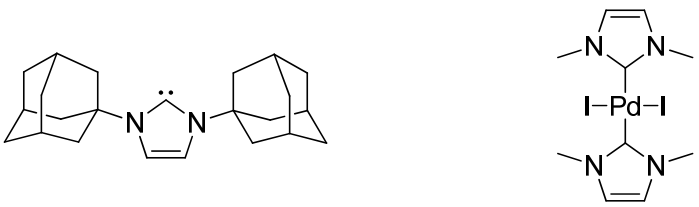

48 **49**

Figure 19: First isolated crystalline carbene 48 by Arduengo and the first NHC-Pd complex 49 used in catalysis by Herrmann.[78, 83-84]

NHCs like 48 are electronically and sterically stabilized, where the sterical shielding increases the lifetime of the carbene species. Nevertheless, the most important interactions for the stability of NHCs are orbital interactions of the empty p-orbital with the adjacent lone pairs of the nitrogen atoms. Therefore NHCs are electron rich species, in contrast to most other carbenes, and thus acting as nucleophiles. As a consequence, NHCs are neutral σ-donor ligands resulting in very strong NHC-metal bonds. From NMR studies it can be concluded that NHCs are more electron rich than most phosphines.[88]

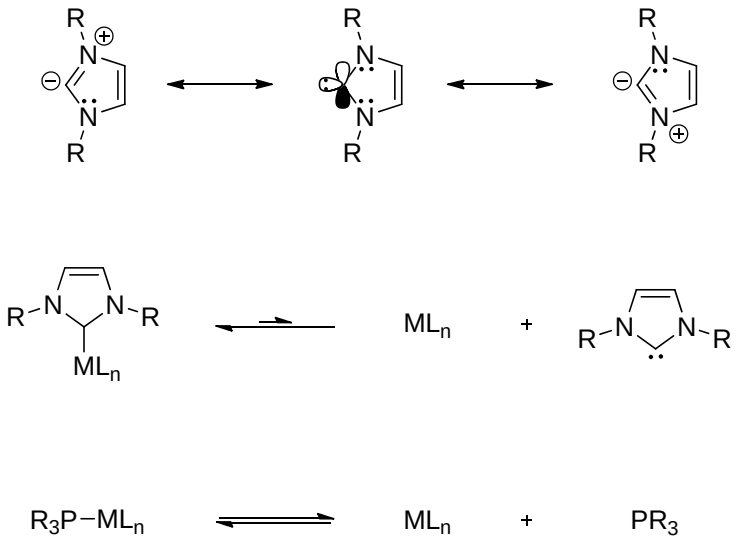

Scheme 12: Resonance structures of NHCs (top) and complex formation equilibriums of NHC (center) and phosphorus ligands (bottom).

Whereas NHCs are delicate species in their free form, their metal complexes exhibit an extraordinary stability. Compared to phosphines the complex stabilities are much higher, and thus the equilibrium is shifted almost completely to the metal complex side (Scheme 12). The low concentration of free carbene increases the thermal and chemical stability of the resulting complexes. This high stability of such species is especially beneficial for reactions performed in water at elevated temperatures.

One example for this kind of reaction is the palladium catalyzed hydroxycarbonylation[89] of aryl halides in aqueous media, giving rise to the corresponding carboxylic acids. This has proven to be a valuable tool in the synthesis of many biologically active compounds.[90] The mechanism involves the oxidative addition of a Pd(0) species to an aryl halide resulting in a Pd(II) complex (Scheme 13). Coordination of CO and migratory insertion leads to the formation of a Pd(II)-acyl complex, which is attacked by a nucleophile followed by reductive elimination to regenerate the Pd(0) species and the product. Besides the simple carboxylic acids, also esters can be synthesized by varying the nucleophiles.

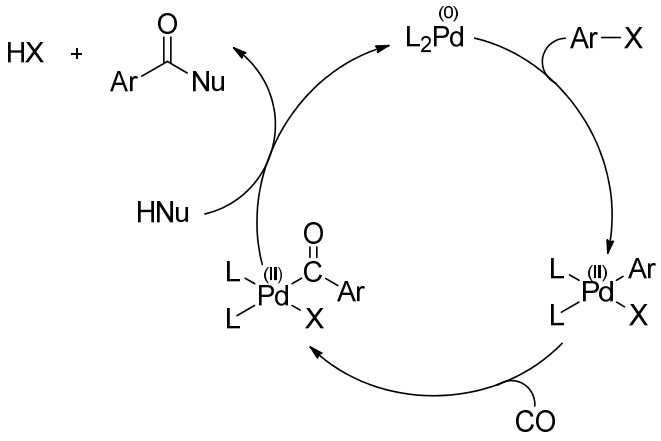

Scheme 13: Mechanism of the hydroxycarbonylation according to Yamamoto.[91]

In order to recycle the catalyst after the hydroxycarbonylation, a pyrene tagged NHC ligand was envisioned. Due to the fact that symmetrical NHC complexes are easily accessible and provide stronger π-π interactions by two pyrene moieties, the bis-pyrene tagged complex 19 was synthesized (Scheme 14). Starting from readily available 50, 1-methylimidazole 51 was fused to yield the imidazolium precursor 52 in excellent yield. Finally, 19 was synthesized by reaction with $Pd(OAc)_2$. 19 could be immobilized onto Co@C nanoparticles by sonication in water successfully (TEM micrographs in Figure 20).

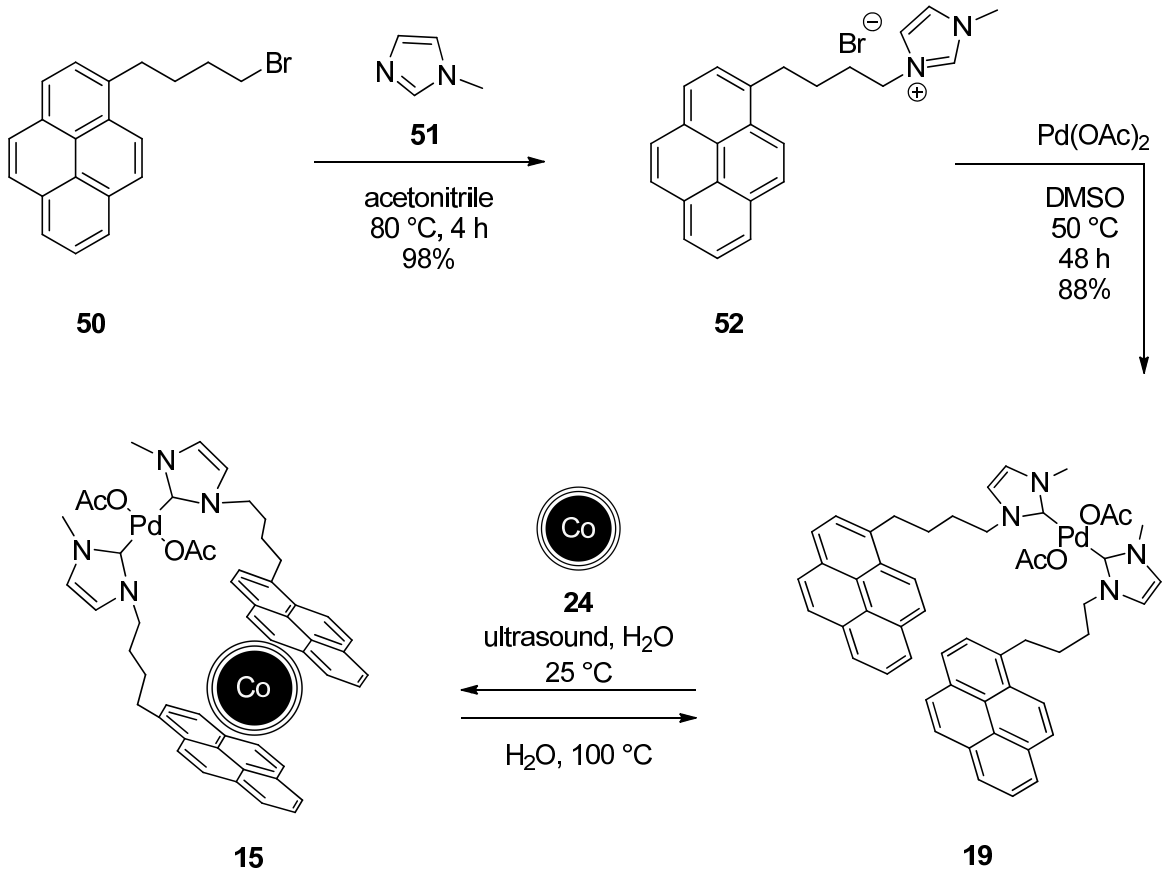

Scheme 14: Synthesis and immobilization of the pyrenyl tagged Pd-NHC catalyst 19.

The catalyst loading and desorption behavior of the nanocomposite 15 was determined by inductively coupled plasma atomic emission spectroscopy (ICP-OES) and was found to be consistent with the observations made by 45. In this way a loading of 0.1 mmol/g 19 could be achieved on Co@C nanobeads. After filtration of 15 with boiling water, 63% of 19 were desorbed from the nanobeads, indicating a partial desorption of the complex at elevated temperatures.

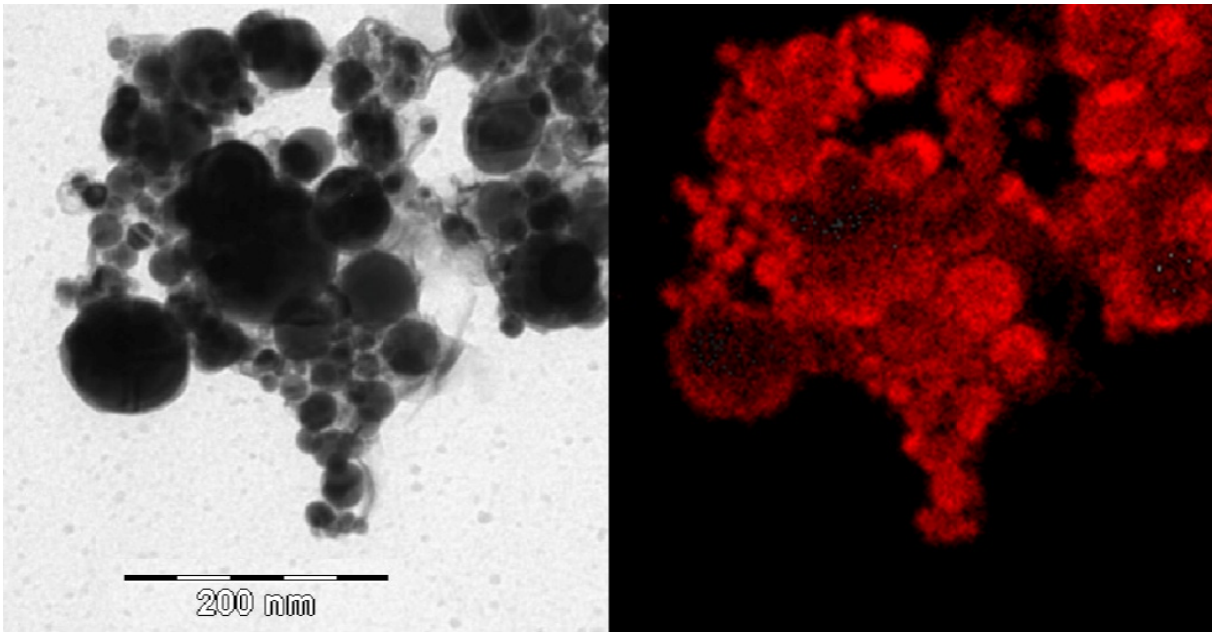

Figure 20: TEM pictures of 19 immobilized on Co@C nanoparticles (left) and Co atom mapping by EELS-TEM (electron energy loss spectroscopy) (right).

The palladium-NHC complex 19 immobilized on Co@C nanoparticles proved to be an effective catalyst for the hydroxycarbonylation of aryl halides with carbon monoxide in water at 100 °C (Table 2). In total 16 consecutive reactions with six different substrates were carried out. Due to the highly magnetic character of the nanobeads, each recycling step of the catalyst via magnetic decantation was very efficient (Figure 21).

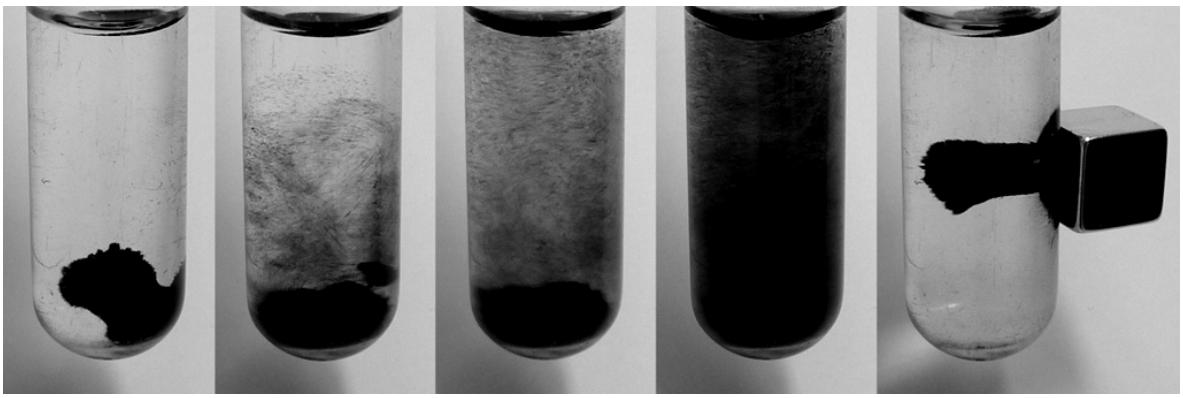

Figure 21: 19 on Co@C nanoparticles at different stages of dispersion and simple recovery by applying an external magnet (right).

Ten consecutive runs were performed with the model reaction depicted in Table 2. The leaching of palladium into the product was negligible according to ICP-OES measurements

(0.7 ppm). Additional determination of the particle loading before and after the first run showed a distinct drop from 0.1 mmol/g to 0.08 mmol/g. This is most probably attributable to residual non-immobilized compounds arising from the catalyst preparation. Nevertheless, the loading remained almost constant in the next nine runs, resulting in a loading of 0.07 mmol/g after the 10th run. The excellent performance of the recycled composite is in accordance with these findings. Only after the seventh run a prolonged reaction time was necessary to ensure complete conversion of the starting material (Table 2, entries 8-10).

Table 2: Recycling experiments of the hydroxycarbonylation of 4-iodophenol with CO in water using the immobilized catalyst 15.[a]

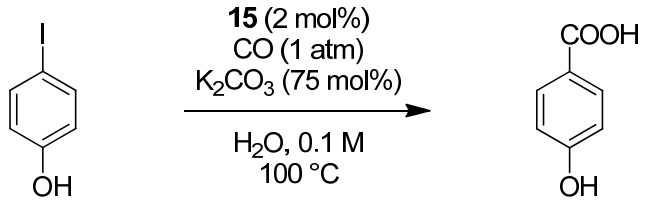

53 **54**

entry	run	time / h	yield / %[b]
1	1	10	95
2	2	10	94
3	3	10	87
4	4	10	93
5	5	10	92
6	6	10	94
7	7	10	90
8	8	14	93
9	9	14	93
10	10	14	91

[a] 4-Iodophenol (0.5 mmol) in Millipore water (5 mL), K_2CO_3 (0.375 mmol), catalyst 15 (2.0 mol%), CO (1 atm), 100 °C. [b] Yields of isolated products.

TEM micrographs recorded before and after the reactions gave further hint that no undesired palladium nanoparticles were formed (Figure 22). Thus, indicating that the palladium-NHC complexes are stable under the reaction conditions in multiple recycling steps.

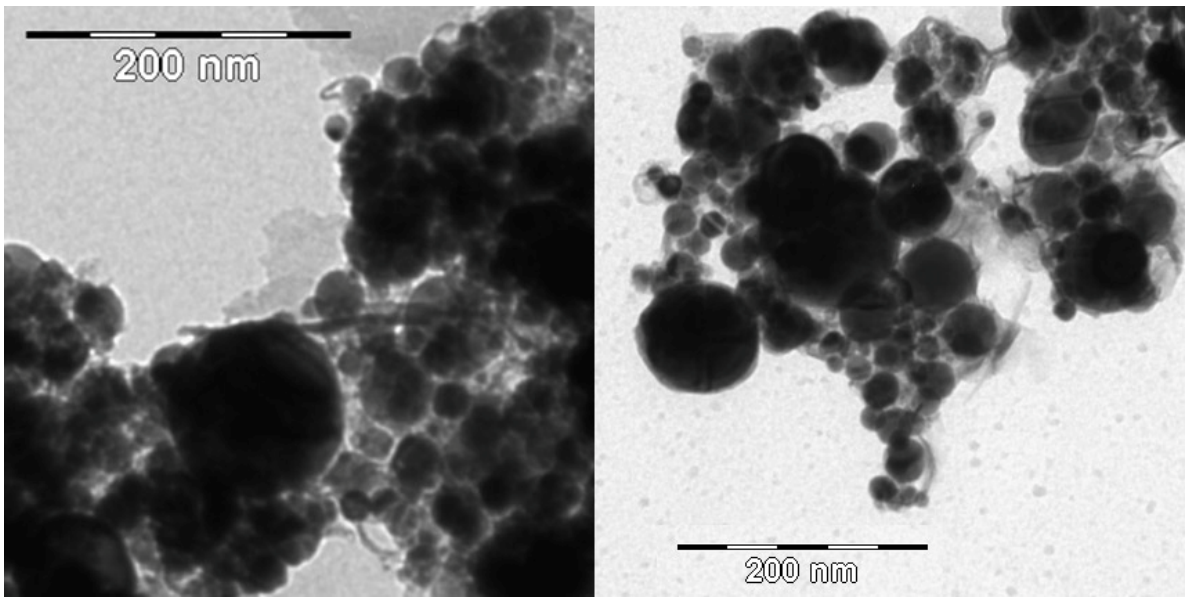

Figure 22: TEM-images of Co/C-nanoparticle grafted palladium-complex 15 before (left) and after five catalytic cycles (right).

After the first ten recycling runs the nanobeads were still highly active and were used in the hydroxycarbonylation of different substrates (Table 3). In six further runs aryl iodides and also aryl bromides were converted to the corresponding benzoic acids. After the last run the catalyst grafted on Co@C nanoparticles was removed from the vessel. The empty vessel failed to catalyze the hydroxycarbonylation of 53, which proves that the catalyst was only immobilized on the graphene like coated particles.

Table 3: Hydroxycarbonylation of different aryl halides with CO in water using the immobilized catalyst 15.[a]

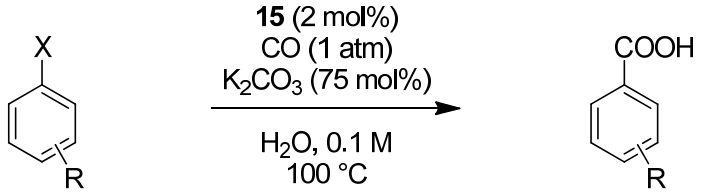

54a: R = 4-OH
54b: R = 4-COOH
54c: R = 3,5-Me 4-OH
54d: R = 3-COOH 4-OH

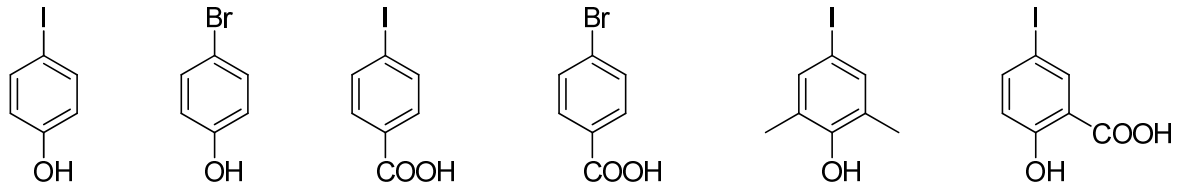

53 **55** **56** **57** **58** **59**

entry	run	aryl halide	time / h	yield / %[b]
1	11	55	20	81
2	12	56	20	89
3	13	57	36	86
4	14	58	24	79
5	15	59	36	75
6	16	53	16	88
7[c]	-	53	48	< 1

[a] Aryl halide (0.5 mmol) in Millipore water (5 mL), K_2CO_3 (0.375 mmol), catalyst 15 (2.0 mol%), CO (1 atm), 100 °C. [b] Yields of isolated products. [c] Catalyst 15 was removed from the reaction vessel prior to the addition of 53.

In conclusion, a method for the reversible immobilization of the pyrene-tagged palladium catalyst 19 on highly magnetic Co@C nanoparticles by π-π stacking interactions was developed. This grafting proved to be temperature dependent on polar solvents like water, giving rise to a catch and release system where the catalyst dissociates from the heterogeneous support into the homogeneous phase at elevated temperatures. The

palladium catalyst 19 was highly active in more than 16 iterative runs and could be recycled as Co@C-nanoparticle-immobilized catalyst 15 by magnetic decantation.

3.3 Immobilization of a proline catalyst on Co@C and Fe@C Nanoparticles

Asymmetric enamine catalysis has gained considerable attention in the last years.[92] Especially proline, one of the most efficient catalysts out of the chiral pool, has faced tremendous effort to improve its catalytic abilities. Although the bifunctional activation mode resembles enzyme type I aldolase,[93] which works in an aqueous environment, proline shows no selectivity for aldol reactions in water.[94] In contrast, there are numerous examples for aldol reactions catalyzed by proline in polar organic solvents like DMSO[95] or DMF.[96] In terms of green chemistry, it is highly desirable to develop recyclable organocatalysts[97] such as proline or derivatives thereof, which exhibit high activity also in environmentally benign solvents like water.

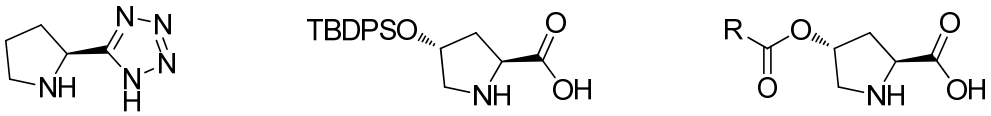

60 **61** **62**

Figure 23: Catalysts for aldol reactions in or in the presence of water.

Yamamoto[98], Hayashi[99] and Noto[100] to name only few have recently developed highly active and selective catalysts for aldol reactions in or in the presence of water (Figure 23). Most of these catalysts have one significant moiety in common - at least one large apolar group attached to the proline backbone.

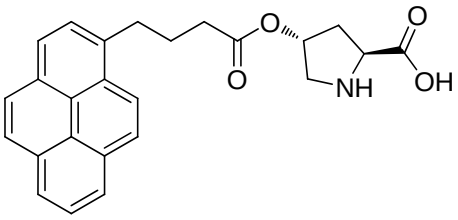

62a

Figure 24: A pyrene tagged proline catalyst used for asymmetric aldol reactions in aqueous media.

In 2008 Noto et al. have shown that 62a catalyzes the asymmetric aldol reaction between cyclic ketones and aromatic aldehydes with excellent activity and selectivity.[100] In order to recycle the catalyst 62a it was envisioned to utilize π-π-interactions between the pyrene scaffold of the organocatalyst and the aromatic surface of metal nanoparticles coated with several graphene shells. Since π–π-interactions are in an aqueous environment sufficiently strong to force pyrene moieties onto aromatic surfaces, catalyst 62a seems to be suitable for immobilization on carbon coated nanoparticles, which makes it amenable to recycling *via* simple magnetic decantation. Moreover, this noncovalent immobilization method offers the possibility to recycle also the nanoparticle support by desorption of the aged catalyst after a few cycles.

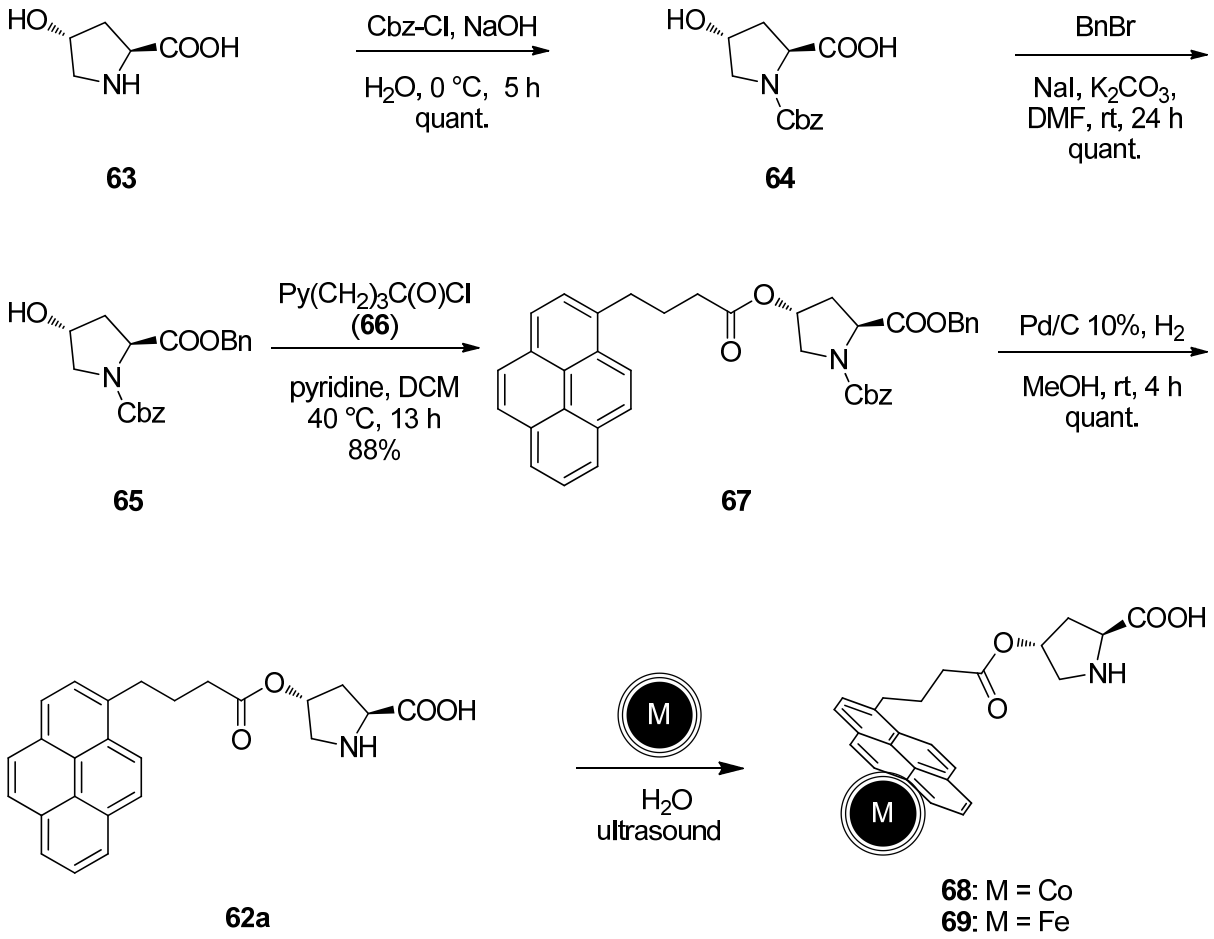

Scheme 15: Synthesis and immobilization of 62a on magnetic Co@C and Fe@C nanoparticles.

Starting from L-*trans*-4-hydroxyproline 63, Cbz and benzyl protection furnished 65 in excellent yield. Subsequent reaction with 66 followed by removal of the protecting groups with Pd/C gave 62a in good yields. To immobilize 62a on Co@C nanobeads 24, the catalyst

was sonicated with an appropriate amount of nanobeads in water for 1 h. After thoroughly washing several times with water and ethyl acetate the beads were isolated and dried under vacuum. IR spectroscopy and elemental microanalysis proved that 0.32 mmol/g of 62a was immobilized on the particles. The same procedure furnished 0.08 mmol/g for the Fe@C particles 27.

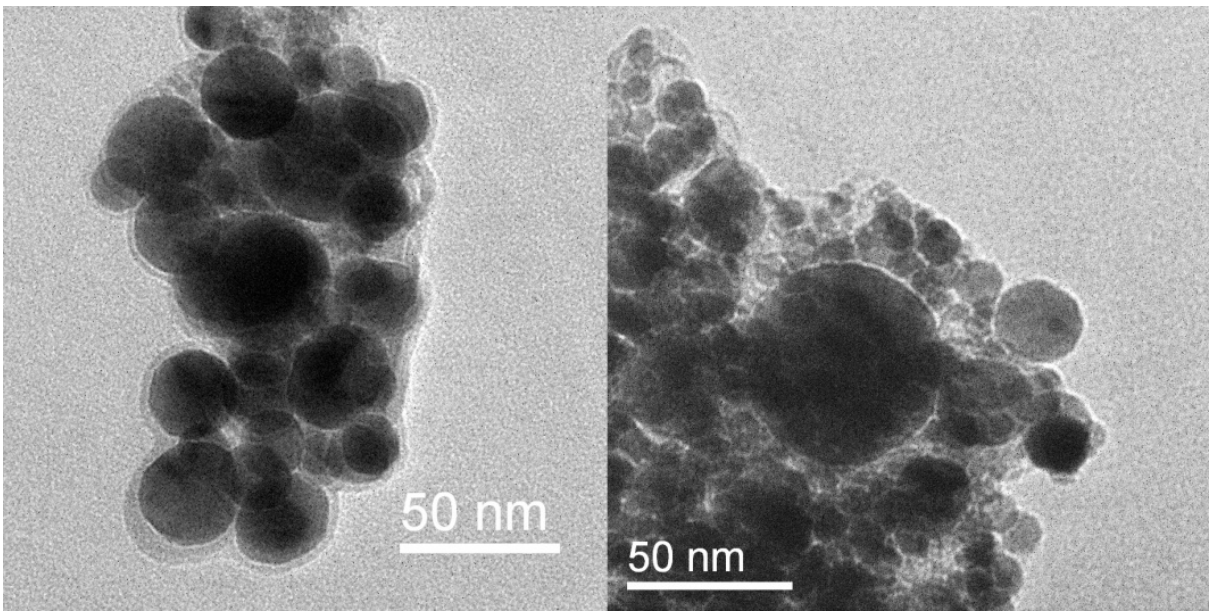

Figure 25: TEM images of 62a immobilized on magnetic Co@C (left) and Fe@C particles (right).

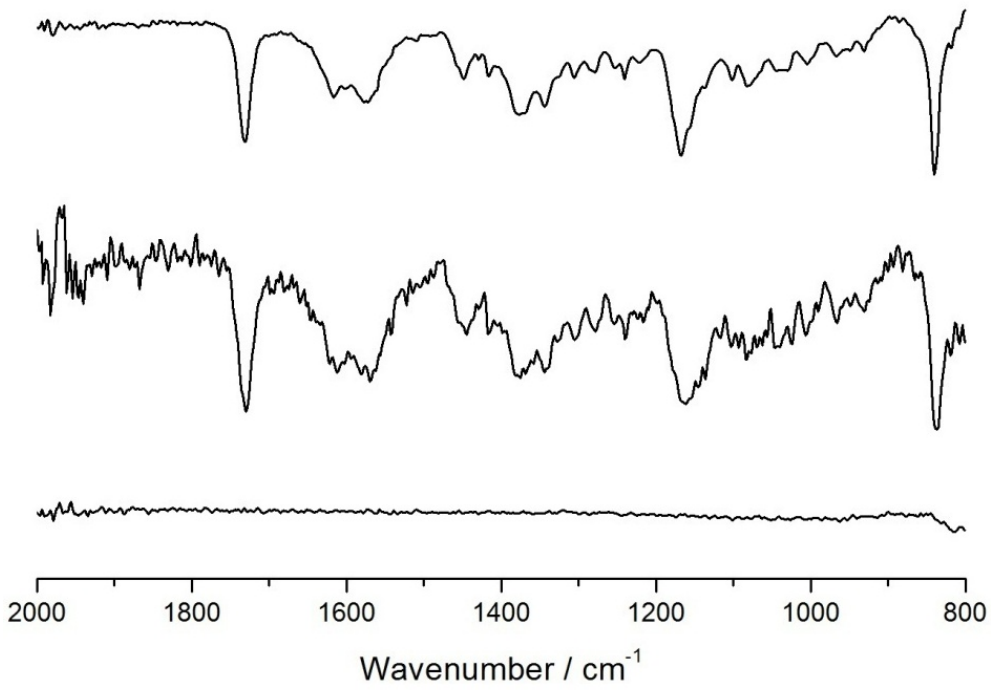

Figure 26: ATR-IR spectra of unfunctionalized particles 24 (bottom), 62a (top) and functionalized particles 68 (center).

The first attempts to use the catalyst 68 in aldol reactions with the initial conditions of Noto et al. failed. Even higher temperatures and different solvents did not have an impact on the reaction rates (Table 4). Only when coordinating additives like ethylenediaminetetraacetic acid (Titriplex III) were added to the solution, the reaction proceeded smoothly with excellent conversion and selectivity (Table 6).

Table 4: First attempts to catalyze an aldol reaction with the immobilized catalyst 6.

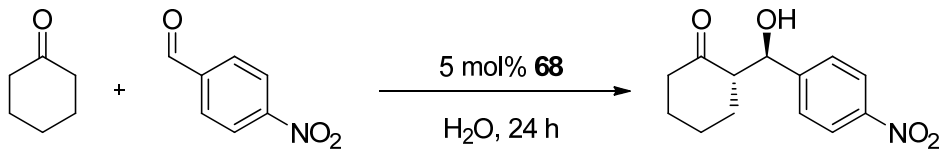

70 **71** **72**

entry	temperature / °C	conversion[a,b] / %	*anti*/*syn*[b]
1	rt	3	6/1
2	50	6	2/1

[a] Combined conversion for *anti*-72 and *syn*-72. [b] Determined by ^{1}H-NMR of the crude product.

This behavior could possibly be explained by the coordination of cobalt ions by proline, which has precedents in literature.[101] The cobalt ions are most likely artifacts of the particle synthesis, resulting from not completely coated particles and leaching from the metal core. Adding a strong chelating agent like EDTA to the reaction mixture renders the active proline catalyst. It is known that amino acids form 1:2 complexes with metal(II) ions (Scheme 16). In analogy one could propose that cobalt ions were coordinating to proline molecules, influencing the performance of the catalyst 68.

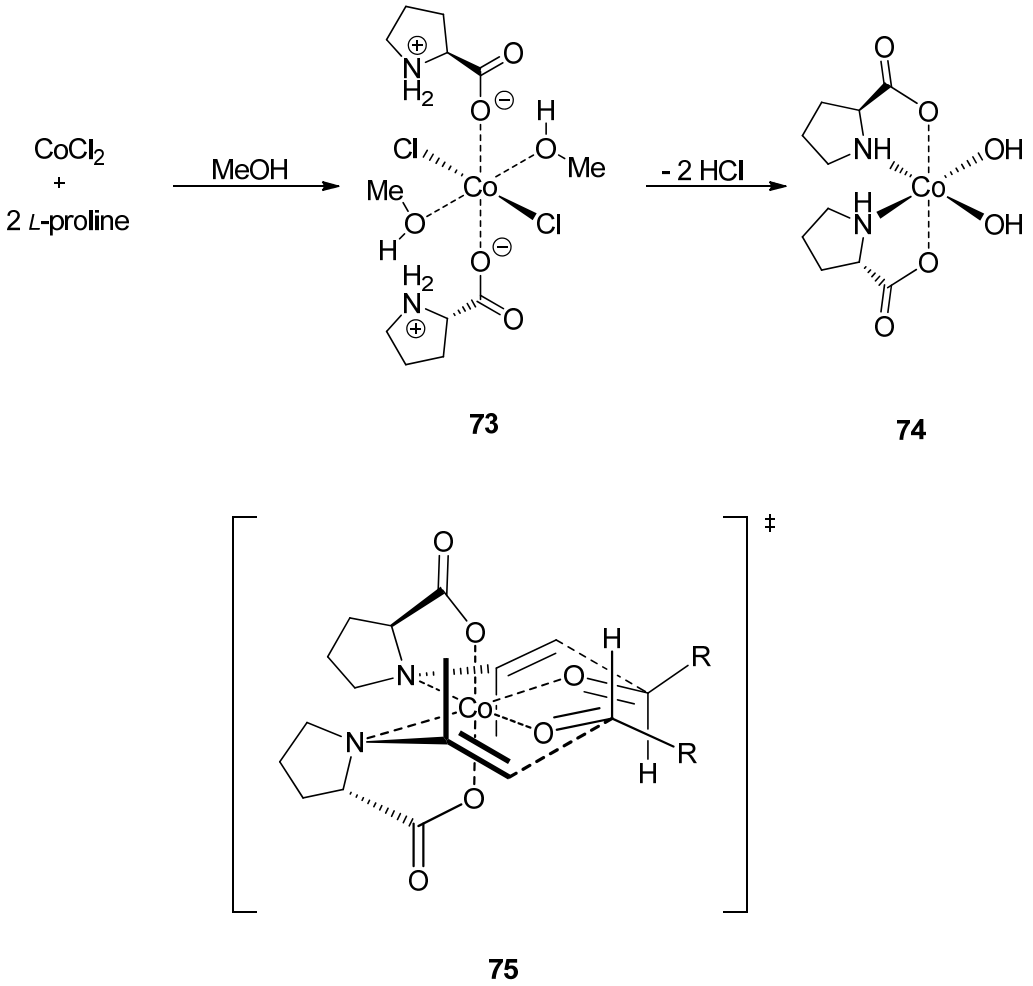

Scheme 16: Formation of the C_2-symmetrical cobalt proline complex 74 and the proposed transition state 75 in the asymmetric aldol reaction.

In order to test this hypothesis we performed a series of aldol reactions catalyzed by *L*-proline with varying amounts of $CoCl_2$ (Table 5). With increasing $CoCl_2$/proline ratio the yield drops dramatically. A fivefold excess of $CoCl_2$ causes a complete shutdown of the reaction (Table 5, entry 9). Surprisingly, at a $CoCl_2$/proline ratio of 1:2 the diastereo- and enantioselectivity as well as the yield reaches excellent values, even better then proline itself. The catalytically active species was assumed to be the C_2-symmetrical cobalt-proline complex 74 (Scheme 16). These results were utilized by Karmakar in various aldol reactions catalyzed by a 1:2 complex of $CoCl_2$/proline with excellent results.[102]

Table 5: Results of the $CoCl_2$/proline ratio screening in the aldol reaction of 70 and 71 using 20 mol% L-proline.[a]

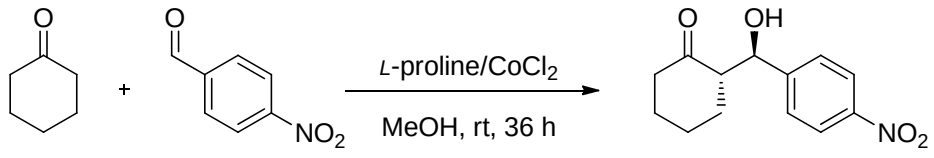

70 **71** **72**

entry	$CoCl_2$ / L-proline	yield / %[b]	*anti* / *syn*[c]	*ee* / %[d]
1	proline only	89	3:1	58
2	1:4	92	5:1	89
3	1:2	91	10:1	98
4[e]	1:2	53	10:1	96
5	1:1	78	5:1	92
6	1.5:1	71	3:1	88
7	2:1	59	2:1	86
8	2.5:1	41	1:1	74
9	5:1	< 10	-	-

[a] Results from reference.[102] Reaction conditions: Aldehyde 71 (0.85 mmol), ketone 70 (2.5 mmol), L-proline (0.17 mmol, 20 mol%), $CoCl_2$, MeOH (0.09 mL), 25 °C, 36 h. [b] Combined isolated yield of *anti*-72 and *syn*-72. [c] Determined by ^{1}H-NMR of the crude product. [d] Determined by HPLC using a chiral stationary phase. [e] 10 mol% of L-proline were used.

Nevertheless, also reactions with the cobalt nanoparticle supported catalyst 68 in the presence of EDTA were performed. Under these conditions the aldol reaction between cyclohexanone and 4-nitro-benzaldehyde proceeded smoothly within 24 h. Up to four iterative runs could be performed and selectivity remained high during all runs, although levels decreased in the fourth run (Table 6). The crude NMR of the product showed no traces of the catalyst during all the runs.

Table 6: Results of the catalysis with 68 + EDTA.[a]

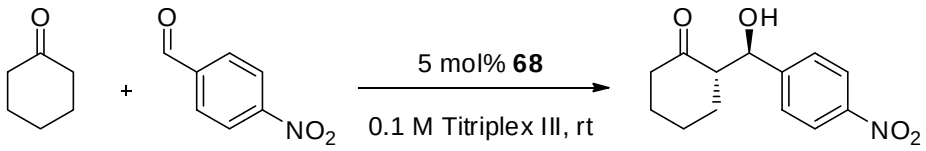

70 **71** **72**

run	conversion[b] / %	*anti* / *syn*[b]	*ee*[c] / %
1	> 95	23/1	97
2	> 95	29/1	99
3	> 95	26/1	99
4	84	22/1	99

[a] Reaction conditions: Cyclohexanone 70 (260 µL, 2.5 mmol), aldehyde 71 (75.5 mg, 0.5 mmol), 0.1 M Titriplex III solution (175 µL), 25 °C, 24 h. [b] Determined by ^{1}H-NMR of the crude product. [c] Determined by HPLC using a chiral stationary phase.

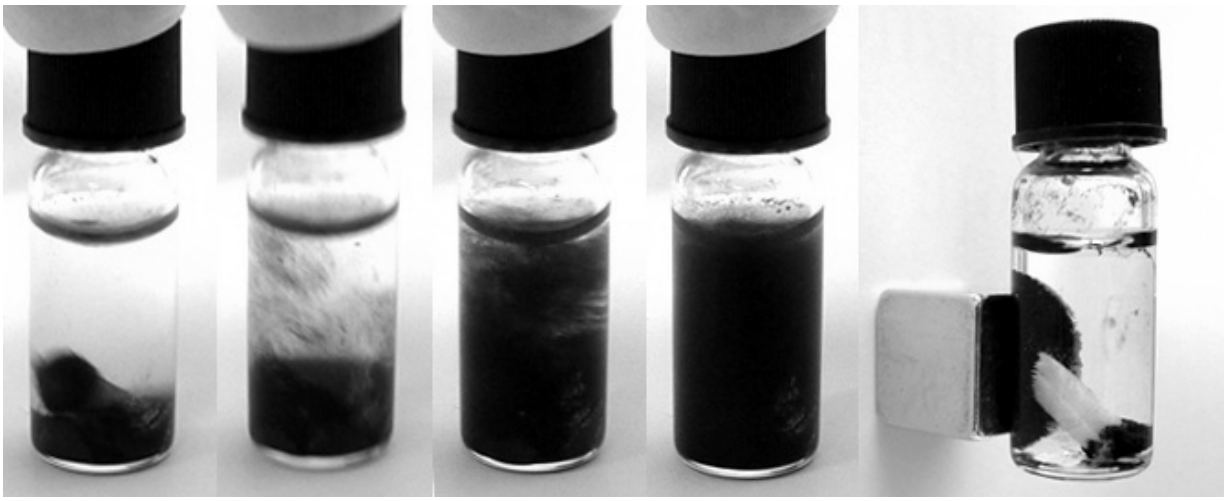

Figure 27: Nanobeads 68 at different stages of dispersion (left) and simple workup *via* magnetic decantation (right).

To avoid the use of an EDTA solution, we assumed that Fe@C particles would lead to a reduced leaching and less interfering iron ions. Indeed, by performing the same reaction as depicted in Table 7 (Entry 1-4) catalyst 69 led to excellent conversion and good selectivity, albeit somewhat inferior results when compared to 68 (Table 6).

Table 7: Results of the catalysis with 69 (without EDTA entry 1-4, with EDTA entry 5-8).

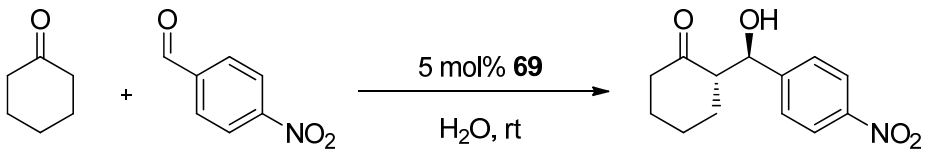

70 **71** **72**

entry	run	conversion[c] / %	*anti* / *syn*[c]	*ee*[d] / %
1[a]	1	> 95	19/1	98
2[a]	2	> 95	19/1	99
3[a]	3	50	14/1	96
4[a]	4	23	12/1	nd
5[b]	1	> 95	23/1	98
6[b]	2	> 95	25/1	99
7[b]	3	94	24/1	94
8[b]	4	19	16/1	nd

[a] Reaction conditions: Cyclohexanone 70 (2.5 mmol), aldehyde 71 (0.5 mmol), H_2O, 25 °C, 24 h. [b] 0.1 M Titriplex III solution as additive. [c] Determined by ^{1}H-NMR of the crude product. [d] Determined by HPLC using a chiral stationary phase.

Conventional polymeric supports like polystyrene or MeOPEG can only be used until the catalytic system is not active anymore.[1d, 103] One advantage of a noncovalent immobilization is the possibility to replace the aged catalyst after four runs with fresh catalyst 62a. Simple washing with hot methanol allows removing the aged catalyst from the surface of the nanobeads and opens the way for subsequent immobilization of a new catalyst batch. This renewed system showed the same activity in four runs as its antecessor (Table 8, Run 5-8).

Table 8: Results of the catalysis with the recycled support 4@Co@C + EDTA.[a]

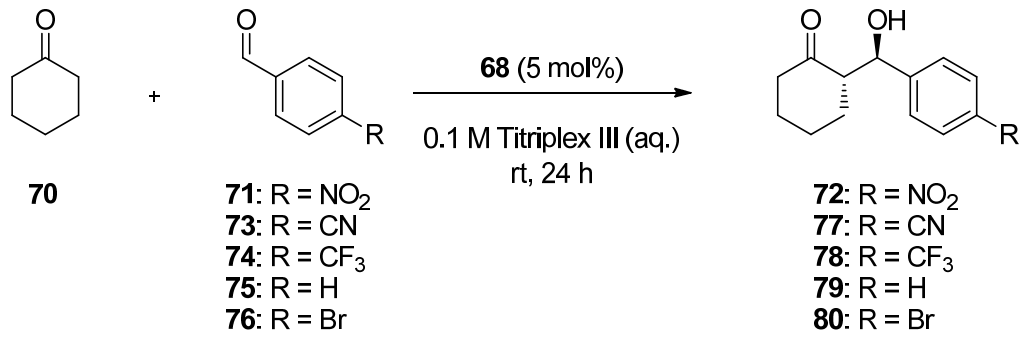

70

71: R = NO_2
73: R = CN
74: R = CF_3
75: R = H
76: R = Br

72: R = NO_2
77: R = CN
78: R = CF_3
79: R = H
80: R = Br

run	aldehyde	conversion[b] / %	*anti*/*syn*[b]	*ee*[c] / %
1	71	> 95	23/1	97
2	71	> 95	29/1	99
3	71	> 95	26/1	99
4	71	84	22/1	99
5	71	> 95	26/1	99
6	71	> 95	25/1	99
7	71	> 95	26/1	99
8	71	79	23/1	99
9	73	> 95	26/1	99
10	74	> 95	15/1	97
11	75	> 95	14/1	89
12	76	93	22/1	91

[a] Reaction conditions: Cyclohexanone 70 (2.5 mmol), aldehyde (0.5 mmol), 0.1 M Titriplex III solution, 25 °C, 24 h. [b] Determined by ^{1}HNMR of the crude product. [c] Determined by HPLC using a chiral stationary phase.

68 was also employed, after a second ´revitalization´, in the aldol reaction of cyclohexanone with a variety of benzaldehydes. As in the first eight runs, the system showed good conversion and selectivities (Table 8, run 9-12).

In conclusion, a new method for the reversible immobilization of the pyrene tagged organocatalyst 62a was developed. The reaction has been performed in a 0.1 M Tritriplex III solution due to the disturbing influence of metal-(II) ions leaching from the nanoparticle core. The catalyst was reusable in the asymmetric aldol reaction of cyclic ketones with aromatic aldehydes for three times without significant loss in activity or selectivity. Moreover, after four cycles the catalyst loading could be renewed without affecting the performance in the next runs. In addition, the 1:2 complex of *L*-proline and $CoCl_2$ proved to be an effective catalyst for aldol reactions. Compared to proline itself the system performed significantly better.

4. Catalysts immobilized on polymer coated magnetic nanoparticles

4.1 A palladium NHC-pincer complex for covalent immobilization

Pincer type ligands appear as a particularly attractive type of complexes for the immobilization of catalysts. Their high stability as a consequence of the chelating effect predestines them for multiple recycling runs. Palladium NHC-pincer complexes in particular exhibit extreme stability against heat, moisture and air.[84c, 104] It was already demonstrated by Luo[105] and Kühn[106] that Pd-pincer complexes like 91 can be immobilized onto polymeric supports bearing benzyl bromide groups in the backbone (Scheme 17). The resulting polymer supported complex 92 was used in the Suzuki-Miyaura cross coupling reaction between aryl bromides and phenylboronic acid 94 where yields ranged from 15 - 66% after 24 h and TOFs from 150 – 530 h^{-1}.

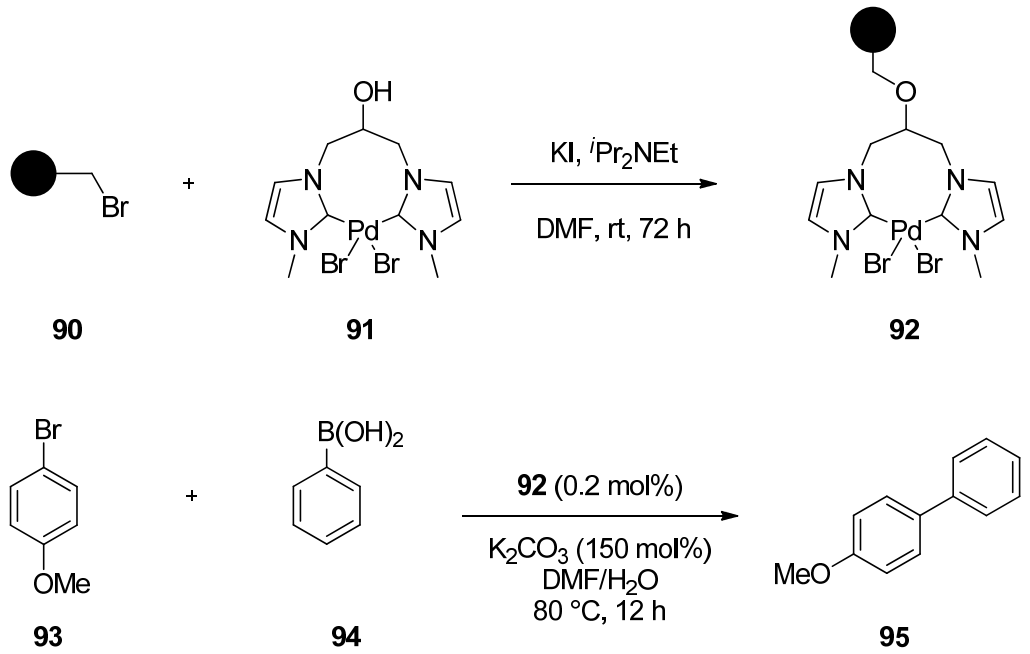

Scheme 17: Immobilization of the Pd-NHC-pincer complex 91 onto a polymeric support by a nucleophilic substitution reaction (top) and Suzuki-Miyaura cross coupling with the polymer supported catalyst 92 (bottom).

In cooperation with the CNRS Toulouse, nanoparticles and dendrimers as two types of globular supports were compared. As a widely applicable anchoring group for dendrimer- and nanoparticle- functionalization, a phenol moiety was chosen. The synthesis of the Pd

NHC-pincer complex 100 starts with a nucleophilic substitution on readily available 96 with the imidazole 97 (Scheme 18). The double imidazolium salt 98 was further converted to the isolable silver complex 99.[107]

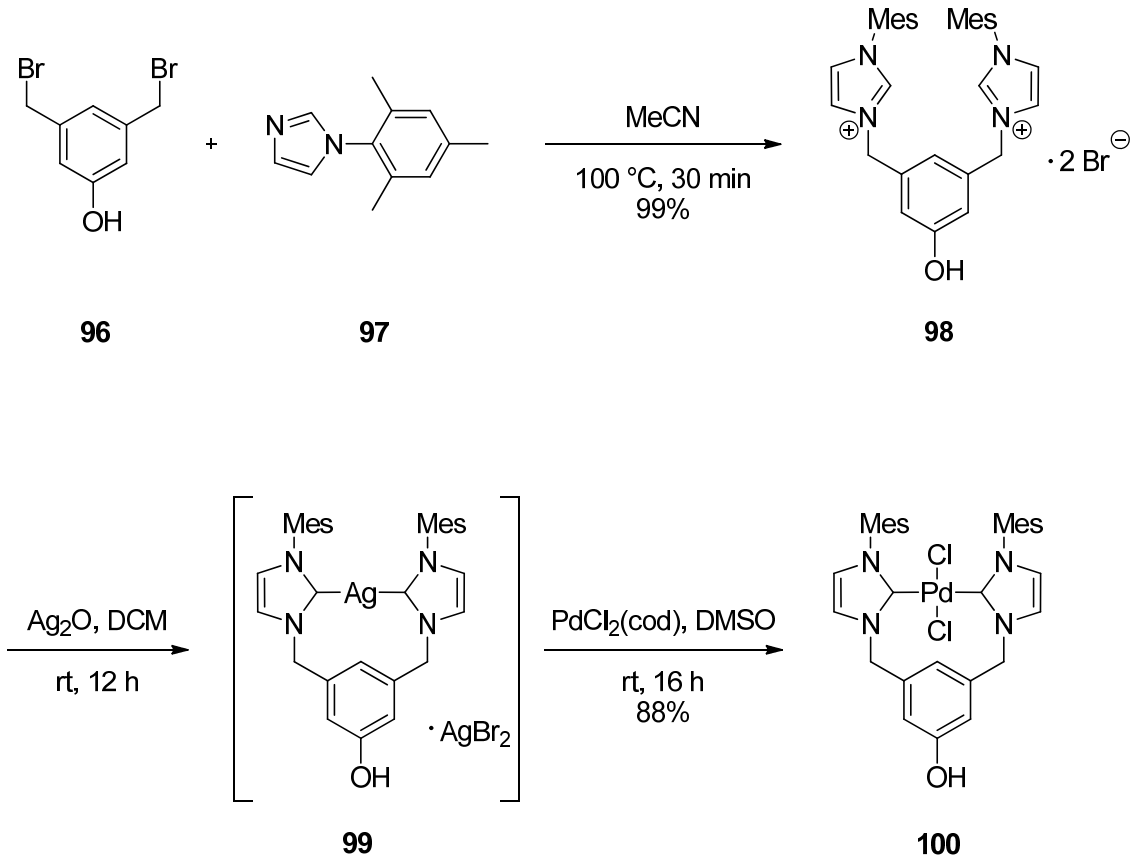

Scheme 18: Synthesis of the palladium pincer NHC complex for covalent immobilization onto the polymer coated particles 101.

In situ transmetallation of 99 with $PdCl_2$(cod) provided the desired pincer Pd-NHC complex 100 in good yield. The 1-methyl imidazole substituted complexes could not be synthesized in this reaction sequence because of the extreme poor solubility of the corresponding methyl substituted Pd-NHC complex.[108] 100 gave in the ^{1}H-NMR spectra only very broad signals, therefore it was not possible to obtain a convincing ^{13}C-NMR spectrum. Attempting to resolve the peaks that correspond to different isomers, the complex was heated to 80°C during the NMR measurement, but only little or no change in the spectra could be observed. This indicates that the broadening does not arise from restricted rotation around bonds within the molecule, but is probably due to either rapid *cis*/*trans* isomerisation, or a dynamic 'ring flip' in which the aromatic ring may interchange between different

configurations (Figure 28). A behavior like this was already shown to complicate the NMR analysis of bridged Pd-NHC complexes.[109] All conditions applied in order to obtain crystals of 100 suitable for X-ray crystallography resulted in amorphous platelets. Crystallization of the precursor 98 caused no problems (Figure 29).

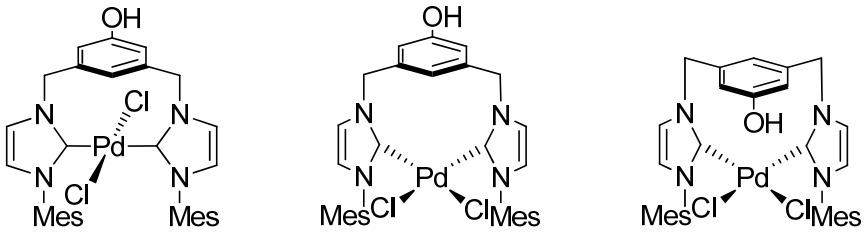

Figure 28: Three possible conformations of complex 100.

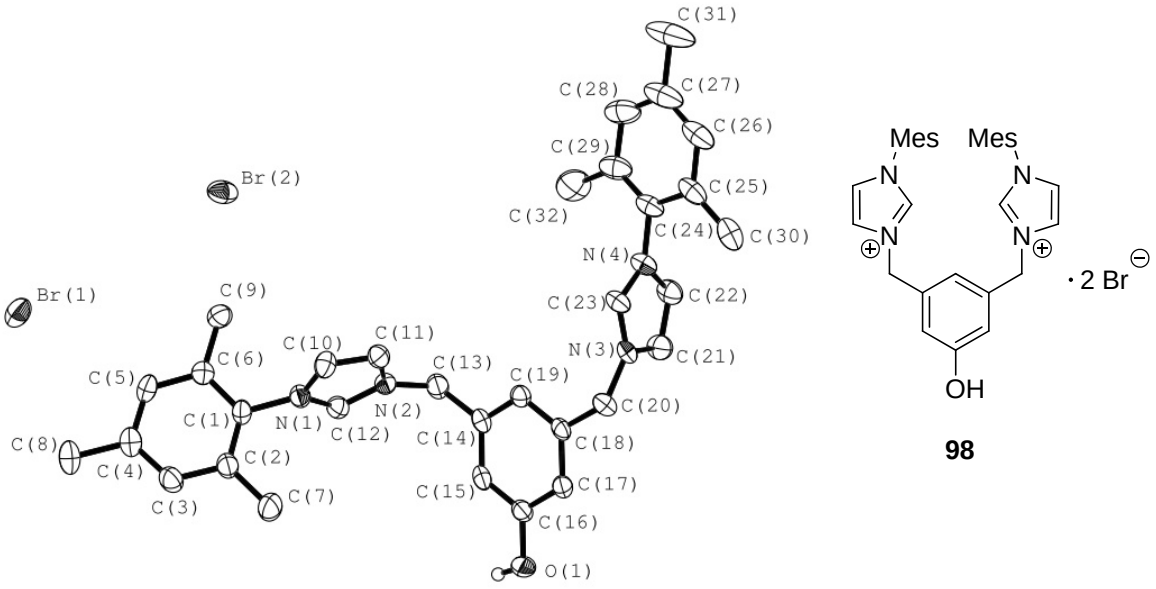

Figure 29: X-ray structure of 98, non-polar H atoms are omitted for clarity.

The functionalization of the polymer coated particles 37 was accomplished by a simple Williamson ether synthesis with the Pd-NHC complex 100 in the presence of K_2CO_3 (Scheme 19). The loading typically achieved under these conditions was 0.6 mmol/g as determined by ICP-OES measurement.

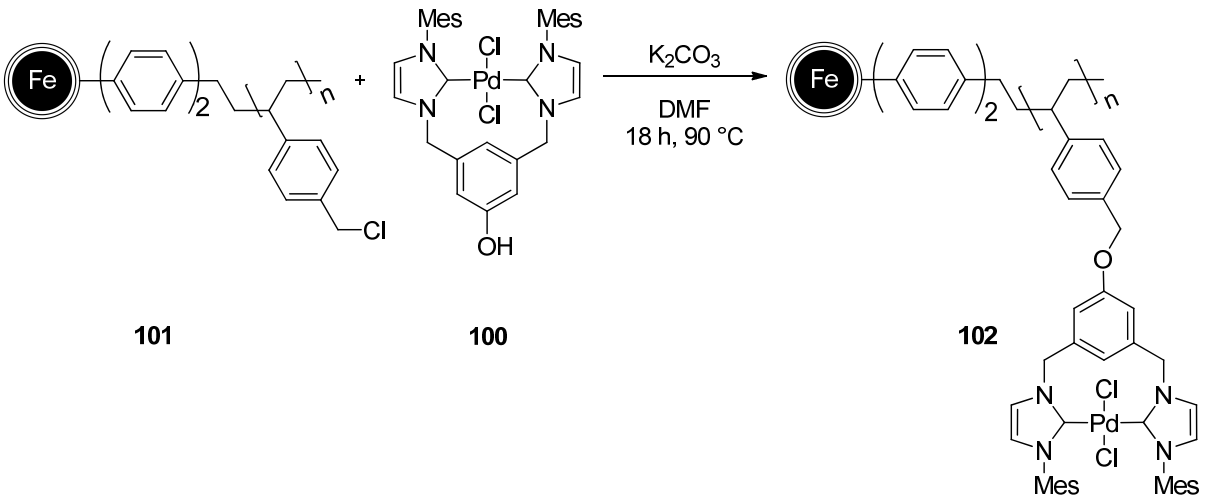

101 100 102

Scheme 19: Functionalization of polyvinylbenzylchloride coated iron nanoparticles 101 with the palladium NHC complex 100.

Functionalization of the polymer coated nanomagnets 101 was monitored by IR spectroscopy (Figure 30). The polymer coated particles 101 showed a distinct peak at 1260 cm^{-1} which was assigned to the stretching of the C-Cl bond. During the functionalization process this peak vanished and new peaks corresponding to aromatic (1230 cm^{-1}) and aliphatic (1150 cm^{-1}) ether groups appeared.

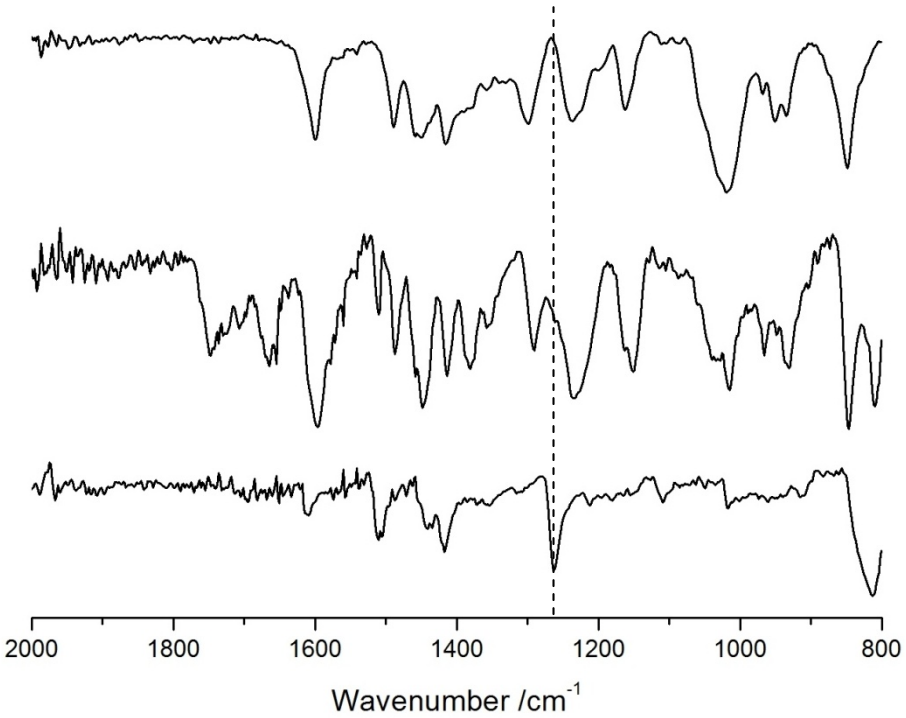

Figure 30: ATR-IR spectra of polymer coated particles 101 (bottom), catalyst 100 (top) and functionalized particles 102 (center).

The resulting catalyst 102 was subsequently applied in the Suzuki cross coupling reaction of 4-bromoanisole with phenylboronic acid. The complex 102 gave full conversion determined by GC with 95% isolated yield after 10 h and a maximum TOF of 165 h^{-1} (Figure 31). Under the same conditions, several recycling experiments were carried out. After six runs, the catalyst showed nearly the same performance as in the first run (Table 9) and was recovered via magnetic decantation efficiently.

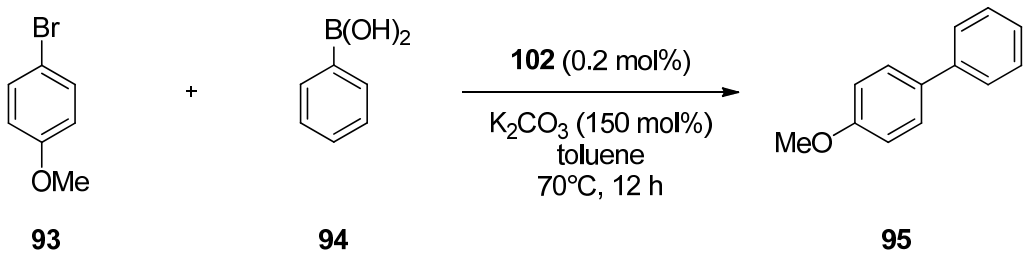

93 **94** **95**

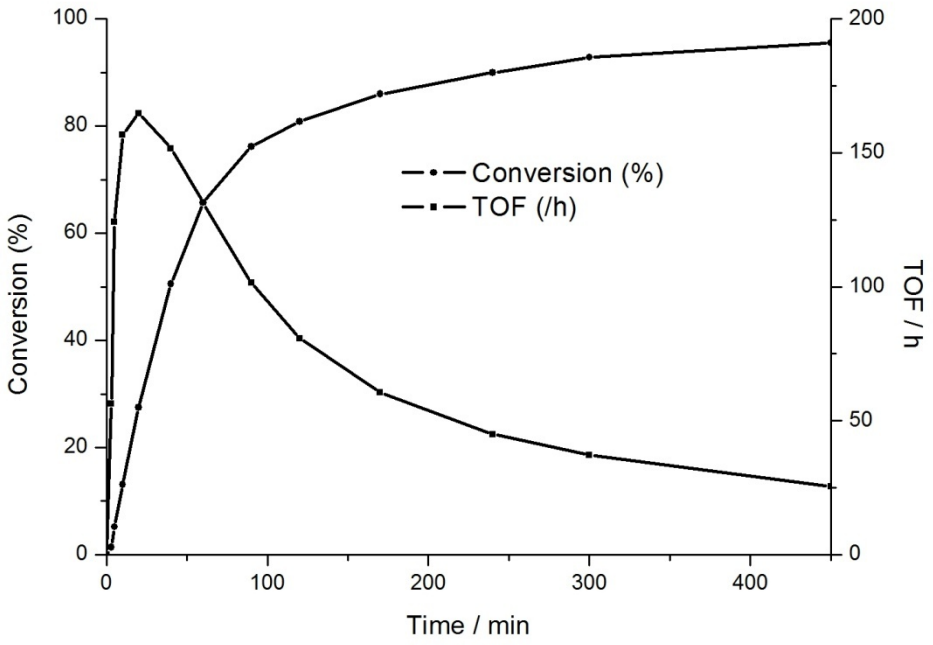

Figure 31: Time-conversion and time-TOF curves of 102 in the Suzuki-Miyaura cross coupling reaction.

Table 9: Suzuki-Miyaura reaction catalyzed by 102.[a]

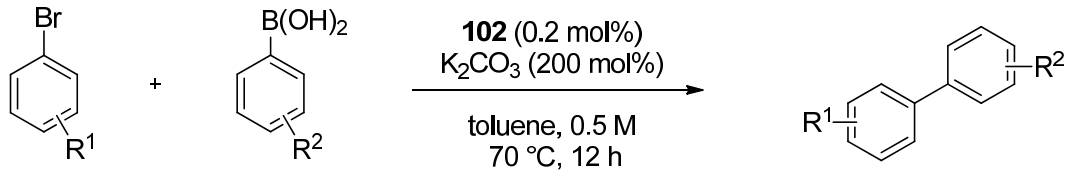

93: R^1 = 4-OMe
103: R^1 = 2,6-Me
104: R^1 = 4-NO_2
105: R^1 = 4-C(O)Me
106: R^1 = H

94: R^2 = H
107: R^2 = 4-Me

95: R^1 = 4-OMe, R^2 = H
108: R^1 = 2,6-Me, R^2 = H
109: R^1 = 4-NO_2, R^2 = H
110: R^1 = 4-C(O)Me, R^2 = H
111: R^1 = H, R^2 = 4-Me

entry	run	R^1	R^2	conversion[b] / %
1	1	4-OMe	-	> 95[b]
2	2	4-OMe	-	> 95[b]
3	3	4-OMe	-	> 95[b]
4	4	4-OMe	-	> 95[b]
5	5	4-OMe	-	> 95[b]
6	6	4-OMe	-	> 95[b]
7	1	2,6-Me	-	61[c]
8	2	4-NO_2	-	95[c]
9	3	4-C(O)Me	-	93[c]
10	4	-	4-Me	91[c]
11	5	4-OMe	-	89[c]

[a] Reaction conditions: 0.5 mmol aryl halide, 0.55 mmol phenylboronic acid, 1.0 mmol K_2CO_3, 0.2 mol% catalyst 102, 2 mL toluene, 70 °C, 12 h. [b] Determined by ^{1}H-NMR. [c] Isolated yield after column chromatography.

As the magnetic Co@C 24 and Fe@C 27 nanoparticles comprise of a metallic core and a conductive shell, conceivably these particles absorb microwave irradiation quite efficiently. To test this hypothesis, different nanoparticles were subjected to microwave heating in toluene, a solvent which is due to its low dipolar polarization inappropriate for microwave

applications (Figure 32). At a fixed power of 200 W, neat toluene reached a temperature of 145 °C. By adding Co@C nanobeads the heating rate as well as the maximum temperature (240 °C) could be increased significantly. At higher power levels, the heating rate as well as the reached temperature and the concomitant pressure levels are exceeding the security limits of the employed microwave apparatus.

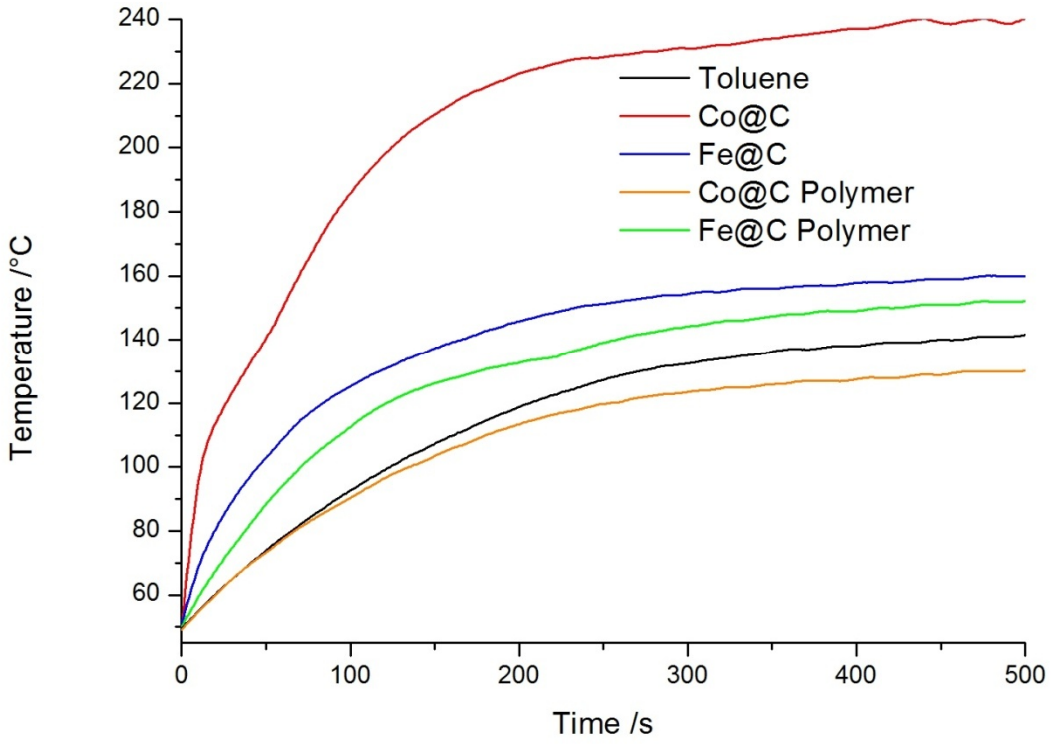

Figure 32: Microwave heating profiles of toluene and different magnetic nanoparticles at a fixed power of 200 W.

Since it is known that aryl halides decompose under biphasic reaction conditions during microwave irradiation, a process in an organic solvent would be advantageous.[110] Due to the fact that aryl chlorides are quite unreactive coupling partners in the Suzuki-Miyaura reaction, the competing decomposition leads with prolonged reaction times also to a decreased yield. For this reason the catalyst 102 was again employed in the Suzuki-Miyaura in toluene with Cs_2CO_3 as a heterogeneous base (Table 10). The microwave irradiation should mainly heat the metal nanoparticles with the result that the surrounding of the particles (where the catalyst is located) is heated most efficiently. The reaction of 4-iodotoluene 112 with phenylboronic acid gave quantitative yield of biphenyl within 5 min of

microwave irradiation at 200 W resulting in a constant temperature of 160 °C after 4 min. The tested bromide 93 converted within 20 minutes to the product. As expected, the aryl chloride 113 took significantly longer to reach full conversion. After the fist cycle, a distinct decrease in the yield as determined by GC could be observed. This is most probably due to decomposition and aging of the catalyst under the elongated reaction time at harsh reaction conditions.

Table 10: Suzuki-Miyaura reaction catalyzed by 102 – microwave conditions.[a]

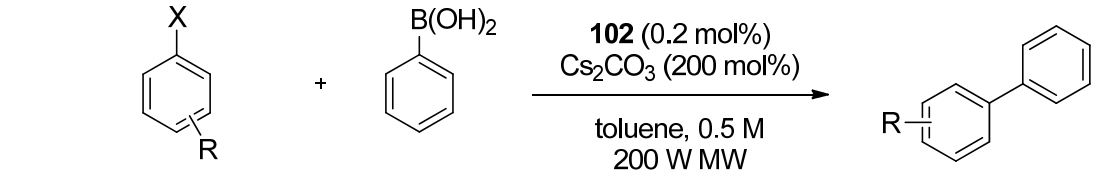

93: R = 4-OMe, X = Br
112: R = 4-Me, X = I
113: R = 4-C(O)Me, X = Cl

94

95: R = 4-OMe
110: R = 4-C(O)Me
114: R = 4-Me

entry	run	aryl halide	time / min	yield[b] / %
1	1	112	5	98
2	2	93	20	96
3	3	93	20	94
4	4	93	20	95
5	1	113	60	95
6	2	113	60	80
7	3	113	60	68
8	4	113	60	49

[a] Reaction conditions: 0.5 mmol aryl halide, 0.55 mmol phenylboronic acid, 1.0 mmol Cs_2CO_3, 0.2 mol% catalyst 102, 2 mL toluene, 200 W microwave heating (fixed power). [b] Determined by GC analysis with diethylene glycol-di-*n*-butyl ether as internal standard.

Due the the fact that palladium pincer complexes can serve as a reservoir for palladium nanoparticles being the active catalyst species a mercury drop test was performed.[111] In order to test whether the reactions are catalyzed by the molecular complex 102, or by

palladium nanoparticles species resulting from complex leaching.[112] The test relies on the formation of an amalgam with colloidal palladium. Catalyst 102 showed in the Suzuki reaction (Scheme 17) between phenylboronic acid 94 and 4-bromoanisole 93 with 100 equivalents of Hg (corresponding to Pd) improved performance of the catalytic system (83% conversion compared to 54% without Hg). Nevertheless, this result could have also been distorted by microwave heating of elemental mercury resulting in a faster temperature increase. In the case of hydrogenation reactions, it has been shown before that mercury can affect the nature of the reactivity, or even improve reaction rates.[113]

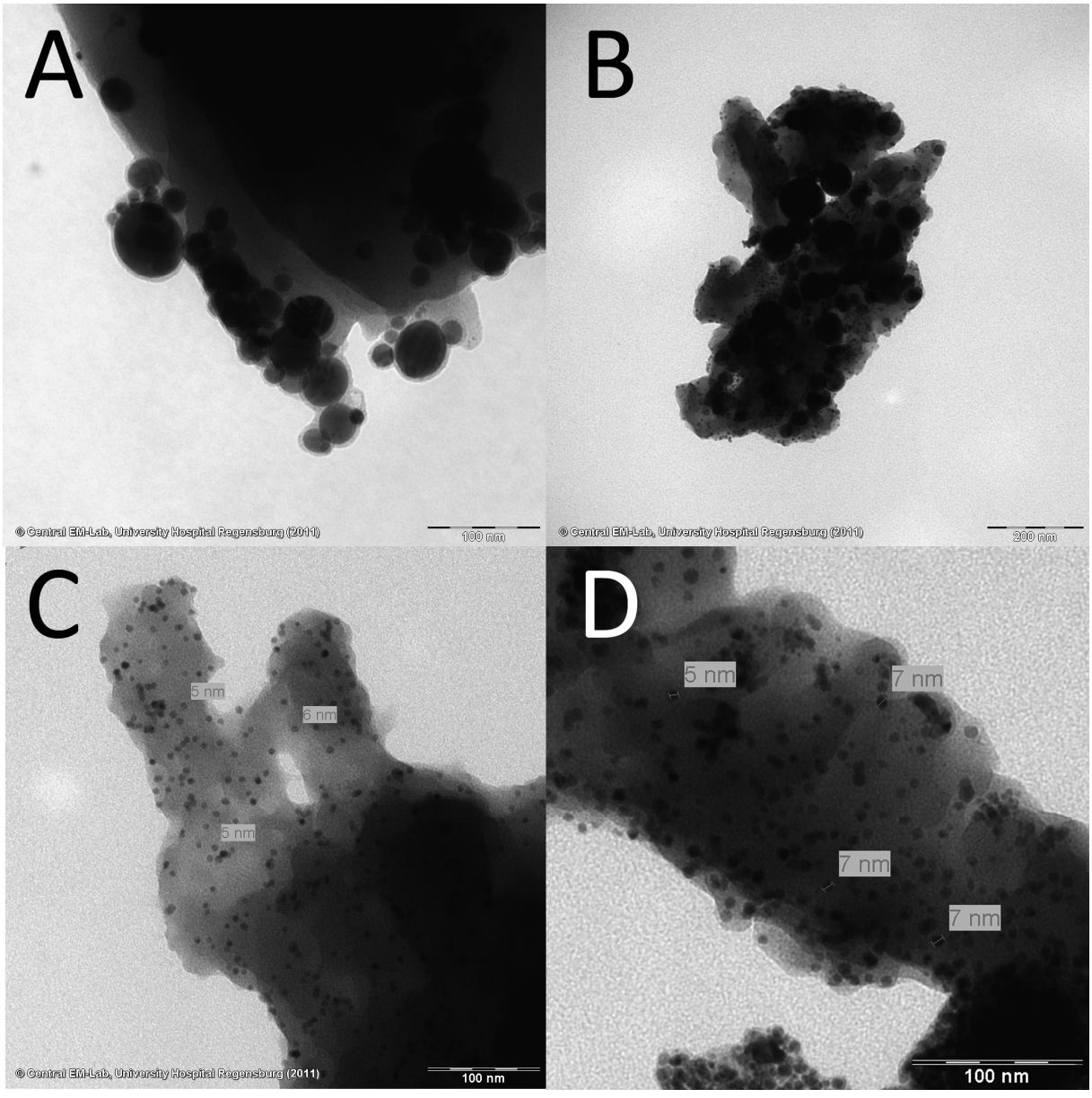

Figure 33: TEM micrographs of freshly prepared 102 (A), after one cycle in the microwave (B) and after one (C) or four (D) cycles with conventional heating. C and D show the formation of Pd nanoparticles.

However, the mercury test, as pointed out by Whitesides, is a useful but not universally applicable technique for differentiating homogenous and heterogeneous reaction behavior.[114] For this reason, the leaching of palladium was determined by ICP-OES measurement. In the case of conventional heating 1.8 ppm Pd and by microwave heating 1.3 ppm Pd were leaching into the product. The reduced leaching under microwave irradiation can probably be attributed to the significantly shorter reaction times. To test if Pd nanoparticles were formed during the reactions, TEM micrographs before and after one and four cycles in the microwave were recorded (Table 10, Entries 5-8). As clearly can be seen from Figure 33 A, no palladium nanoparticles were present directly after preparation of the catalyst. However, after the Suzuki reaction palladium nanoparticles are visible. The size of the particles does not increase significantly when multiple cycles are performed. After one and four cycles the size of the formed nanoparticles stays at about 5-7 nm, which indicates a stabilizing effect of the functionalized polymer.[115] In conclusion, the mercury test seems not to be reliable in the case of polymer embedded palladium nanoparticles. Nevertheless, the polymer 102 was found to be an efficient catalyst for the Suzuki-Miyaura cross coupling reaction, even with aryl chlorides, under microwave heating.

4.2 Supported ionic liquid phases as catalyst supports

Ionic liquids (ILs) have received tremendous interest in the last years as an alternative reaction media to replace volatile organic solvents. Their ionic character, easy accessibility and the ability to tune their properties makes them attractive candidates for catalytic processes. The cations in ILs are mostly large organic cations like imidazolium salts or alkylated pyridines. The anions can be divided into two groups. Anions like Cl^-, Br^- or I^- yield hydrophilic ILs whereas fluorinated anions like PF_6^-, BF_4^-, $CF_3SO_3^-$ or NTf_2^- yield hydrophobic ILs[114], which results in an almost infinite number of possible combinations, thus allowing to tailor the properties of ILs. However, most ionic liquids are quite expensive and hence should not be used in reactions requiring a large amount of solvent. One of the main problems of ionic liquids is their high viscosity, which causes problems in terms of diffusion. Wasserscheid et al. have shown that this problem can be avoided if the ionic liquid is immobilized as a thin film onto a solid support with high surface area.[115] These supported ionic liquid phase (SILP) catalysts have, due to the fact that they use the IL in a more efficient way, evoked great interest.[116] Different supports, mainly porous silica gels,[117] zeolites, clays but also organic polymers[118] and carbon nanofibers[119] have been used as carrier materials for ILs.

The majority of SILP systems aim for applications in gas phase catalysis. Nevertheless, there are some adoptions of this technology for homogeneous catalysis in liquid media. The first demonstration of such a system was reported by Noto et al. using proline, embedded in layer of IL to perform aldol reactions between different benzaldehydes and acetone.[120]

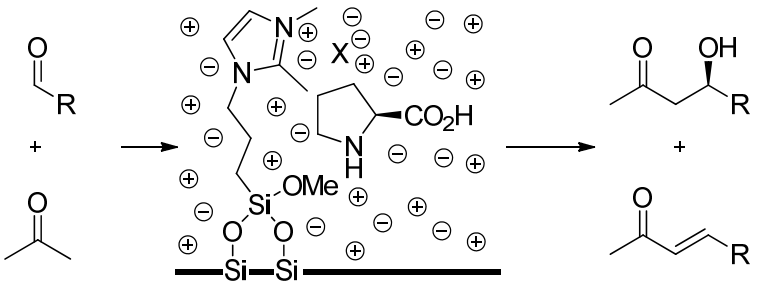

Scheme 20: L-Proline catalyzed asymmetric aldol reaction using a SILP system (reproduced from [120]). The IL layer, consisting of either [bmim][BF_4] or [bmim][PF_6] is represented by the charges.

Especially interesting is SILP catalysis for expensive chiral complexes in order to simplify or enable recycling. A privileged class of such catalysts is represented by copper bisoxazoline complexes. Hardacre et al. used the complexes 115 and 116 in a layer of $[C_2mim][NTf_2]$, which were immobilized on different supports like AC, CNTs, zeolite and different silica materials.[121]

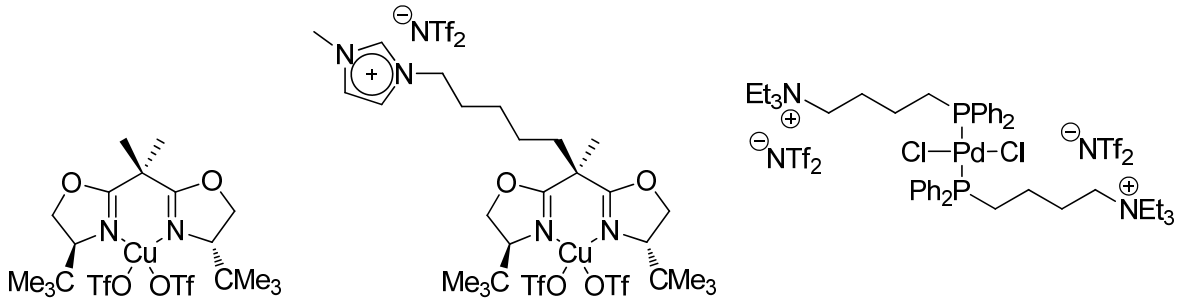

115 **116** **117**

Figure 34: Copper-(II)-bisoxazoline complexes 115 and 116 together with the palladium complex 117[122] used in SILP catalysis.

To immobilize different catalysts, a versatile and simple way to functionalize ionic liquid precursors was envisioned. Such a functionalization strategy is the Huisgen 1,3-dipolar cycloaddition of an azide with a terminal alkynes catalyzed by copper(I), also known as click-reaction. For this purpose 118 was reacted with 1,2-dimethylimidazole 119 followed by an anion exchange to yield the azide tagged ionic liquid 122.

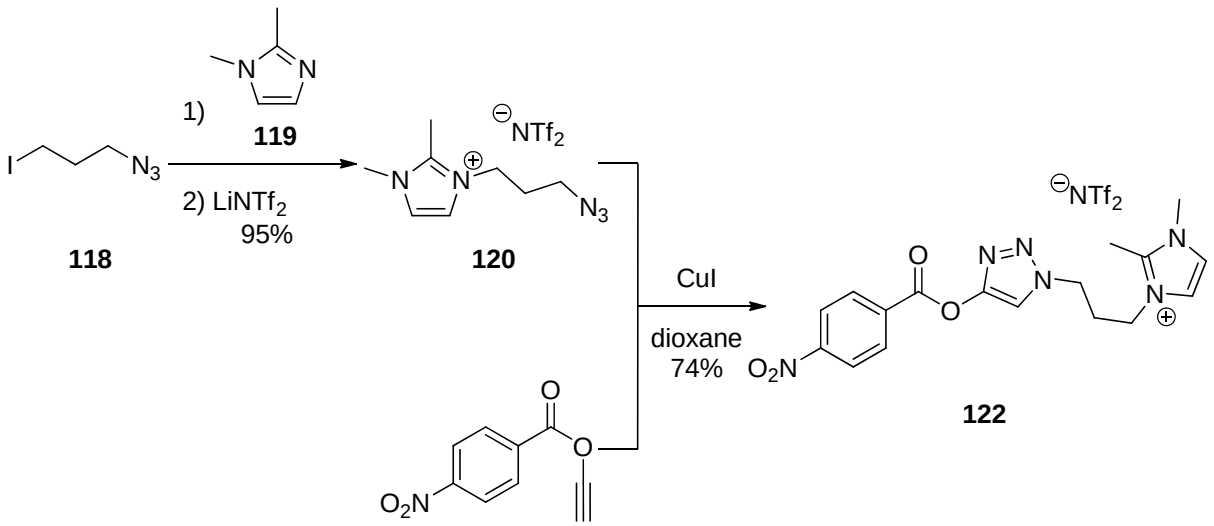

Scheme 21: Synthesis of the nitrophenol tagged IL 122 by click chemistry.

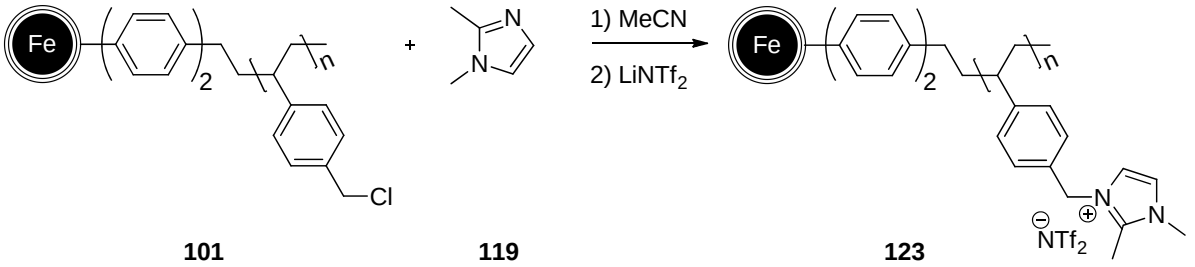

101 **119** **123**

Scheme 22: Synthesis of polymer coated nanoparticles 123 by nucleophilic substitution with 119 followed by anion exchange.

In order to test the feasibility of this concept, a nitrophenol ester was attached to the ionic liquid. As already shown with the nitrophenole tagged pyrene derivative 45 it was envisioned to determine the strength of the binding forces in different solvents by means of UV/Vis measurements. For this purpose, also the polymer coated particles 101 were functionalized with a shell of ionic liquid (Scheme 22). Again, the functionalization could be easily followed by IR spectroscopy (Figure 35). Determination of the nitrogen content of 123 by elemental analysis revealed a loading of 1.6 mmol/g.

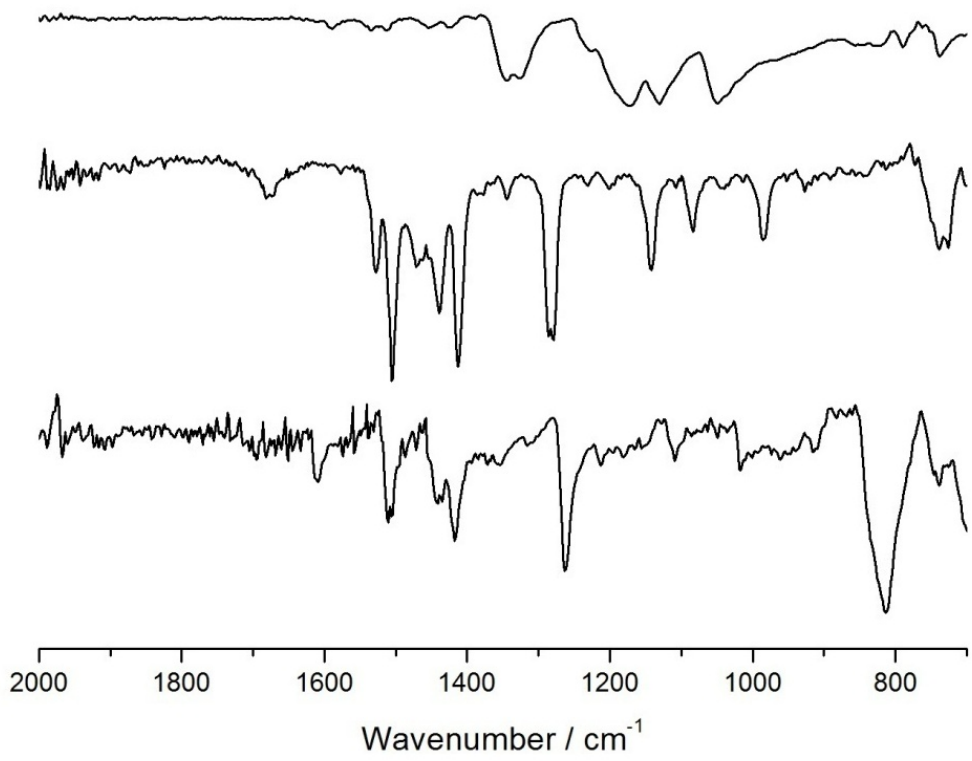

Figure 35: ATR-IR spectra of unfunctionalized particles 101 (bottom), dimethylimidazole 119 (top) and functionalized particles 123 (center).

The ability of the particles 123 to immobilize the ionic liquid 122 was determined by dispersing both compounds in ether, DCM and THF in a 1:2.5 (123:122) ratio. UV/Vis measurement of the hydrolyzed supernatant solution revealed that in ether 2.1 eq. of the initial 2.5 eq. 122 were immobilized on the particles. In each of the following three washing steps 1% of 122 was found to be desorbed from the particles. After three times washing with ether still 2 eq. 122 per imidazole unit on the particles 123 was present. In DCM and THF only a small amount (0.82 and 0.31 eq.) was adsorbed on the particles. In the first washing cycle nearly all of the remaining IL was desorbed from the particles. Thus, only ether proved to be a suitable solvent for the immobilization and reactions with ionic liquid tagged catalysts.

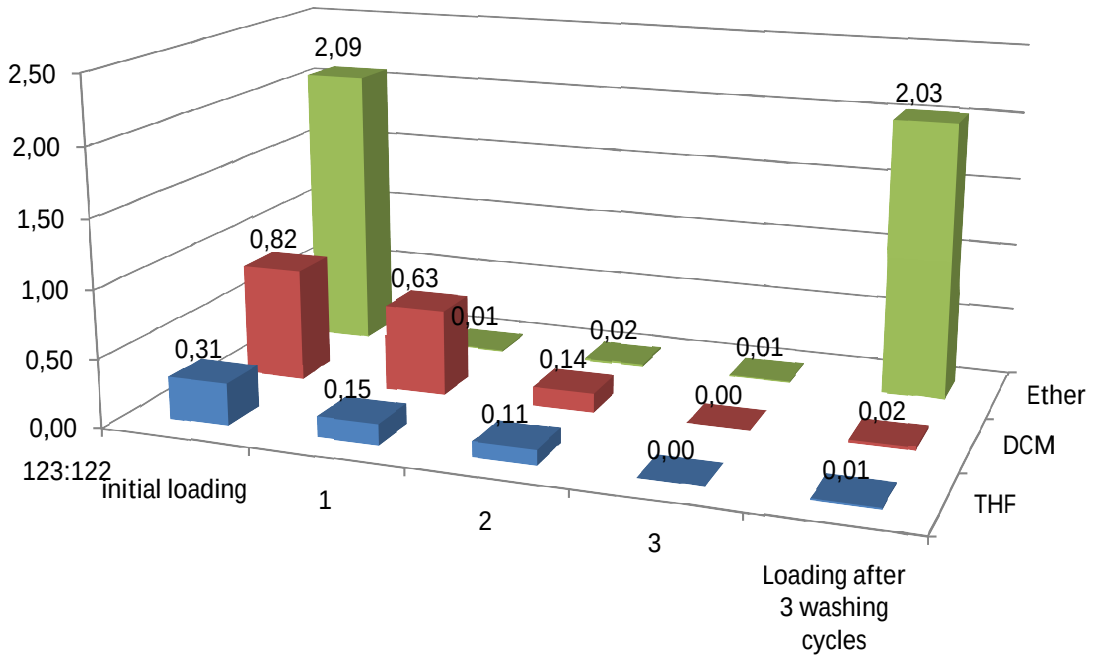

Scheme 23: Relative amount of 122 compared to 123 after stirring with 2.5 eq. 122 in the corresponding solvent (row 1), after washing one, two or three times (rows 1, 2 and 3) and residual amount of 122 on the particles after three washing steps (last row).

The low amount of leaching observed during the washing experiments in ether was the basis for the synthesis of ionic liquid functionalized catalysts. As a first model system, the IL tagged TEMPO derivative 126 was synthesized (Scheme 24). Both precursors 120 and 125 were soluble in dioxane. However, the product 126 formed a second ionic liquid layer and could be isolated in almost quantitative yield by simple decantation and filtration.

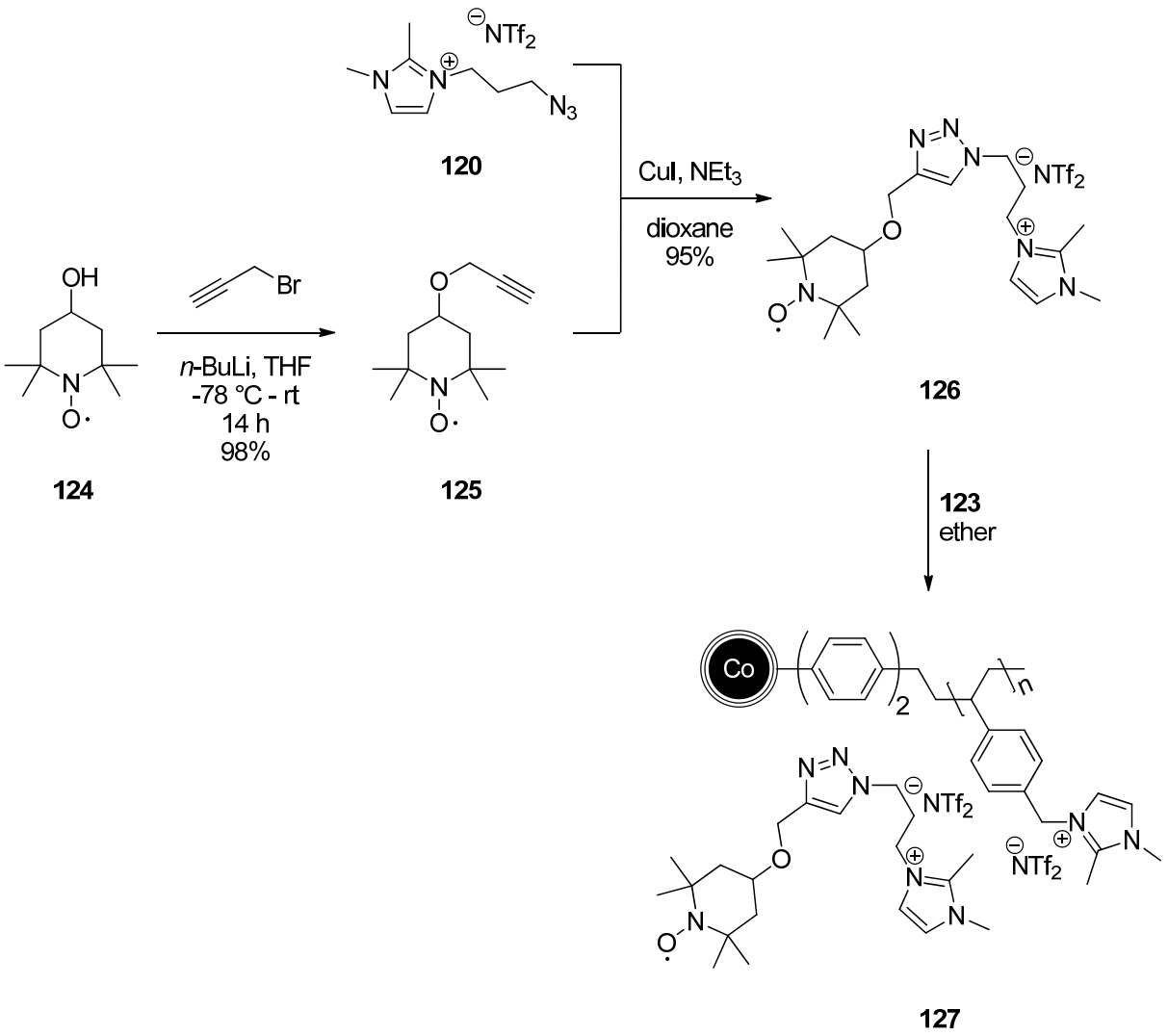

Scheme 24: Synthesis of the ionic liquid tagged TEMPO catalyst 126 and immobilization as supported ionic liquid layer.

The catalyst 126 was then tested in the chemoselective oxidation of *p*-tolylmethanol 128 with 129 as terminal oxidant.[123] Using 126 as homogenous catalyst in toluene or dioxane resulted in complete conversion after 7 or 6 h, respectively (Table 11). The long reaction time is not surprising as Piancatelli already pointed out that solvents with high dielectric constants accelerate the reaction significantly. Thus, the reaction with the IL tagged particles 127 resulted in shorter reaction times because of the high dielectric constant of the ionic liquid layer.

By adding additional [bmim][BF_4] to the particles, the layer was further extended. With this system the reaction times could be decreased to 3.5 hours, after which the recycling of the nanobeads was possible. Three consecutive runs without an observable loss in activity could be performed.

Table 11: Chemoselective oxidation of 128 to the corresponding aldehyde with 129 as oxidant.[a]

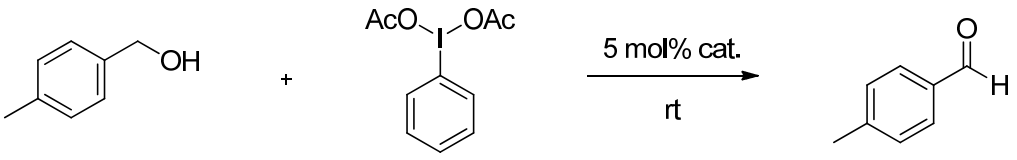

128 **129** **130**

entry	catalyst	run	solvent	time / h	conversion[b] / %
1	126	1	toluene	7	> 95
2	126	1	dioxane	6	> 95
3	127	1	ether	5	> 95
4	127	2	ether	5	> 95
5	127	3	ether	5	> 95
6	127 + [bmim][BF_4]	1	ether	3.5	> 95
7	127 + [bmim][BF_4]	2	ether	3.5	> 95
8	127 + [bmim][BF_4]	3	ether	3.5	> 95

[a] Conditions: 0.5 mmol alcohol, 0.55 mmol 129, 5 mol% catalyst, 2 mL solvent, rt. [b] Determined by ^{1}H-NMR spectroscopy.

The preparation of the IL tagged azabis(oxazoline) complex 132 could be carried out in the same manner as shown for 126 (Scheme 25). Unfortunately the well known benzoylation of racemic diols and the Michael addition of benzylidene malonates to indoles gave poor results.

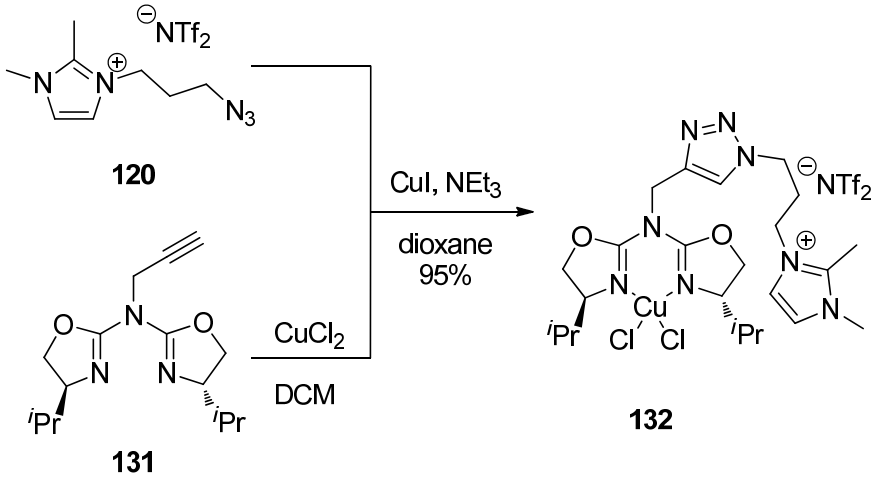

Scheme 25: Preparation of the IL tagged azabis(oxazoline) complex 132 by click chemistry.

5. Assessment of relative catalyst activities

The determination of the activities of two ligands in metal catalysis requires usually the meticulous measurement of increments over an extended time period to determine the reaction kinetics. This means that after defined intervals aliquots of the reaction mixture have to be taken and worked up prior to the determination of conversion or selectivity. Thus, a simpler and less time consuming method would be desirable. By employing a mixture of two competitive ligands in a reaction, each with antipodal chiral induction, one could determine from the resulting cumulative product *ee* value the relative activities of the catalysts.[124] For this measurement only the *ee* values of the sole catalysts and the resulting *ee* value of the mixture have to be known. For the calculation the following formula can be used:

$$v_{rel} = \frac{X_2(ee_2 + ee_r)}{X_1(ee_1 - ee_r)}$$

v_{rel} = relative reaction rate

ee_1 = enantioselectivity of ligand 1

ee_2 = enantioselectivity of ligand 2

ee_r = resulting product enantioselectivity using both ligands

X_1 = amount of catalyst 1

X_2 = amount of catalyst 2

As a model reaction the Friedel-Crafts alkylation of indoles with benzylidene malonate was chosen because the two similar ligand classes bis(oxazolines) and azabis(oxazolines) show high activities and selectivities. The results of the catalytic runs are summarized in Table 12.

Table 12: Asymmetric Friedel-Crafts alkylation of indole with different bis(oxazoline)- and azabis(oxazoline)-copper(II) complexes.[a]

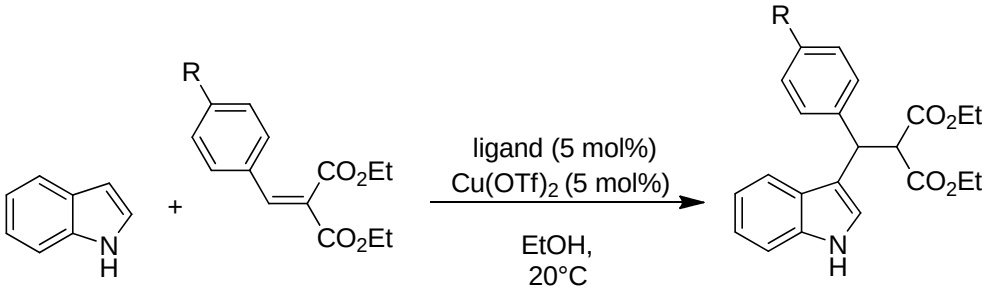

132

133a: R = H
133b: R = Me
133c: R = Cl
133d: R = OMe

134 a-d

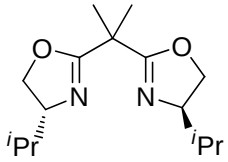

135

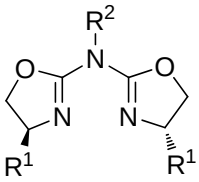

(*S*,*S*)-**136a**: R^1=^{i}Pr, R^2=H
(*S*,*S*)-**136b**: R^1=^{i}Pr, R^2=Me
(*S*,*S*)-**136c**: R^1=Bn, R^2=H
(*R*,*R*)-**136d**: R^1=Ph, R^2=H

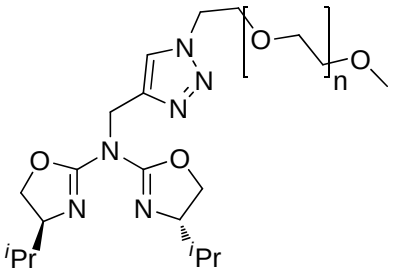

137

entry	ligand	R	product	yield (%)	*ee* (%)[b]
1[c]	(*R*,*R*)- 135	H (133a)	134a	89	99 (*R*)
2[c]	(*S*,*S*)- 136a	H (133a)	134a	97	99 (*S*)
3	(*R*,*R*)- 135	H (133a)	134a	93	90 (*R*)
4	(*S*,*S*)- 136a	H (133a)	134a	90	98 (*S*)
5	(*S*,*S*)- 136b	H (133a)	134a	84	77 (*S*)
6	(*S*,*S*)- 136c	H (133a)	134a	90	81 (*S*)
7	(*R*,*R*)- 136d	H (133a)	134a	63	57 (*R*)
8	(*R*,*R*)- 135	Cl (133c)	134c	84	80 (*R*)
9	(*S*,*S*)- 136a	Cl (133c)	134c	87	76 (*S*)
10	(*R*,*R*)- 135	Me (133b)	134b	79	84 (*R*)
11	(*S*,*S*)- 136a	Me (133b)	134b	66	78 (*S*)
12	(*R*,*R*)- 135	OMe (133d)	134d	80	83 (*R*)
13	(*S*,*S*)- 136a	OMe (133d)	134d	47	71 (*S*)
14	(*S*,*S*)- 137	H (133a)	134a	81	87 (*S*)

[a] Results from reference [124]. Reagents and conditions: 1.2 mmol indole, 1.0 mmol benzylidene malonate, 5 mol% ligand, 5 mol% $Cu(OTf)_2$, 20°C, 16h, solvent: 4 mL EtOH. [b] Determined by chiral HPLC. [c] 4.8 mol% $Cu(OTf)_2$, taken from reference [125].

With these results in hand the comparison of two ligands was carried out. From two runs each combination the averaged yields and *ee* values were calculated. The relative reaction rate could then be easily calculated with the values from Table 12 and the aid of the aforementioned formula.

Table 13: Comparison of different ligands with antipodal stereochemical induction. [a]

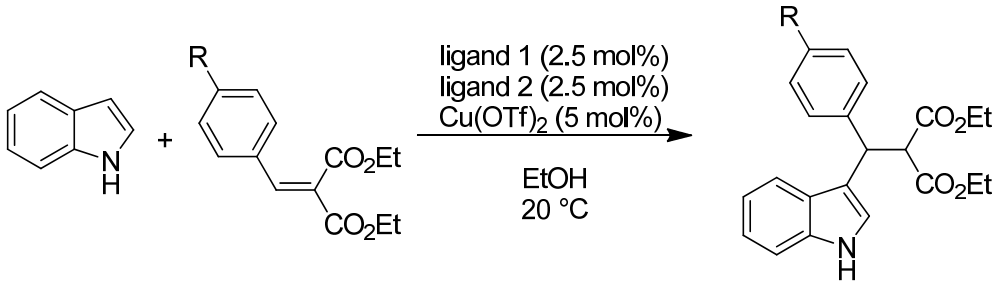

132

133a: R = H
133b: R = Me
133c: R = Cl
133d: R = OMe

134a: R = H
134b: R = Me
134c: R = Cl
134d: R = OMe

entry	ligand 1	ligand 2	R	yield (%)[b]	*ee* (%)[c]	$\nu_{rel.}$
1	135	136a	H (7a)	90	- 53	4.1
2	135	136b	H (7a)	89	- 63	5.2
3	135	136c	H (7a)	90	- 58	4.4
4	*ent*-135	*ent*-136d	H (7a)	92	- 80	13.7
5	136c	*ent*-136d	H (7a)	84	+ 48	3.2
6	135	136a	Cl (7b)	87	- 41	3.0
7	135	136a	Me (7c)	65	- 49	3.7
8	135	136a	OMe (7d)	44	- 55	4.6
9	135	137	H (7a)	71	- 52	3.6

[a] Results from M. Hager and S. Wittmann. Reagents and conditions: 1.2 mmol indole, 1.0 mmol malonate, 2.5 mol% ligand 1, 2.5 mol% ligand 2, 5 mol% $Cu(OTf)_2$, 20 °C, 16 h, solvent: 4 mL EtOH; [b] Average of two runs; [c] Determined by chiral HPLC; average of two runs.

In conclusion, the measurement of relative catalyst activites could be achieved in the case of bis(oxazoline)-copper(II) catalyzed Friedels-Craft reaction of indoles with benzylidenmalonates. As this method is an endpoint measurement, effects like induction times or nonlinear effects cannot be assessed. However, considering the high reproducibility obtained in the aforementioned reactions for different substrates, this tool might be useful in a screening process where detailed kinetics are difficult to assess.

6. Iridium catalyzed allylation of alcohols – recycling of the catalyst

Polyketide natural products are within the most interesting targets for organic chemists. Therefore, a vast library of methods for the allylation of carbonyl compounds has been developed in the last years. Since 1964 the first isolable allylboranes and silanes were synthesized also enantioselective and catalytic variants have been developed. One major drawback of all these methods is that soichiometric amounts of byproducts are produced, which are in some cases even highly toxic and difficult to separate. A more efficient approach consists the use of allylcaetates, allylalcohols or allylhalides as allyl donors.

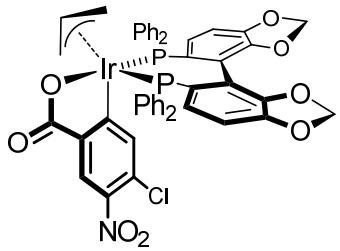

138

Figure 36: Iridium π-allyl complex 138 used for asymmetric allylations of aldehydes and alcohols.

One catalytic system that comprises of all above mentioned points was developed by Krische et al. in 2008.[126] Using the cyclometallated, *in situ* formed, iridium complex 138 allowed to allylate various alcohols and aldehydes under transfer hydrogenation conditions in excellent yield and enantioselectivity. Due to the fact that the reaction is performed under transfer hydrogenation conditions, Krische was able to use aldehydes with isopropanol as the reductant or directly alcohols as substrates. This method is even more powerful when one considers the allylation of unstable aldehydes like malonaldehyde.[127] This aldehyde is highly reactive and not isolable in pure form at ambient conditions. The corresponding alcohol 1,3-propanediol is a cheap bulk chemical. The initial studies focused on the *in situ* generation of the catalyst from $[Ir(cod)Cl]_2$. This iridium precursor forms with chrial bisphosphines, 3,4-substituted benzoic acids and allyl acetate under the reaction conditions the active catalyst species. Later it was discovered that this catalyst outlasts the reaction and can be easily

separated by column chromatography from the products of the catalysis. In most cases it is also possible to form the catalyst prior to the reaction from $[Ir(cod)Cl]_2$ (Scheme 26).

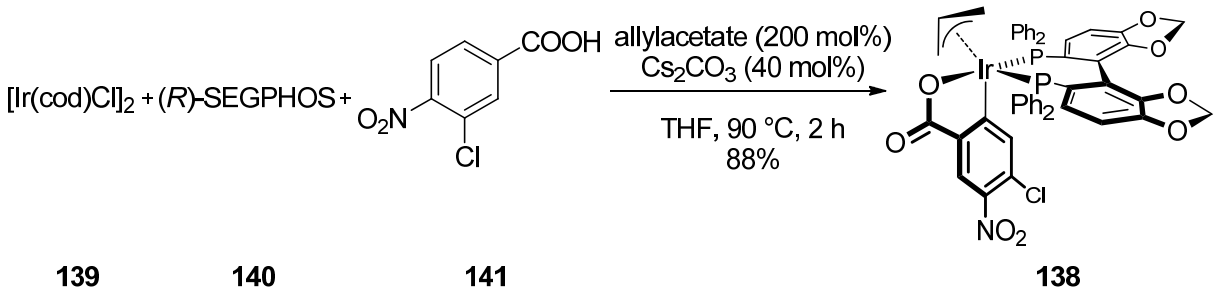

139 **140** **141** **138**

Scheme 26: Preparation of the catalyst 138.

Surprisingly, the use of preformed complexes increased the reaction rate as well as the selectivities in most of the reactions performed so far. In principle it should be possible to recover this catalyst after an allylation reaction and to recycle it, because 138 represents the resting state. This would be highly desirable if one considers that the price of of the iridium precursor $[Ir(cod)Cl]_2$ (1 g ≈ 500 €). Unfortunately this approach is limited to simple allylations because all other Ir-π-allyl complexes originating from substituted allyl molecules are not isolable.

To explore the recyclability of the preformed complex 138 some reaction conditions were screened (Table 14). In order to mimic the "in situ" conditions, also the carboxylic acid 141 was added. The additive caused an increased conversion (Entry 2) as well as an enhanced catalyst recovery (Entry 8).

Table 14: Optimization of the reaction conditions.

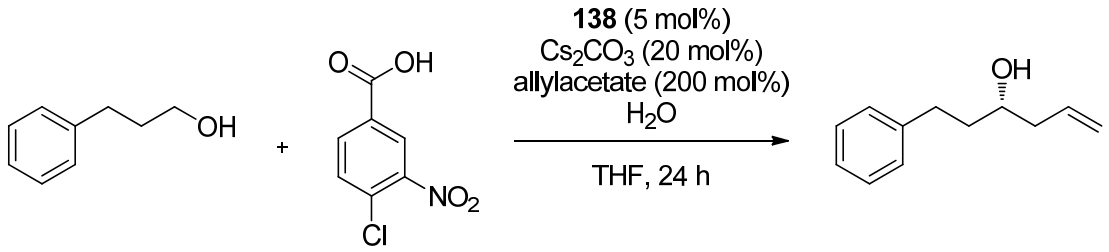

142 **141** **143**

entry	temperature /°C	concentration /mol/L	n(142) /mmol	141 /mol%	H_2O /mol%	conversion /%[a]	catalyst recovery /%[b]
1	110	0.2	0.2	5	5	99	nd
2	90	0.2	0.2	0	5	78	nd
3	90	0.2	0.2	5	5	52	nd
4	110	0.2	0.2	5	2	52	nd
5	90	0.2	0.2	5	2	77	nd
6	110	0.4	0.2	5	2	99	nd
7	110	0.4	1	0	2	99	69
8	110	0.4	1	5	2	99	85

[a] Determined by ^{1}H-NMR of the crude product. [b] Isolated yield after column and precipitation.

Having the optimized conditions in hand different substrates were tested and the catalyst was recovered by precipitation after column chromatography (Scheme 27). Benzylic, allylic and aliphatic alcohols could be functionalized in good yield and excellent enantioselectivity. The catalyst could be recovered after column chromatography by precipitation with hexane. ^{31}P-NMR spectra of a fresh prepared and recovered catalyst sample showed no significant difference.

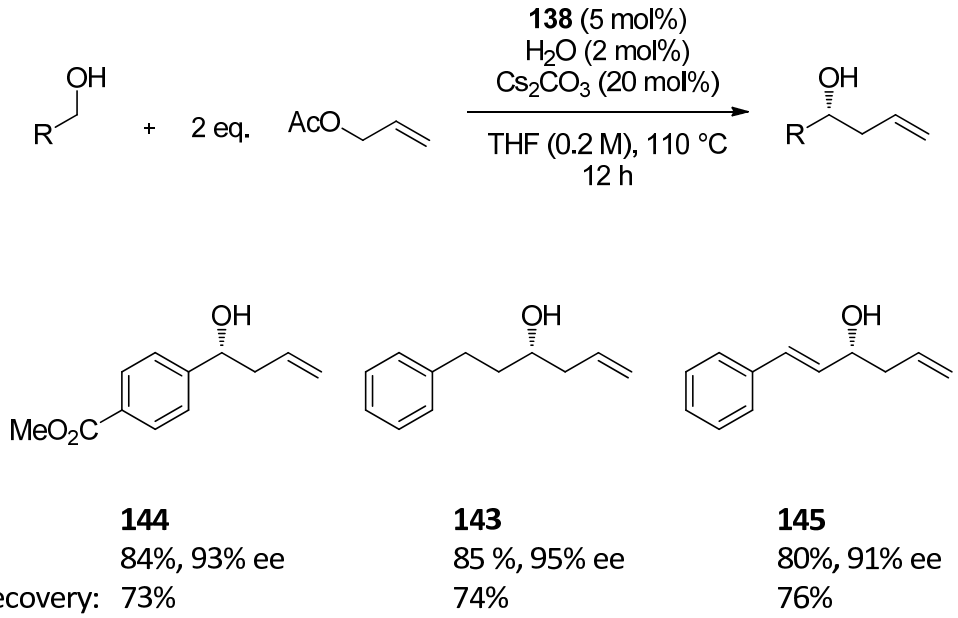

	144	**143**	**145**
	84%, 93% ee	85 %, 95% ee	80%, 91% ee
catalyst recovery:	73%	74%	76%

Scheme 27: Recycling studies of 138 under the optimized reaction conditions with different substrates.

The recycled catalyst 138 was also employed in a second cycle and showed similar activity and selectivity. In summary a simple and efficient recycling protocol for the expensive Ir catalyst 138 was established.

7. References

[1] (a) J. A. Gladysz, *Chem. Rev.* 2002, *102*, 3215-3216; (b) J. Lu, P. H. Toy, *Chem. Rev.* 2009, *109*, 815-838; (c) M. Benaglia, A. Puglisi, F. Cozzi, *Chem. Rev.* 2003, *103*, 3401-3430; (d) D. E. Bergbreiter, J. Tian, C. Hongfa, *Chem. Rev.* 2009, *109*, 530-582; (e) V. Polshettiwar, R. Luque, A. Fihri, H. Zhu, M. Bouhrara, J.-M. Basset, *Chem. Rev.* 2011, *111*, 3036-3075; (f) S. Shylesh, V. Schünemann, W. R. Thiel, *Angew. Chem.* 2010, *122*, 3504-3537; (g) S. Shylesh, V. Schünemann, W. R. Thiel, *Angew. Chem. Int. Ed.* 2010, *49*, 3428-3459; (h) A. Schätz, O. Reiser, W. J. Stark, *Chem.-Eur. J.* 2010, *16*, 8950-8967.

[3] (a) S. Iijima, *Nature* 1991, *354*, 56-58; (b) M. Monthioux, V. L. Kuznetsov, *Carbon* 2006, *44*, 1621-1623.

[10] (a) P. Serp, M. Corrias, P. Kalck, *Appl. Catal., A* 2003, *253*, 337-358; (b) N. Karousis, N. Tagmatarchis, D. Tasis, *Chem. Rev.* 2010, *110*, 5366-5397.

[11] K. Yang, B. Xing, *Chem. Rev.* 2010, *110*, 5989-6008.

[13] D. Tasis, N. Tagmatarchis, A. Bianco, M. Prato, *Chem. Rev.* 2006, *106*, 1105-1136.

[19] (a) D. Baskaran, J. W. Mays, X. P. Zhang, M. S. Bratcher, *J. Am. Chem. Soc.* 2005, *127*, 6916-6917; (b) Y.-L. Zhao, J. F. Stoddart, *Acc. Chem. Res.* 2009, *42*, 1161-1171; (c) M. Á. Herranz, C. Ehli, S. Campidelli, M. Gutiérrez, G. L. Hug, K. Ohkubo, S. Fukuzumi, M. Prato, N. Martín, D. M. Guldi, *J. Am. Chem. Soc.* 2007, *130*, 66-73; (d) N. Nakashima, Y. Tomonari, H. Murakami, *Chem. Lett.* 2002, *31*, 638-639; (e) Q. Su, S. Pang, V. Alijani, C. Li, X. Feng, K. Müllen, *Adv. Mater.* 2009, *21*, 3191-3195; (f) P. Wu, X. Chen, N. Hu, U. C. Tam, O. Blixt, A. Zettl, C. R. Bertozzi, *Angew. Chem.* 2008, *120*, 5100-5103; (g) P. Wu, X. Chen, N. Hu, U. C. Tam, O. Blixt, A. Zettl, C. R. Bertozzi, *Angew. Chem. Int. Ed.* 2008, *47*, 5022-5025; (h) G. M. A. Rahman, D. M. Guldi, S. Campidelli, M. Prato, *J. Mater. Chem.* 2006, *16*, 62-65; (i) X. Wang, Y. Liu, W. Qiu, D. Zhu, *J. Mater. Chem.* 2002, *12*, 1636-1639.

[35] (a) R. N. Grass, E. K. Athanassiou, W. J. Stark, *Angew. Chem.* 2007, *119*, 4996-4999; (b) R. N. Grass, E. K. Athanassiou, W. J. Stark, *Angew. Chem. Int. Ed.* 2007, *46*, 4909-4912; (c) I. K. Herrmann, R. N. Grass, D. Mazunin, W. J. Stark, *Chem. Mater.* 2009, *21*, 3275-3281.

[37] A. Schätz, R. N. Grass, W. J. Stark, O. Reiser, *Chem.-Eur. J.* 2008, *14*, 8262-8266.

[38] A. Schätz, R. N. Grass, Q. Kainz, W. J. Stark, O. Reiser, *Chem. Mater.* 2009, *22*, 305-310.

[48] (a) T. Rajh, L. X. Chen, K. Lukas, T. Liu, M. C. Thurnauer, D. M. Tiede, *J. Phys. Chem. B* 2002, *106*, 10543-10552; (b) C. Xu, K. Xu, H. Gu, R. Zheng, H. Liu, X. Zhang, Z. Guo, B. Xu, *J. Am. Chem. Soc.* 2004, *126*, 9938-9939; (c) N. Kohler, G. E. Fryxell, M. Zhang, *J. Am. Chem. Soc.* 2004, *126*, 7206-7211; (d) Y. Lu, Y. Yin, B. T. Mayers, Y. Xia, *Nano Lett.* 2002, *2*, 183-186; (e) A. Schätz, M. Hager, O. Reiser, *Adv. Funct. Mater.* 2009, *19*, 2109-2115.

[49] Y. Bao, K. M. Krishnan, *J. Magn. Magn. Mater.* 2005, *293*, 15-19.

[50] W. Gong, *J. Appl. Phys.* 1991, *69*, 5119.

[51] (a) M. Zeltner, A. Schatz, M. L. Hefti, W. J. Stark, *J. Mater. Chem.* 2011, *21*, 2991-2996; (b) A. Schaetz, M. Zeltner, T. D. Michl, M. Rossier, R. Fuhrer, W. J. Stark, *Chem.-Eur. J.* 2011, *17*, 10566-10573.

[52] M. d. F. F. Lelis, J. D. Fabris, W. d. N. Mussel, A. Y. Takeuchi, *Materials Research* 2003, *6*, 145-150.

[53] R. N. Panda, N. S. Gajbhiye, G. Balaji, *J. Alloys Compd.* 2001, *326*, 50-53.

[54] Z. L. Liu, Z. H. Ding, K. L. Yao, J. Tao, G. H. Du, Q. H. Lu, X. Wang, F. L. Gong, X. Chen, *J. Magn. Magn. Mater.* 2003, *265*, 98-105.
[55] D. K. Yi, S. S. Lee, G. C. Papaefthymiou, J. Y. Ying, *Chem. Mater.* 2006, *18*, 614-619.
[56] H. Bönnemann, W. Brijoux, R. Brinkmann, N. Matoussevitch, N. Waldöfner, N. Palina, H. Modrow, *Inorg. Chim. Acta* 2003, *350*, 617-624.
[57] Y. Kobayashi, M. Horie, M. Konno, B. Rodríguez-González, L. M. Liz-Marzán, *J. Phys. Chem. B* 2003, *107*, 7420-7425.
[58] (a) N. S. Sobal, M. Hilgendorff, H. Möhwald, M. Giersig, M. Spasova, T. Radetic, M. Farle, *Nano Lett.* 2002, *2*, 621-624; (b) M. Chen, *J. Appl. Phys.* 2003, *93*, 7551.
[59] (a) A.-H. Lu, W.-C. Li, N. Matoussevitch, B. Spliethoff, H. Bonnemann, F. Schuth, *Chem. Commun.* 2005, 98-100; (b) F. Michalek, A. Lagunas, C. Jimeno, M. A. Pericas, *J. Mater. Chem.* 2008, *18*, 4692-4697.
[60] (a) L. E. Euliss, S. G. Grancharov, S. O'Brien, T. J. Deming, G. D. Stucky, C. B. Murray, G. A. Held, *Nano Lett.* 2003, *3*, 1489-1493; (b) X. Liu, Y. Guan, Z. Ma, H. Liu, *Langmuir* 2004, *20*, 10278-10282; (c) R. Hong, N. O. Fischer, T. Emrick, V. M. Rotello, *Chem. Mater.* 2005, *17*, 4617-4621; (d) Y. Sahoo, H. Pizem, T. Fried, D. Golodnitsky, L. Burstein, C. N. Sukenik, G. Markovich, *Langmuir* 2001, *17*, 7907-7911; (e) M. Kim, Y. Chen, Y. Liu, X. Peng, *Adv. Mater.* 2005, *17*, 1429-1432.
[61] (a) T. Hayashi, S. Hirono, M. Tomita, S. Umemura, *Nature* 1996, *381*, 772-774; (b) W. Teunissen, F. M. F. de Groot, J. Geus, O. Stephan, M. Tence, C. Colliex, *J. Catal.* 2001, *204*, 169-174; (c) W. S. Seo, J. H. Lee, X. Sun, Y. Suzuki, D. Mann, Z. Liu, M. Terashima, P. C. Yang, M. V. McConnell, D. G. Nishimura, H. Dai, *Nat. Mater.* 2006, *5*, 971-976.
[62] M. A. Zalich, V. V. Baranauskas, J. S. Riffle, M. Saunders, T. G. St. Pierre, *Chem. Mater.* 2006, *18*, 2648-2655.
[63] Y. Lu, Z. Zhu, Z. Liu, *Carbon* 2005, *43*, 369-374.
[64] W. Xian-Wen, et al., *Nanotechnology* 2006, *17*, 4307.
[65] Y.-C. Liang, K. C. Hwang, S.-C. Lo, *Small* 2008, *4*, 405-409.
[66] Q. Kainz, Master thesis, Universität Regensburg (Regensburg), 2010.
[67] (a) M. Delamar, R. Hitmi, J. Pinson, J. M. Saveant, *J. Am. Chem. Soc.* 1992, *114*, 5883-5884; (b) P. Allongue, M. Delamar, B. Desbat, O. Fagebaume, R. Hitmi, J. Pinson, J.-M. Savéant, *J. Am. Chem. Soc.* 1997, *119*, 201-207; (c) C. Bourdillon, M. Delamar, C. Demaille, R. Hitmi, J. Moiroux, J. Pinson, *J. Electroanal. Chem.* 1992, *336*, 113-123.
[68] (a) R. Matsuno, K. Yamamoto, H. Otsuka, A. Takahara, *Macromolecules* 2004, *37*, 2203-2209; (b) S. Gu, T. Shiratori, M. Konno, *Colloid Polym. Sci.* 2003, *281*, 1076-1081; (c) F. Caruso, M. Spasova, A. Susha, M. Giersig, R. A. Caruso, *Chem. Mater.* 2000, *13*, 109-116; (d) L. P. Ramírez, K. Landfester, *Macromol. Chem. Phys.* 2003, *204*, 22-31.
[69] H. W. Kroto, J. R. Heath, S. C. O'Brien, R. F. Curl, R. E. Smalley, *Nature* 1985, *318*, 162-163.
[70] (a) S. B. Sinnott, R. Andrews, *Crit. Rev. Solid State Mater. Sci.* 2001, *26*, 145-249; (b) B. Sitharaman, X. Shi, X. F. Walboomers, H. Liao, V. Cuijpers, L. J. Wilson, A. G. Mikos, J. A. Jansen, *Bone* 2008, *43*, 362-370; (c) A. Javey, J. Guo, Q. Wang, M. Lundstrom, H. Dai, *Nature* 2003, *424*, 654-657.
[71] (a) Y. F. Yin, T. Mays, B. McEnaney, *Langmuir* 1999, *15*, 8714-8718; (b) K. Yang, B. Xing, *Environ. Pollut.* 2007, *145*, 529-537.
[72] D. Tasis, N. Tagmatarchis, V. Georgakilas, M. Prato, *Chem.-Eur. J.* 2003, *9*, 4000-4008.
[73] Y. Tomonari, H. Murakami, N. Nakashima, *Chem.-Eur. J.* 2006, *12*, 4027-4034.
[74] D. E. Bergbreiter, in *Recoverable and Recyclable Catalysts*, John Wiley & Sons, Ltd, 2009, pp. 117-153.

[75] (a) K. Eugenii, *J. Electroanal. Chem.* 1994, *365*, 157-164; (b) H. Jaegfeldt, T. Kuwana, G. Johansson, *J. Am. Chem. Soc.* 1983, *105*, 1805-1814; (c) R. J. Chen, Y. Zhang, D. Wang, H. Dai, *J. Am. Chem. Soc.* 2001, *123*, 3838-3839.

[76] W. A. Herrmann, C. W. Kohlpaintner, *Angew. Chem., Int. Ed. Engl.* 1993, *32*, 1524-1544.

[77] (a) A. F. Littke, G. C. Fu, *Angew. Chem.* 2002, *114*, 4350-4386; (b) A. F. Littke, G. C. Fu, *Angew. Chem. Int. Ed.* 2002, *41*, 4176-4211; (c) R. R. Tykwinski, *Angew. Chem.* 2003, *115*, 1604-1606; (d) R. R. Tykwinski, *Angew. Chem. Int. Ed.* 2003, *42*, 1566-1568; (e) A. C. Frisch, M. Beller, *Angew. Chem.* 2005, *117*, 680-695; (f) A. C. Frisch, M. Beller, *Angew. Chem. Int. Ed.* 2005, *44*, 674-688; (g) A. Zapf, *Angew. Chem. Int. Ed.* 2003, *42*, 5394-5399; (h) A. Zapf, *Angew. Chem.* 2003, *115*, 5552-5557.

[78] (a) W. A. Herrmann, *Angew. Chem. Int. Ed.* 2002, *41*, 1290-1309; (b) W. A. Herrmann, *Angew. Chem.* 2002, *114*, 1342-1363.

[79] W. von E. Doering, A. K. Hoffmann, *J. Am. Chem. Soc.* 1954, *76*, 6162-6165.

[80] (a) H. W. Wanzlick, E. Schikora, *Angew. Chem.* 1960, *72*, 494-494; (b) H.-W. Wanzlick, E. Schikora, *Chem. Ber.* 1961, *94*, 2389-2393.

[81] K. Öfele, *J. Organomet. Chem.* 1968, *12*, P42-P43.

[82] H.-J. Schönherr, H.-W. Wanzlick, *Chem. Ber.* 1970, *103*, 1037-1046.

[83] A. J. Arduengo, R. L. Harlow, M. Kline, *J. Am. Chem. Soc.* 1991, *113*, 361-363.

[84] (a) W. A. Herrmann, M. Elison, J. Fischer, C. Köcher, G. R. J. Artus, *Angew. Chem., Int. Ed. Engl.* 1995, *34*, 2371-2374; (b) W. A. Herrmann, L. J. Goossen, C. Köcher, G. R. J. Artus, *Angew. Chem., Int. Ed. Engl.* 1996, *35*, 2805-2807; (c) W. A. Herrmann, C. Köcher, *Angew. Chem., Int. Ed. Engl.* 1997, *36*, 2162-2187.

[85] D. Enders, H. Gielen, G. Raabe, J. Runsink, J. H. Teles, *Chem. Ber.* 1996, *129*, 1483-1488.

[86] M. Scholl, T. M. Trnka, J. P. Morgan, R. H. Grubbs, *Tetrahedron Lett.* 1999, *40*, 2247-2250.

[87] (a) S. Diez-Gonzalez, N. Marion, S. P. Nolan, *Chem Rev* 2009, *109*, 3612-3676; (b) *N-heterocyclic carbenes in transition metal catalysis*, Glorius, Frank ed., Springer, Berlin, 2007.

[88] H. V. Huynh, Y. Han, R. Jothibasu, J. A. Yang, *Organometallics* 2009, *28*, 5395-5404.

[89] (a) K. Jitsuo, O. Tamon, N. Wataru, K. Hisatoshi, *Chem. Lett.* 1988, *Vol.17* 957-960; (b) T. Okano, I. Uchida, T. Nakagaki, H. Konishi, J. Kiji, *J. Mol. Catal.* 1989, *54*, 65; (c) T. Okano, N. Okabe, J. Kiji, *Bull. Chem. Soc. Jpn.* 1992, *65*, 2589-2593; (d) C. Goux, P. Lhoste, D. Sinou, A. Masdeu, *J. Organomet. Chem.* 1996, *511*, 139-143; (e) L. Cassar, M. Foà, A. Gardano, *J. Organomet. Chem.* 1976, *121*, C55-C56; (f) D. Valentine, J. W. Tilley, R. A. LeMahieu, *J. Org. Chem.* 1981, *46*, 4614-4617; (g) N. A. Bumagin, K. V. Nikitin, I. P. Beletskaya, *J. Organomet. Chem.* 1988, *358*, 563-565.

[90] (a) R. Frenette, J. H. Hutchinson, S. Léger, M. Thérien, C. Brideau, C. C. Chan, S. Charleson, D. Ethier, J. Guay, T. R. Jones, M. McAuliffe, H. Piechuta, D. Riendeau, P. Tagari, Y. Girard, *Bioorganic and Medicinal Chemistry Letters* 1999, *9*, 2391-2396; (b) M. S. Yu, N. H. Baine, *Tetrahedron Lett.* 1999, *40*, 3123-3124; (c) P. Henley, J. Kilburn, *Chem. Commun.* 1999, 1335-1336; (d) W. H. Miller, W. E. Bondinell, R. D. Cousins, K. F. Erhard, D. R. Jakas, R. M. Keenan, T. W. Ku, K. A. Newlander, S. T. Ross, R. C. Haltiwanger, J. Bradbeer, F. H. Drake, M. Gowen, S. J. Hoffman, S.-M. Hwang, I. E. James, M. W. Lark, B. Lechowska, D. J. Rieman, G. B. Stroup, J. A. Vasko-Moser, D. L. Zembryki, L. M. Azzarano, P. C. Adams, K. L. Salyers, B. R. Smith, K. W. Ward, K. O. Johanson, W. F. Huffaman, *Bioorganic Medicinal Chemistry Letters* 1999, *9*, 1807-

1812; (e) J. R. Young, S. X. Huang, I. Chen, T. F. Walsh, R. J. DeVita, M. J. Wyvratt Jr, M. T. Goulet, N. Ren, J. Lo, Y. T. Yang, J. B. Yudkovitz, K. Cheng, R. G. Smith, *Bioorganic Medicinal Chemistry Letters* 2000, *10*, 1723-1727.

[91] A. Yamamoto, *Bull. Chem. Soc. Jpn.* 1995, *68*, 433-446.

[92] S. Mukherjee, J. W. Yang, S. Hoffmann, B. List, *Chem. Rev.* 2007, *107*, 5471-5569.

[93] E. R. Jarvo, S. J. Miller, *Tetrahedron* 2002, *58*, 2481-2495.

[94] A. Cordova, W. Notz, C. F. Barbas III, *Chem. Commun.* 2002, 3024-3025.

[95] B. List, R. A. Lerner, C. F. Barbas, *J. Am. Chem. Soc.* 2000, *122*, 2395-2396.

[96] Z. G. Hajos, D. R. Parrish, *J. Org. Chem.* 1974, *39*, 1615-1621.

[97] (a) H. Li, Y.-Y. Luk, M. Mrksich, *Langmuir* 1999, *15*, 4957-4959; (b) C. Ó Dálaigh, S. A. Corr, Y. Gun'ko, S. J. Connon, *Angew. Chem.* 2007, *119*, 4407-4410; (c) C. Ó Dálaigh, S. A. Corr, Y. Gun'ko, S. J. Connon, *Angew. Chem. Int. Ed.* 2007, *46*, 4329-4332; (d) O. Gleeson, R. Tekoriute, Y. K. Gun'ko, S. J. Connon, *Chem.-Eur. J.* 2009, *15*, 5669-5673; (e) S. Luo, X. Zheng, H. Xu, X. Mi, L. Zhang, J.-P. Cheng, *Adv. Synth. Catal.* 2007, *349*, 2431-2434; (f) G. Chouhan, D. Wang, H. Alper, *Chem. Commun.* 2007, 4809-4811; (g) M. Gruttadauria, F. Giacalone, R. Noto, *Chem. Soc. Rev.* 2008, *37*, 1666-1688; (h) M. Benaglia, G. Celentano, F. Cozzi, *Adv. Synth. Catal.* 2001, *343*, 171-173; (i) K. Kondo, T. Yamano, K. Takemoto, *Die Makromolekulare Chemie* 1985, *186*, 1781-1785; (j) V. D'Elia, H. Zwicknagl, O. Reiser, *J. Org. Chem.* 2008, *73*, 3262-3265; (k) I. Mager, K. Zeitler, *Org. Lett.* 2010, *12*, 1480-1483.

[98] (a) H. Torii, M. Nakadai, K. Ishihara, S. Saito, H. Yamamoto, *Angew. Chem. Int. Ed.* 2004, *43*, 1983-1986; (b) H. Torii, M. Nakadai, K. Ishihara, S. Saito, H. Yamamoto, *Angew. Chem.* 2004, *116*, 2017-2020.

[99] (a) Y. Hayashi, T. Sumiya, J. Takahashi, H. Gotoh, T. Urushima, M. Shoji, *Angew. Chem. Int. Ed.* 2006, *45*, 958-961; (b) Y. Hayashi, T. Sumiya, J. Takahashi, H. Gotoh, T. Urushima, M. Shoji, *Angew. Chem.* 2006, *118*, 972-975; (c) S. Aratake, T. Itoh, T. Okano, N. Nagae, T. Sumiya, M. Shoji, Y. Hayashi, *Chem.-Eur. J.* 2007, *13*, 10246-10256.

[100] F. Giacalone, M. Gruttadauria, P. L. Meo, S. Riela, R. Noto, *Adv. Synth. Catal.* 2008, *350*, 2747-2760.

[101] K. Kustin, S.-T. Liu, *J. Chem. Soc., Dalton Trans.* 1973, 278-284.

[102] A. Karmakar, T. Maji, S. Wittmann, O. Reiser, *Chem.-Eur. J.* 2011, *17*, 11024–11029.

[103] (a) C. A. McNamara, M. J. Dixon, M. Bradley, *Chem. Rev.* 2002, *102*, 3275-3300; (b) D. E. Bergbreiter, *Chem. Rev.* 2002, *102*, 3345-3384; (c) T. J. Dickerson, N. N. Reed, K. D. Janda, *Chem. Rev.* 2002, *102*, 3325-3344; (d) N. E. Leadbeater, M. Marco, *Chem. Rev.* 2002, *102*, 3217-3274.

[104] (a) F. E. Hahn, M. C. Jahnke, V. Gomez-Benitez, D. Morales-Morales, T. Pape, *Organometallics* 2005, *24*, 6458-6463; (b) F. E. Hahn, M. C. Jahnke, T. Pape, *Organometallics* 2006, *25*, 5927-5936; (c) F. E. Hahn, M. C. Jahnke, T. Pape, *Organometallics* 2006, *26*, 150-154; (d) D. Pugh, A. A. Danopoulos, *Coord. Chem. Rev.* 2007, *251*, 610-641; (e) N. Selander, K. I. n. J. Szabó, *Chem. Rev.* 2010, *111*, 2048-2076; (f) W. A. Herrmann, V. P. W. Böhm, C. W. K. Gstöttmayr, M. Grosche, C.-P. Reisinger, T. Weskamp, *J. Organomet. Chem.* 2001, *617-618*, 616-628.

[105] T. Kang, Q. Feng, M. Luo, *Synlett* 2005, *2005*, 2305-2308.

[106] N. B. Jokic, C. S. Straubinger, S. Li Min Goh, E. Herdtweck, W. A. Herrmann, F. E. Kühn, *Inorg. Chim. Acta* 2010, *363*, 4181-4188.

[107] W. Chen, B. Wu, K. Matsumoto, *J. Organomet. Chem.* 2002, *654*, 233-236.

[108] M. V. Baker, B. W. Skelton, A. H. White, C. C. Williams, *J. Chem. Soc., Dalton Trans.* 2001, 111-120.
[109] (a) E. Alcalde, R. M. Ceder, C. Lopez, N. Mesquida, G. Muller, S. Rodriguez, *Dalton Trans.* 2007, 2696-2706; (b) A. M. Magill, D. S. McGuinness, K. J. Cavell, G. J. P. Britovsek, V. C. Gibson, A. J. P. White, D. J. Williams, A. H. White, B. W. Skelton, *J. Organomet. Chem.* 2001, *617-618*, 546-560.
[110] (a) R. K. Arvela, N. E. Leadbeater, *Org. Lett.* 2005, *7*, 2101-2104; (b) R. K. Arvela, N. E. Leadbeater, *J. Org. Chem.* 2005, *70*, 1786-1790.
[111] N. T. S. Phan, M. Van Der Sluys, C. W. Jones, *Adv. Synth. Catal.* 2006, *348*, 609-679.
[112] D. R. Anton, R. H. Crabtree, *Organometallics* 1983, *2*, 855-859.
[113] (a) G. C. Georgiades, P. A. Sermon, *J. Chem. Soc., Chem. Commun.* 1985, 975-976; (b) C. S. Consorti, F. R. Flores, J. Dupont, *J. Am. Chem. Soc.* 2005, *127*, 12054-12065.
[114] R. Marcilla, M. L. Curri, P. D. Cozzoli, M. T. Martínez, I. Loinaz, H. Grande, J. A. Pomposo, D. Mecerreyes, *Small* 2006, *2*, 507-512.
[115] (a) A. Riisager, P. Wasserscheid, R. van Hal, R. Fehrmann, *J. Catal.* 2003, *219*, 452-455; (b) A. Riisager, R. Fehrmann, S. Flicker, R. van Hal, M. Haumann, P. Wasserscheid, *Angew. Chem.* 2005, *117*, 826-830; (c) A. Riisager, R. Fehrmann, S. Flicker, R. van Hal, M. Haumann, P. Wasserscheid, *Angew. Chem. Int. Ed.* 2005, *44*, 815-819.
[116] (a) A. Riisagera, R. Fehrmanna, M. Haumannb, P. Wasserscheidb, *Top. Catal.* 2006, *40*, 91-102; (b) H. Olivier-Bourbigou, L. Magna, D. Morvan, *Appl. Catal., A* 2010, *373*, 1-56; (c) C. Van Doorslaer, J. Wahlen, P. Mertens, K. Binnemans, D. De Vos, *Dalton Trans.* 2010, *39*, 8377-8390.
[117] (a) A. Riisager, B. Jorgensen, P. Wasserscheid, R. Fehrmann, *Chem. Commun.* 2006, 994-996; (b) L.-L. Lou, X. Peng, K. Yu, S. Liu, *Catal. Commun.* 2008, *9*, 1891-1893.
[118] (a) D. W. Kim, D. Y. Chi, *Angew. Chem. Int. Ed.* 2004, *43*, 483-485; (b) D. W. Kim, D. Y. Chi, *Angew. Chem.* 2004, *116*, 489-491.
[119] (a) M. Ruta, I. Yuranov, P. J. Dyson, G. Laurenczy, L. Kiwi-Minsker, *J. Catal.* 2007, *247*, 269-276; (b) L. Rodriguez-Perez, E. Teuma, A. Falqui, M. Gomez, P. Serp, *Chem. Commun.* 2008, 4201-4203.
[120] M. Gruttadauria, S. Riela, P. Lo Meo, F. D'Anna, R. Noto, *Tetrahedron Lett.* 2004, *45*, 6113-6116.
[121] (a) S. Doherty, P. Goodrich, C. Hardacre, V. Pârvulescu, C. Paun, *Adv. Synth. Catal.* 2008, *350*, 295-302; (b) P. Goodrich, C. Hardacre, C. Paun, A. Ribeiro, S. Kennedy, M. J. V. Lourenço, H. Manyar, C. A. N. de Castro, M. Besnea, V. I. Pârvulescu, *Adv. Synth. Catal.* 2011, *353*, 995-1004.
[122] M. Lombardo, M. Chiarucci, C. Trombini, *Green Chem.* 2009, *11*, 574-579.
[123] A. De Mico, R. Margarita, L. Parlanti, A. Vescovi, G. Piancatelli, *J. Org. Chem.* 1997, *62*, 6974-6977.
[124] M. Hager, S. Wittmann, A. Schätz, F. Pein, P. Kreitmeier, O. Reiser, *Tetrahedron: Asymmetry* 2010, *21*, 1194-1198.
[125] R. Rasappan, M. Hager, A. Gissibl, O. Reiser, *Org. Lett.* 2006, *8*, 6099-6102.
[126] (a) I. S. Kim, M.-Y. Ngai, M. J. Krische, *J. Am. Chem. Soc.* 2008, *130*, 14891-14899; (b) I. S. Kim, M.-Y. Ngai, M. J. Krische, *J. Am. Chem. Soc.* 2008, *130*, 6340-6341.
[127] Y. Lu, I. S. Kim, A. Hassan, D. J. Del Valle, M. J. Krische, *Angew. Chem. Int. Ed.* 2009, *48*, 5018-5021.

C. Summary

1. Noncovalent attachment of catalysts

The noncovalent immobilization of catalysts offers promising features that the covalent linkage is lacking. For example, it is possible to perform reactions in a homogeneous way by desorbing the catalyst during the reaction at elevated temperature or to renew the catalyst loading after a few runs.

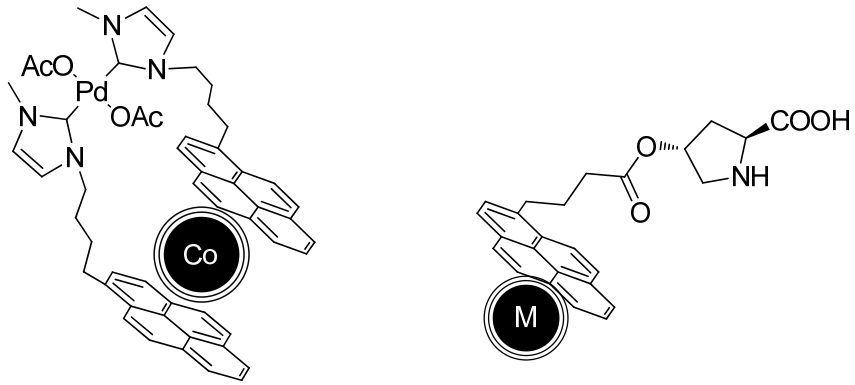

15 **68**: M = Co
69: M = Fe

Figure 37: Catalysts 15, 68 and 69 immobilized by π-π interactions on magnetic carbon coated metal nanoparticles.

π-π interactions between the aromatic surfaces of magnetic carbon coated metal nanoparticles and pyrene moieties create sufficiently strong forces to bind the catalysts 15, 68 and 69 in aqueous media to the surface of the particles and to recover them by magnetic decantation (Figure 38). In comparison to covalent linkage on the nanobeads almost twice as much loading could be achieved.[37, 48e]

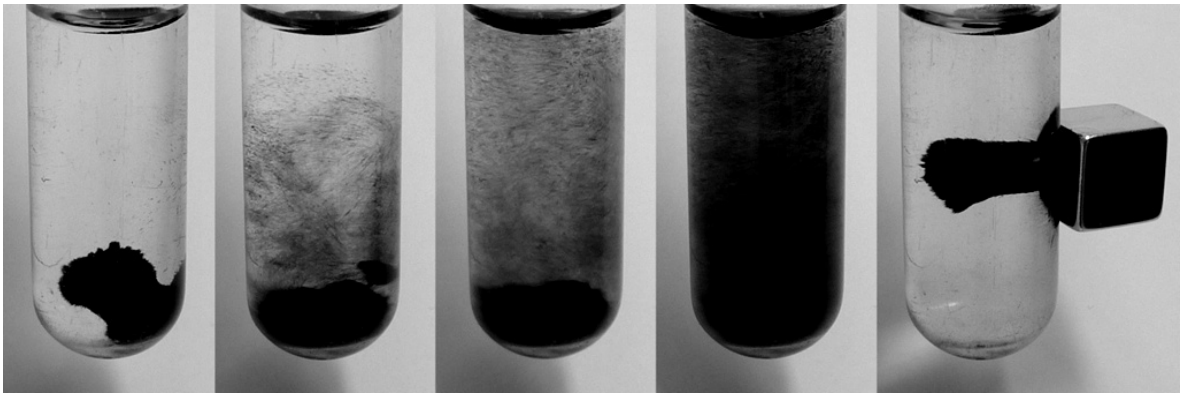

Figure 38: 15 on Co@C nanoparticles on different stages of dispersion and simple recovery by applying an external magnet (right).

The catalyst 15 was tested in the hydroxycarbonylation of aryl halides with carbon monoxide in water at elevated temperatures.[44] Desorption studies suggest that the catalyst can desorb at elevated temperatures from the surface of the nanoparticle and catalyze the reaction in a homogeneous way. After cooling down to ambient temperature the catalyst could be recovered quantitatively by applying an external magnet. 18 runs were performed with this catalyst with little loss in activity.

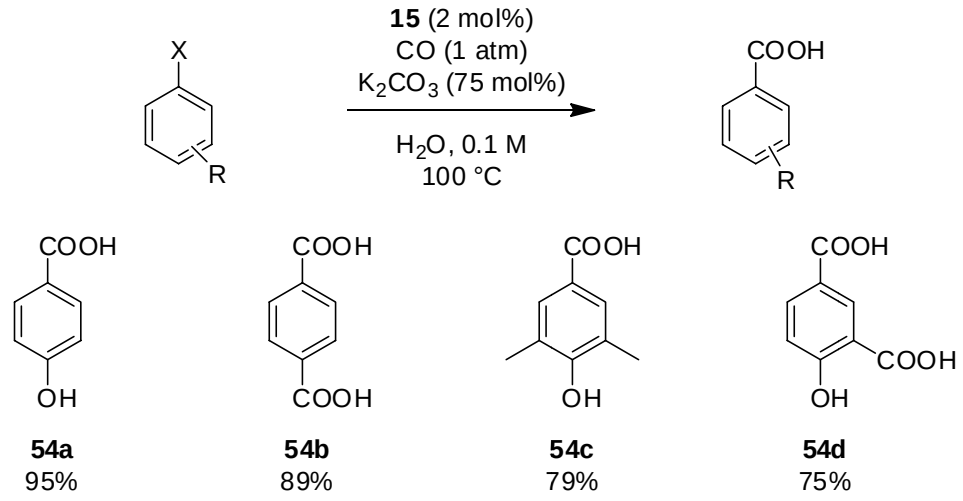

Figure 39: Scope of the hydroxycarbonylation catalyzed by the noncovalent catalytic system 15.

The possibility to renew the catalyst loading after a few cycles was demonstrated the pyrene tagged proline catalyst 68. Catalysts of this type have been recycled only up to 5 times, after which the catalyst attached to the support has to be exchanged.[97g] In the case of the

pyrene tagged proline 68 the loading was renewed by simply desorbing the altered catalyst with methanol. After the immobilization of a new batch of 62a, the system could be reused four more times with the same performance.

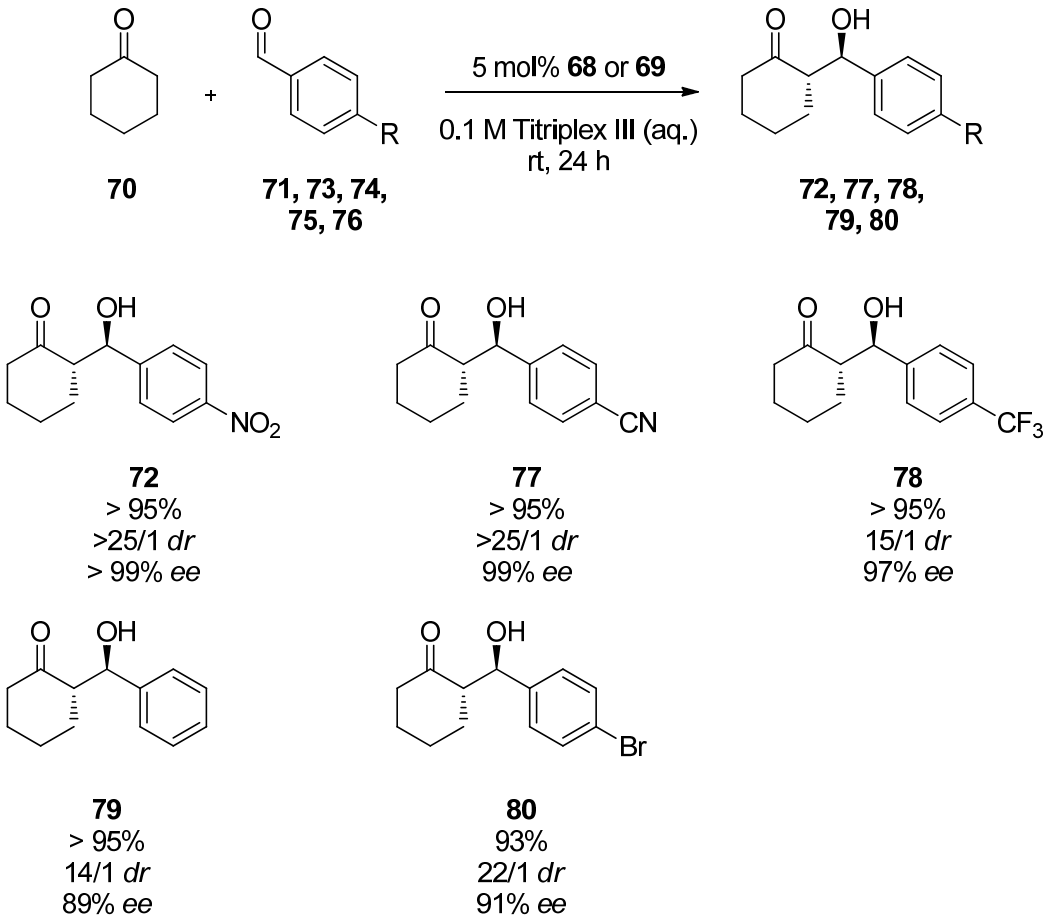

Figure 40: Substrate scope of the aldol reaction catalyzed by the noncovalent catalytic systems 68 and 69.

In summary, a new noncovalent immobilization method based on π-π interactions between graphene like coated magnetic nanoparticles and pyrene tagged catalysts was established. The hydroxycarbonylation of aryl halides with 15 could be carried out in 16 consecutive runs yielding the corresponding carboxylic acids in good to excellent yields. In the case of the by the hydroxyproline derivative 62a catalyzed aldol reaction the renewal of the catalyst loading allowed twelve consecutive runs with the same support.

2. Covalent attachment of catalysts

As pointed out in the introduction, the covalent immobilization of catalysts onto polymeric supports is a topic of great interest. One of the main problems of this approach is the necessity to precipitate soluble polymers after the reaction in order to recover them. One way to overcome this problem is the attachment of the polymer onto a magnetic support to simply recover the hybrid system by applying an external magnet. The covalent attachment of the Pd-NHC complex 100 provided a loading of 0.6 mmol/g catalyst on polymer coated magnetic iron nanoparticles. This value is seven times higher than the previously used covalent immobilization methods without the aid of a polymer.[37, 48e]

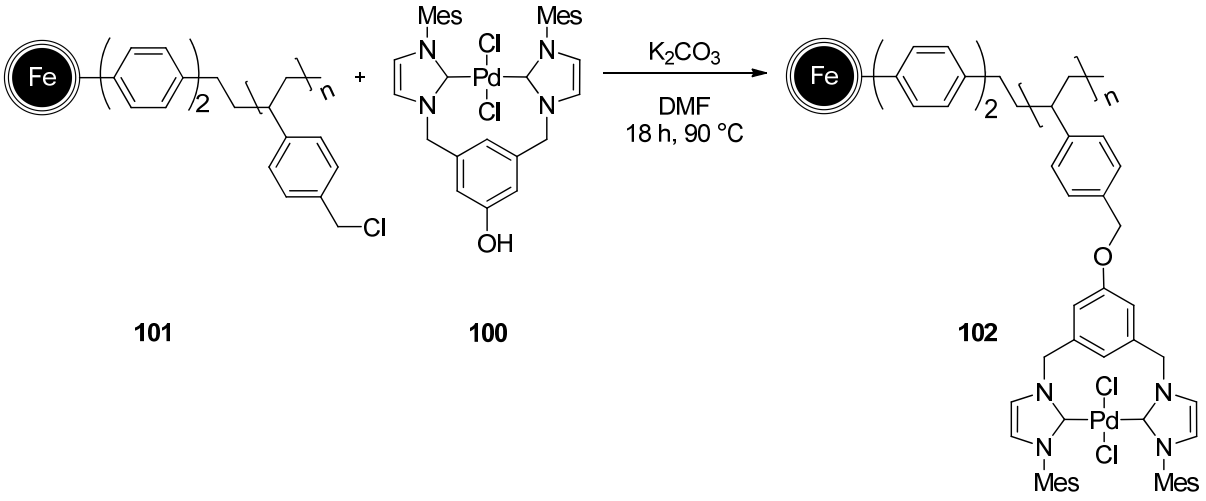

101 **100** **102**

Scheme 28: Covalent immobilization of the Pd-NHC complex 100 onto polymer coated magnetic iron nanoparticles 101.

The catalyst 102 was tested in the Suzuki-Miyaura cross coupling of aryl halides with arylboronic acids and proved to be highly active. Even aryl chlorides were amenable under microwave conditions whereby the nanoparticle core could be used as an internal microwave absorber. After the reaction the catalyst could be recovered by magnetic decantation.

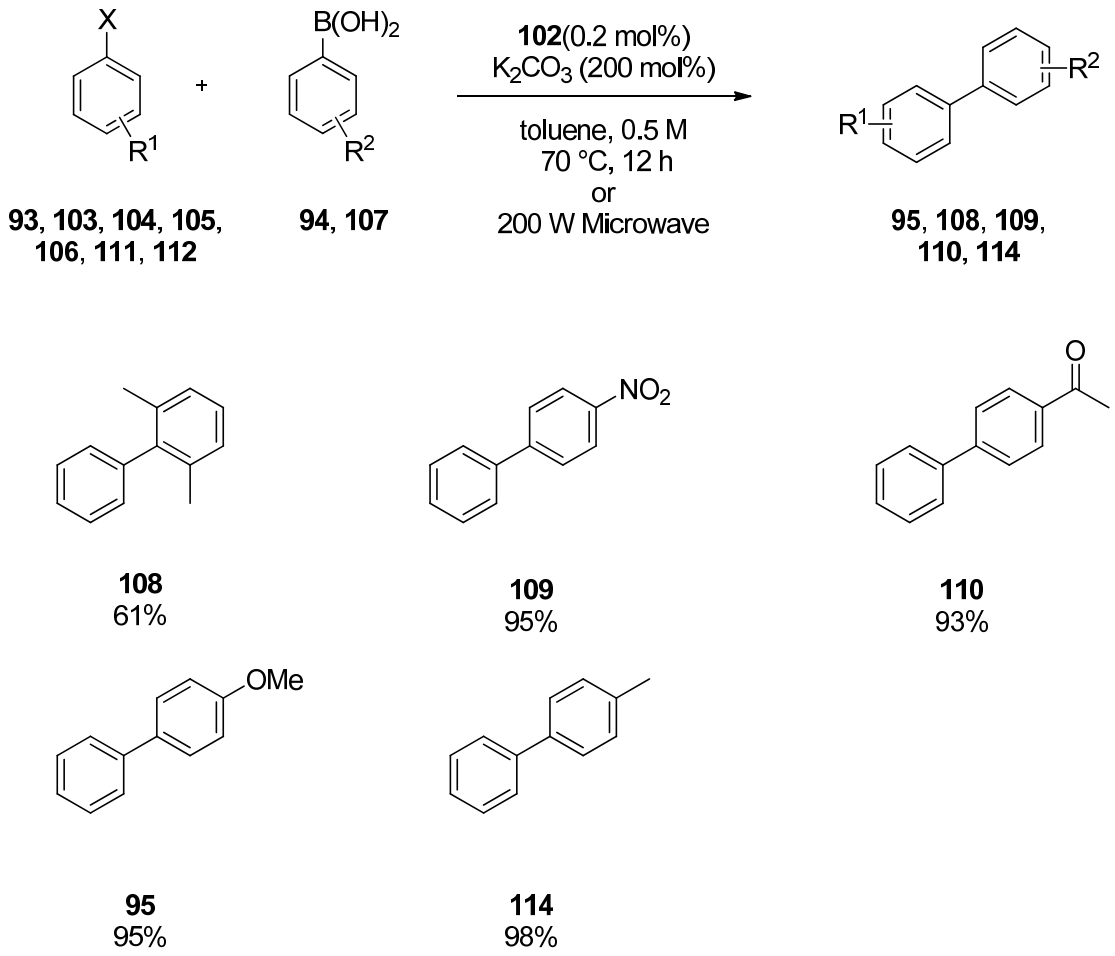

Figure 41: Substrate scope of the Suzuki coupling catalyzed by the polymeric supported catalyst 102.

In summary a versatile Pd-NHC complex could be synthesized, which was successfully grafted onto polymer coated magnetic iron nanoparticles. The resulting catalytic system was active in the Suzuki-Miyaura cross coupling of aryl halides, particularly chlorides, under microwave conditions.

3. Assessment of relative reaction rates

Beside the approaches to immobilize various catalysts on nanoparticles a new simple approach for the assessment of catalyst activities was developed in cooperation with M. Hager. The well known Michael-addition of benzylidene malonates to indoles was chosen as a model reaction.[124]

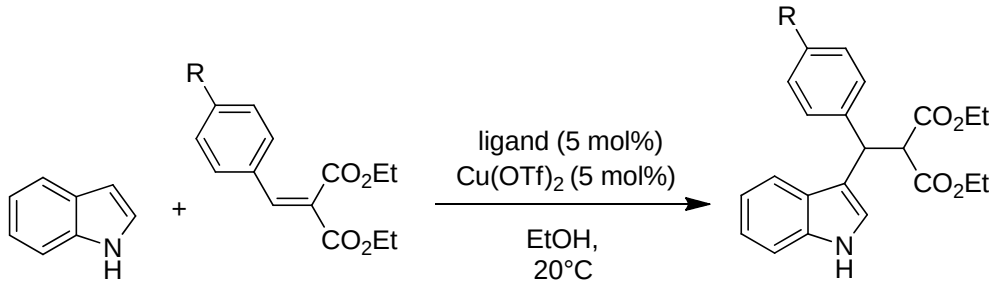

132 **133 a-d** **134 a-d**

Scheme 29: Michael-addition of benzylidene malonates to indole catalyzed by copper(II) catalysts.

Unlike most other methods that require the meticulous measurement of increments over a long time, the developed method uses only the resulting enantioselectivity of a competitive experiment of two ligands with antipodal stereochemical induction. For the deduction of relative reaction rate by the following formula was derived:

$$v_{rel} = \frac{ee_r - ee_2}{ee_1 - ee_r}$$

v_{rel} = relative reaction rate

ee_1 = enantioselectivity of ligand 1

ee_2 = enantioselectivity of ligand 2

ee_r = resulting enantioselectivity using both ligands

Various bis(oxazoline) and azabis(oxazoline) ligands were tested in competitive reactions and their relative reaction rates were determined according to the aforementioned formula by measurement of the resulting *ee* value. The results of the comparison experiments are depicted in Scheme 30.

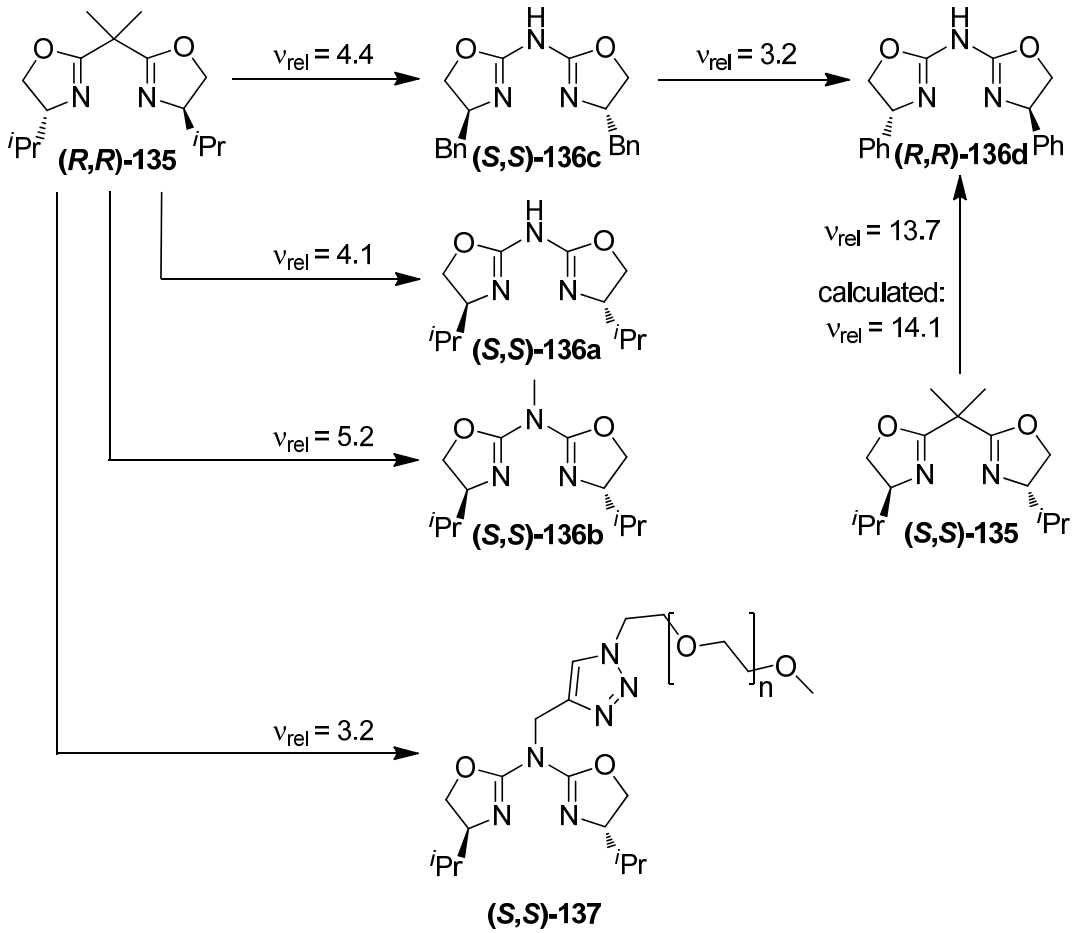

Scheme 30: Overview of the tested ligand combinations with the corresponding calculated relative reaction rates.

Notably, the calculated value of the ligands (*R*,*R*)-135 and (*S*,*S*)-135 could be reproduced in good accordance to the competition experiment showing the high reliability of this approach. Moreover, not only homogeneous ligands were tested, but also the activity of ligand 137 immobilized on MeOPEG resin could be accessed. As this method is an endpoint measurement effects like induction times or nonlinear effects cannot be assessed with this approach. In summary the newly established method is applicable for the rapid and simple determination of relative rate ratios of catalyst.

4. References

[37] A. Schätz, R. N. Grass, W. J. Stark, O. Reiser, *Chem.-Eur. J.* 2008, *14*, 8262-8266.

[44] (a) S. Wittmann, A. Schätz, R. N. Grass, W. J. Stark, O. Reiser, *Angew. Chem. Int. Ed.* 2010, *49*, 1867-1870; (b) S. Wittmann, A. Schätz, R. N. Grass, W. J. Stark, O. Reiser, *Angew. Chem.* 2010, *122*, 1911-1914.

[48] (a) T. Rajh, L. X. Chen, K. Lukas, T. Liu, M. C. Thurnauer, D. M. Tiede, *J. Phys. Chem. B* 2002, *106*, 10543-10552; (b) C. Xu, K. Xu, H. Gu, R. Zheng, H. Liu, X. Zhang, Z. Guo, B. Xu, *J. Am. Chem. Soc.* 2004, *126*, 9938-9939; (c) N. Kohler, G. E. Fryxell, M. Zhang, *J. Am. Chem. Soc.* 2004, *126*, 7206-7211; (d) Y. Lu, Y. Yin, B. T. Mayers, Y. Xia, *Nano Lett.* 2002, *2*, 183-186; (e) A. Schätz, M. Hager, O. Reiser, *Adv. Funct. Mater.* 2009, *19*, 2109-2115.

[97] (a) H. Li, Y.-Y. Luk, M. Mrksich, *Langmuir* 1999, *15*, 4957-4959; (b) C. Ó Dálaigh, S. A. Corr, Y. Gun'ko, S. J. Connon, *Angew. Chem.* 2007, *119*, 4407-4410; (c) C. Ó Dálaigh, S. A. Corr, Y. Gun'ko, S. J. Connon, *Angew. Chem. Int. Ed.* 2007, *46*, 4329-4332; (d) O. Gleeson, R. Tekoriute, Y. K. Gun'ko, S. J. Connon, *Chem.-Eur. J.* 2009, *15*, 5669-5673; (e) S. Luo, X. Zheng, H. Xu, X. Mi, L. Zhang, J.-P. Cheng, *Adv. Synth. Catal.* 2007, *349*, 2431-2434; (f) G. Chouhan, D. Wang, H. Alper, *Chem. Commun.* 2007, 4809-4811; (g) M. Gruttadauria, F. Giacalone, R. Noto, *Chem. Soc. Rev.* 2008, *37*, 1666-1688; (h) M. Benaglia, G. Celentano, F. Cozzi, *Adv. Synth. Catal.* 2001, *343*, 171-173; (i) K. Kondo, T. Yamano, K. Takemoto, *Die Makromolekulare Chemie* 1985, *186*, 1781-1785; (j) V. D'Elia, H. Zwicknagl, O. Reiser, *J. Org. Chem.* 2008, *73*, 3262-3265; (k) I. Mager, K. Zeitler, *Org. Lett.* 2010, *12*, 1480-1483.

[124] M. Hager, S. Wittmann, A. Schätz, F. Pein, P. Kreitmeier, O. Reiser, *Tetrahedron: Asymmetry* 2010, *21*, 1194-1198.

D. Experimental

1. General comments

All reactions were carried out in oven dried glassware under an atmosphere of dry nitrogen gas unless otherwise indicated. Commercially available reagents were used as received. Carbon coated cobalt nanoparticles were donated from Prof. W. J. Stark (ETH Zürich). Magnetic nanobeads were dispersed with the aid of an ultrasound bath (Sonorex RK 255 H-R, Bandelin) and recovered with the aid of a neodymium based magnet (N48, W-12-N, Webcraft GmbH, side length 12 mm) unless stated otherwise. The following solvents and reagents were purified prior to use: Dichloromethane (DCM) was distilled from calcium hydride. Ethanol (EtOH) and methanol (MeOH) were distilled from magnesium and stored over molecular sieves (3 Å). Tetrahydrofurane (THF) was distilled from sodium wire. Toluene was dried with CaH_2, distilled and stored over sodium wire. Ethylacetate (EA) and hexanes (PE) for chromatographic separations were distilled before use.
Analytical thin layer chromatography was performed on Merck TLC aluminum sheets silica gel 60 F254. Visualization was accomplished with UV light and vanillin solution followed by heating. Liquid chromatography was performed using Merck silica gel 60 (70-230 mesh ASTM).

NMR spectroscopy
^1H (300 MHz) NMR spectra were recorded on a Bruker AC 300 spectrometer at ambient temperature. Chemical shift in ppm from internal $CHCl_3$ (7.27 ppm) as standard on the δ scale, multiplicity (b = broad, s = singlet, d = doublet, t = triplet, q = quartet and m = multiplet), integration and coupling constant (Hz). ^{13}C (75.5 MHz) NMR spectra were recorded on a Bruker AC 300 spectrometer at ambient temperature. Chemical shifts are reported in ppm from internal $CHCl_3$ (77 ppm) as standard on the δ scale.

HPLC

Chiral HPLC was performed on a Varian 920 LC using chiral-pack AS-H, OD-H, OJ-H and OJ columns.

GC

Gas chromatography was performed on a Fisons GC 8000. CP-Chirasil-Dex CB (25m x 0.25mm Di, 0.25µm Film) was used as chiral stationary phase.

Melting points

The melting points were meassured on a Büchi SMP-20 apparatus in silicon oilbath. Values thus obtained were not corrected.

Alpha

The optical rotation was determined in a Perkin Elmer 241 polarimeter at 589 nm wavelength (sodium-d-line) in a 1.0 dm measuring cell of 2 mL volume.

Mass spectrometry

Mass spectrometry was performed using a Finnigan ThermoQuest TSQ 7000 at the Central Analytical Laboratory of the Universität Regensburg.

IR spectroscopy

ATR-IR spectroscopy was carried out on a Biorad Excalibur FTS 3000 spectrometer, equipped with a Specac Golden Gate Diamond Single Reflection ATR-System.

Elemental microanalysis

Elemental microanalysis was performed on a LECO CHN-900 at the ETH Zürich.
At the Universität Regensburg a HERAEUS Mikro-Rapid CHN was used.

TEM

ETH-Zürich:

Transmission electron microscopy was carried out with a Philips CM30 ST equipped with a LaB_6 cathode and operated at 300 kV point resolution (~ 4 Å) at the ETH Zürich.

Universitätsklinikum Regensburg:

For TEM measurements sample suspension drops were placed on Formvar- and carbon-coated positively glow-discharge treated cupper grid (400 mesh) and subsequently blotted dry with a filter paper. The samples were examined in a LEO912AB electron microscope (Zeiss, Oberkochen/Germany) operating at 100 kV, equipped with a side-mounted CCD-camera capable to record images with 1kx1k pixels. The documentation was done with the iTEM-software, Ver. 5.0 (Olympus Soft Imaging Solutions GmbH, Muenster/Germany).

ICP-OES

Samples were examined on a Spectro Analytical Instruments ICP Modula EOP.

UV/Vis

Spectra were recorded at Varian Cary 50 Bio UV/VIS spectrometer.

2. Syntheses of literature-known compounds

The following compounds were prepared according to literature procedures:

4-nitrophenyl 4-(pyren-1-yl)butanoate (45)[128], 1-(4-bromo-butyl)-pyrene (50)[129], (2*S*,4*R*)-4-(4-(pyren-1-yl)butanoyloxy)pyrrolidine-2-carboxylic acid (62a)[100], 3,5-bis(bromomethyl)-phenol (96)[130], 1-mesityl-1H-imidazole (97)[131], 1-azido-3-iodopropane (118)[132], 1-(nitrophenyl)-2-propyn-1-one (121)[133], 2,2,6,6-tetramethyl-4-(prop-2-ynyloxy)piperidine-1-oxyl (125)[37], (*S*)-4-*iso*propyl-N-((*S*)-4-*iso*propyl-4,5-dihydrooxazol-2-yl)-*N*-(prop-2-ynyl)-4,5-dihydrooxazol-2-amine (131)[134], diethyl 2-benzylidenemalonate (133a)[135], diethyl 2-(4-methyl-benzylidene)malonate (133b)[135], diethyl 2-(4-chlorobenzylidene)-malonate (133c)[135], MEOPEG-N_3 (146)[136].

3. Synthesis of ligands and complexes

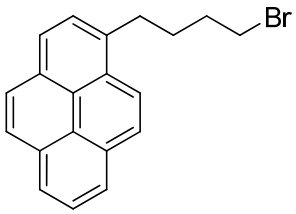

1-(4-bromobutyl)pyrene (50):

Prepared by a modified procedure according to Smith.[129]

To a solution of 800 mg (2.9 mmol) 4-(pyren-1-yl)butan-1-ol in 20 mL DCM 920 mg (3.5 mmol, 1.2 eq.) of PPh_3 were added. After cooling down to 0 °C, 1.94 g (5.9 mmol, 2 eq.) CBr_4 were added and the solution was warmed to ambient temperature. After 20 minutes the reaction was quenched with 30 mL sat. $NaHCO_3$-solution, the phases were separated and the aqueous layer was extracted twice with DCM. The combined organic layers were dried over Na_2SO_4 and the solvent was removed under reduced pressure. Further purification of the crude product by silica gel column chromatography (PE/EA 24:1) furnished 605 mg (1.8 mmol) of 50 as a light sensitive pale brown powder in 62% yield.

^{1}H-NMR (300 MHz, $CDCl_3$): δ = 8.26 (d, J=9.3, 1H), 8.21 - 8.09 (m, 4H), 8.06 - 7.96 (m, 3H), 7.89 - 7.81 (m, 1H), 3.53 - 3.41 (m, 2H), 3.41 - 3.30 (m, 2H), 2.09 - 1.95 (m, 4H); - ^{13}C-NMR (75.5 MHz, $CDCl_3$): δ = 136.1, 131.5, 131.0, 130.0, 128.6, 127.5, 127.3, 127.2, 126.7, 125.8, 125.1, 125.0, 124.9, 124.8, 124.7, 123.2, 33.6, 32.6, 32.6, 30.2.

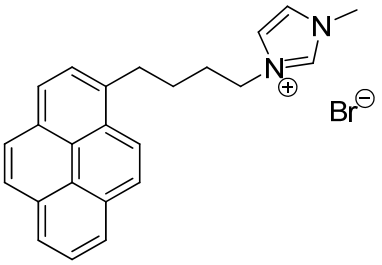

1-methyl-3-(4-(pyren-1-yl)butyl)-1H-imidazol-3-ium bromide (52):

To a solution of 250 mg (0.74 mmol) 4-(4-bromobutyl)pyrene 50 dissolved in 25 mL acetonitrile 60 µL (0.74 mmol, 1.0 eq.) 1-methyimidazole 51 were added and refluxed for 20 h. After evaporating the solvent, silica gel column chromatography of the residue (DCM/MeOH 9:1) afforded 305 mg (0.73 mmol) 52 as a yellow solid in 98% yield.

^{1}H-NMR (300 MHz, DMSO): δ = 1.76 (m, 2H), 1.96 (m, 2H), 3.38 (m, 2H), 3.83 (s, 3H), 4.26 (t, 2H, J = 7.0Hz), 7.71 (t, 1H, J = 1.6Hz), 7.81 (t, 1H, J = 1.6Hz), 8.20 (m, 8H), 9.18 (s, 1H); - ^{13}C-NMR (75.5 MHz, DMSO): δ = 136.4, 136.2, 130.8, 130.3, 129.2, 128.0, 127.4, 127.3, 127.2, 126.5, 126.1, 125.0, 124.9, 124.7, 124.1, 124.0, 123.5, 123.3, 122.2, 48.5, 35.7, 31.8, 29.4, 27.8; - IR (neat) $\tilde{\nu}$ = 1774, 1589, 1509, 1485, 1413, 1341, 1216, 1159, 1106, 1094, 927, 838, 738, 710, 680, 649, 610, 581, 526, 459; - MS (EI): m/z = 338.9 (M^+), 339.9; - HRMS (LSI-MS) [M^+]: found 339.1861, calculated 339.1860.

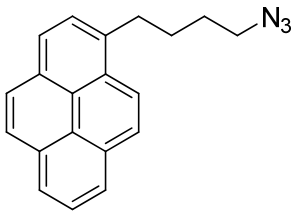

1-(4-azidobutyl)pyrene (147):

250 mg (0.74 mmol) 1-(4-bromobutyl)pyrene 50 were stirred with 480 mg NaN_3 (7.4 mmol, 10.0 eq.) in 30 mL DMF at 70 °C. After 24 hours 20 mL DCM were added to the mixture. Subsequent extraction with water, followed by drying over $MgSO_4$ and evaporation of the solvent furnished 219 mg (0.73 mmol) of 147 in 99% yield.

^{1}H-NMR (300 MHz, $CDCl_3$) δ = 8.25 - 7.75 (m, 9H), 3.30 (dt, *J* = 11.8, 7.1, 4H), 1.90 (ddd, *J* = 11.9, 9.7, 7.3, 2H), 1.72 (tt, *J* = 6.9, 3.7, 2H); - ^{13}C-NMR (75 MHz, $CDCl_3$) δ = 136.1, 131.5, 130.9, 129.9, 128.6, 127.5, 127.4, 127.2, 126.7, 125.9, 125.1, 125.0, 125.0, 124.8, 124.8, 123.2, 51.4, 33.0, 28.9, 28.8; - IR (neat) $\tilde{\nu}$ = 3045, 2938, 2865, 2090, 1601, 1582, 1486, 1466, 1414, 1208, 1279, 1245, 1183, 1102, 892, 839, 816, 758, 726, 709, 680, 667, 645, 608; - MS (EI): m/z (%) = 299. 1 ($M^{+\bullet}$, 55), 242.1 (33), 227 (81), 215 (M-$C_3H_6N_3^+$, 100), 213 (22); - HRMS (EIMS) [$M^{+\bullet}$]: found 299.1422, calculated 299.1422.

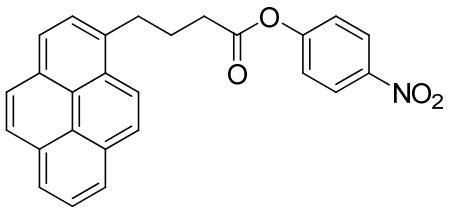

4-nitrophenyl 4-(pyren-1-yl)butanoate (45):

Prepared by a modified procedure according to Ueno.[128]

A solution of 300 mg (1.0 mmol) 43, 307 mg (1.0 mmol, 1.0 eq.) DCC and 13 mg (0.1 mmol, 0.1 eq.) DMAP in 60 mL DCM was stirred at room temperature for 20 minutes. After the addition of 150 mg (1.1 mmol, 1.05 eq.) of 4-nitrophenol 44 the mixture was stirred for additional 7 h. Subsequent evaporation of the solvent the crude mixture was purified by a

silica gel column (PE/DCM 1:1) to yield 389 mg (0.95 mmol) of 45 in 91% yield as a pale yellow solid.

^{1}H-NMR (300 MHz, $CDCl_3$): δ = 8.31 (d, J=9.3, 1H), 8.23 - 8.10 (m, 6H), 8.07 - 7.97 (m, 3H), 7.89 (d, J=7.8, 1H), 7.21 - 7.10 (m, 2H), 3.54 - 3.41 (m, 2H), 2.72 (t, J=7.2, 2H), 2.43 - 2.25 (m, 2H); - ^{13}C-NMR (75.5 MHz, $CDCl_3$): δ = 171.0, 155.3, 145.2, 135.0, 131.4, 130.9, 130.2, 128.8, 127.6, 127.5, 127.4, 126.9, 126.0, 125.2, 125.0, 124.9, 124.9, 123.1, 122.3, 33.8, 32.6, 26.4.

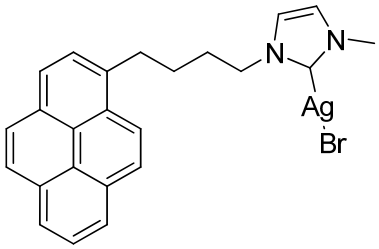

(1-methyl-3-(4-(pyren-1-yl)butyl)-2,3-dihydro-1H-imidazol-2-yl)silver(II) bromide (148):
To a solution of 210 mg (0.5 mmol) of 1-methyl-3-(4-(pyren-1-yl)butyl)-1H-imidazol-3-ium bromide 52 in 10 mL MeOH 70 mg (0.3 mmol, 0.6 eq.) Ag_2O were added. After stirring 24 hours in the dark the solution was filtered. Evaporation of the solvent gave 195 mg (0.37 mmol) of an off-white powder as product in 74% yield.

^{1}H-NMR (300 MHz, MeOD): δ = 7.84 - 7.72 (m, 2H), 7.71 - 7.62 (m, 1H), 7.61 - 7.48 (m, 5H), 7.17 (d, J=7.8, 1H), 6.61 (s, 2H), 3.13 (d, J=5.9, 2H), 2.94 (s, 3H), 2.65 (dd, J=11.9, 3.6, 2H), 1.25 - 1.07 (m, 4H); - ^{13}C-NMR (75.5 MHz, MeOD): δ = 170.3, 136.9, 132.5, 132.0, 131.0, 129.5, 128.4, 128.2, 128.1, 127.6, 127.0, 126.0, 125.9, 125.8, 125.7, 124.1, 123.2, 122.3, 51.9, 38.3, 33.2, 31.7, 29.2; - MS (ESI-MS, m/z) $C_{48}H_{44}AgN_4^+$ [L_2Ag^+]: 783.3.

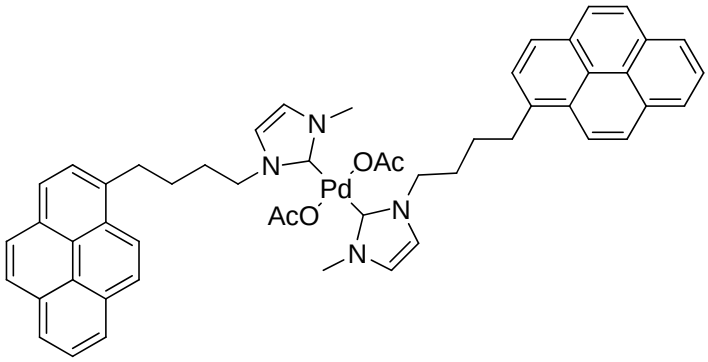

bis(1-methyl-3-(4-(pyren-1-yl)butyl)-1H-imidazol-2(3H)-ylidene)palladium(II) acetate (19): 100 mg (0.24 mmol) of 52 were stirred together with 27 mg $Pd(OAc)_2$ in 10 mL DMSO at 50 °C under nitrogen atmosphere for 48 h. After evaporation of the solvent, the residue was purified by column chromatography (DCM/MeOH 9:1) to afford 99 mg (0.1 mmol) of 19 in 88% yield.

^{1}H-NMR (300 MHz, $CDCl_3$): δ = 1.99 (m, 4H), 2.30 (m, 4H), 3.46 (t, 4H, J=7.7Hz), 3.65 (s, 6H), 4.07 (s, 6H), 4.52 (t, 4H, J=7.5Hz), 6.77 (d, 4H, J=1.7Hz), 6.82 (d, 2H, J=1.9Hz), 7.63 (t, 2H, J=1.3Hz), 7.91 (d, 2H, J=7.8Hz), 8.06 (m, 12H); - ^{13}C-NMR (75.5 MHz, $CDCl_3$): δ = 148.9, 140.3, 136.4, 131.4, 130.9, 130.3, 129.8, 128.6, 127.5, 127.4, 127.3, 126.6, 125.8, 125.0, 125.0, 124.8, 124.8, 124.7, 123.5, 122.8, 121.7, 119.8, 51.0, 38.4, 34.2, 33.0, 30.2, 28.8; - IR (neat) $\tilde{\nu}$ = 3132, 2924, 2854, 1736, 1603, 1535, 1470, 1420, 1376, 1233, 1108, 847, 743, 687, 667, 618, 525, 460; - MS (ESI-MS, m/z) $C_{50}H_{47}N_4O_2Pd^-$ $[(L_2Pd^{2+} + OAc^-)^+]$: 841.3.

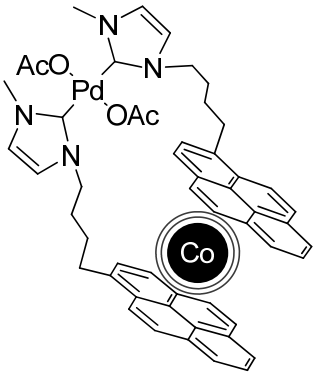

Immobilization of 19 on Co@C nanoparticles (15):

200 mg Co@C nanoparticles and 20 mg of 19 in 5 mL water were sonicated for 1 hour. After stirring overnight and one hour sonication the particles were washed 10 times with 10 mL of water. With the aid of a neodymium based magnet the particles were recovered and dried under vacuum to afford 205 mg of 15.

IR (neat) $\tilde{\nu}$ = 2929, 2857, 1737, 1465, 1376, 1266, 1230, 1106, 1024, 848, 747, 683, 649, 609, 581, 458.

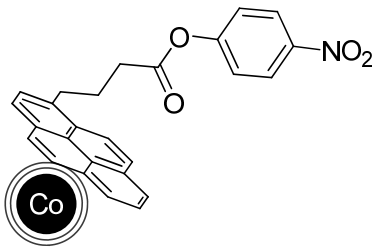

4-nitrophenyl 4-(pyren-1-yl)butanoate noncovalently immobilized on Co@C nanoparticles (46):

12 mg of Co@C nanoparticles and 8 mg 45 in 3 mL water were sonicated for 1 hour. After stirring overnight and one hour sonication the particles were washed 10 times with each 10 mL water. The particles were recovered with the aid of a neodymium based magnet and dried under vacuum.

IR (neat) $\tilde{\nu}$ = 1759, 1592, 1522, 1345, 1208, 1117, 844, 746, 608, 581, 525, 461.

Leaching experiments:

Solid samples were dissolved in 3 mL of aqua regia, diluted with water to a final volume of 50 mL and subjected to ICP-OES analysis after filtration. Calibration was performed using freshly prepared palladium standard solutions and investigation of a blank sample approved contamination-free pre-treatment procedure.

Desorption experiments:

Magnetic nanoparticles with either 19 or 45 attached to the surface were placed on a frit and washed with 0.5 L of boiling water. After drying under vacuum the recovered particles 19 were subjected to ICP-OES analysis and respectively basic hydrolysis followed by UV measurement for 45.

Magnetic nanoparticles with 45 attached to the surface were placed in a flask. After adding 10 mL water the mixture was heated to 100 °C. Subsequently, a magnet was placed on the outside of the flask and the supernatant was decanted. This procedure was repeated four respectively eight times. After drying under vacuum the recovered particles 45 were subjected to basic hydrolysis followed by UV measurement.

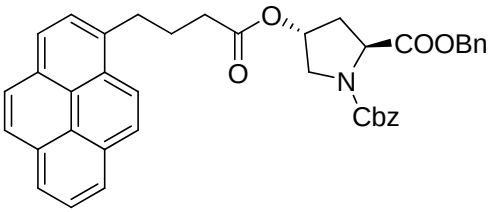

(2*S*,4*R*)-dibenzyl 4-(4-(pyren-1-yl)butanoyloxy)pyrrolidine-1,2-dicarboxylate (67):

Prepared in a modified procedure according to Noto[100]:

500 mg (1.73 mmol, 1.2 eq.) of 4-(pyren-1-yl)butanoic acid 43 were dissolved in 50 mL DCM_{abs}. Afterwards 1.1 g (9 mmol, 5 eq.) $SOCl_2$ was added dropwise. After refluxing for 3 hours the solvent was evaporated under reduced pressure. The resulting off white solid was added to 500 mg (1.4 mmol, 1 eq.) 65 and 3 mL pyridine in 50 mL DCM. After refluxing for 13 hours the organic layer was washed with 10% HCl and $NaCl_{sat.,}$ dried over Na_2SO_4 and evaporated. The residue was further purified by column chromatography with DCM/MeOH 19:1 and by a second column with PE/EA 7:1 to yield 773 mg (1.24 mmol) 67 as a white powder in 88% yield.

^{1}H-NMR (300 MHz, $CDCl_3$): δ = 8.39 - 7.93 (m, 9H), 7.83 (dd, J=7.7, 2.3, 1H), 7.43 - 7.14 (m, 10H), 5.34 - 5.09 (m, 3H), 5.02 (d, J=13.7, 2H), 4.50 (dt, J=23.3, 8.0, 1H), 3.86 - 3.69 (m, 2H), 3.46 - 3.29 (m, 2H), 2.51 - 2.29 (m, 3H), 2.27 - 2.09 (m, 3H).

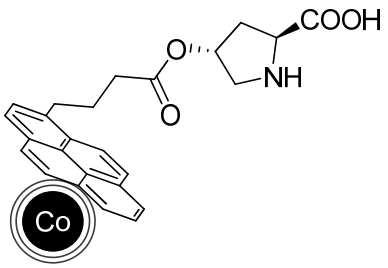

Immobilization of 62a on Co@C nanoparticles (68):

100 mg Co@C particles and 7 mg (17.5 μmol) of 62a in 5 mL water were sonicated for one hour. After stirring overnight and another hour sonication the particles were washed 10 times with 10 mL water. With the aid of a neodymium based magnet the particles were recovered and dried under vacuum to afford 101 mg of 68.

IR (neat) $\tilde{\nu}$ = 3050, 1731, 1575, 1374, 1166; - elemental microanalysis (%): C, 15.94; N, 0.54; H, 0.89.

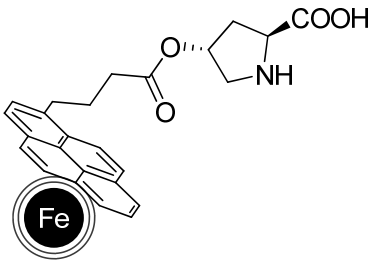

Immobilization of 62a on Fe@C nanoparticles (69):

100 mg Fe@C particles and 7 mg (17.5 μmol) of 62a in 5 mL water were sonicated for one hour. After stirring overnight and another hour sonication the particles were washed 10 times with 10 mL water. With the aid of a neodymium based magnet the particles were recovered and dried under vacuum to afford 99 mg of 69.

IR (neat) $\tilde{\nu}$ = 3050, 1731, 1575, 1374, 1166; - elemental microanalysis (%): C, 11.72; N, 0.22; H, 0.27.

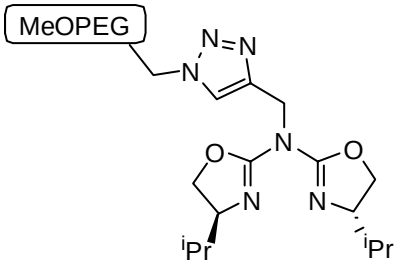

Bis-{(4-*iso*propyl-4,5-dihydro-oxazol-2-yl)-[methoxypolyethylenglycol-etyl]-1H-[1,2,3]triazol-4-ylmethyl}-amin (137):

Propargyl-azabis(oxazoline) 131 (70 mg, 0.3 mmol, 1.5 eq.) and MeOPEG-N_3 (1.0 g, 0.2 mmol, 1.0 eq.) were dissolved in 5 mL degassed DCM under N_2-atmosphere before CuI (3 mg, 0.02 mmol, 0.1 eq.) and NEt_3 (42 µL, 0.3 mmol, 1.5 eq.) were added. The mixture was stirred at ambient temperature for 20 h before the solvent was evaporated. The residue was separated between DCM (10 mL) and Titriplex III (5 mL of a 0.1 M solution) until the color of the aqueous phase remained colorless. The organic layer was dried over $MgSO_4$ and concentrated. The product was dissolved in DCM and precipitated with Et_2O to obtain 854 mg of 137 as a white solid with a loading of 60%.

^{1}H-NMR (300 MHz, $CDCl_3$): δ = 7.75 (d, 1H, *J* = 17.02 Hz), 5.10 (d, 2H, *J* = 2.47 Hz), 4.53 - 4.46 (m, 2 H), 4.40 - 4.33 (m, 2H), 3.88 - 3.81 (m, CH_2CH_2OPEG), 3,62 (s, PEG), 3.36 (s, $PEGOCH_3$), 1.77 - 1.64 (m, 2H), 0.90 (d, 6H, *J* = 6.86 Hz), 0.81 (d, 6H, *J* = 6.59 Hz).

Procedure for preparing the active catalyst:

The MeOPEG supported ligand 137 (1.2 g, 0.13 mmol, 1.0 eq.) was dissolved in DCM (5 mL) and $Cu(OTf)_2$ (47 mg, 0.13 mmol, 1.0 eq.) were added. The mixture was stirred at ambient temperature for 3 h and subsequently separated between DCM (10 mL) and Titriplex III (5 mL of a 0.1 M solution) until the color of the aqueous phase remained colorless. The organic layer was dried over $MgSO_4$ and concentrated. The residue was dissolved in DCM and added to Et_2O. The precipitated catalyst was filtered off.

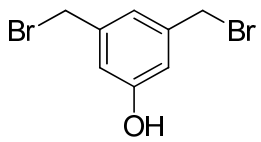

3,5-bis(bromomethyl)phenol (96):

Prepared by a modified procedure according to Vogt[130]:

7.6 g (49 mmol) (5-hydroxy-1,3-phenylene)dimethanol were dissolved in 70 mL $THF_{abs.}$ and 9.4 mL (98 mmol, 2 eq.) PBr_3 were added drop wise. The mixture was stirred for 4 days. Afterwards the solvent was evaporated and the residue was purified by column chromatography (PE/EA 4:1). Further purification was performed by recrystallization from hexanes to yield 8.6 g (31 mmol) of the product as a white solid in 62% yield.

^{1}H-NMR (300 MHz, $CDCl_3$): δ = 6.98 (d, J=1.3, 1H), 6.81 (d, J=1.5, 2H), 4.89 (s, 1H), 4.40 (s, 4H); - ^{13}C-NMR (75 MHz, $CDCl_3$): δ = 155.8, 140.0, 122.1, 116.2, 32.7.

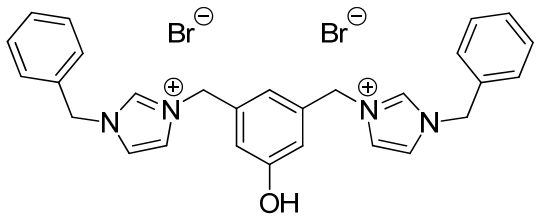

3,3'-(5-hydroxy-1,3-phenylene)bis(methylene)bis(1-benzyl-1H-imidazol-3-ium) bromide (149):

291 mg (1.04 mmol) 3,5-bis(bromomethyl)phenol 96 and 330 mg (2.09 mmol, 2 eq.) 1-benzyl-1H-imidazole were stirred in 3 mL MeCN at 90 °C for 30 minutes. After cooling down to ambient temperature the white precipitate was washed thrice with MeCN and acetone to yield 550 mg (0.9 mmol) product as a white solid in 88% yield.

^{1}H-NMR (300 MHz, DMSO): δ = 9.94 (s, 1H), 9.51 (s, 2H), 7.88 (t, J=1.7, 2H), 7.84 (t, J=1.7, 2H), 7.50 - 7.31 (m, 10H), 6.96 (s, 1H), 6.77 (d, J=1.1, 2H), 5.48 (s, 4H), 5.37 (s, 4H); - ^{13}C-NMR (75 MHz, DMSO): δ = 158.2, 136.7, 136.3, 134.7, 128.9, 128.7, 128.3, 122.9, 122.7, 118.6, 115.3, 51.9, 51.6; - IR (neat) $\tilde{\nu}$ = 3061, 3039, 1703, 1600, 1557, 1455, 1355, 1309, 1146, 1027,

867, 822, 747, 712, 644; - MS (EI): m/z (%) = 217.9 (M^{2+}); - HRMS (EIMS) [M^{2+}-H^{+}]: found 435.2184, calculated 435.2263; - m.p.: 138 °C (decomposition).

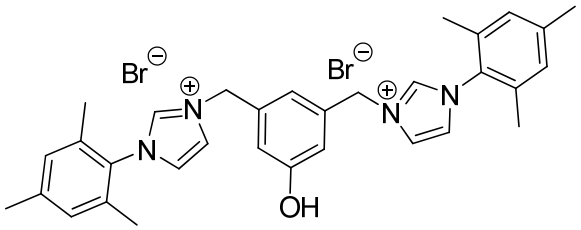

3,3'-(5-hydroxy-1,3-phenylene)bis(methylene)bis(1-mesityl-1H-imidazol-3-ium) bromide (98):

711 mg (2.54 mmol) 3,5-bis(bromomethyl)phenol 96 and 946 mg (5.08 mg, 2 eq.) 1-mesityl-1H-imidazole 97 were stirred in 5 mL MeCN at 90 °C in a sealed tube for 1 h. After cooling down to ambient temperature the white precipitate was washed thrice with MeCN and acetone to yield 1.42 g (2.2 mmol) product as a white solid in 86% yield.

^{1}H-NMR (300 MHz, DMSO): δ = 10.01 (s, 1H), 9.71 (s, 2H), 8.11 (s, 2H), 8.00 (s, 2H), 7.15 (s, 4H), 7.07 (s, 1H), 6.84 (s, 2H), 5.52 (s, 4H), 2.33 (s, 6H), 2.01 (s, 12H); - ^{13}C-NMR (75 MHz, DMSO): δ = 158.3, 140.2, 137.6, 136.7, 134.1, 131.0, 129.2, 124.1, 123.2, 118.4, 115.2, 108.4, 51.9, 20.5, 16.9; - IR (neat) $\tilde{\nu}$ = 3387, 3061, 1703, 1601, 1557, 1497, 1456, 1355, 1310, 1231, 1147, 1107, 1030, 1009, 876, 749, 714, 698, 663; - MS (EI): m/z = 246.0 (M^{2+}); - HRMS (EIMS) [M^{2+}]: found 246.1450, calculated 246.1439; - m.p.: 145 °C (decomposition);

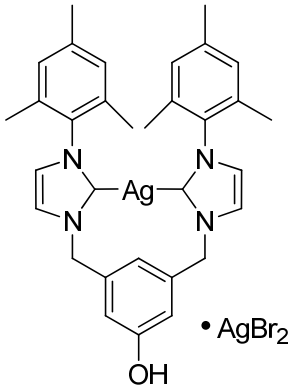

(3,3'-(5-hydroxy-1,3-phenylene)bis(methylene)bis(1-mesityl-1H-imidazolium-2,2'-diyliden))-di-silver(I)-dibromide (99):

To 50 mg (0.77 mmol) of 98 in 2 mL DCM, 20 mg (0.84 mmol, 1.1 eq.) Ag_2O were added. The slurry was stirred for 16 h under the exclusion of light. Subsequent filtration through a syringe filter and evaporation of the solvent furnished 60 mg (0.7 mmol) as white powder in 90% yield.

^{1}H-NMR (300 MHz, $CDCl_3$): δ = 7.34 (s, 2H), 6.89 (s, 4H), 6.85 (d, J=1.2, 4H), 6.69 (s, 2H), 6.42 (s, 1H), 5.12 (s, 4H), 2.35 (s, 6H), 1.79 (s, 12H); - ^{13}C-NMR (75 MHz, $CDCl_3$): δ = 139.1, 137.8, 135.5, 134.8, 129.2, 122.5, 122.3, 116.6, 77.2, 55.6, 21.2, 17.8; - IR (neat) $\tilde{\nu}$ = 2917, 1978, 1599, 1488, 1447, 1411, 1302, 1238, 1196, 1031, 1009, 919, 850, 728; - MS (ESMS): [M^+, - $AgBr_2^-$] m/z = 597.3, 598.3, 599.3, 600.3; - m.p.: 184 °C (decomposition);

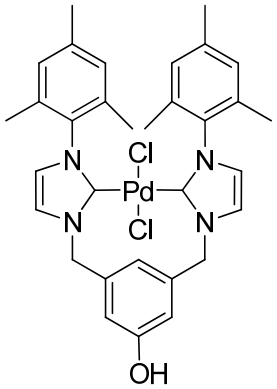

(3,3'-(5-hydroxy-1,3-phenylene)bis(methylene)bis(1-mesityl-1H-imidazolium-2,2'-diyliden))palladium(II)-dichloride (100):

To 250 mg (0.38 mmol) of 98 in 10 mL DCM, 98 mg (0.42 mmol, 1.1 eq.) of Ag_2O were added. The slurry was stirred for 4 h under the exclusion of light. Subsequent filtration trough a syringe filter and evaporation of the solvent furnished a white powder. This powder was dissolved in 10 mL of degassed DCM. After the addition of 110 mg (0.38 mmol) of $PdCl_2$(cod) the reaction mixture was stirred 16 h. Filtration trough a syringe filter and subsequent evaporation of the solvent furnished a yellow powder which was purified by precipitation of a saturated DCM solution with pentane. Centrifugation of the precipitate and subsequent recrystallization from $CHCl_3$ gave 219 mg (0.33 mmol) of amorphous yellow platelets in 86% yield.

^{1}H-NMR (300 MHz, DMSO): δ = 7.35 - 6.93 (m, br, 5H), 6.93 - 6.41 (m, br, 7H), 5.80 - 5.39 (m, br, 2H), 5.24 (m, br, 2H), 2.43 (m, br, 3H), 2.30 (m, br, 1H), 2.08 (m, br, 5H), 1.97 (m, br, 3H), 1.82 (m, br, 7H); - IR (neat) $\tilde{\nu}$ = 2916, 1598, 1487, 1448, 1415, 1297, 1233, 1160, 1033, 968, 934, 848, 728, 702; - MS (ESMS): [M^{2+} - 2 Cl^- - H^+] m/z = 593.3, 594.1, 595.2, 597.1, 599.1, 600.1; - CHN ($C_{32}H_{34}Cl_2N_4OPd$): calculated: C 57.54, H 5.13, N 8.39, found: C 58.12, H 5.37, N 7.26; - m.p.: > 200 °C (decomposition).

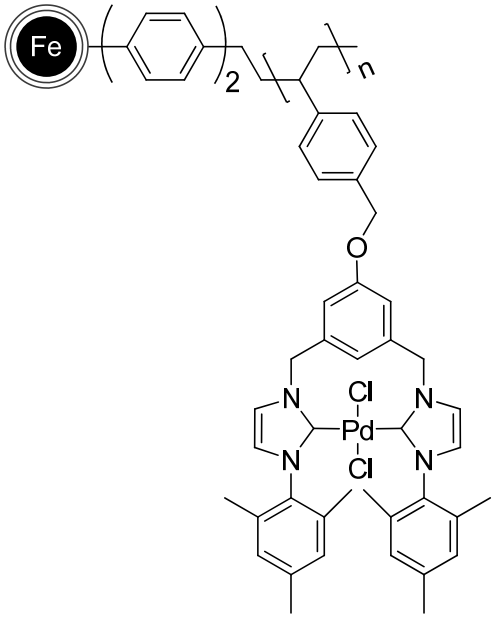

Immobilization of 100 on polymer coated Fe@C nanoparticles (102):

To 25 mg (corresponding to 0.095 mmol BzCl) of 101 in 3 mL $DMF_{abs.}$ 70 mg (0.105 mmol, 1.1 eq.) 100 and 30 mg (0.2 mmol, 2 eq.) of K_2CO_3 were added. After vigorously stirring at 60 °C for 18 h, the particles were recovered by the aid of an external magnet and subsequently washed with acetone, water, acetone and DCM. After drying 37 mg of the particles with a loading of 0.6 mmol/g were recovered.

IR (neat) $\tilde{\nu}$ = 3651, 2915, 2117, 1748, 1664, 1596, 1510, 1487, 1448, 1413, 1381, 1357, 1291, 1235, 1151, 1034, 1015, 931, 847, 810, 726, 700, 654; - elemental microanalysis (%): C, 70.71; H, 4.43; N, 3.92.

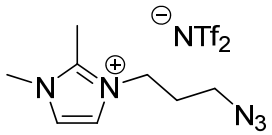

3-(3-azidopropyl)-1-methyl-1H-imidazol-3-ium bis(trifluoromethylsulfonyl)amide (120):

To a solution of 92 mg (1.0 mmol) 1,2-dimethyl-1H-imidazole 119 in 5 mL MeCN 202 mg (1.0 mmol) 1-azido-3-iodopropane 118 were added. After stirring for 3 days the solvent was evaporated. The resulting IL was subsequently dissolved in 10 mL water and 275 mg (1.0

mmol) $LiNTf_2$ were added. After stirring for 18 h the mixture was extracted twice with 10 mL DCM. Drying over Na_2SO_4 and evaporation of the solvent yielded 402 mg (0.9 mmol) of a viscous yellow liquid in 95% yield.

^{1}H-NMR (300 MHz, Acetone): δ = 7.57 (dd, J=12.1, 2.1, 2H), 4.62 – 4.30 (m, 2H), 3.91 (s, 3H), 3.50 (t, J=6.5, 2H), 2.76 (s, 3H), 2.16 (dt, J=13.4, 6.6, 2H); - ^{13}C-NMR (75 MHz, Acetone): δ = 145.9, 127.3, 123.6, 123.1, 121.9, 118.8, 114.6, 48.6, 46.4, 35.6, 29.6, 9.8; - ^{19}F NMR (282 MHz, Acetone): δ = -78.72; - IR (neat) $\tilde{\nu}$ = 2112, 1353, 1332, 1228, 1196, 1141, 1058; - MS (EI): [M^+] m/z = 180.0; - HRMS (EIMS, m/z) [M^+]: found: 180.1249, calculated: 180.1244.

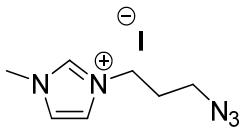

3-(3-azidopropyl)-1-methyl-1H-imidazol-3-ium iodide (150):

To a solution of 510 µL (6.4 mmol, 1.1 eq.) of 1-methyl-1H-imidazole 51 in 5 mL MeCN 1.23 g (5.82 mmol) 1-azido-3-iodopropane 118 were added. After stirring for 3 days the solvent and remaining 1-methyl-1H-imidazole was evaporated to yield 1.65 g (5.6 mmol) of the product as viscous oil in 98% yield.

^{1}H-NMR (300 MHz, Acetone): δ = 9.71 (s, 1H), 7.98 (t, J=1.8, 1H), 7.85 (t, J=1.7, 1H), 4.57 (t, J=7.1, 2H), 4.11 (s, 3H), 3.58 (t, J=6.7, 2H), 2.36 - 2.14 (m, 2H); - ^{13}C-NMR (75 MHz, Acetone): δ = 138.2, 124.7, 123.5, 48.8, 47.7, 37.0, 30.3; - IR (neat): 3069, 2097, 1572, 1456, 1165, 856, 760; - MS (EI): [M^+] m/z = 166.0; - HRMS (EIMS, m/z) [M^+]: calc.: 166.1087, found: 166.1086.

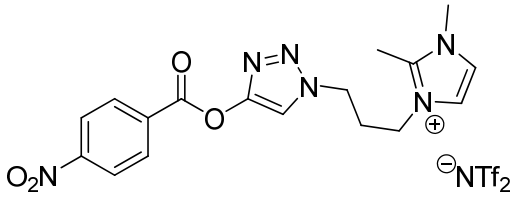

1,2-dimethyl-3-(3-(4-(4-nitrobenzoyloxy)-1H-1,2,3-triazol-1-yl)propyl)-1H-imidazol-3-ium bis(trifluoromethylsulfonyl)amide (122):

To a solution of 60.5 mg (0.13 mmol) 120, 25.2 mg (0.13 mmol) 121 and 2.5 mg (0.1 eq.) CuI 3 mL of dioxane$_{abs}$ were added. The resulting mixture was stirred for 18 hours and subsequent filtration and evaporation of the solvent furnished 63 mg (0.1 mmol) of a yellow liquid in 74% yield.

^{1}H-NMR (300 MHz, Acetone): δ = 8.88 (s, 1H), 8.45 - 8.30 (m, 2H), 7.71 (d, *J*=2.0, 1H), 7.61 (ddd, *J*=10.3, 4.8, 2.4, 4H), 4.77 (t, *J*=6.8, 2H), 4.59 - 4.43 (m, 2H), 3.97 (s, 3H), 2.84 (s, 3H), 2.70 (dt, *J*=13.7, 6.8, 2H); - ^{13}C-NMR (75 MHz, Acetone): δ = 158.9, 156.1, 146.6, 146.2, 139.2, 131.0, 126.2, 123.9, 123.7, 123.1, 122.0, 118.9, 48.1, 46.4, 35.7, 9.9.

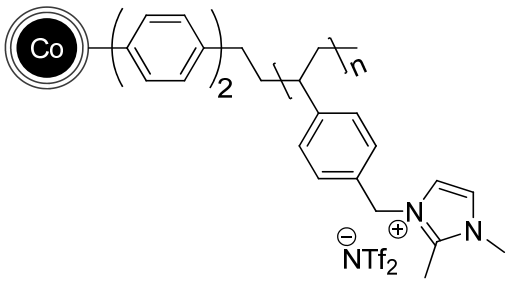

Ionic liquid tagged magnetic particles (123):

To a suspension of 100 mg nanobeads 101 (corresponding to 0.37 mmol BzCl) in 3 mL MeCN 1 mL 119 was added. After stirring for 3 days at 90 °C the particles were recovered with the aid of an external magnet and subsequently washed with acetonitrile, acetone and water. After drying under vacuum the particles were dispersed in 3 mL H_2O and 100 mg $LiNTf_2$ (0.35 mmol) were added. After stirring for 24 h the particles were recovered and washed with water, acetone and ether. Evaporation of residual solvent gave 120 mg particles with a loading of 1.62 mmol/g.

IR (neat) $\tilde{\nu}$ = 1588, 1513, 1452, 1428, 1345, 1327, 1173, 1129, 1049, 817, 767, 738; - elemental microanalysis (%): C, 36.88; N, 6.87; H, 3.06.

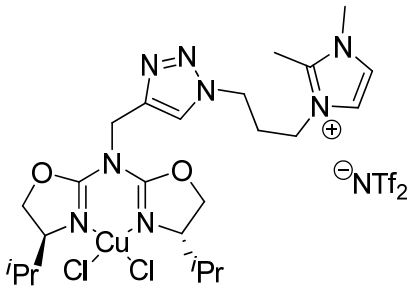

3-(3-(4-((bis((*S*)-4-*iso*propyl-4,5-dihydrooxazol-2-yl)amino)methyl)-1H-1,2,3-triazol-1-yl)propyl)-1,2-dimethyl-1H-imidazol-3-ium bis(trifluoromethylsulfonyl)amide·$CuCl_2$ (132): 295 mg 131 (1.06 mmol) and 143 mg $CuCl_2$ (1.06 mmol) were placed in a Schlenk tube and were stirred in 5 mL $DCM_{abs.}$ for 3 h. Afterwards the solvent was evaporated and the remaining green solid was dissolved in 5 mL dioxane. After the addition of 475 mg 120 (1.06 mmol) and 138 µL NEt_3 (1.06 mmol) a second liquid layer was formed. After 10 h stirring this layer was separated, filtrated and washed thrice with 5 mL dioxane each. Evaporation of the remaining solvent furnished the product (820 mg, 0.94 mmol) in 88% yield.

IR (neat) $\tilde{\nu}$ = 2986, 2356, 1745, 1681, 1591, 1494, 1465, 1348, 1179, 1134, 1087, 1053, 945, 874, 787; - MS (EI): [M^+] m/z = 590.2, 591.2, 592.2, 593.2, 594.2, 595.2, 596.2, 597.2.

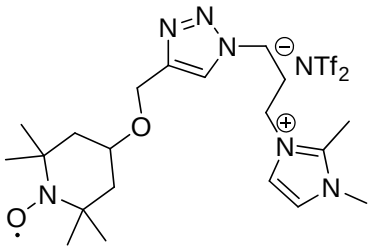

3-(1,2-dimethyl-1H-imidazol-3-ium-3-yl)-1-(4-((1-hydroxy-2,2,6,6-tetramethylpiperidin-4-oxyl)methyl)-1H-1,2,3-triazol-1-yl)propan-1-ide (126)

To a solution of 140 mg (0.67 mmol) 2,2,6,6-tetramethyl-4-(prop-2-ynyloxy)piperidine-1-oxyl 125 in 5 mL dioxane$_{abs.}$ 306 mg (0.67 mmol) 120, 13 mg (0.07 mmol, 0.1 eq.) CuI and 47 mL (0.33 mmol, 0.5 eq.) NEt_3 were added. After a short period a second layer consisting of IL was formed and after 3 hours the product layer was separated, filtered and washed three times with 5 mL dioxane$_{abs.}$ to afford 420 mg (0.63 mmol) of a red viscous oil in 94% yield.

IR (neat) $\tilde{\nu}$ = 3147, 2976, 1540, 1349, 1182, 1136, 1055, 874, 789; - MS (EI): [M^+] m/z = 390.0; - HRMS (EIMS, m/z) [M^+]: calc.: 390.2738, found: 390.2739.

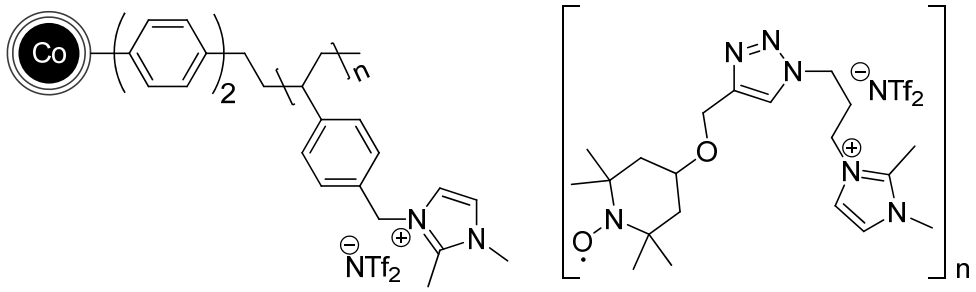

126 immobilized on IL functionalized nanoparticles (127):

67 mg (0.1 mmol) of 126 were dissolved in a minimal amount of DCM. After addition of 62 mg (0.1 mmol) 123, 2 mL Et_2O was added drop wise. After stirring for one hour the solvent was evaporated and the particles were washed 5 times with Et_2O. Subsequent drying under vacuum gave 120 mg nanoparticles 127.

IR (neat) $\tilde{\nu}$ = 1347, 1177, 1133, 1051, 823, 788, 739.

4. Catalysis

General procedure for the hydroxycarbonylation with 15 (GP1):

Co@C supported catalyst 15 (2 mol%) was suspended in 5 mL Millipore water in a Schlenk tube. Subsequently, 110 mg (0.5 mmol) 4-Iodophenol 53a and 54 mg K_2CO_3 (0.375 mmol, 0.75 eq.) were added. After evacuating the Schlenk tube with superimposed reflux condenser the system was flushed with CO from a balloon. This procedure was repeated 3 times. After stirring 10 hours at 100 °C the reaction was complete (monitored by to TLC, DCM:MeOH 9:1). The catalyst was separated from the cooled reaction mixture by magnetic decantation and washed 5 times with 5 mL of a 10% NaOH solution. The combined extracts were treated with dilute HCl until it was acidic to litmus and subsequently extracted five times with 10 mL EtOAc. After drying over $MgSO_4$ the evaporation of the solvent gave 66 mg (0.48 mmol) of 54 in 95% yield.

Before using the catalyst for the next reaction, Millipore water was added and stirred for 10 minutes. This procedure was repeated until the water showed a neutral pH.

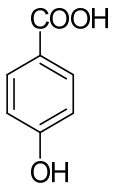

4-hydroxybenzoic acid (54a):

Starting from 4-bromophenol

Prepared following GP1.

4-bromophenol 55 (87 mg, 0.5 mmol) and 54 mg K_2CO_3 (0.375 mmol, 0.75 eq.) were used as starting materials to obtain 56 mg (0.4 mmol) 54a in 81 % yield.

^{1}H-NMR (300 MHz, DMSO): δ = 6.83 (d, 2H, J=8.7Hz), 7.80 (d, 2H, J=8.7Hz, 10.22 (s, 1H), 12.43 (s, 1H); - ^{13}C-NMR (75.5 MHz, DMSO): δ = 167.1, 161.5, 131.4, 121.2, 115.0.

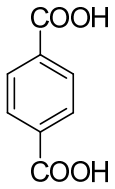

Terephthalic acid (54b):

Starting from 4-iodobenzoicacid:

Prepared following GP1.

4-iodobenzoicacid 56 (124 mg, 0.5 mmol) and 54 mg K_2CO_3 (0.375 mmol, 0.75 eq.) were used as starting materials to obtain 74 mg (0.45 mmol) 54b in 89 % yield.

Starting from 4-bromobenzoicacid:

Prepared following GP1.

4-bromobenzoicacid 57 (101 mg, 0.5 mmol) and 54 mg K_2CO_3 (0.375 mmol, 0.75 eq.) were used as starting materials to obtain 72 mg (0.44 mmol) 54b in 87 % yield.

^{1}H-NMR (300 MHz, DMSO): δ = 8.04 (s, 4H), 13.29 (s, 2H); - ^{13}C-NMR (75.5 MHz, DMSO): δ = 166.6, 134.3, 129.3.

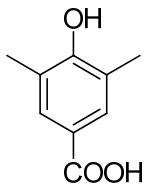

4-hydroxy-3,5-dimethylbenzoic acid (54c):

Prepared following GP1.

4-iodo-2,6-dimethylphenol 58 (124 mg, 0.5 mmol) and 54 mg K_2CO_3 (0.375 mmol, 0.75 eq.) were used as starting materials to obtain 66 mg (0.4 mmol) 54c in 79 % yield.

^{1}H-NMR (300 MHz, DMSO): δ = 2.19 (s, 6H), 7.54 (s, 2H), 9.02 (s, 1H), 12.28 (s, 1H); - ^{13}C-NMR (75.5 MHz, DMSO): δ = 167.4, 157.5, 129.9, 123.8, 121.2, 16.5.

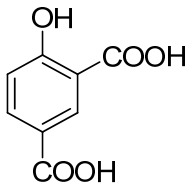

4-hydroxyisophthalic acid (54d):

Prepared following GP1.

2-hydroxy-5-iodobenzoic acid 59 (132 mg, 0.5 mmol) and 54 mg K_2CO_3 (0.75 mmol, 1.5 eq.) were used as starting materials to obtain 66 mg (0.38 mmol) 54d in 75 % yield.

^{1}H-NMR (300 MHz, DMSO): δ = 7.04 (d, 1H, J=8.7Hz), 8.03 (dd, 1H, J=1.9Hz, J=8.7Hz) , 8.38 (d, 1H, J=1.9Hz), 12.90 (s, 1H); - ^{13}C-NMR (75.5 MHz, DMSO): δ = 171.1, 166.2, 164.3, 136.1, 132.1, 121.6, 117.4, 113.0; - MS (EI): m/z (%) = 182.0 ($M^{+\bullet}$, 39), 164 (M-H_2O, 100), 136 (M-H_2O –CO, 41), 119 (46); - HRMS (EIMS, m/z) [$M^{+\bullet}$]: calc.: 182.0215, found: 182.0215.

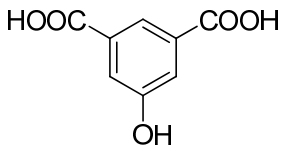

5-hydroxyisophthalic acid (54e):

Prepared following GP1.

3,5-dibromophenol (126 mg, 0.5 mmol) and 54 mg K_2CO_3 (0.75 mmol, 1.5 eq.) were used as starting materials to obtain 31 mg (0.17 mmol) 154 in 34 % yield.

^{1}H-NMR (300 MHz, DMSO): δ = 13.03 (s, 2H), 11.16 - 9.66 (m, 1H), 7.95 (d, J=1.4, 1H), 7.53 (d, J=1.4, 2H); - ^{13}C-NMR (75.5 MHz, DMSO): δ = 166.5, 157.5, 132.3, 120.7, 119.9.

General procedure for aldol reactions with the supported catalysts 68 and 69 (GP2):

To 0.025 mmol (5 mol%) of nanoparticles supported catalyst 68 or 69 75.5 mg (0.5 mmol) 4-nitrobenzaldehyde 72, 260 μL (2.5 mmol, 5 eq.) cyclohexanone 70 and 175 μL 1 M EDTA solution were added. The mixture was stirred for 24 hours at ambient temperature. Subsequently, the vial containing the mixture was washed two times with 2 mL ethyl acetate. The combined organic extracts were washed with water, dried over $MgSO_4$ and concentrated under reduced pressure. From the crude ^{1}H-NMR the conversion and diastereomeric ratio was deduced. The entantiomeric excess was determined by chiral HPLC. Afterwards the compound was purified by column chromatography.
Prior to the next run the catalyst was twice washed with 2 mL Millipore water each and the dried under reduced pressure.

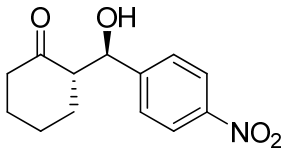

(*S*)-2-((*R*)-hydroxy(4-nitrophenyl)methyl)cyclohexanone (72):
Prepared following GP2 and purified by column chromatography (PE/EA 10:1 - 4:1) to obtain the pure product as a yellow solid.

^{1}H-NMR (300 MHz, $CDCl_3$): δ = 8.11 (d, *J*=8.7, 2H), 7.44 (d, *J*=8.7, 2H), 4.85 (d, *J*=8.2, 1H), 4.11 (s, 1H), 2.55 (ddd, *J*=13.3, 8.0, 5.6, 1H), 2.45 - 2.30 (m, 2H), 2.08 - 1.98 (m, 1H), 1.84 - 1.45 (m, 5H); - ^{13}C-NMR (75.5 MHz, $CDCl_3$): δ = 214.8, 148.5, 147.5, 127.9, 123.5, 73.9, 57.1, 42.6, 30.7, 27.6, 24.6; - $[\alpha]_D^{22}$ = +12.1 (c = 1.0, $CHCl_3$); - HPLC analysis (Chiralcel AS-H, 10% ^{i}PrOH/*n*-heptane, 1.0 mL/min, 254 nm) t_r (*S*) = 34.92 min, t_r (*R*) = 30.41 min; *ee* = 99%.

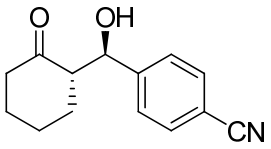

4-((*R*)-hydroxy((*S*)-2-oxocyclohexyl)methyl)benzonitrile (77):

Prepared following GP2 and purified by column chromatography (PE/EA 10:1 - 4:1) to obtain the pure product as a white solid.

^{1}H-NMR (300 MHz, $CDCl_3$): δ = 7.56 (d, J=8.3, 2H), 7.38 (d, J=8.2, 2H), 4.77 (d, J=8.3, 1H), 4.05 (s, 1H), 2.61 - 2.18 (m, 3H), 2.11 - 1.92 (m, 1H), 1.89 - 1.39 (m, 4H); - ^{13}C-NMR (75.5 MHz, $CDCl_3$): δ = 214.7, 146.5, 132.1, 127.8, 118.7, 111.6, 74.1, 57.1, 42.6, 30.7, 27.6, 24.6; - $[\alpha]_D^{22}$ = +22.5 (c = 1.0, $CHCl_3$); - HPLC (Chiralcel AS-H, 10% ^{i}PrOH/*n*-heptane, 0.5 mL/min, 230 nm): t_r (*S*) = 61.92 min, t_r (*R*) = 75.7 min; *ee* = 99%.

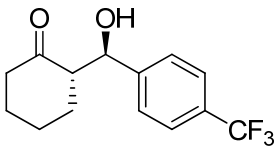

(S)-2-((R)-hydroxy(4-(trifluoromethyl)phenyl)methyl)cyclohexanone (78):

Prepared following GP2 and purified by column chromatography (PE/EA 10:1 - 4:1) to obtain the pure product as a white solid.

^{1}H-NMR (300 MHz, $CDCl_3$): δ = 7.60 (d, J=8.1, 2H), 7.44 (d, J=8.4, 2H), 4.84 (dd, J=8.6, 2.8, 1H), 4.06 (d, J=3.0, 1H), 2.66 - 2.26 (m, 3H), 2.17 - 2.01 (m, 1H), 1.87 - 1.24 (m, 4H); - ^{13}C-NMR (75.5 MHz, $CDCl_3$): δ = 215.1, 145.0, 130.3, 129.8, 127.4, 125.9, 125.4, 125.3, 125.3, 125.2, 122.3, 77.5, 77.1, 76.6, 74.2, 57.3, 42.7, 30.8, 27.7, 24.7; - $[\alpha]_D^{22}$ = +11.0 (c = 1.0, $CHCl_3$, 97% *ee*); - HPLC (Chiralcel OD-H, 5% ^{i}PrOH/*n*-heptane, 0.75 mL/min, 217 nm): t_r (*S*) = 7.91 min, t_r (*R*) = 8.78 min.

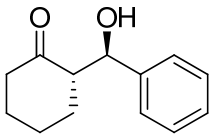

(*S*)-2-((*R*)-hydroxy(phenyl)methyl)cyclohexanone (79):

Prepared following GP2 and purified by column chromatography (PE/EA 10:1 - 4:1) to obtain the pure product as a white solid.

^{1}H-NMR (300 MHz, $CDCl_3$): δ = 7.38 - 7.21 (m, 5H), 4.79 (dd, *J*=8.8, 2.8, 1H), 3.96 (d, *J*=2.8, 1H), 2.65 - 2.53 (m, 1H), 2.51 - 2.29 (m, 2H), 2.15 - 2.02 (m, 1H), 1.90 - 1.47 (m, 5H); - ^{13}C-NMR (75.5 MHz, $CDCl_3$): δ = 215.6, 140.9, 128.4, 127.9, 127.1, 74.8, 57. 5, 42.7, 30.9, 27.8, 24.8; - $[\alpha]_D^{22}$ = +12.1 (c = 1.0, $CHCl_3$); - HPLC (Chiralcel AS-H, 10% ^{i}PrOH/*n*-heptane, 1.0 mL/min, 220 nm): t_r (*S*) = 19.46 min, t_r (*R*) = 25.95 min; *ee* = 89%.

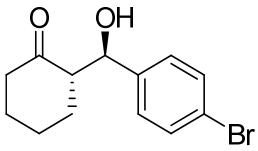

(*S*)-2-((*R*)-(4-bromophenyl)(hydroxy)methyl)cyclohexanone (80):

Prepared following GP2 and purified by column chromatography (PE/EA 10:1 - 4:1) to obtain the pure product as a white solid.

^{1}H-NMR (300 MHz, $CDCl_3$): δ = 7.46 (d, *J*=8.4, 2H), 7.19 (d, *J*=8.3, 2H), 4.74 (dd, *J*=8.7, 2.2, 1H), 3.85 (s, 1H), 2.62 - 2.41 (m, 2H), 2.41 - 2.27 (m, 1H), 2.15 - 2.01 (m, 1H), 1.86 - 1.49 (m, 5H); - ^{13}C-NMR (75.5 MHz, $CDCl_3$): δ = 215.3, 140.0, 131.5, 128.8, 121.7, 74.2, 57.3, 42.7, 30.8, 27.7, 24.7; - $[\alpha]_D^{22}$ = +16.0 (c = 1.0, $CHCl_3$); - HPLC (Chiralcel AS-H, 10% ^{i}PrOH/*n*-heptane, 0.75 mL/min, 217 nm): t_r (*S*) = 15.30 min, t_r (*R*) = 13.21 min; *ee* = 91%.

General procedure for Suzuki-Miyaura cross coupling reactions with the supported catalyst 102 (GP3):

To 102 (0.2 mol%), 1.0 mmol arene, 1.1 mmol (1.1 eq.) boronic acid and 276 mg (2.0 mmol, 2 eq.) K_2CO_3 were added. After the addition of 2 mL toluene the reaction mixture was stirred at 70 °C or heated in a closed microwave vessel at a constant power of 200 W for the indicated time. Afterwards the catalyst was recovered by applying an external magnet. The reaction vessel was washed with each 5 mL of toluene, MeOH, water and MeOH. The combined organic fractions were extracted with 10 mL water and dried over Na_2SO_4, filtered, evaporated under reduced pressure and purified by column chromatography.
The recovered catalyst was dried under reduced pressure and subsequently subjected to the next run.

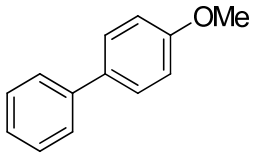

4-methoxybiphenyl (95):
Prepared following GP3 and purified by column chromatography (PE/EA 24:1 - 9:1) to obtain the pure product as a white solid.

^{1}H-NMR (300 MHz, $CDCl_3$): δ = 7.58 - 7.49 (m, 4H), 7.46 - 7.36 (m, 2H), 7.34 - 7.25 (m, 1H), 7.00 - 6.92 (m, 2H), 3.83 (s, 3H); - ^{13}C-NMR (75.5 MHz, $CDCl_3$): δ = 159.2, 140.9, 133.8, 128.8, 128.2, 126.8, 126.7, 114.3, 55.4.

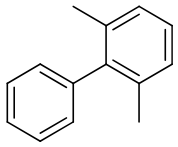

2,6-dimethylbiphenyl (108):

Prepared following GP3 and purified by column chromatography (PE/EA 24:1) to obtain the pure product as colorless oil.

^{1}H-NMR (300 MHz, $CDCl_3$): δ = 7.55 - 7.47 (m, 2H), 7.46 - 7.38 (m, 1H), 7.30 - 7.17 (m, 5H), 2.14 (s, 6H); - ^{13}C-NMR (75.5 MHz, $CDCl_3$): δ = 142.0, 141.2, 136.1, 129.1, 128.5, 127.4, 127.1, 126.7, 21.0.

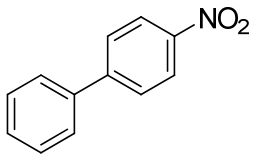

4-nitrobiphenyl (109)

Prepared following GP3 and purified by column chromatography (PE/EA, 24:1 - 9:1) to obtain the pure product as a yellow solid.

^{1}H-NMR (300 MHz, $CDCl_3$): δ = 8.32 - 8.24 (m, 2H), 7.76 - 7.67 (m, 2H), 7.62 (ddd, J=9.6, 5.1, 2.8, 2H), 7.55 - 7.41 (m, 3H); - ^{13}C-NMR (75.5 MHz, $CDCl_3$): δ = 147.6, 147.1, 138.7, 129.2, 129.0, 127.8, 127.4, 124.1.

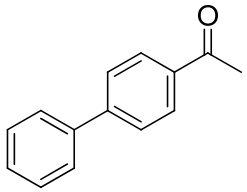

1-(biphenyl-4-yl)ethanone (110):

Prepared following GP3 and purified by column chromatography (PE/EA 24:1 - 9:1) to obtain the pure product as a white solid.

^{1}H-NMR (300 MHz, $CDCl_3$): δ = 8.08 - 8.00 (m, 2H), 7.73 - 7.60 (m, 4H), 7.52 - 7.35 (m, 3H), 2.64 (s, 3H); - ^{13}C-NMR (75.5 MHz, $CDCl_3$): δ = 197.8, 145.8, 139.9, 135.9, 129.0, 128.9, 128.3, 127.3, 127.2, 26.7.

General procedure for the oxidation of alcohols with catalyst 127 (GP6):

61 mg (0.5 mmol) 4-metylbenzyl alcohol 128 and 177 mg (0.55 mmol, 1.1 eq.) BAIB 129 were dissolved in 2 mL of solvent. After the addition of the nanoparticle supported catalyst 127 (0.025 mmol, 5 mol%) and 50 μL [bmim][BF_4] the mixture was stirred at ambient temperature until TLC showed no remaining starting material. Then, the reaction mixture was separated from the nanoparticles by the aid of a neodymium based magnet. The particles were washed three times with ether (3 x 5 mL). The combined organic extracts were dried over $MgSO_4$, filtered and concentrated under vacuum to afford 4-methylbenzaldehyde 130. The recovered nanoparticles were dried in vacuo and reused without further purification and the addition of further [bmim][BF_4].

General procedure for Michael additions with 137 (GP5):

Reactions using MeOPEG supported catalyst:

To a Schlenk tube ligand 137 (0.05 mmol, 0.05 eq.) in 2 mL EtOH was added. To the resulting blue-green solution malonate (1.0 mmol, 1.0 eq.) in EtOH (2 mL) and indole (1.2 mmol, 1.2 eq.) were added. After stirring for 16 h at room temperature, the red colored solution was concentrated under reduced pressure. The residue was dissolved in DCM, dried over $MgSO_4$ and added to Et_2O. The precipitated catalyst was filtered off and the remaining crude product was purified on silica (PE/DCM 1:1, followed by DCM).

Reaction using MeOPEG supported catalyst and unsupported catalyst:

To a Schlenk tube ligand 137 (0.025 mmol, 0.025 eq.) and $Cu(OTf)_2$ (9.05 mg, 0.025 mmol, 1.0 eq.) in 2 mL EtOH were added and stirred for 1 h. To the resulting blue-green solution ligand 135·$Cu(OTf)_2$ (0.025 mmol, 0.025 eq.), malonate (1.0 mmol, 1.0 eq.) in EtOH (2 mL) and indole (1.2 mmol, 1.2 eq.) were added. After stirring for 16 h at room temperature, the red colored solution was concentrated under reduced pressure. The residue was dissolved in CH_2Cl_2, dried over $MgSO_4$ and added to Et_2O. The precipitated catalyst was filtered off and the remaining crude product was purified on silica (PE/DCM 1:1, followed by DCM).

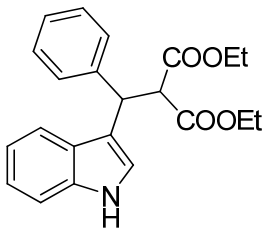

Ethyl 2-ethoxycarbonyl-3-(3-indolyl)-3-phenyl propanoate (134a):

Prepared according to the general procedure GP5 and purified by column chromatography (PE/DCM, 1:1 followed by DCM) to obtain 295 mg of the pure product in 81% yield as a white solid.

^{1}H-NMR (300 MHz, $CDCl_3$): δ = 0.93 - 1.06 (m, 6 H), 3.93 - 4.06 (m, 4 H), 4.30 (d, J = 11.8 Hz, 1 H), 5.09 (d, J = 11.8 Hz, 1 H), 7.00 - 7.07 (m, 1 H), 7.09-7.31 (m, 6 H), 7.37 (d, J = 7.4 Hz, 2

H), 7.56 (d, J = 8.0 Hz, 1 H), 8.07 (bs, 1 H); - ^{13}C-NMR (75 MHz, $CDCl_3$): δ = 168.1, 167.9, 141.4, 136.2, 128.4, 128.2, 126.8, 126.7, 122.3, 120.9, 119.5, 119.4, 117.0, 111.0, 61.5, 61.4, 58.4, 42.9, 13.8, 13.8; - MS (CI): m/z (%) = 383 (MNH_4^+, 89), 366 (MH^+, 3), 206 (100), 178 (5); - HPLC (Chiralcel OJ-H, 30% ^{i}PrOH/*n*-heptane, 1.0 mL/min, 254 nm): t_r (*S*) = 19.46 min, t_r (*R*) = 25.95 min).

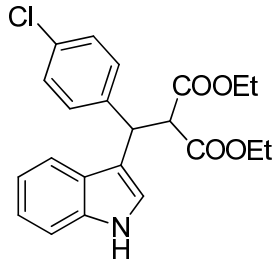

diethyl 2-((4-chlorophenyl)(1H-indol-3-yl)methyl)malonate (134b)

Prepared according to the general procedure GP5 and purified by column chromatography (PE/DCM, 1:1, followed by DCM) to obtain 296 mg of the pure product in 74% yield as a white solid.

^{1}H-NMR (300 MHz, CDCl3): δ = 8.20 (s, 1H), 7.50 (d, J=7.9, 1H), 7.35 - 7.24 (m, 4H), 7.24 - 7.09 (m, 4H), 7.09 – 7.00 (m, 1H), 5.08 (d, J=11.7, 1H), 4.27 (d, J=11.7, 1H), 4.02 (qd, J=7.1, 2.3, 4H), 1.03 (dt, J=19.6, 7.1, 7H). - ^{13}C-NMR (75 MHz, $CDCl_3$): δ = 167.9, 167.8, 140.1, 136.3, 132.5, 129.6, 128.1, 126.5, 122.4, 121.0, 119.6, 119.2, 116.4, 111.2, 61.6, 58.2, 42.3, 13.9, 13.7; - HPLC (Chiralcel OJ-H, 20% ^{i}PrOH/*n*-heptane, 1.0 mL/min, 254 nm): t_r (*S*) = 15.22 min, t_r (*R*) = 19.03 min).

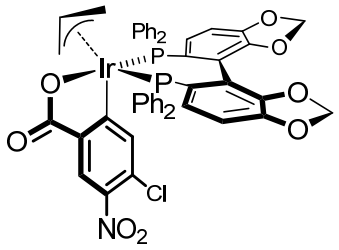

Iridium catalyst 138:

To a mixture of 200 mg $[Ir(cod)Cl]_2$ (0.3 mmol), 364 mg (0.6 mmol, 2eq.) (*R*)-SEGPHOS 140, 388 mg (1.2 mmol, 4 eq.) Cs_2CO_3, 240 mg (1.2 mmol, 4 eq.) 3-chloro-4-nitrobenzoic acid 141 and 162 µL allyl acetate (1.5 mmol, 5 eq.) in a sealed tube under an atmosphere of N_2 6 mL THF (0.05 M) were added. The reaction mixture was stirred for 30 minutes at ambient temperature and heated for 1.5 hours at 80 °C. Upon cooling to ambient temperature, the reaction mixture was diluted with DCM (10 mL), filtered through a celite plug, washed with 50 mL DCM and concentrated in vacuo. The residue was purified by flash chromatography (SiO_2, 20% Et_2O/DCM) and concentrated in vacuo. The light yellow gum was dissolved in THF (3 mL). Rapid addition of hexanes (50 mL) to the stirred solution resulted in precipitation of a yellow powder, which was collected by filtration. Removal of solvents residues in vacuo gave 270 mg (*R*)-138 (0.26 mmol) in 87% yield.

General procedure for the asymmetric allylation of alcohols using catalyst 138 (GP6):

An oven dried sealed tube was charged with 0.3 mmol alcohol, 15.7 mg 138 (0.015 mmol, 0.05 eq.), 3 mg 4-chloro-3-nitrobenzoic acid (0.015 mmol, 0.05 eq.), 19.6 mg Cs_2CO_3 (0.06 mmol, 0.2 eq.) and 65 µL allylacetate (0.6 mmol, 2 eq.) under an atmosphere e of N_2. After addition of 1.5 mL $THF_{abs.}$ the tube was sealed and heated at 90 °C for 48 h. Evaporation of the solvent and purification of the residue by column chromatography afforded the product.

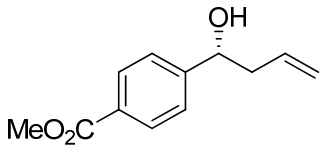

(*R*)-methyl 4-(1-hydroxybut-3-enyl)benzoate (144):

Prepared according to the general procedure GP6 and purified by column chromatography (PE/EA 10:1-5:1) to obtain the pure product as yellow oil in 74% yield.

^{1}H-NMR (400 MHz, $CDCl_3$): δ = 7.93 (d, *J*=8.4 Hz, 2H), 7.34 (d, *J*=8.1 Hz, 2H), 5.82 - 5.62 (m, 1H), 5.16 - 4.99 (m, 2H), 4.72 (dd, *J*=8.0, 4.8 Hz , 1H), 3.83 (s, 3H), 2.54 - 2.32 (m, 2H), 2.28 (s, *J*=2.7 Hz, 1H); - ^{13}C-NMR (101 MHz, $CDCl_3$): δ = 167.0, 149.0, 133.8, 129.7, 129.2, 125.7, 118.9, 72.7, 52.1, 43.8; - IR (neat): 3427, 2951, 1719, 1610, 1434, 1415, 1210, 1276, 1191, 1176, 1110, 1053, 1018, 965, 916, 856, 767, 726, 707; - MS (EI): m/z (%) = 165, 189 ($M-H_2O^+$), 207 (M^+); - HRMS (EIMS, m/z) [M^+]: calc.: 206.0949, found: 206.0922; - HPLC (Chiralpak AD-H column, hexane/^{i}PrOH = 95:5, 0.6 mL/min, 254 nm): t_{major} = 24.8 min, t_{minor} = 28.0 min; *ee* = 93%.

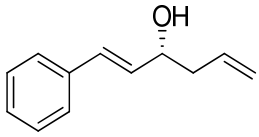

(*R*,*E*)-1-phenylhexa-1,5-dien-3-ol (145):

Prepared according to the general procedure GP6 and purified by column chromatography (PE/EA 10:1-5:1) to obtain the pure product as yellow oil in 76% yield.

^{1}H-NMR (400 MHz, $CDCl_3$): δ = 7.42 - 7.37 (m, 2H), 7.36 - 7.30 (m, 2H), 7.29 - 7.24 (m, 1H), 6.62 (dd, *J*=15.9, 1.1, 1H), 6.26 (dd, *J*=15.9, 6.4, 1H), 5.88 (ddt, *J*=17.2, 10.2, 7.1, 1H), 5.20 – 5.15 (m, 1H), 4.36 (tt, *J*=20.5, 10.4, 1H), 2.51 – 2.33 (m, 2H), 2.26 (dd, *J*=12.9, 2.4, 1H); - ^{13}C-NMR (101 MHz, $CDCl_3$): δ = 136.7, 134.1, 131.7, 130.3, 128.6, 127. 7, 126.5, 118.4, 71.8, 42.0; - IR (neat): 3357, 3077, 3025, 2903, 1640, 1493, 1448, 1294, 1068, 1028, 964, 914, 868, 746, 691. - MS (EI): m/z = 156, 157, 158 ($M-H_2O^+$), 173 (M^+); - HRMS (EIMS, m/z) [M^+]: calc.:

175.1045, found: 174.1045; - HPLC (Chiralpak OD-H column, hexane/^{i}PrOH = 93:7, 0.5 mL/min, 254 nm): t_{major} = 17.0 min, t_{minor} = 23.7 min; *ee* = 91%.

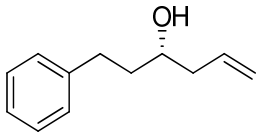

(S)-1-phenylhex-5-en-3-ol (145):

Prepared according to the general procedure GP6 and purified by column chromatography (PE/EA 10:1-5:1) to obtain the pure product as yellow oil in 74% yield.

^{1}H-NMR (400 MHz, $CDCl_3$): δ = 7.35 - 7.28 (m, 2H), 7.26 - 7.18 (m, 2H), 5.91 - 5.78 (m, 1H), 5.20 - 5.16 (m, 1H), 5.16 - 5.13 (m, 1H), 3.70 (ddd, *J*=12.2, 7.5, 5.0, 1H), 2.89 - 2.66 (m, 2H), 2.40 - 2.29 (m, 1H), 2.26 - 2.17 (m, 1H), 1.87 (s, 1H), 1.85 - 1.77 (m, 2H); - ^{13}C-NMR (101 MHz, $CDCl_3$): δ 142.0, 134.7, 128.5, 128.4, 125.9, 118.3, 67.0, 42.1, 38.5, 32.1; - IR (neat): 3363, 3063, 3026, 2926, 1640, 1602, 1495, 1453, 1046, 1030, 993, 912, 864, 745, 698. - MS (EI): m/z (%) = 157, 158, 159 ($M-H_2O^+$); - HRMS (EIMS, m/z) [M^+]: calc.: 176.1201, found: 176.1200; - HPLC (Chiralpak OD-H column, hexane/^{i}PrOH = 97:3, 0.5 mL/min, 254 nm): t_{major} = 19.7 min, t_{minor} = 15.5 min; *ee* = 95%.

5. A formula for the simple assessment of relative catalyst activities

The selectivity of two catalysts is constituted by their *ee*-values ee_1 and ee_2. Furthermore, the resulting *ee*-value of the mixture of both catalysts is constituted by ee_r. In the following the rate ratio $v_{rel} = \frac{R_1 + S_1}{R_2 + S_2}$ of the two catalysts will be derivated by means of the aforementioned values.

According to the definition of the *ee*-value it is deemed to be:

$$ee_1 = \frac{R_1 - S_1}{R_1 + S_1} \qquad (1)$$

$$ee_2 = \frac{R_2 - S_2}{R_2 + S_2} \qquad (2)$$

$$ee_r = \frac{R_r - S_r}{R_r + S_r} = \frac{(R_1 + R_2) - (S_1 + S_2)}{(R_1 + R_2) + (S_1 + S_2)} \qquad (3)$$

By variables substitution one can simplify the problem.

$$p = R_1 + S_1 \qquad (4)$$

$$\hat{p} = R_1 - S_1 \qquad (5)$$

$$q = R_2 + S_2 \qquad (6)$$

$$\hat{q} = R_2 - S_2 \qquad (7)$$

From the last formulas ensues:

$$ee_1 = \frac{\hat{p}}{p} \qquad (8)$$

$$ee_2 = \frac{\hat{q}}{q} \qquad (9)$$

$$ee_r = \frac{\hat{p}+\hat{q}}{p+q} \qquad (10)$$

With the variable order ($\hat{p}$; p; $\hat{q}$; q) we get the following homogeneous system of equations (row order (10,9,8)):

$$\begin{pmatrix} \hat{q} \\ q \\ \hat{p} \\ p \end{pmatrix} = \lambda \begin{pmatrix} \frac{ee_1 ee_r - {ee_r}^2}{ee_r - ee_2} - ee_1 + ee_r \\ \frac{ee_1 - ee_r}{ee_r - ee_2} \\ ee_1 \\ 1 \end{pmatrix}$$

$$v_{rel} = \frac{R_1 + S_1}{R_2 + S_2} = \frac{p}{q} = \frac{\lambda \cdot 1}{\lambda \cdot \frac{ee_1 - ee_r}{ee_r - ee_2}} = \frac{ee_r - ee_2}{ee_1 - ee_r}$$

The sought formula is:

$$v_{rel} = \frac{ee_r - ee_2}{ee_1 - ee_r}$$

For the utilization of this formula one has to convert all values to either the *R* or *S* enantiomer:

$$ee_x(R) = -ee_x(S); x \in \{1,2,r\}$$

Hence, the final formula for a 1:1 ratio of the 2 catalysts is:

$$\boxed{v_{rel} = \frac{ee_2 + ee_r}{ee_1 - ee_r}}$$

For the general formula:

$$v_{rel} = \frac{X_2(R_1 + S_1)}{X_1(R_2 + S_2)}$$

X_1 and X_2 are the ratios of Catalyst 1 and Catalyst 2 respectively.

As stated above:

$$v_{rel} = \frac{X_2(R_1 + S_1)}{X_1(R_2 + S_2)} = \frac{X_2 \cdot p}{X_1 \cdot q} = \frac{X_2 \cdot \lambda \cdot 1}{X_1 \cdot \lambda \cdot \frac{ee_1 - ee_r}{ee_r - ee_2}} = \frac{X_2(ee_2 - ee_r)}{X_1(ee_1 - ee_r)}$$

$$ee_x(R) = -ee_x(S); x \in \{1,2,r\}$$

$$\boxed{v_{rel} = \frac{X_2(ee_2 + ee_r)}{X_1(ee_1 - ee_r)}}$$

6. References

[37] A. Schätz, R. N. Grass, W. J. Stark, O. Reiser, *Chem.-Eur. J.* 2008, *14*, 8262-8266.
[100] F. Giacalone, M. Gruttadauria, P. L. Meo, S. Riela, R. Noto, *Adv. Synth. Catal.* 2008, *350*, 2747-2760.
[128] A. Ueno, I. Suzuki, T. Osa, *J. Am. Chem. Soc.* 1989, *111*, 6391-6397.
[129] A. J. Lampkins, E. J. O'Neil, B. D. Smith, *J. Org. Chem.* 2008, *73*, 6053-6058.
[130] N. J. Ronde, D. Totev, C. Müller, M. Lutz, A. L. Spek, D. Vogt, *ChemSusChem* 2009, *2*, 558-574.
[131] G. Occhipinti, H.-R. Bjørsvik, K. W. Törnroos, A. Fürstner, V. R. Jensen, *Organometallics* 2007, *26*, 4383-4385.
[132] L. Yao, B. T. Smith, J. Aubé, *J. Org. Chem.* 2004, *69*, 1720-1722.
[133] D. A. Fleming, C. J. Thode, M. E. Williams, *Chem. Mater.* 2006, *18*, 2327-2334.
[134] H. Werner, R. Vicha, A. Gissibl, O. Reiser, *J. Org. Chem.* 2003, *68*, 10166-10168.
[135] J. Zabicky, *J. Chem. Soc.* 1961, 683.
[136] A. Gissibl, Universität Regensburg (Regensburg), 2006.

E. Appendix

1. NMR-spectra

^{1}H-NMR (300 MHz, $CDCl_3$): -upper image

^{13}C-NMR (75 MHz, $CDCl_3$): -lower image

Solvent (if not stated otherwise): $CDCl_3$

1-(4-bromobutyl)pyrene (50):

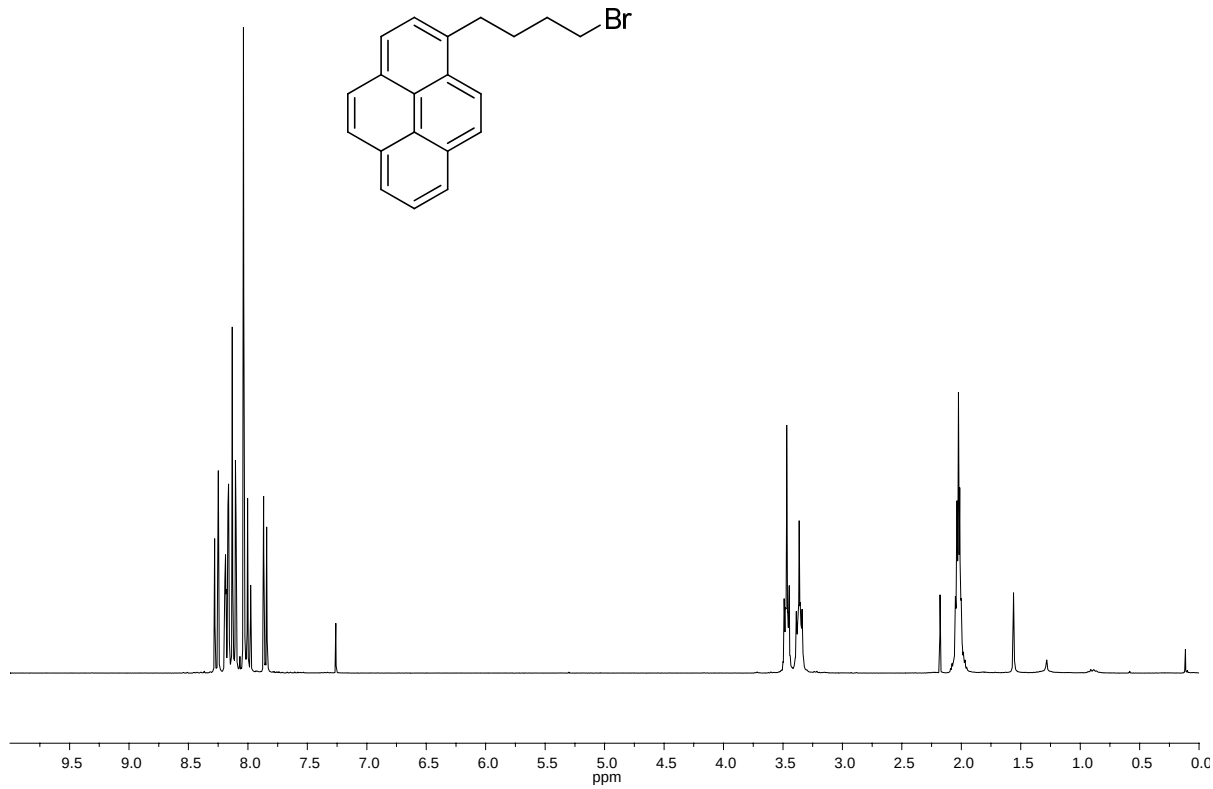

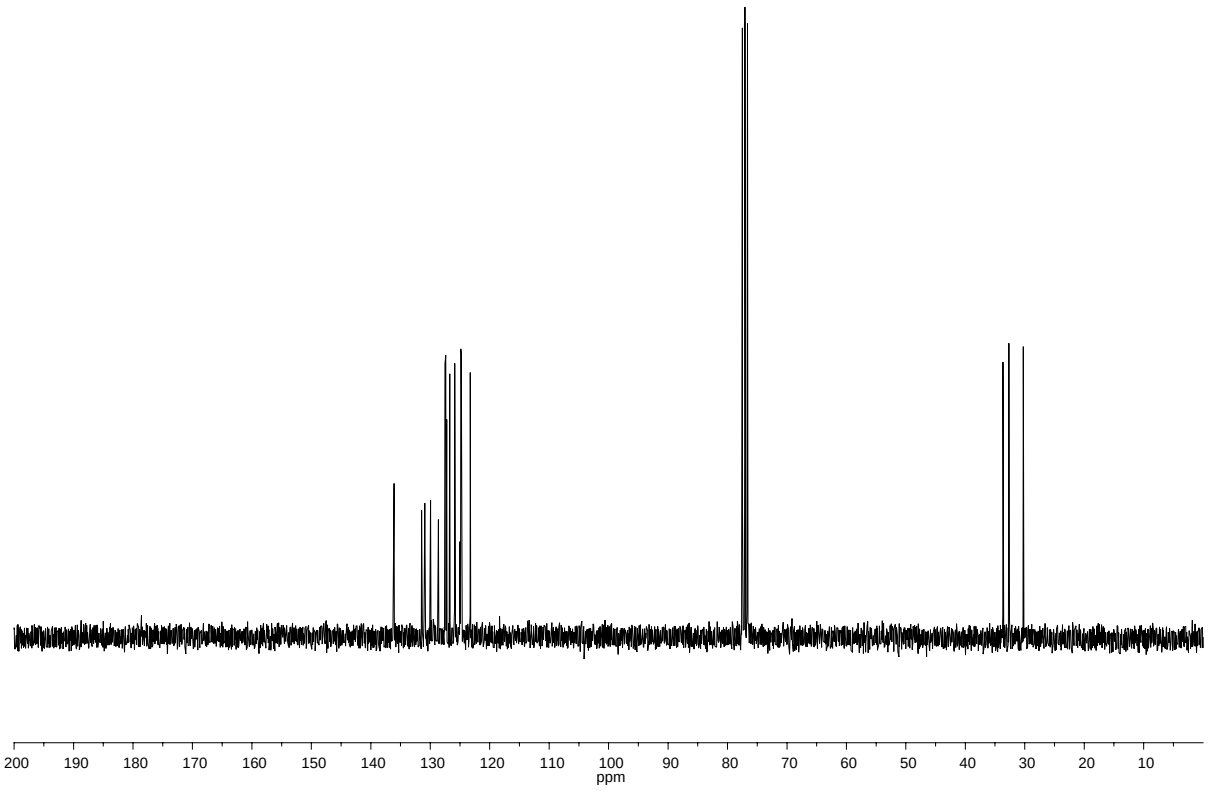

1-methyl-3-(4-(pyren-1-yl)butyl)-1H-imidazol-3-ium bromide (52) (DMSO):

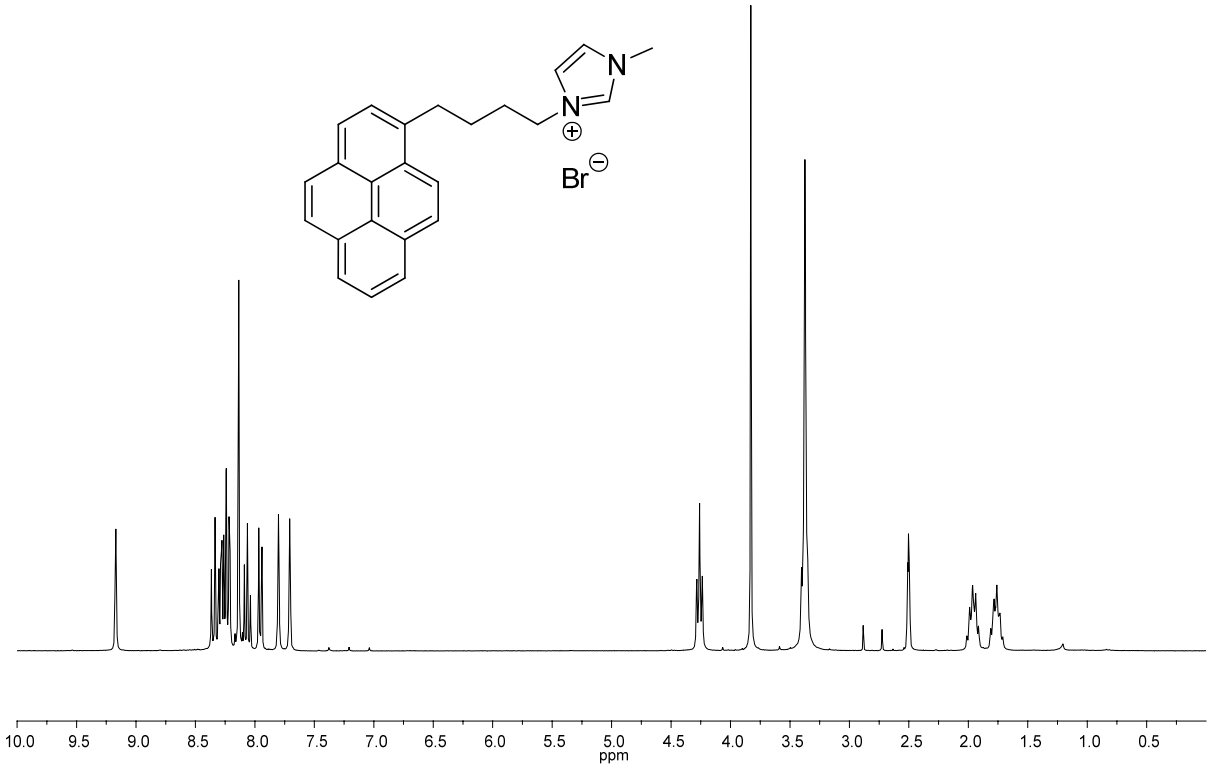

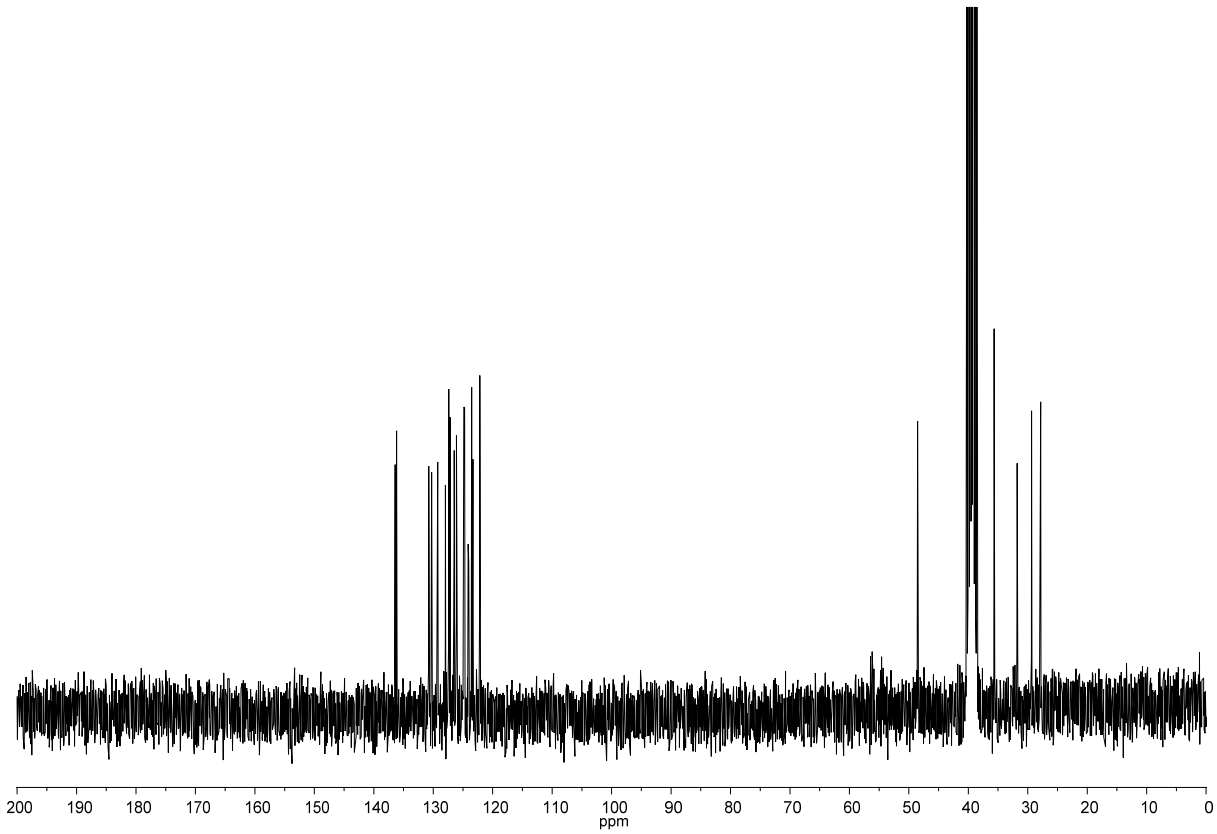

1-(4-azidobutyl)pyrene (147):

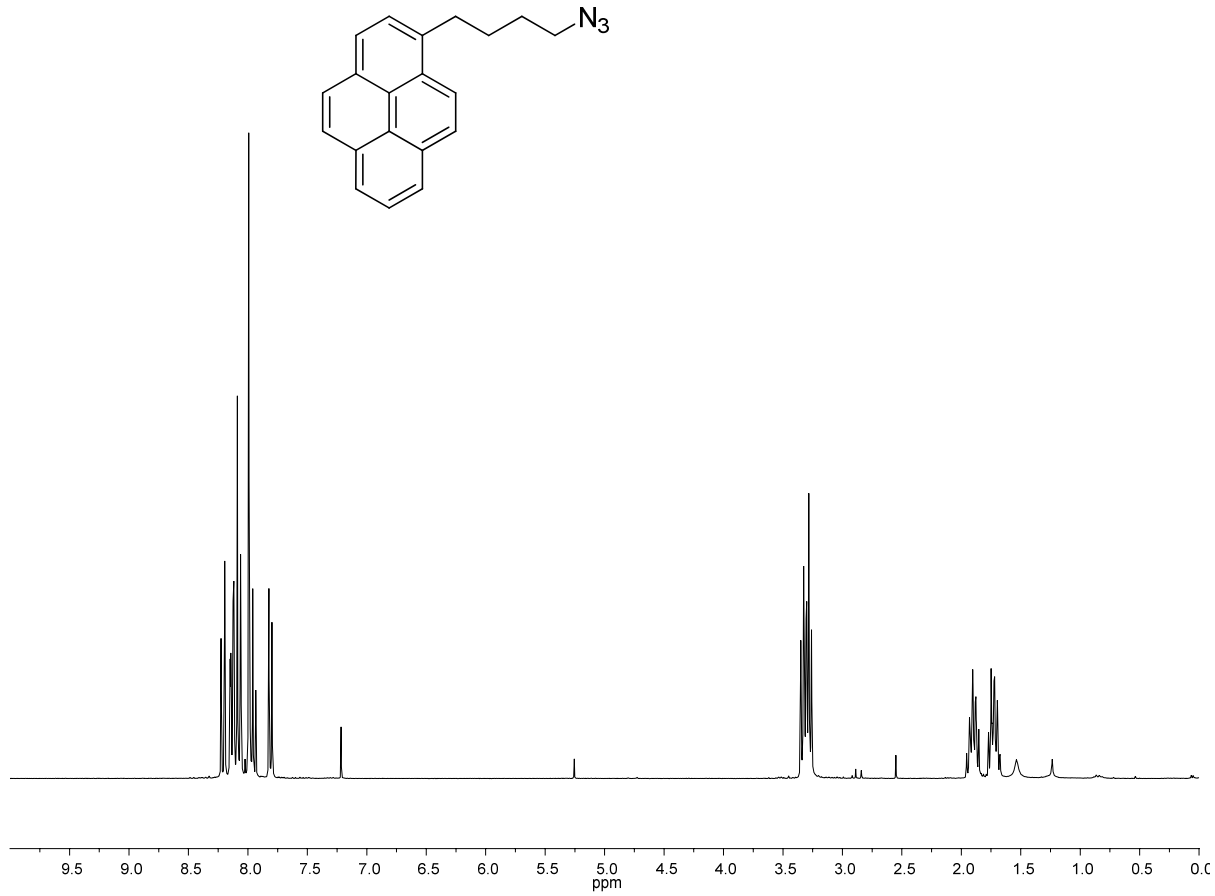

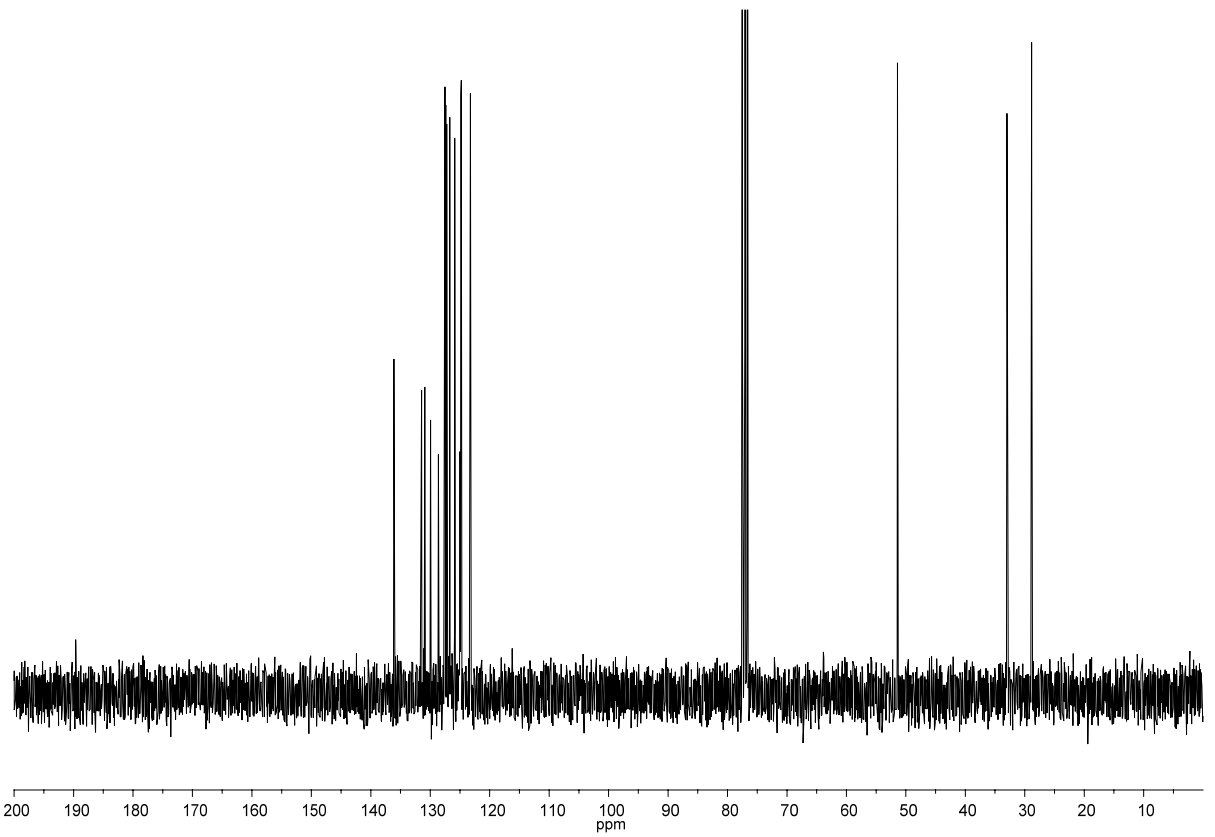

4-nitrophenyl 4-(pyren-1-yl)butanoate (45):

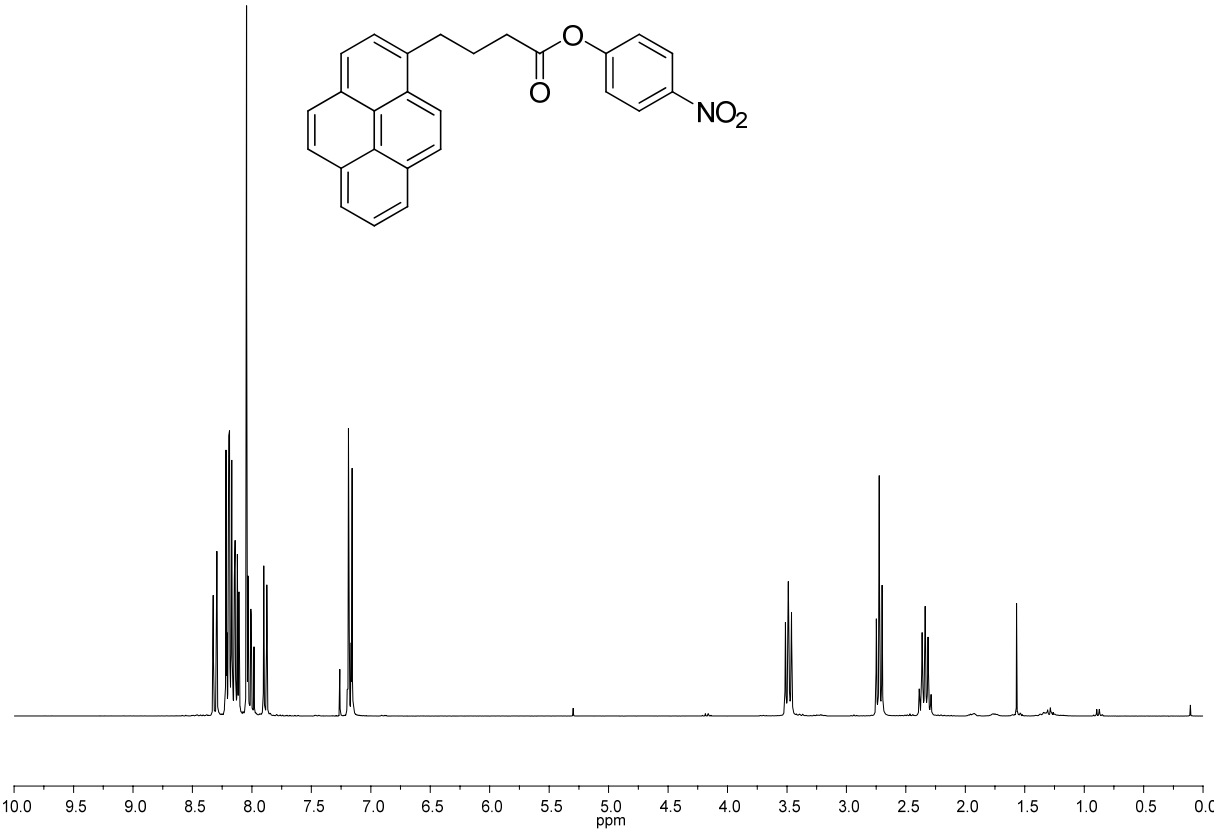

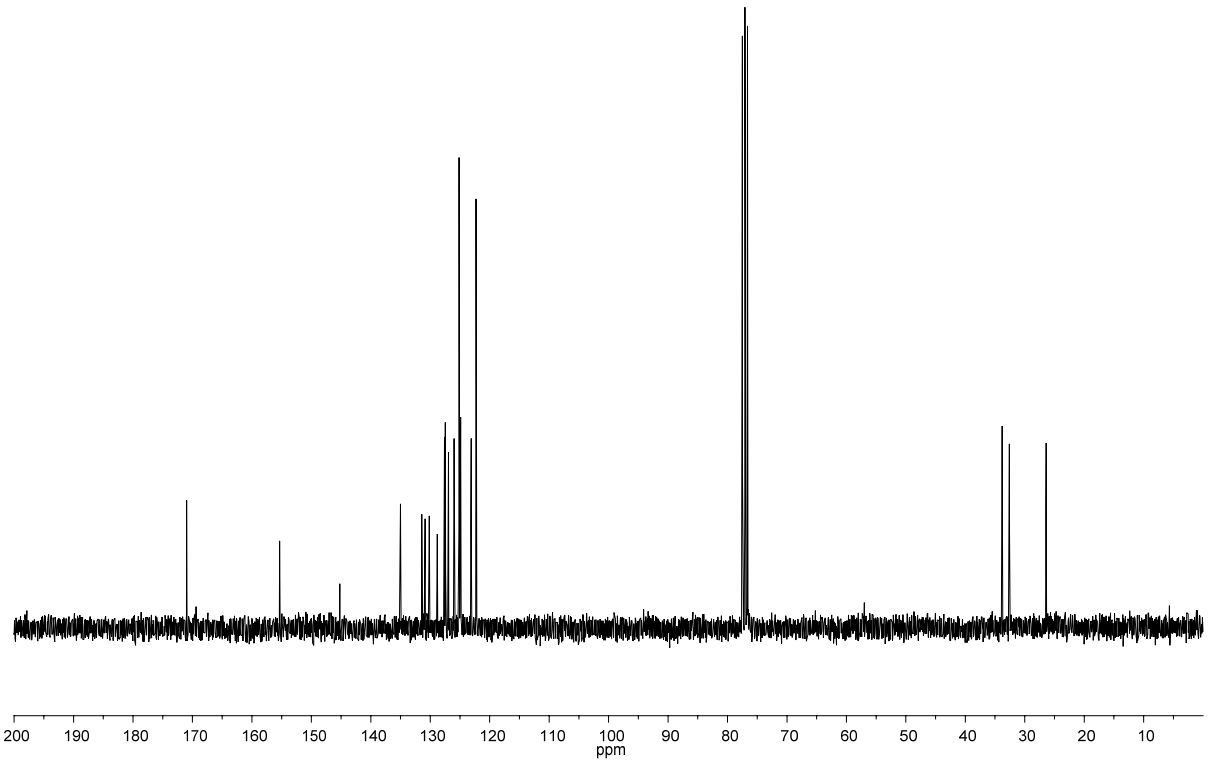

(1-methyl-3-(3-(pyren-1-yl)propyl)-1H-imidazol-2(3H)-ylidene)(1-methyl-3-(4-(pyren-1-yl)butyl)-1H-imidazol-2(3H)-ylidene)silver (148) (MeOD):

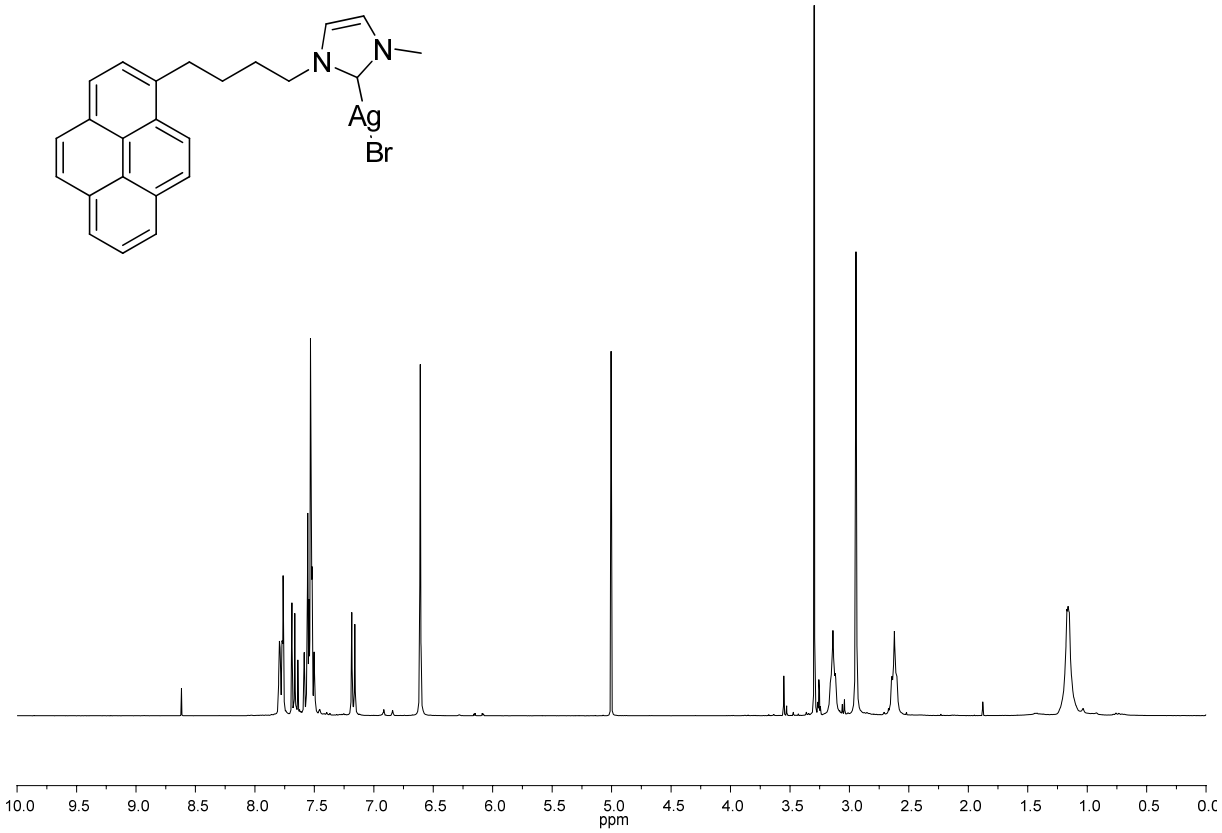

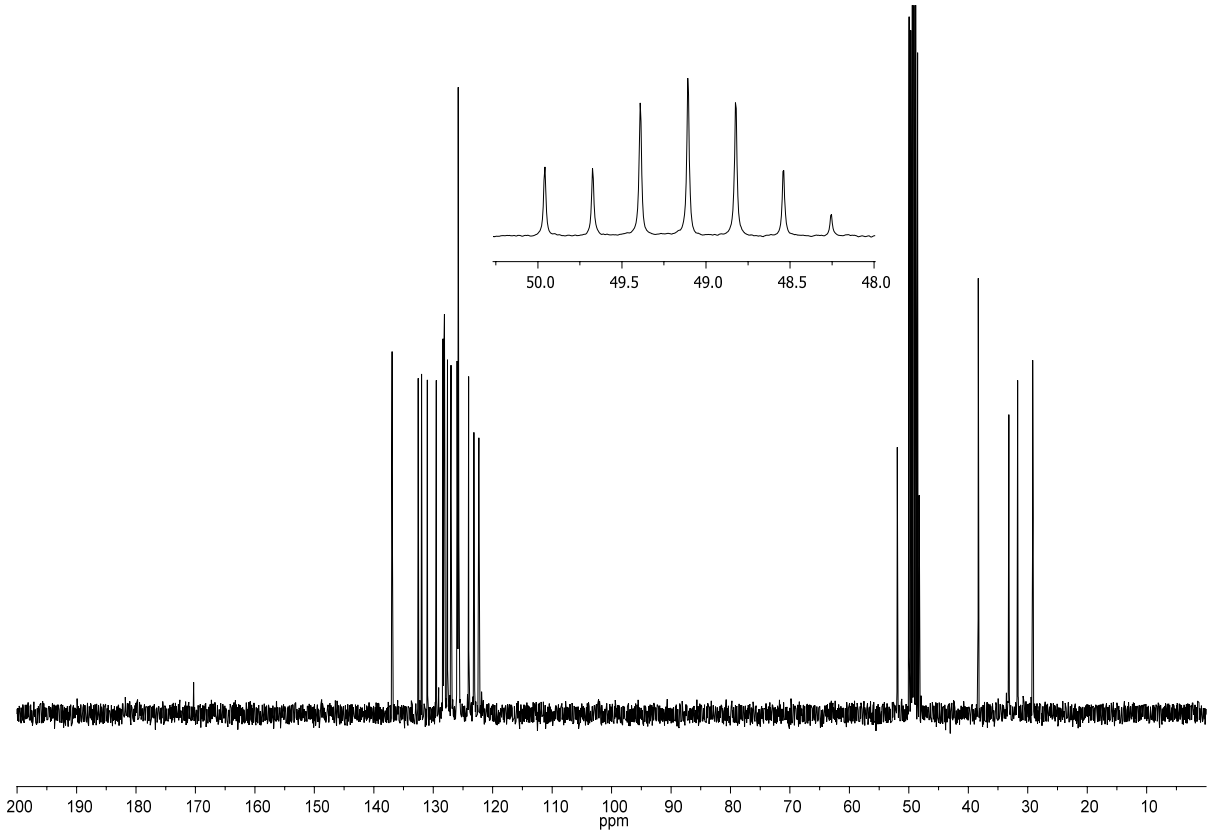

Bis(1-methyl-3-(4-(pyren-1-yl)butyl)-1H-imidazol-2(3H)-ylidene)palladium(II) acetate (19):

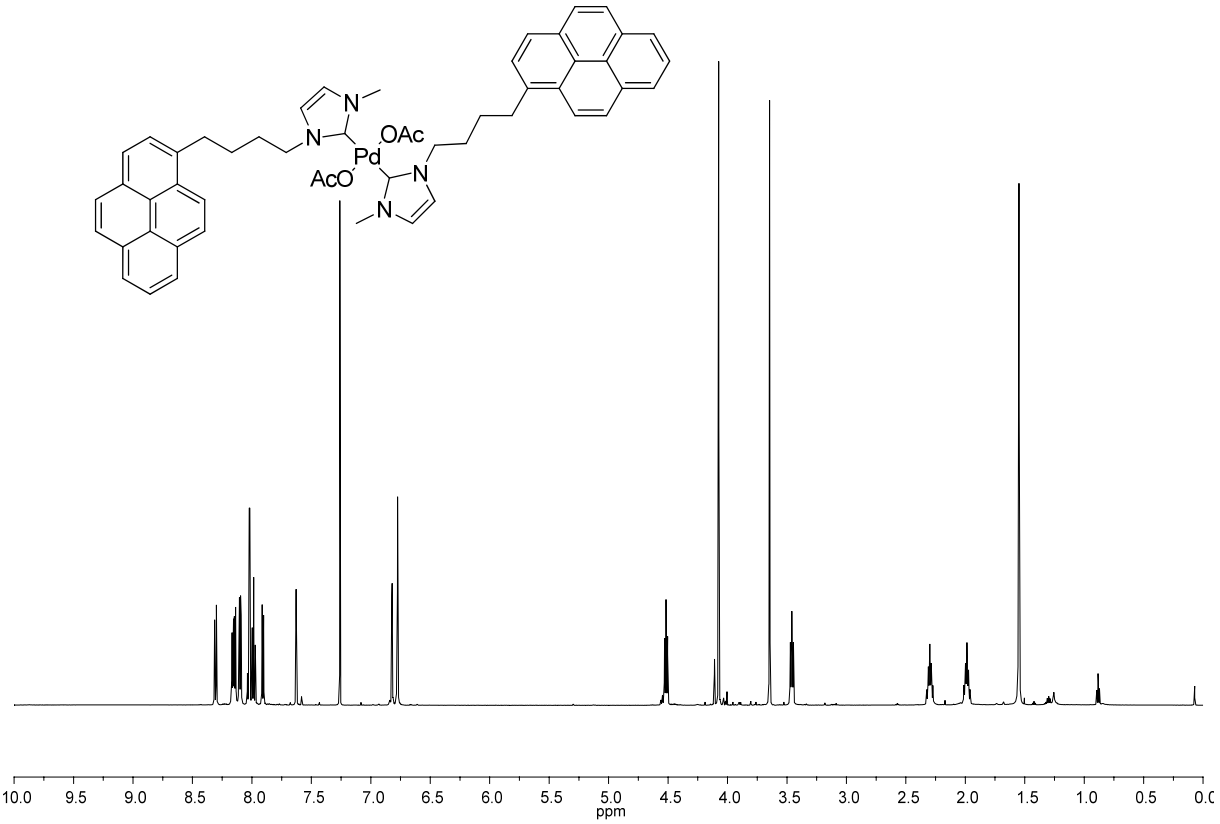

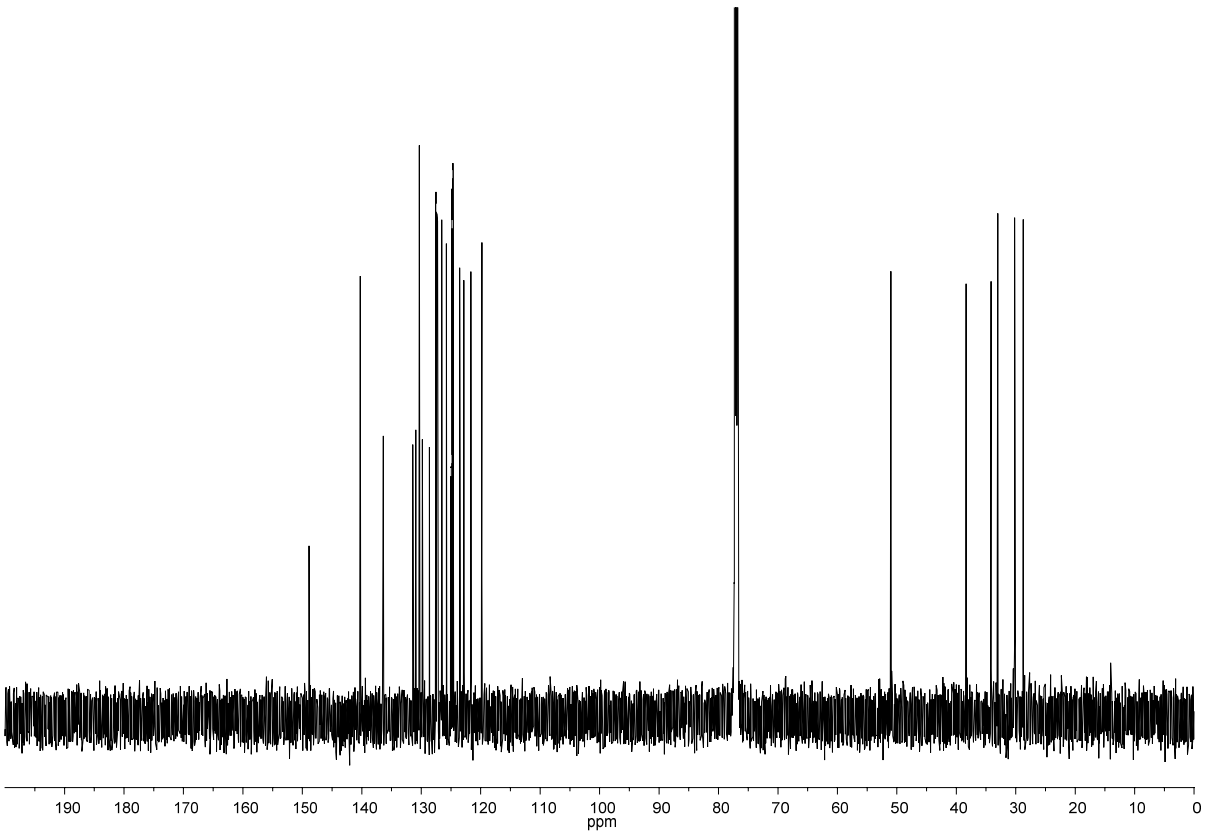

(2*S*,4*R*)-dibenzyl 4-(4-(pyren-1-yl)butanoyloxy)pyrrolidine-1,2-dicarboxylate (67):

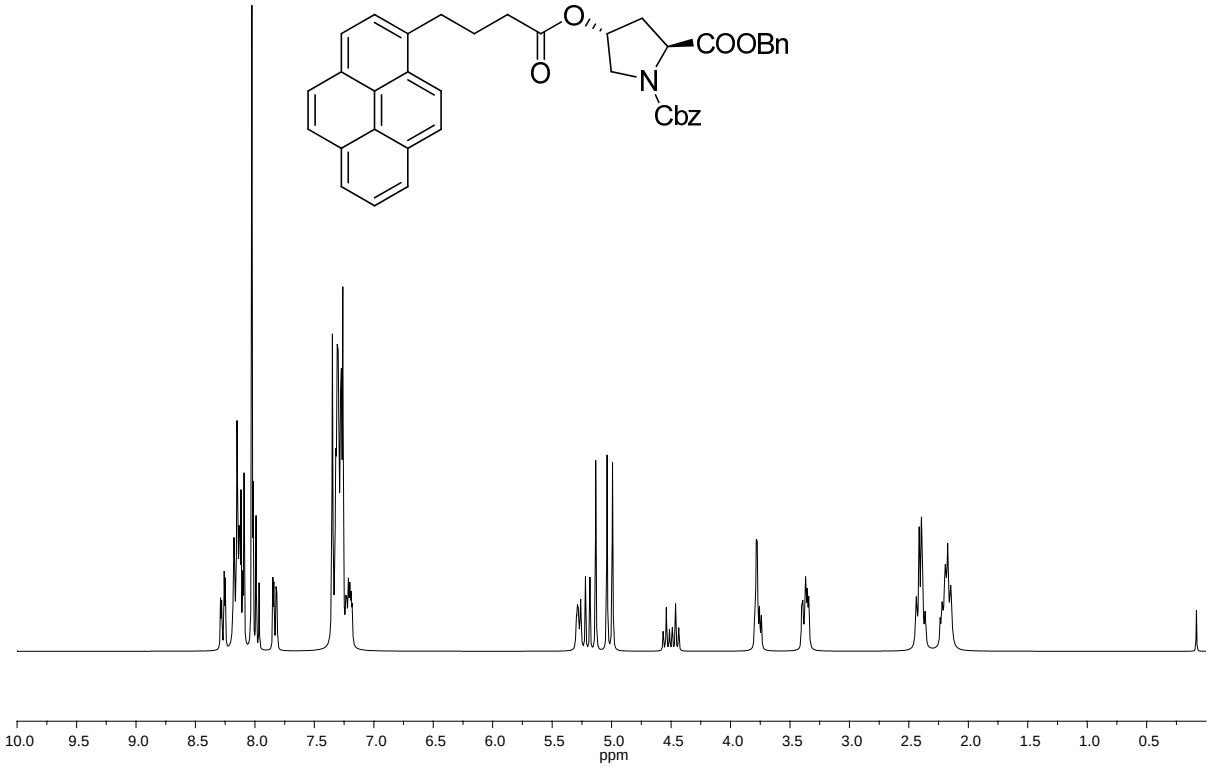

3,5-bis(bromomethyl)phenol (96):

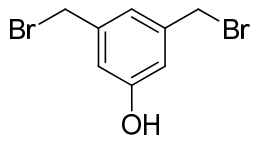

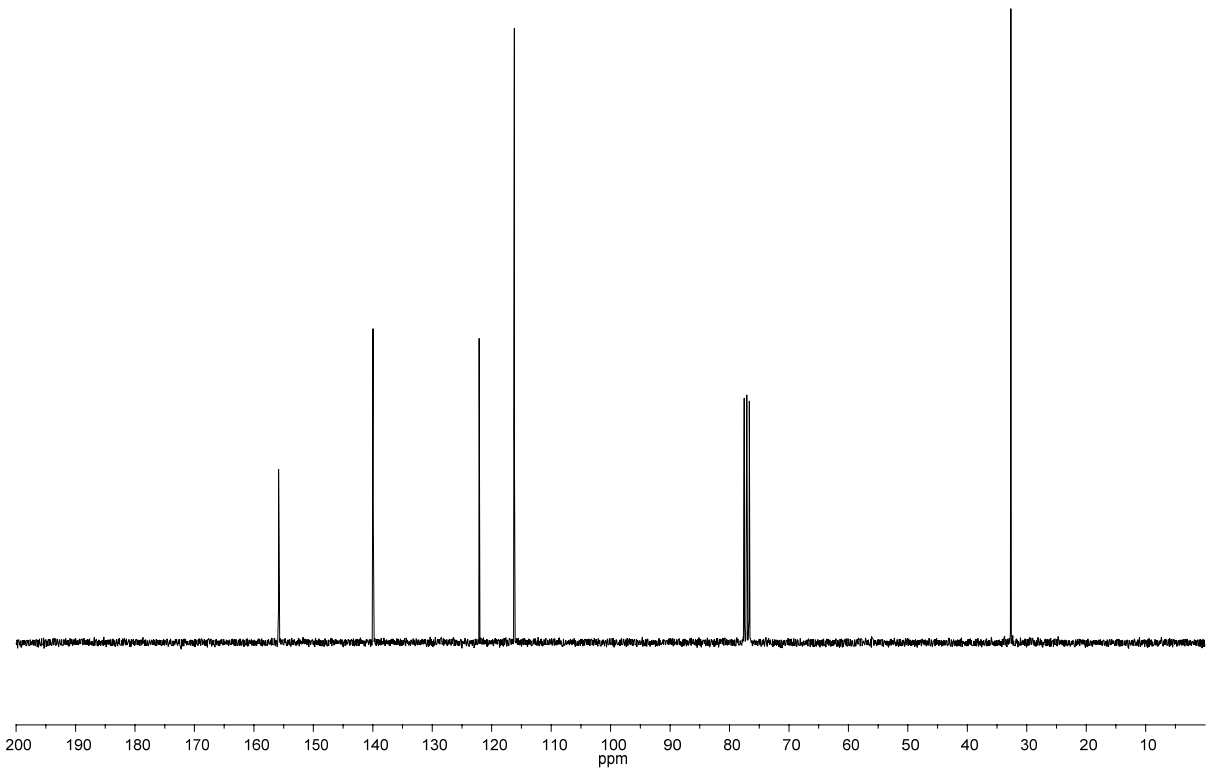

3,3'-(5-hydroxy-1,3-phenylene)bis(methylene)bis(1-benzyl-1H-imidazol-3-ium) bromide (149) (DMSO):

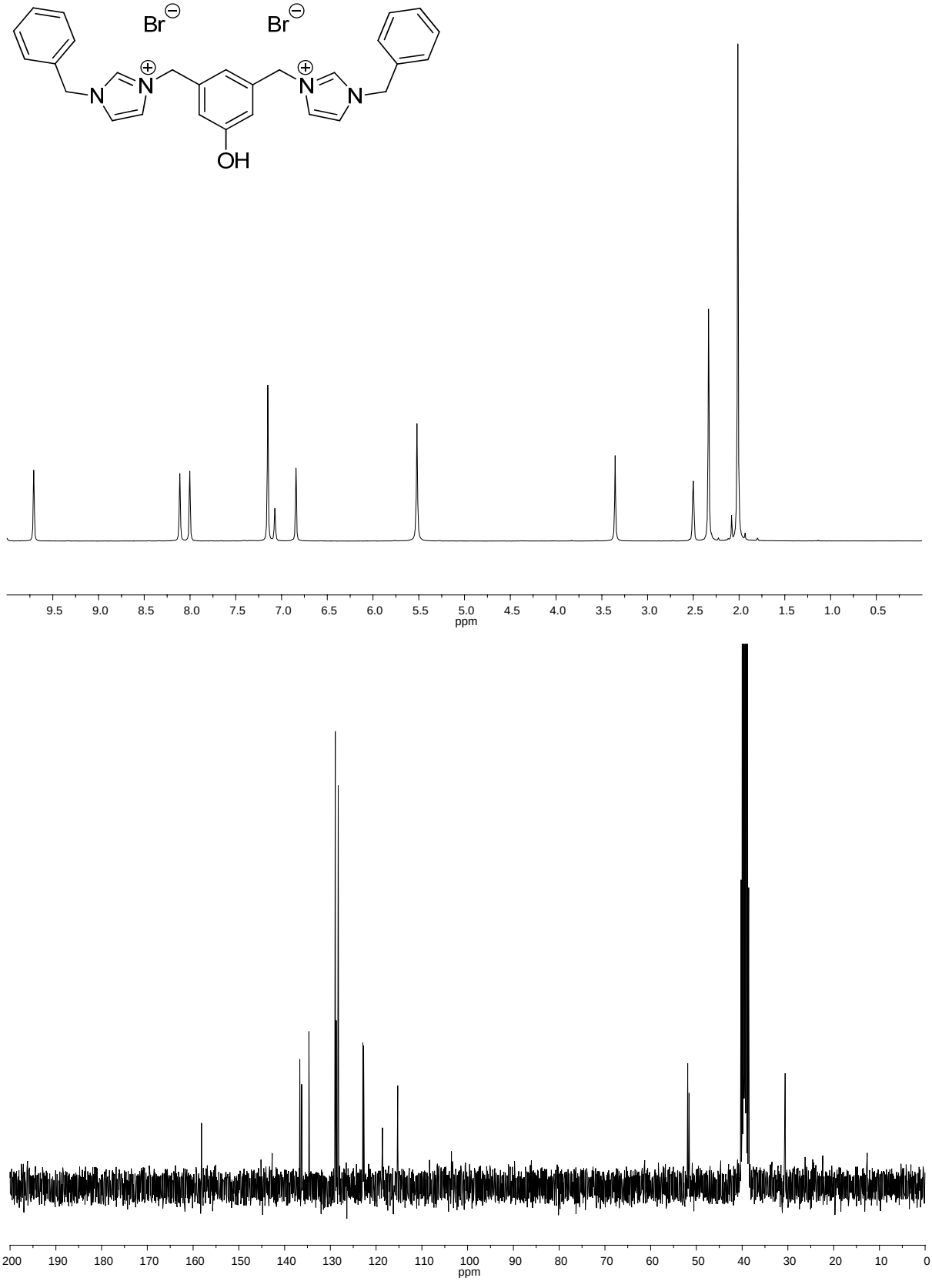

3,3'-(5-hydroxy-1,3-phenylene)bis(methylene)bis(1-mesityl-1H-imidazol-3-ium) bromide (98) (DMSO):

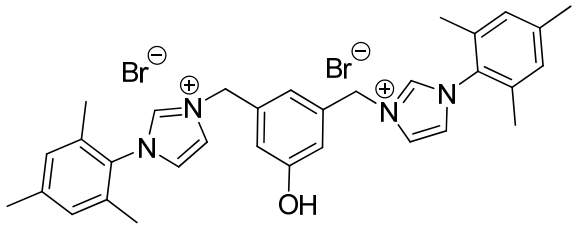

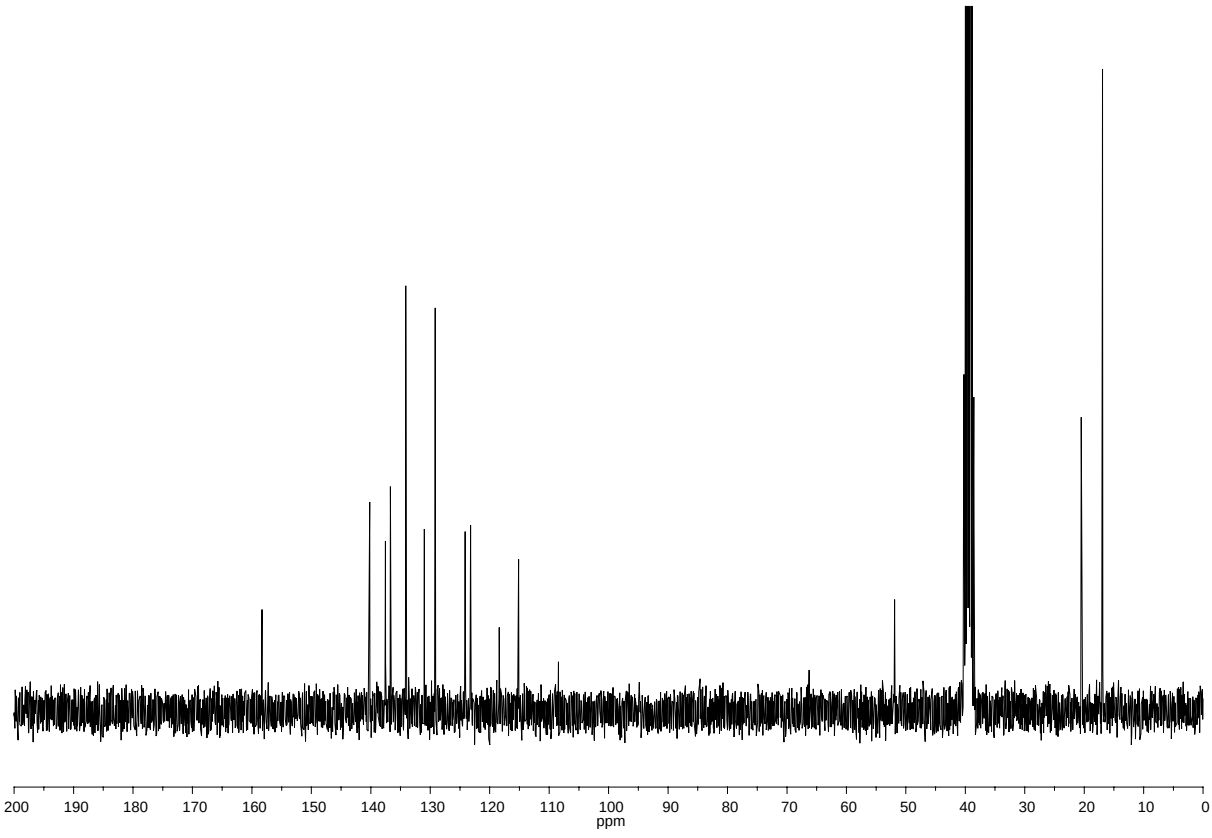

(3,3'-(5-hydroxy-1,3-phenylene)bis(methylene)bis(1-mesityl-1H-imidazolium-2,2'-diyliden))-di-silver(I)-dibromide (99):

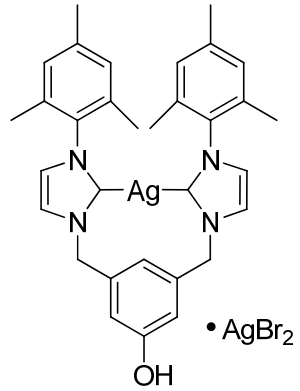

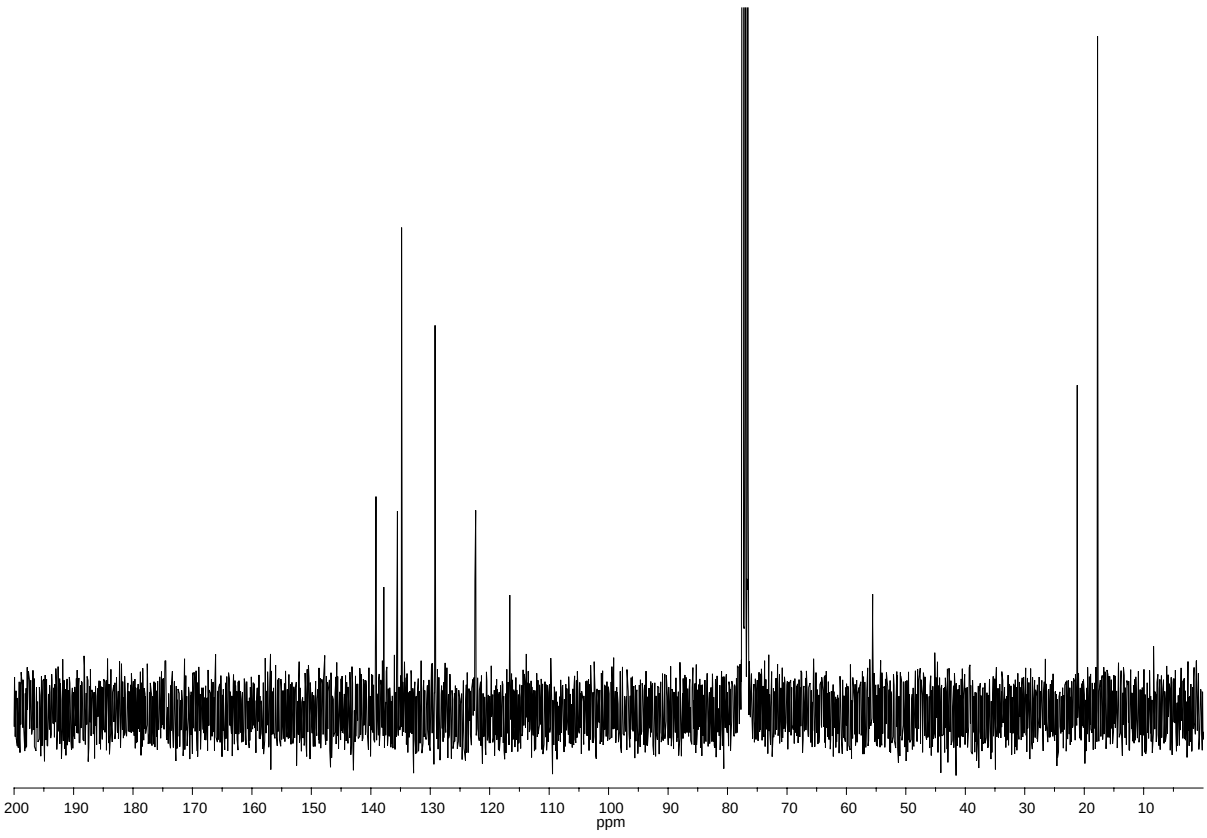

(3,3'-(5-hydroxy-1,3-phenylene)bis(methylene)bis(1-mesityl-1H-imidazolium-2,2'-diyliden))palladium(II)-dichloride (100):

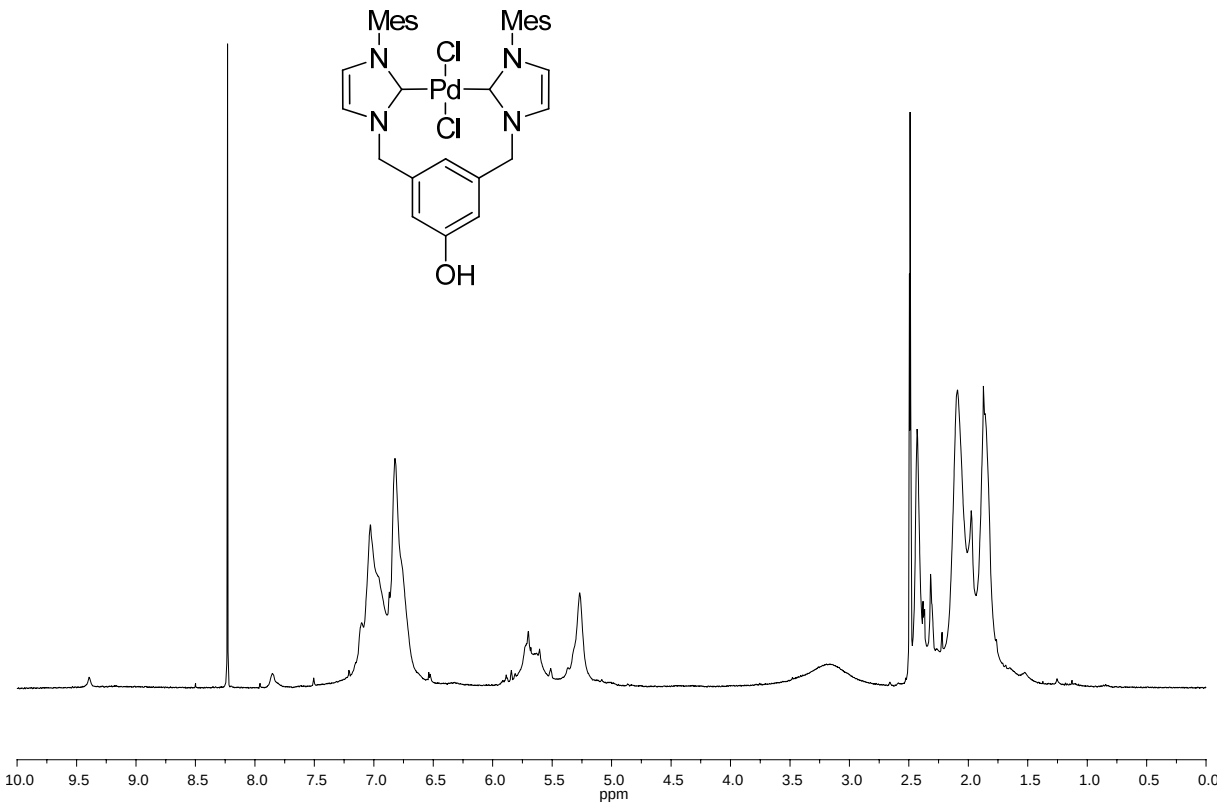

3-(3-azidopropyl)-1-methyl-1H-imidazol-3-ium bis(trifluoromethylsulfonyl)amide (120):

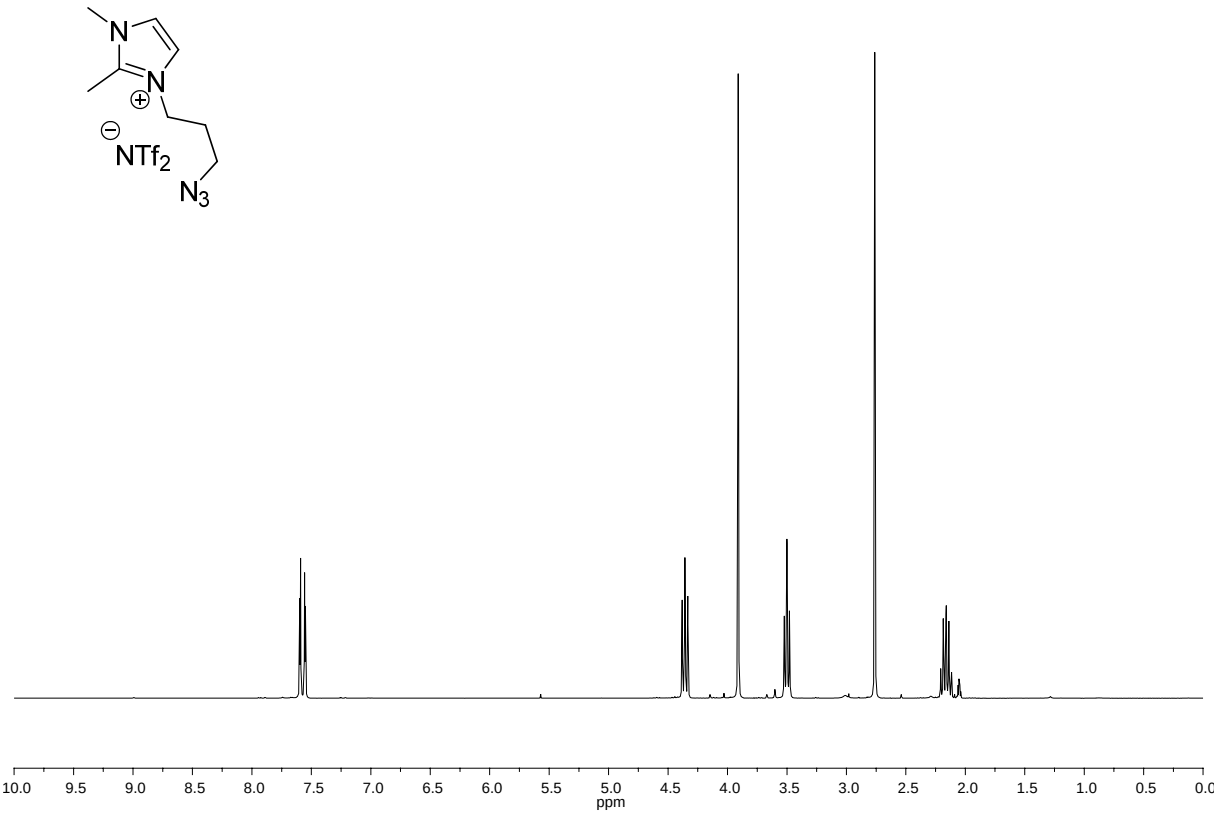

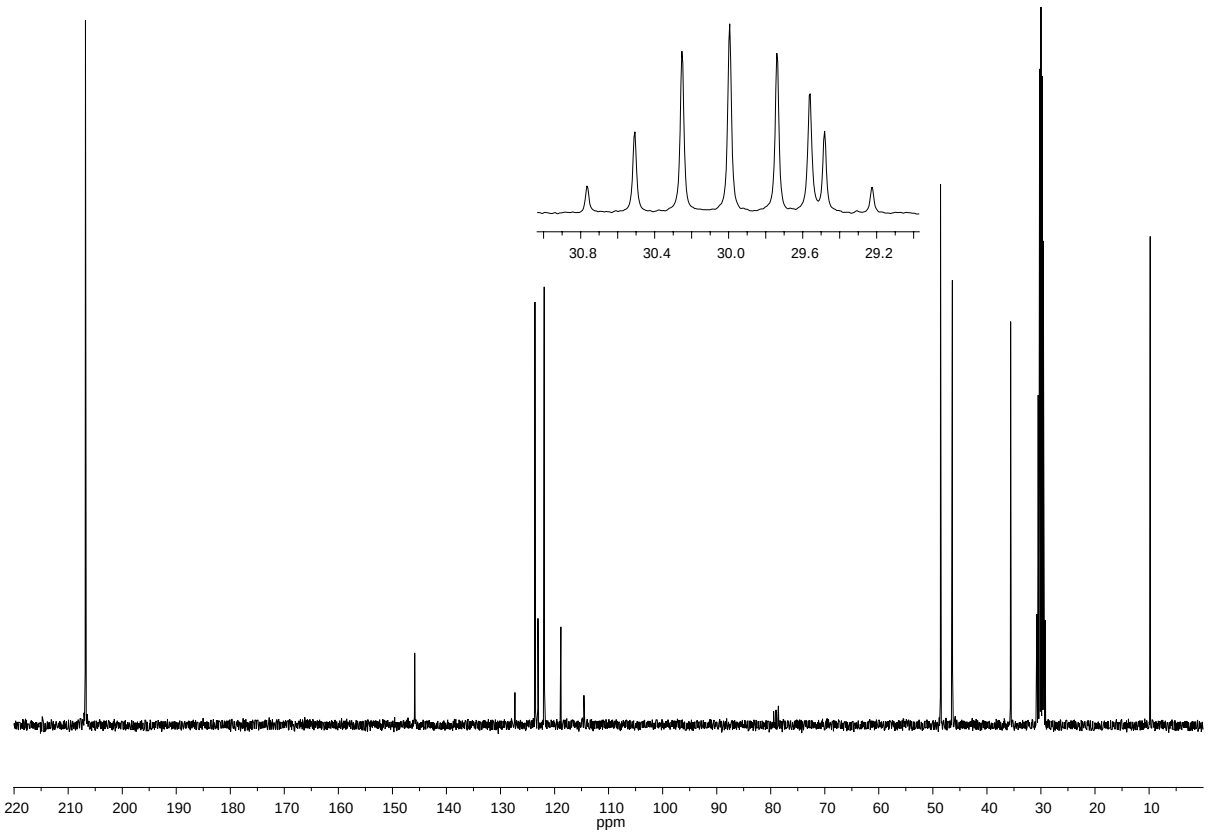

3-(3-azidopropyl)-1-methyl-1H-imidazol-3-ium iodide (150) (acetone):

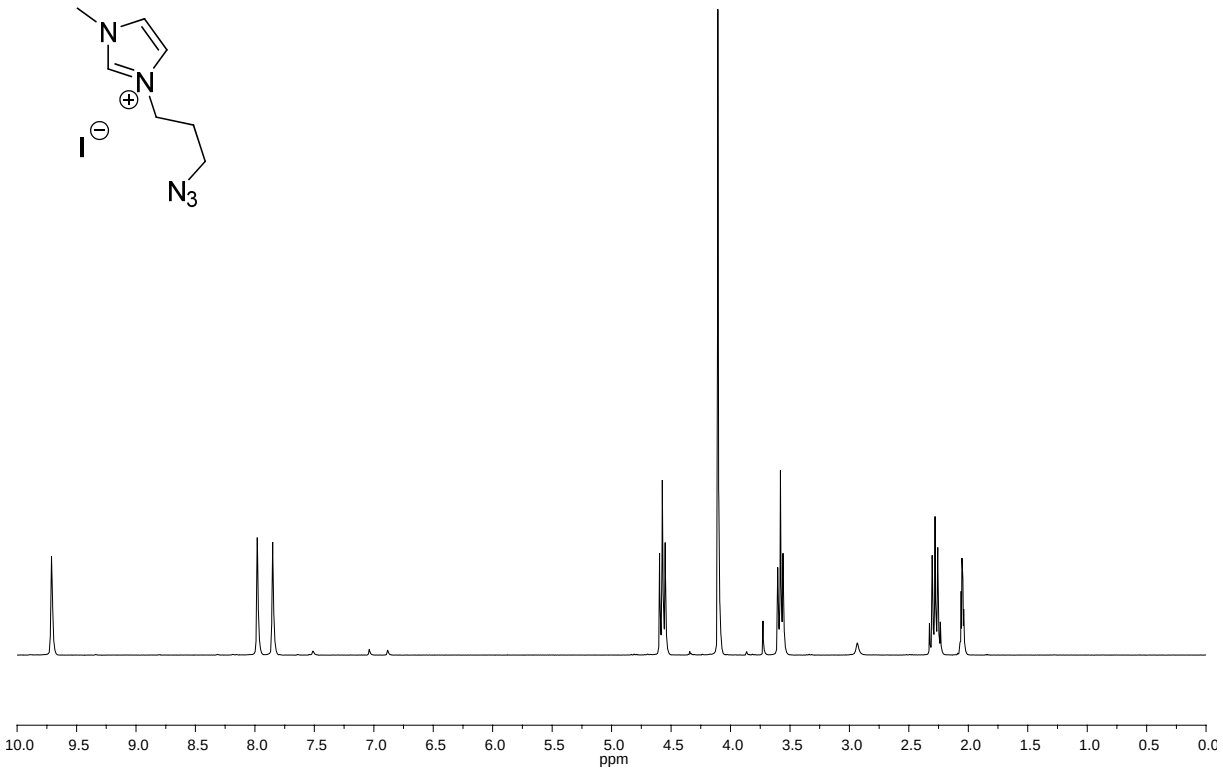

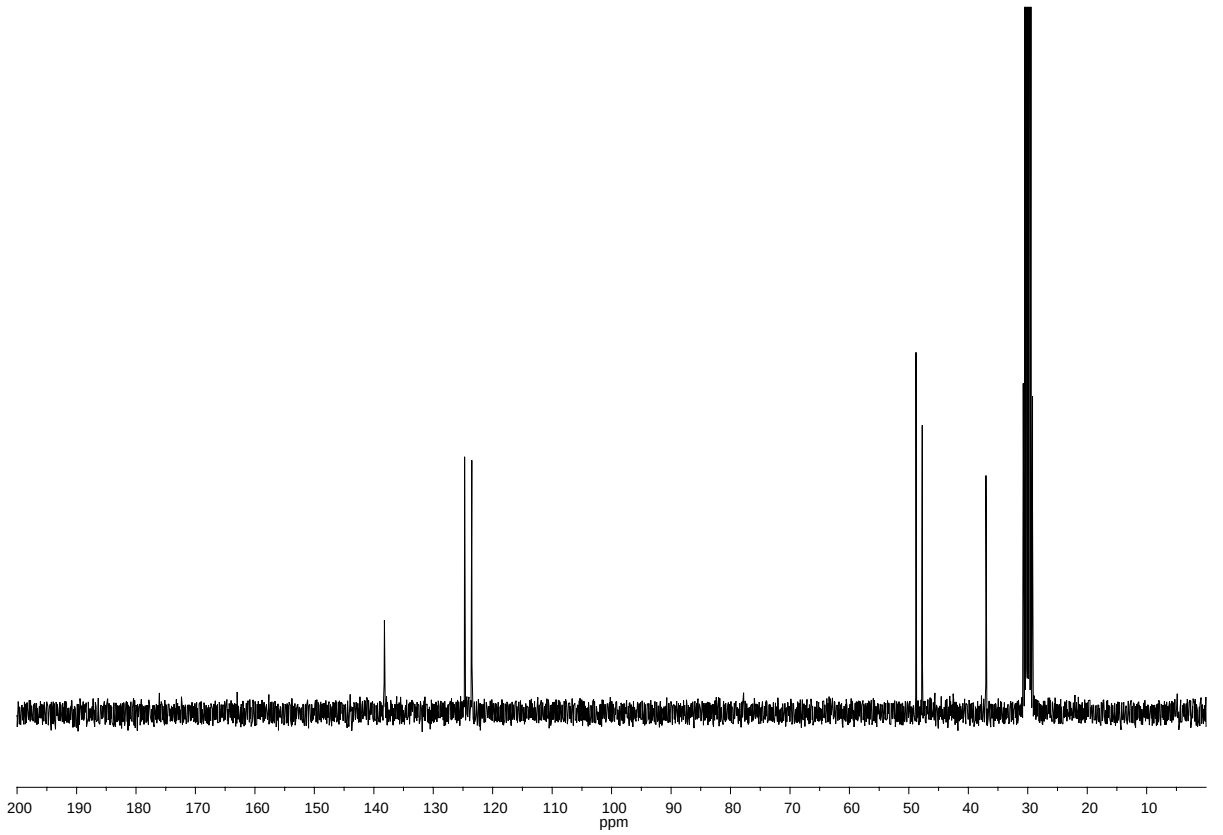

1,2-dimethyl-3-(3-(4-(4-nitrobenzoyloxy)-1H-1,2,3-triazol-1-yl)propyl)-1H-imidazol-3-ium bis(trifluoromethylsulfonyl)amide (122) (acetone):

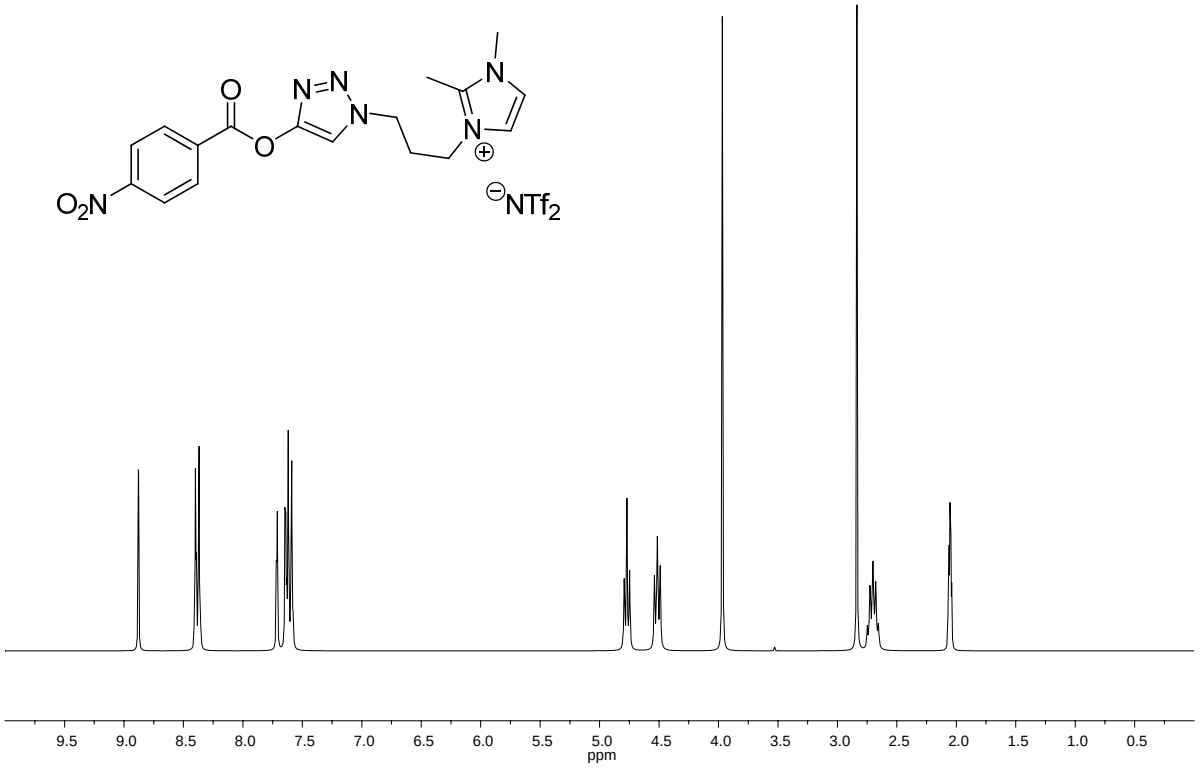

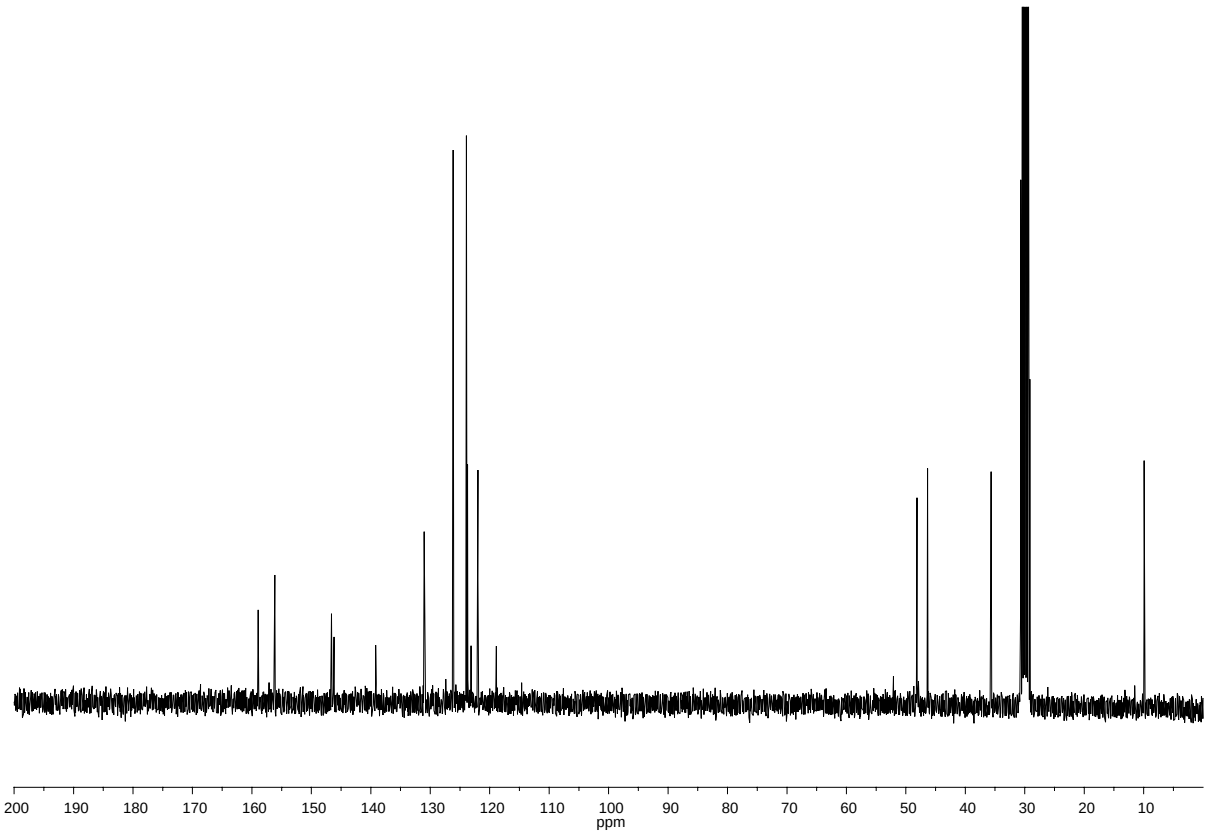

4-hydroxybenzoic acid (54a) (DMSO):

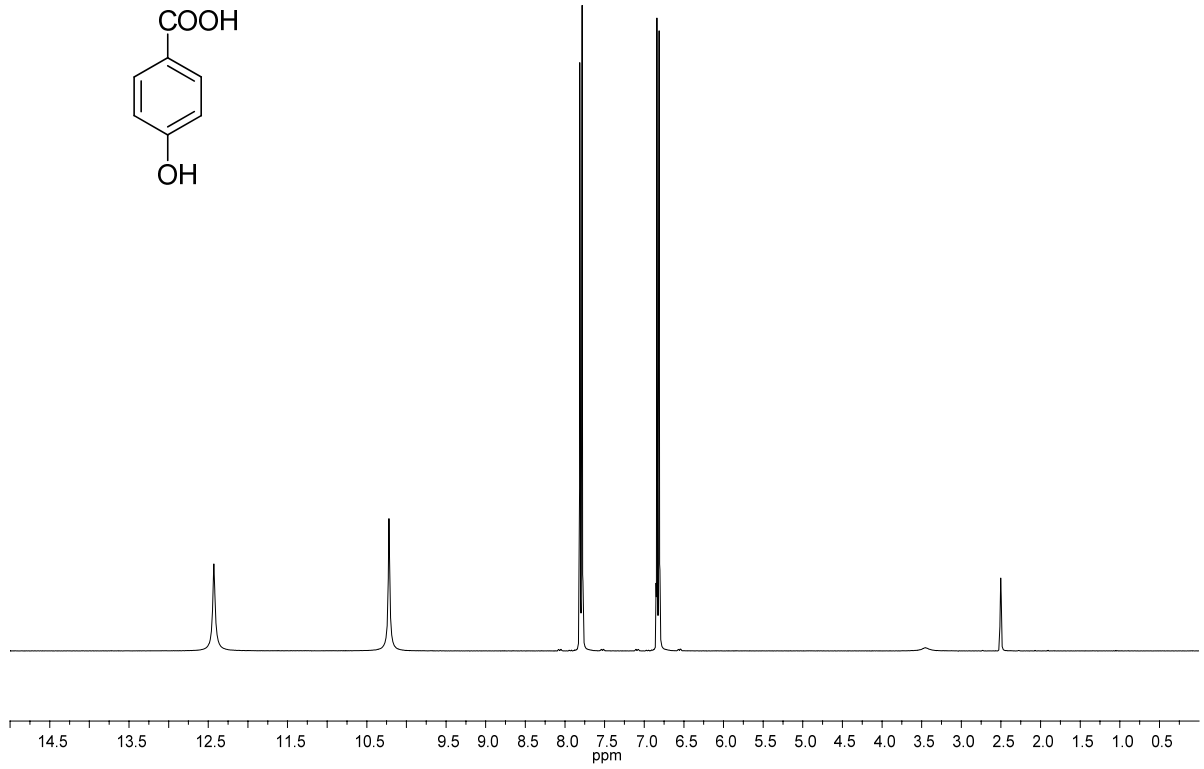

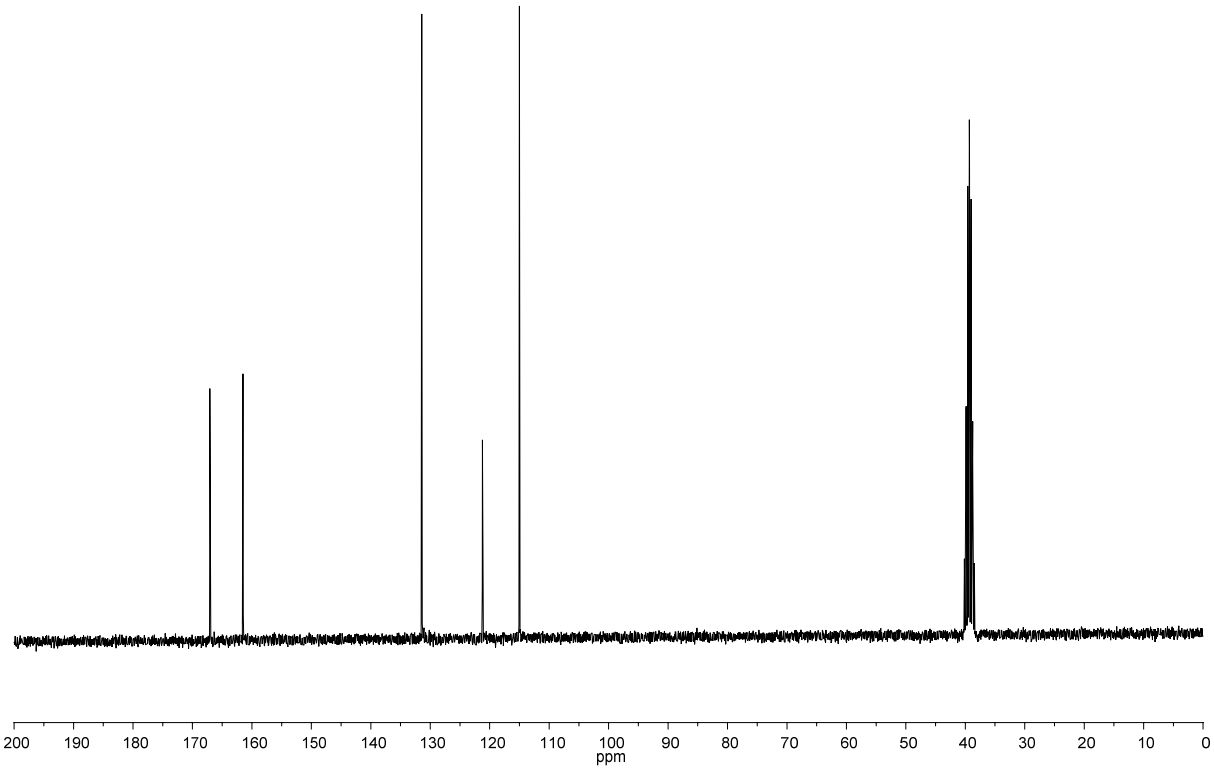

Terephthalic acid (54b) (DMSO):

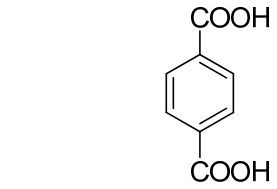

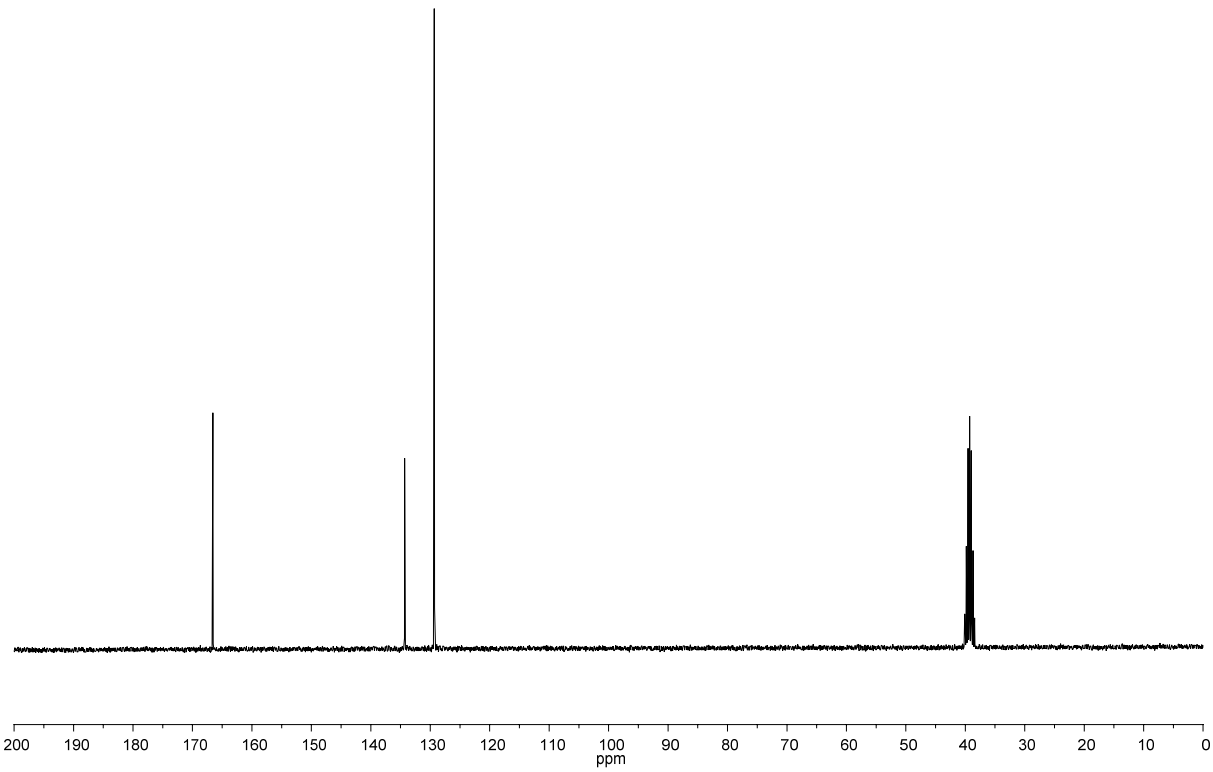

5-hydroxyisophthalic acid (54e) (DMSO):

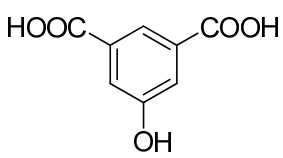

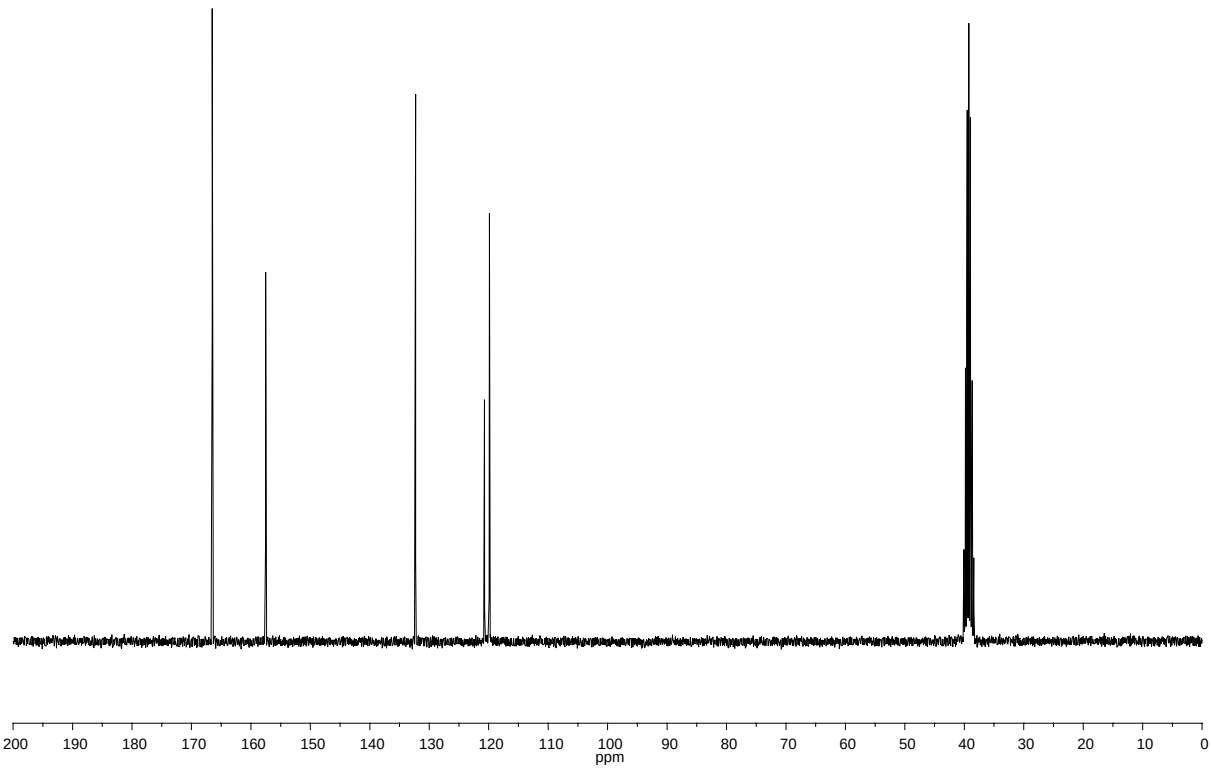

4-hydroxyisophthalic acid (54d) (DMSO):

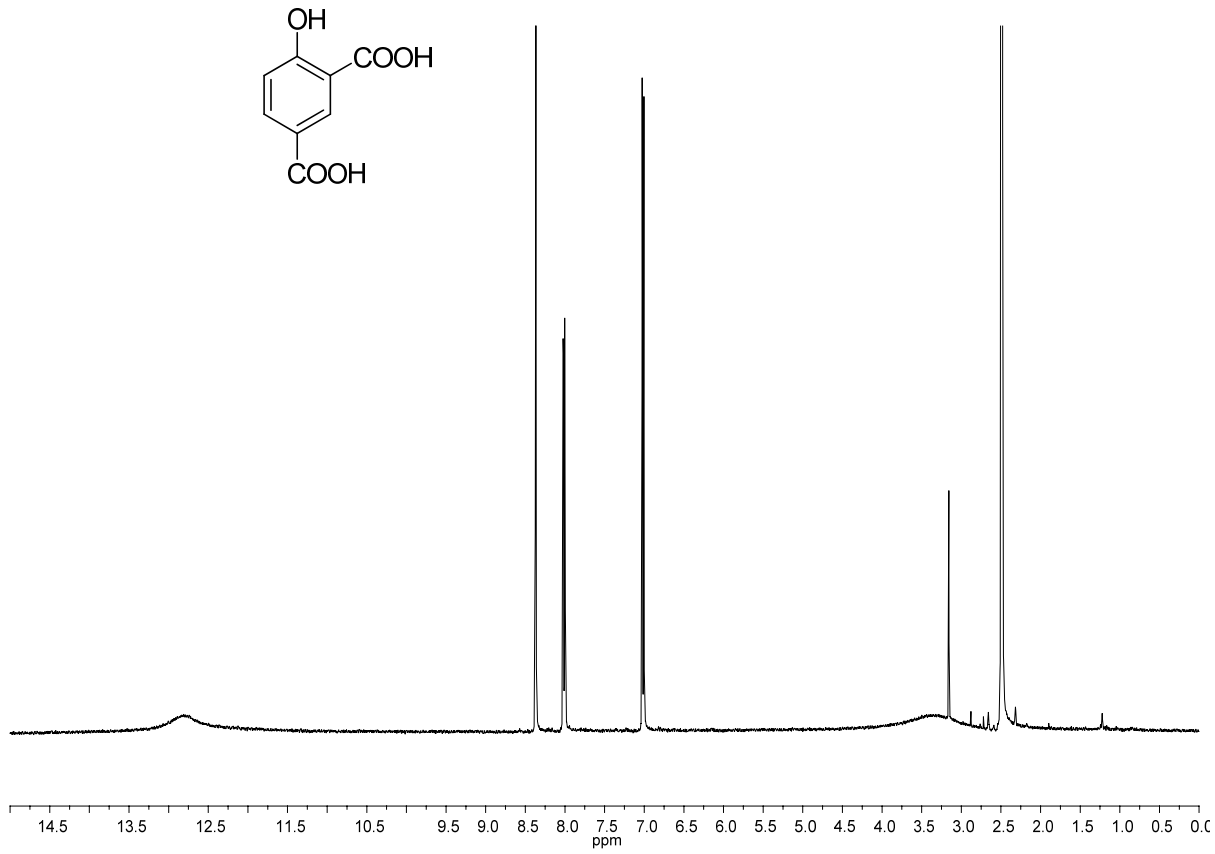

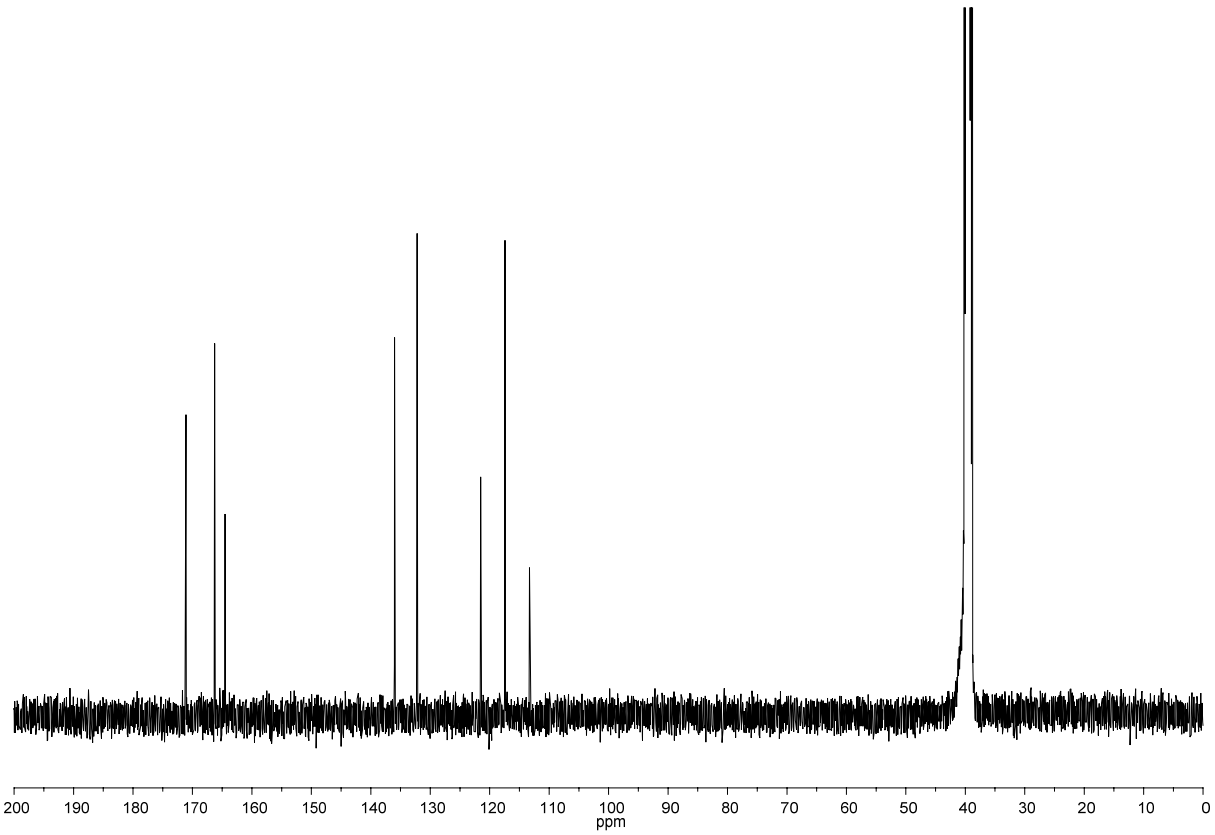

4-hydroxy-3,5-dimethylbenzoic acid (54c) (DMSO):

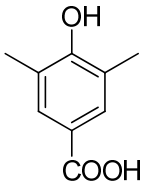

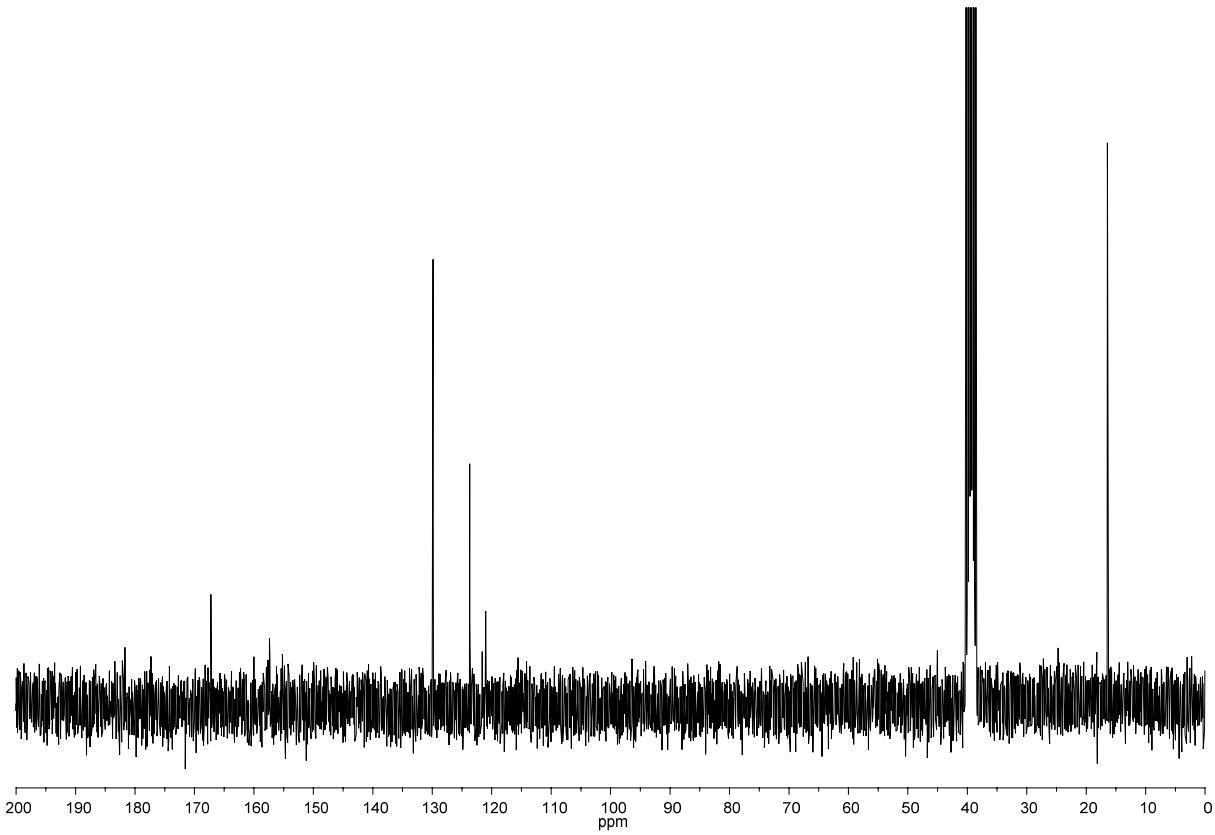

Diethyl 2-((1H-indol-3-yl)(phenyl)methyl)malonate (134a):

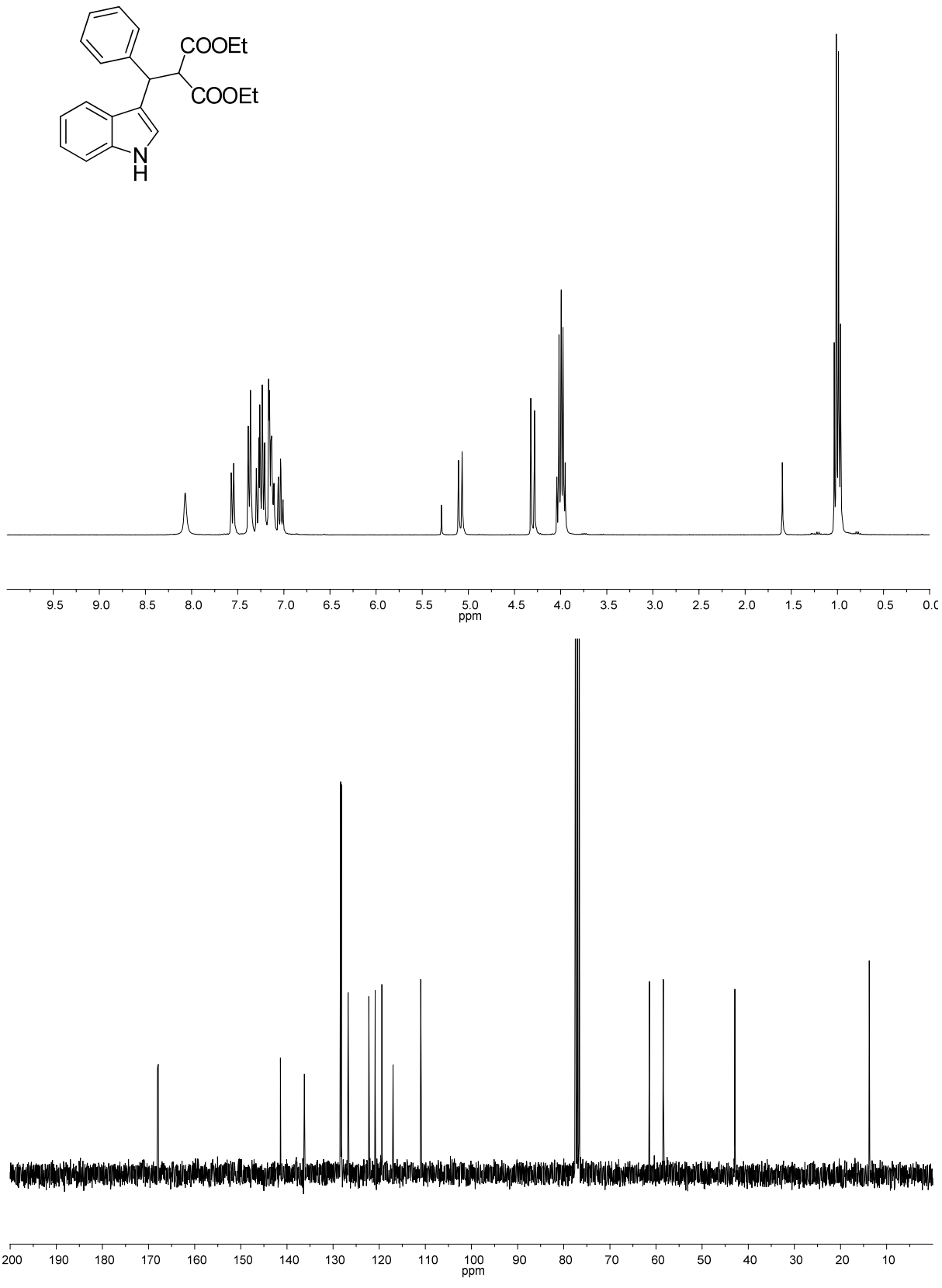

Diethyl 2-((4-chlorophenyl)(1H-indol-3-yl)methyl)malonate (134c):

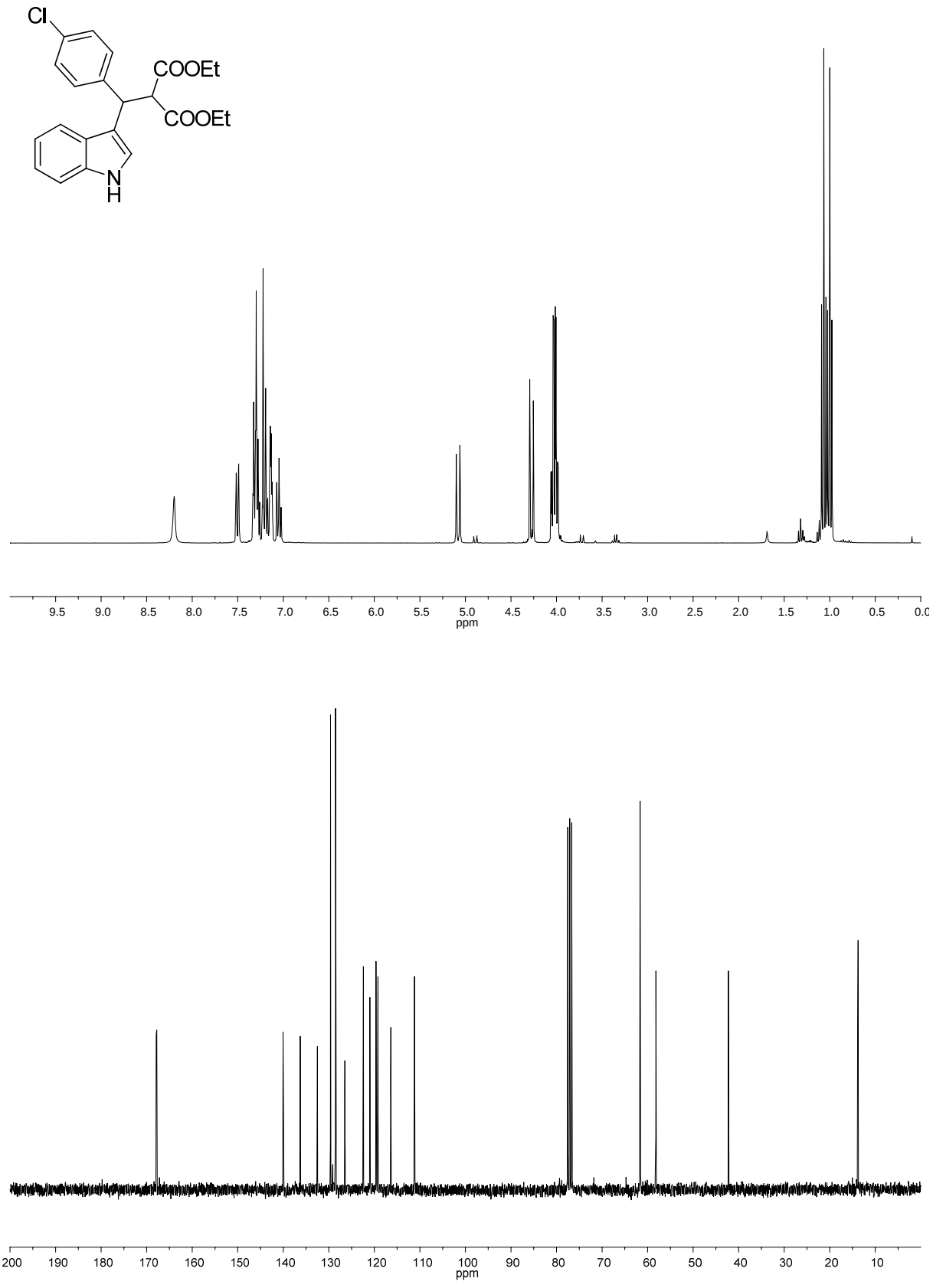

(*S*)-2-((*R*)-hydroxy(4-nitrophenyl)methyl)cyclohexanone (72):

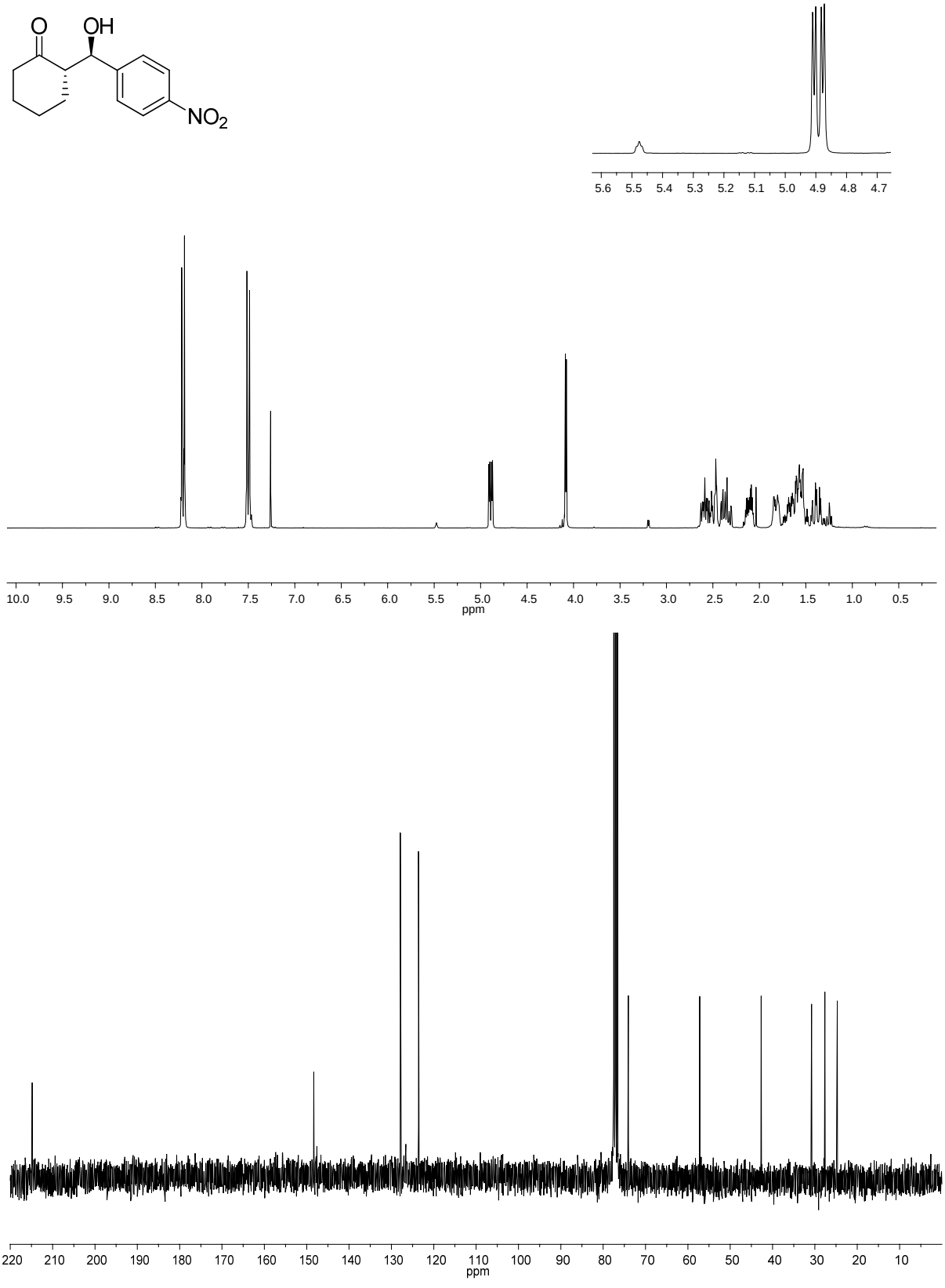

(*S*)-2-((*R*)-(4-bromophenyl)(hydroxy)methyl)cyclohexanone (80):

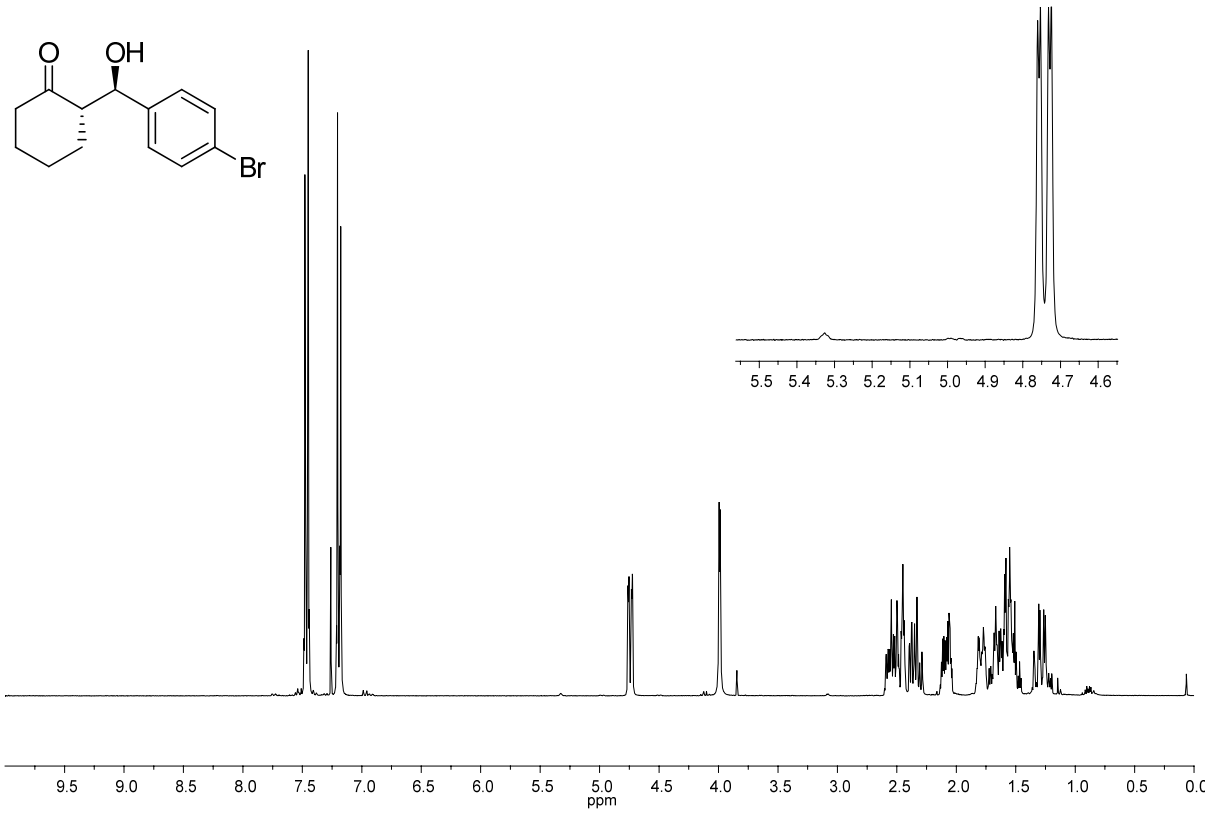

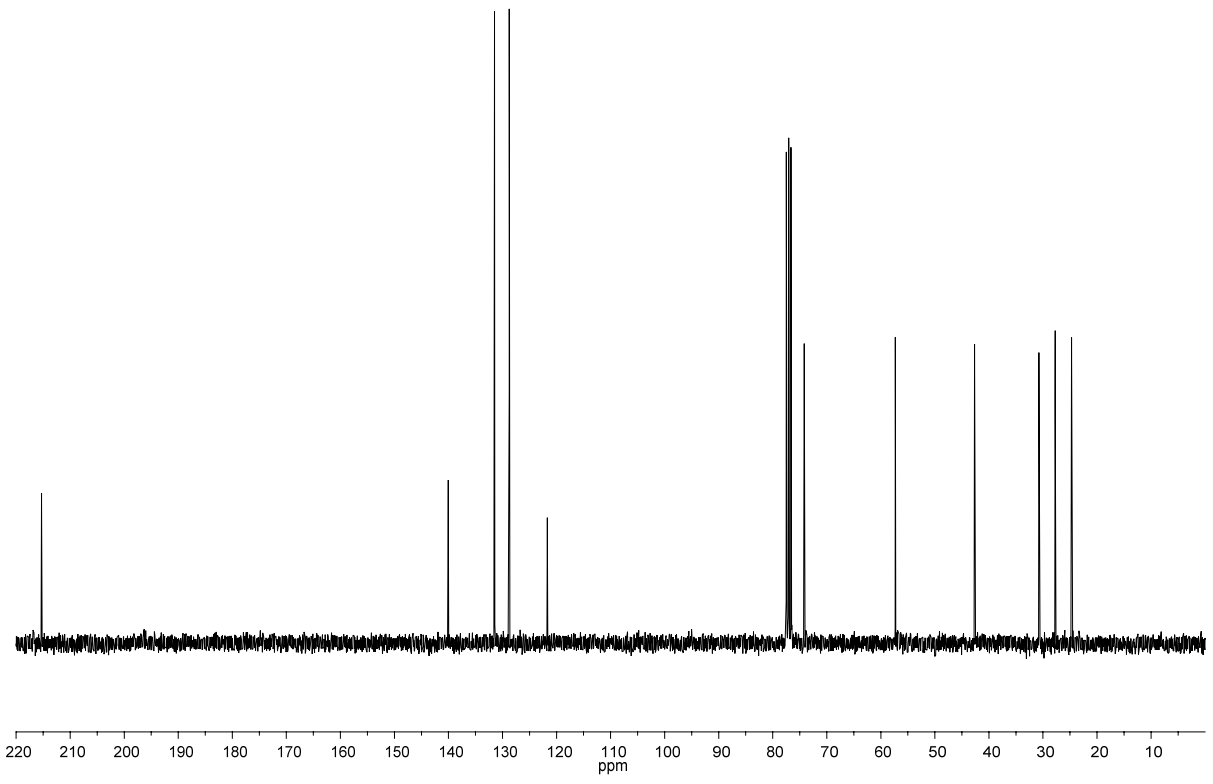

4-((*R*)-hydroxy((*S*)-2-oxocyclohexyl)methyl)benzonitrile (77):

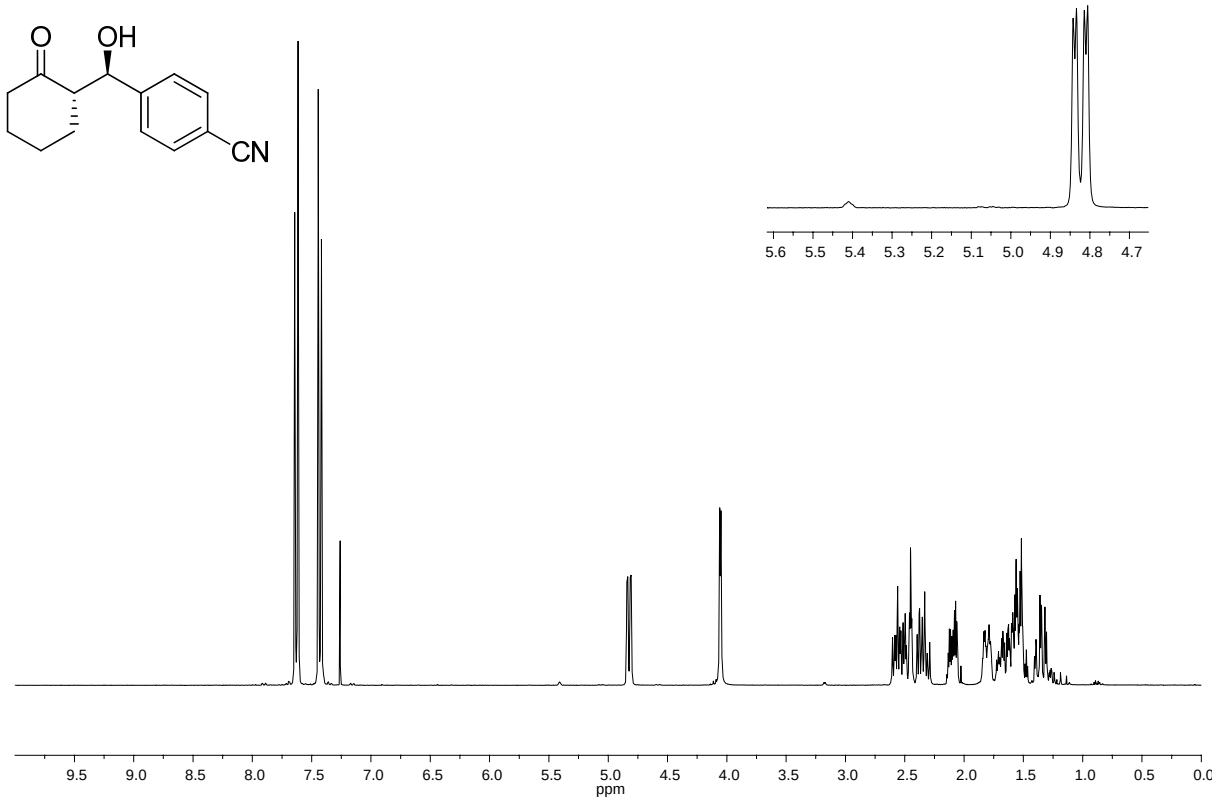

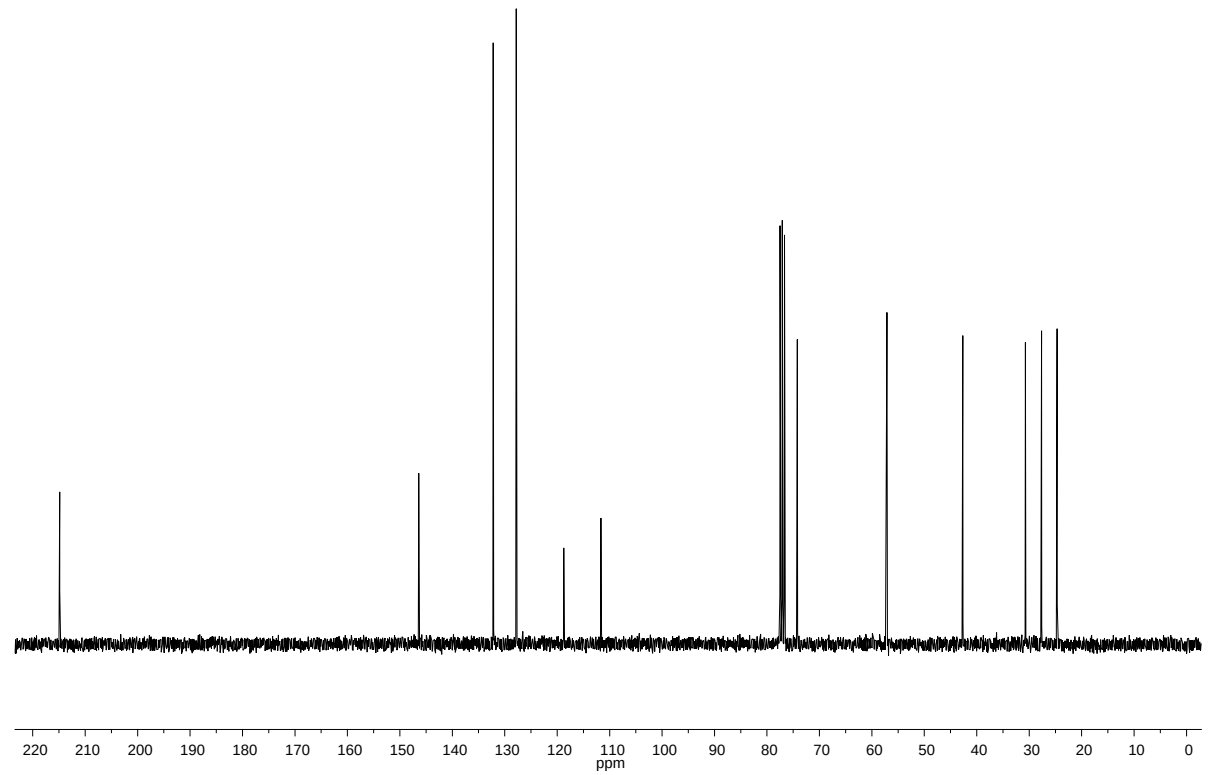

(*S*)-2-((*R*)-hydroxy(4-(trifluoromethyl)phenyl)methyl)cyclohexanone (78):

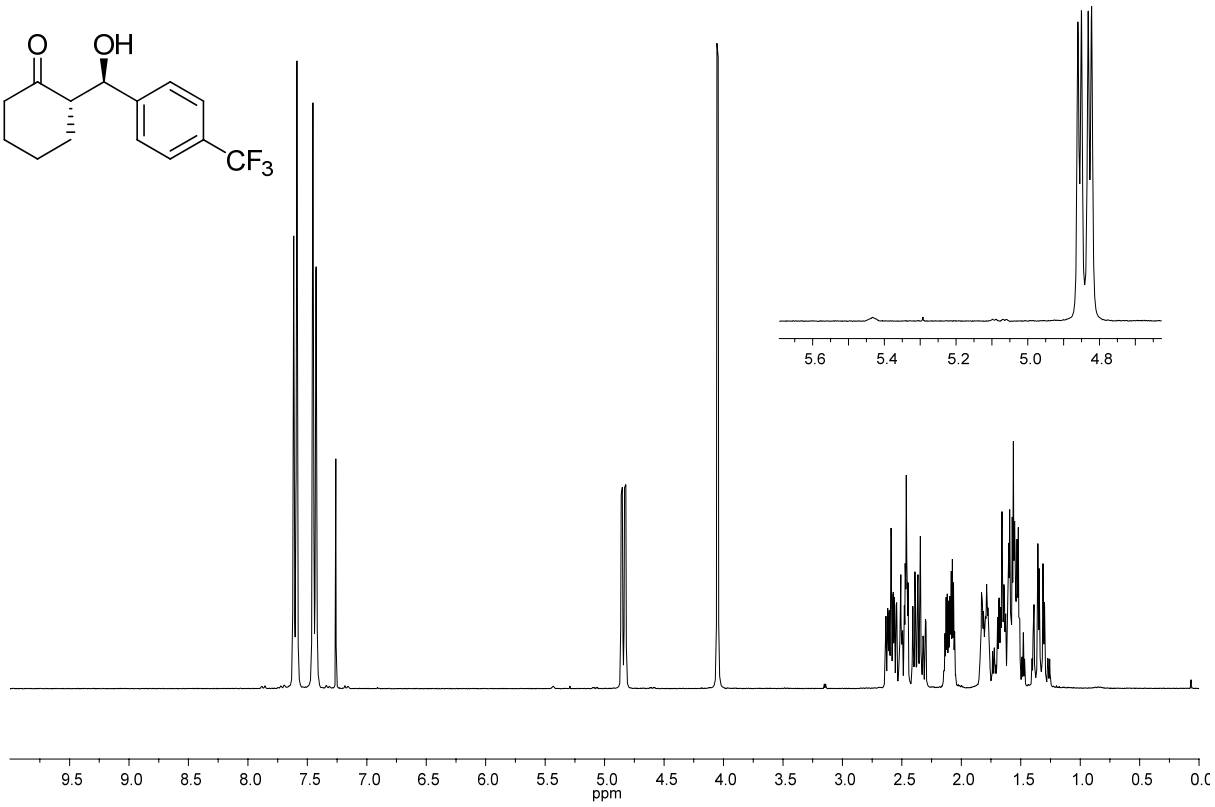

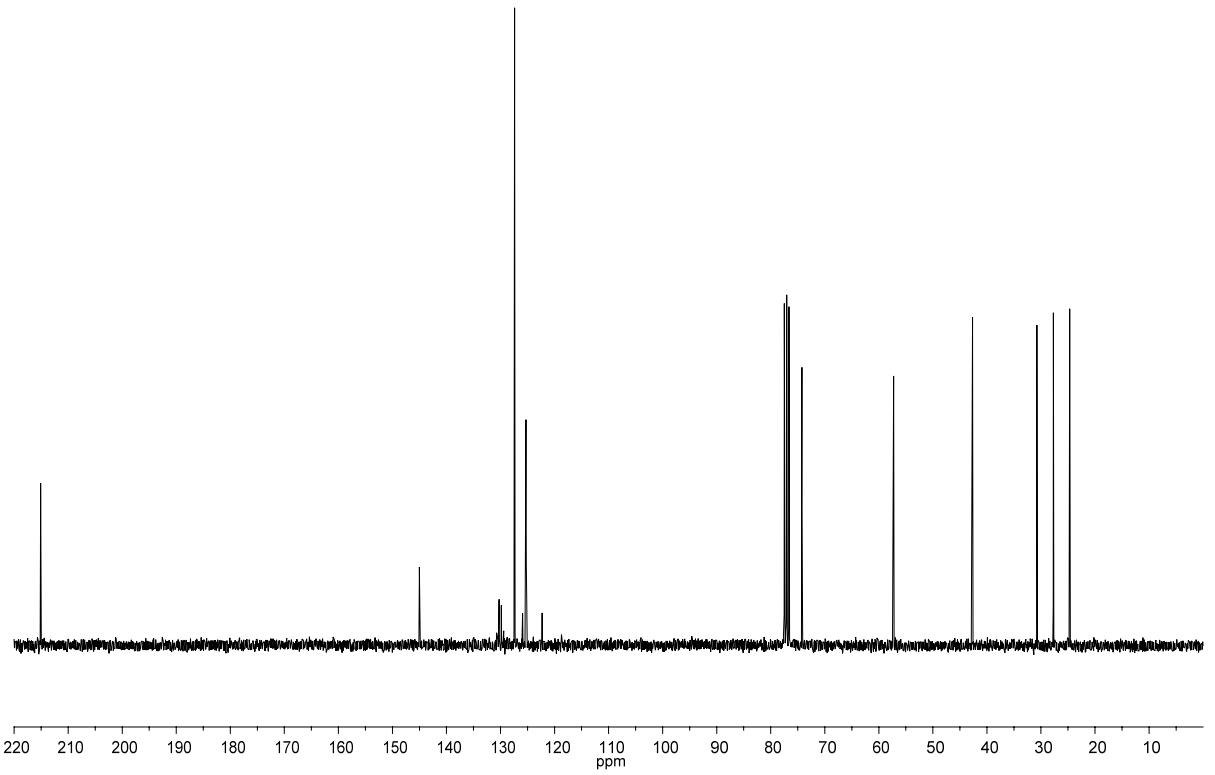

(*S*)-2-((*R*)-hydroxy(phenyl)methyl)cyclohexanone (79):

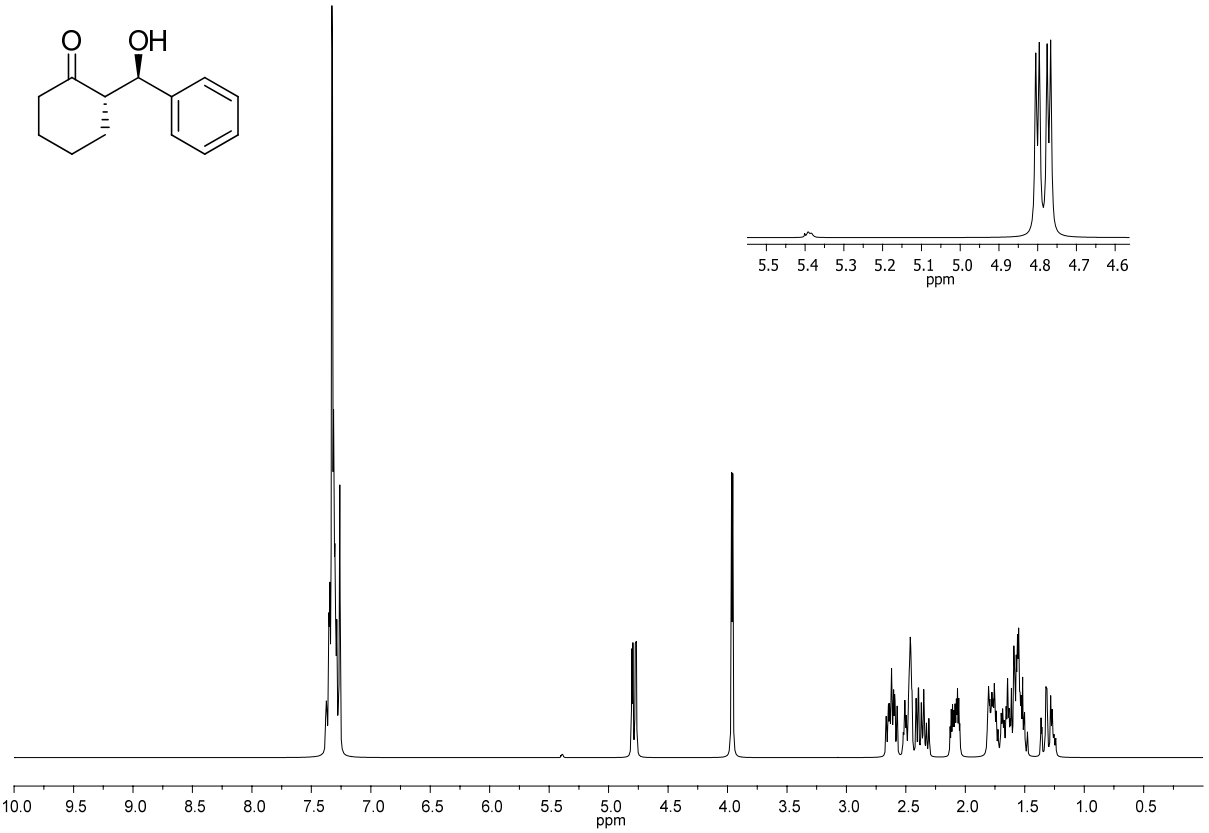

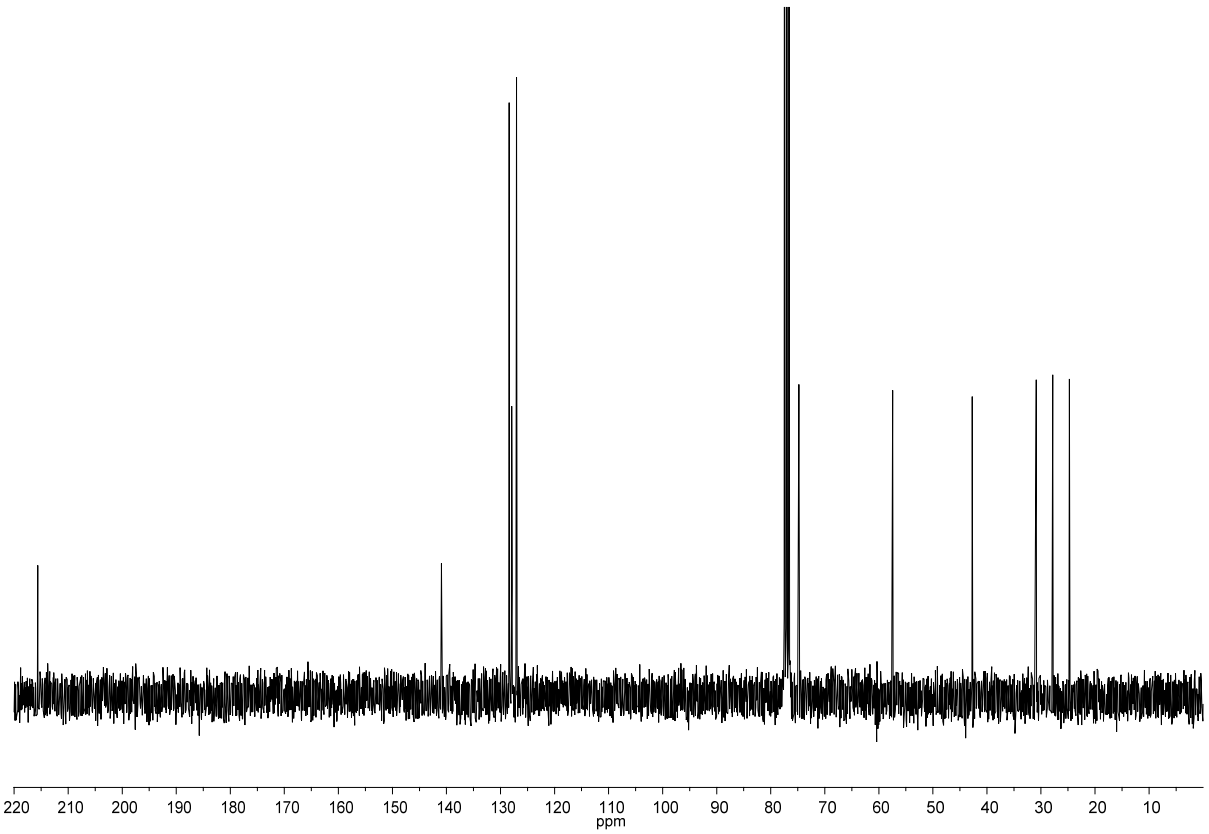

1-(biphenyl-4-yl)ethanone (110):

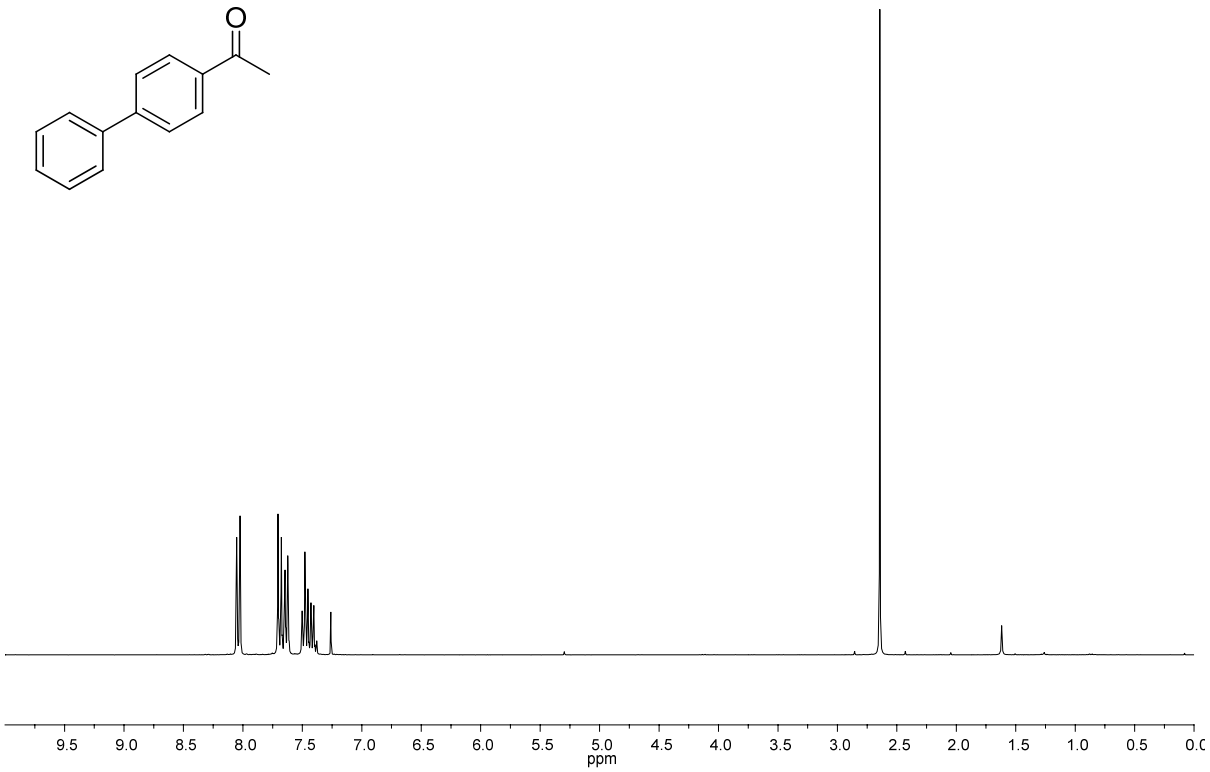

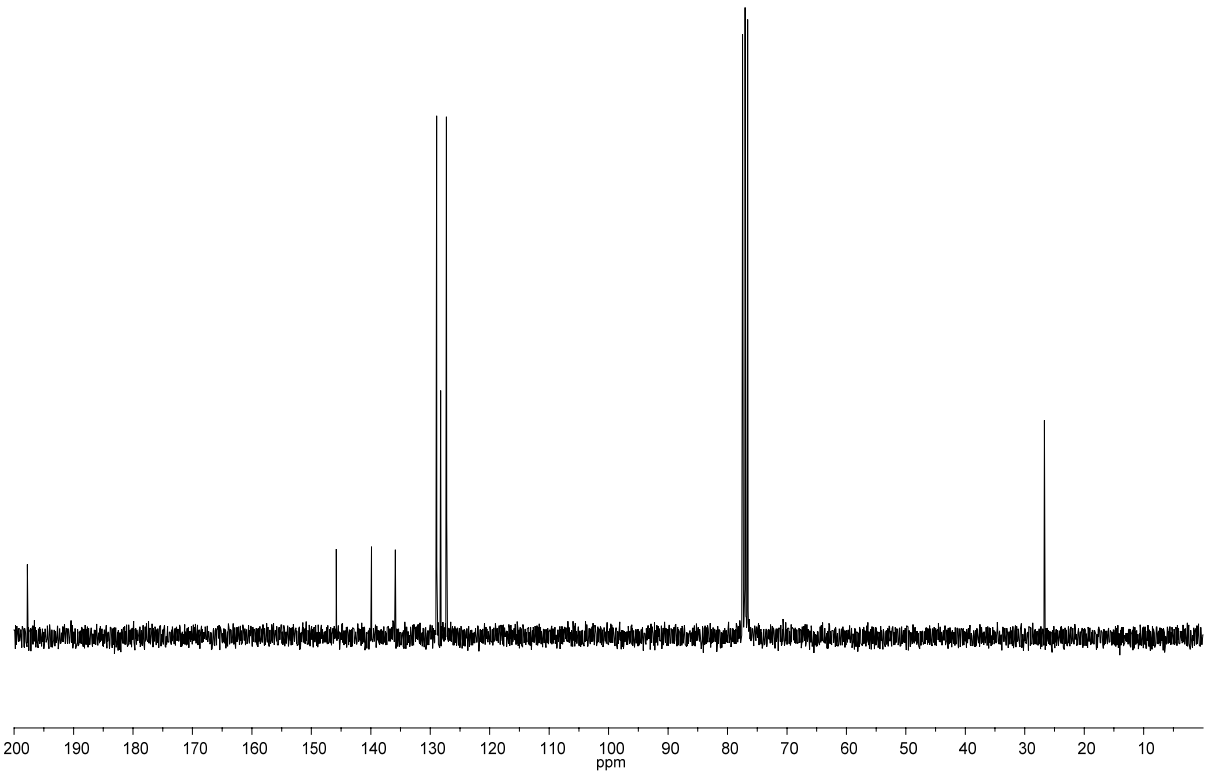

2,6-dimethylbiphenyl (108):

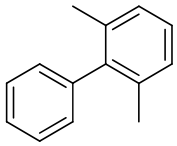

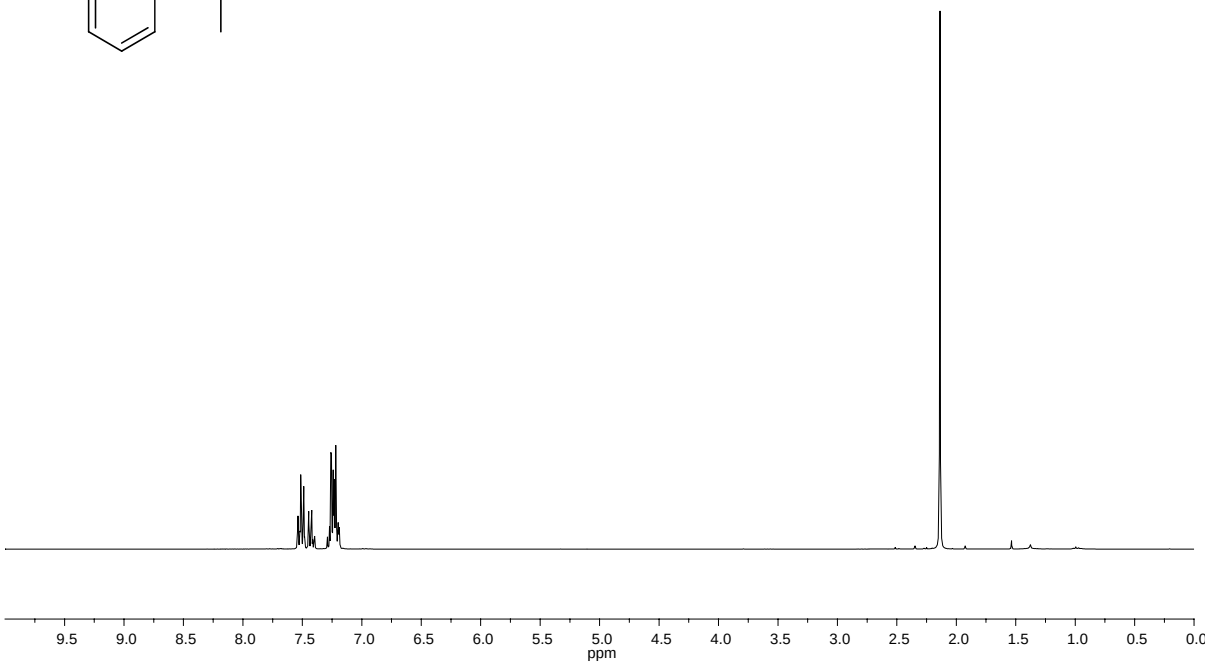

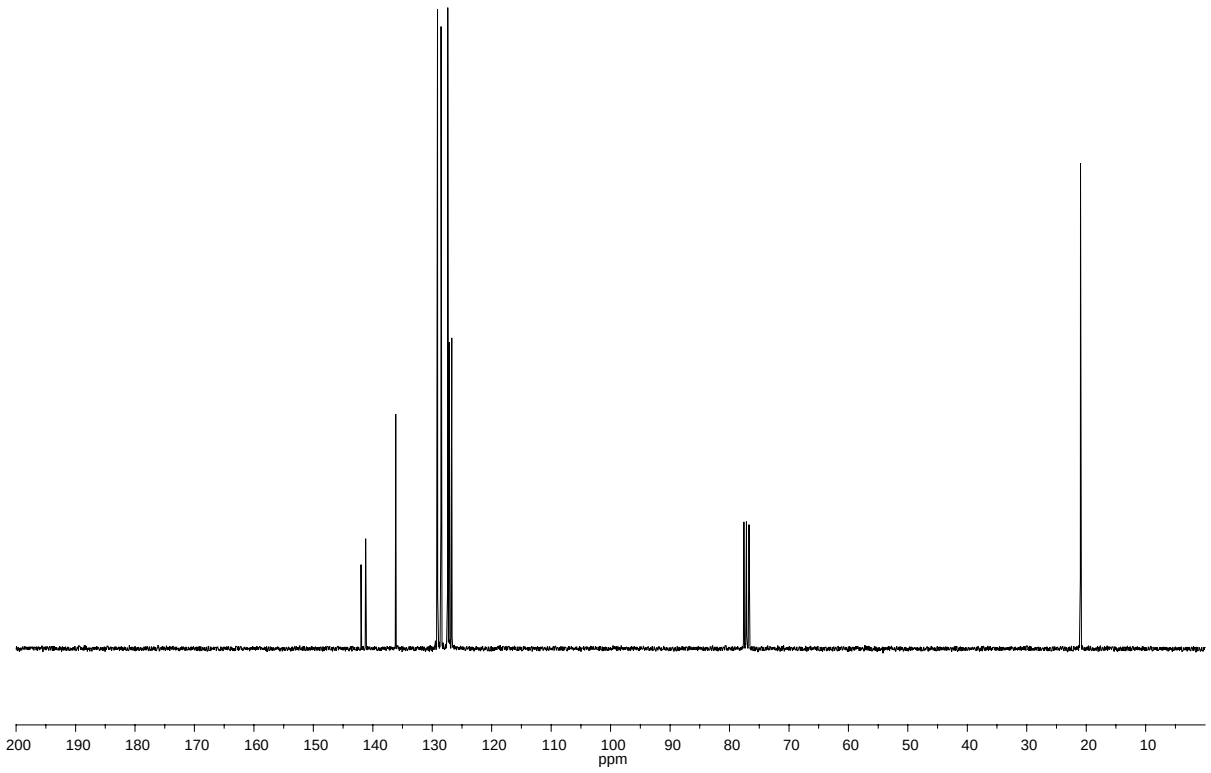

4-nitrobiphenyl (109):

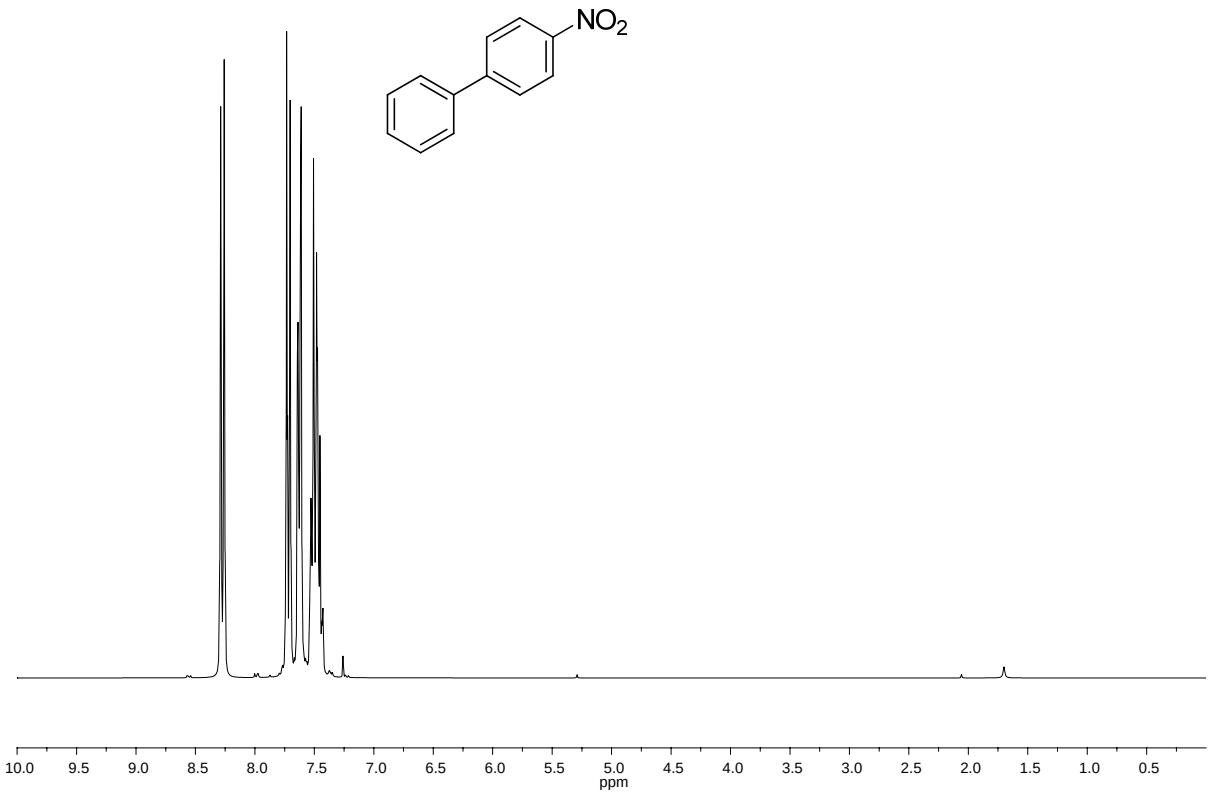

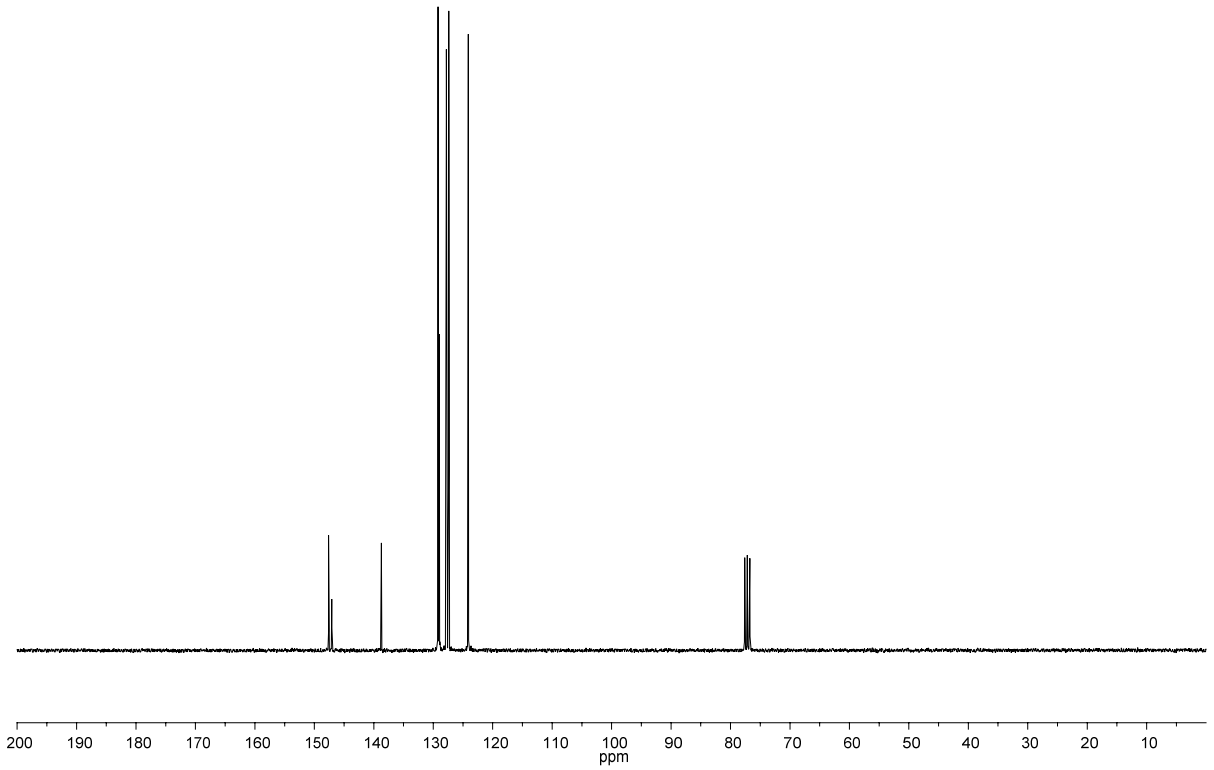

(*R*)-methyl 4-(1-hydroxybut-3-enyl)benzoate (144):

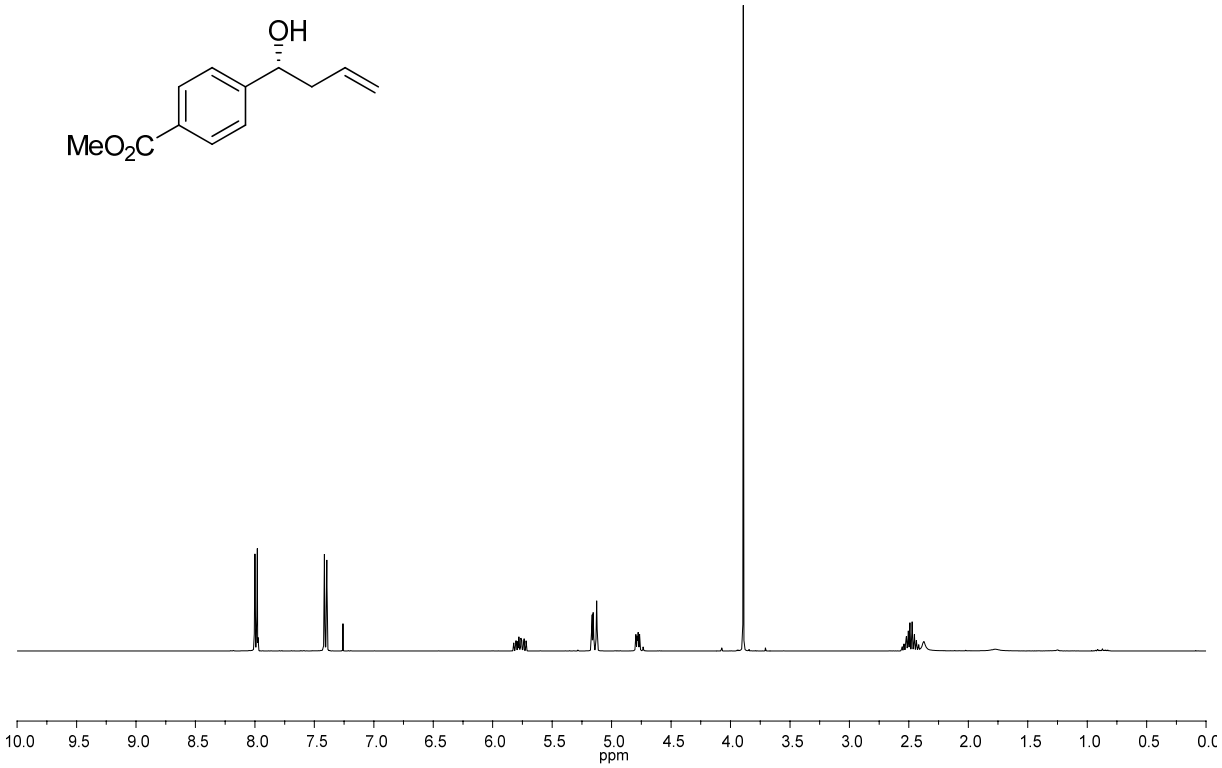

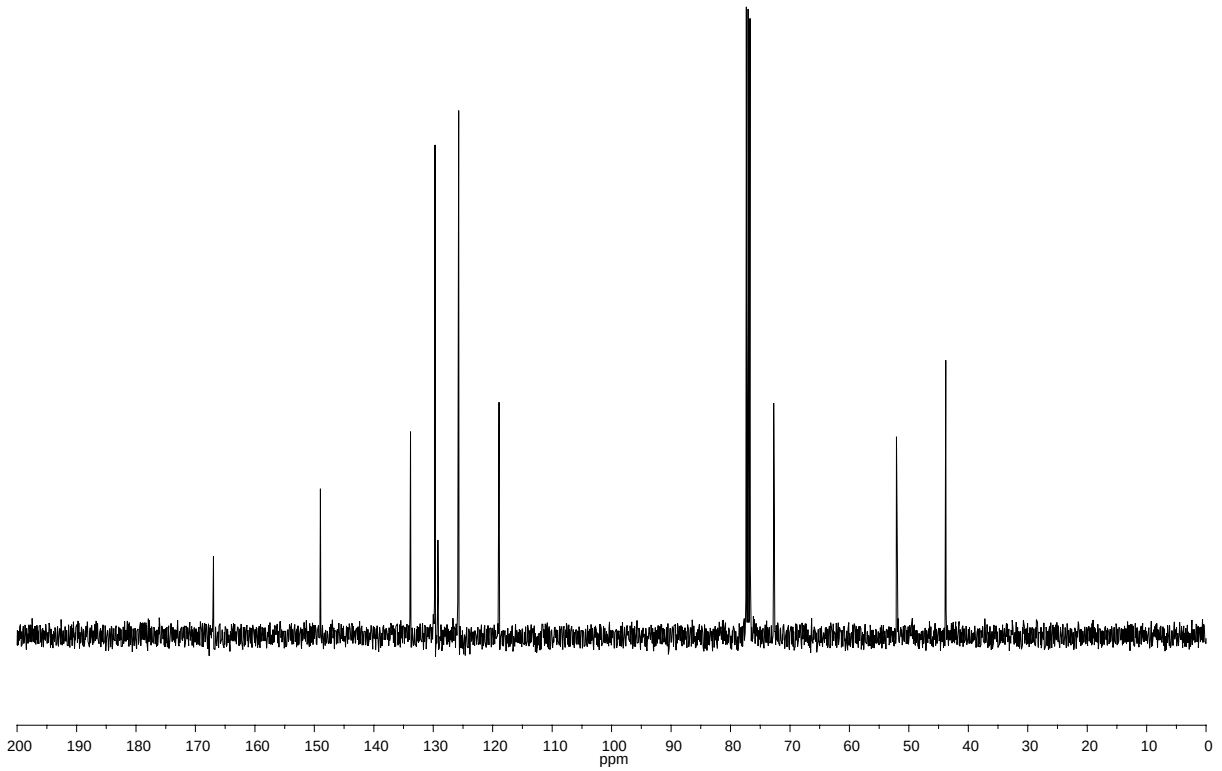

(*R*,*E*)-1-phenylhexa-1,5-dien-3-ol (145):

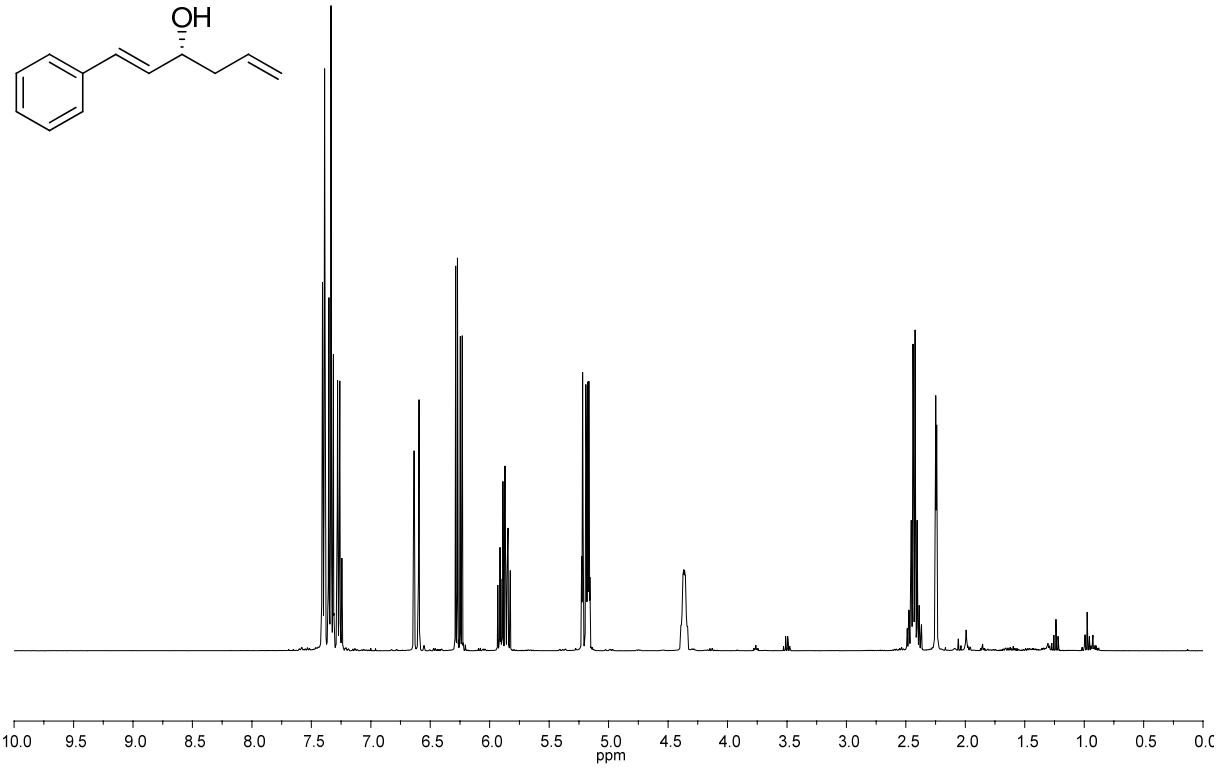

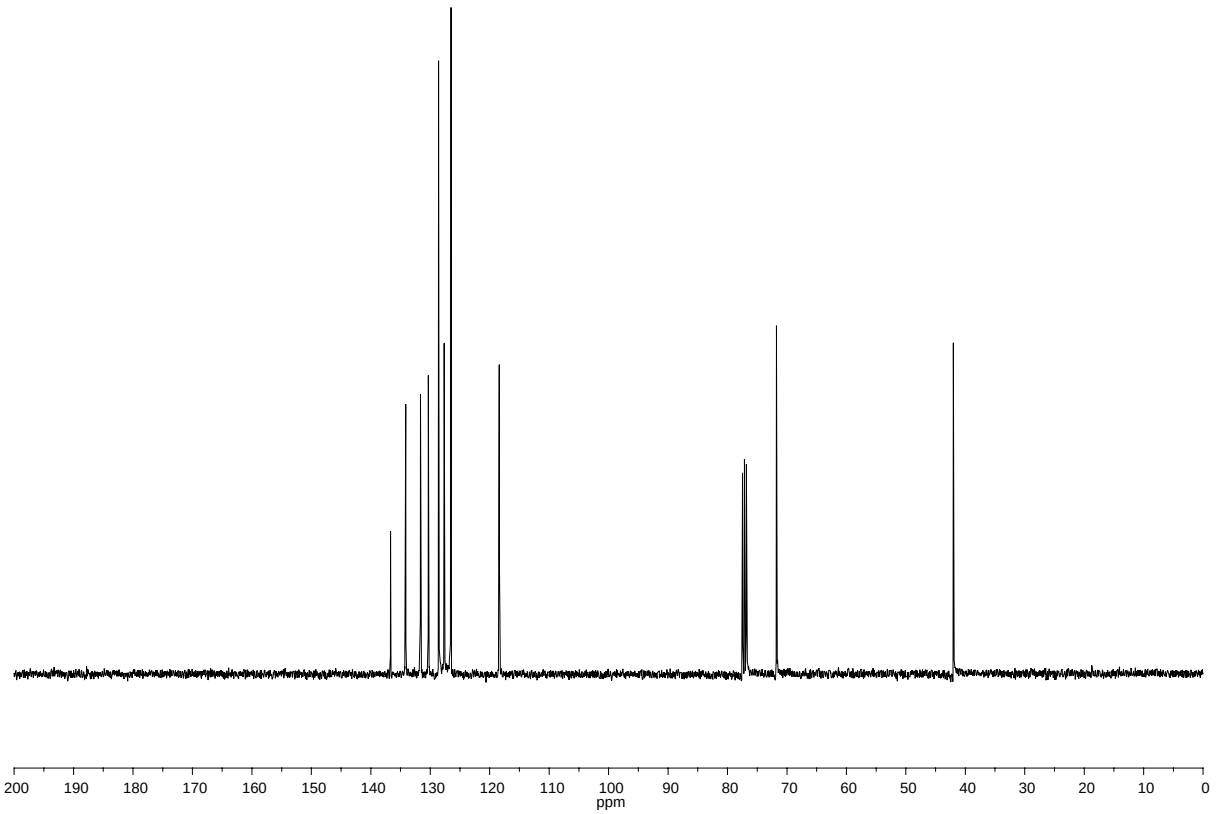

(*S*)-1-phenylhex-5-en-3-ol (143):

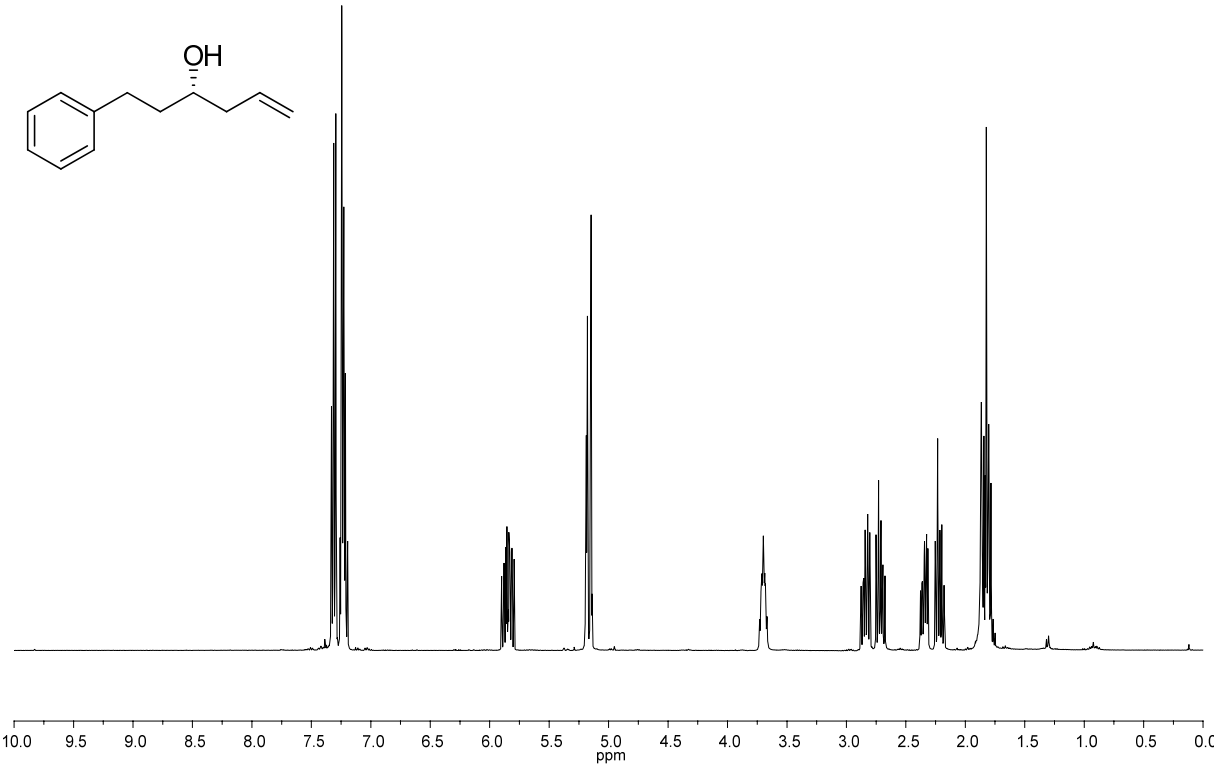

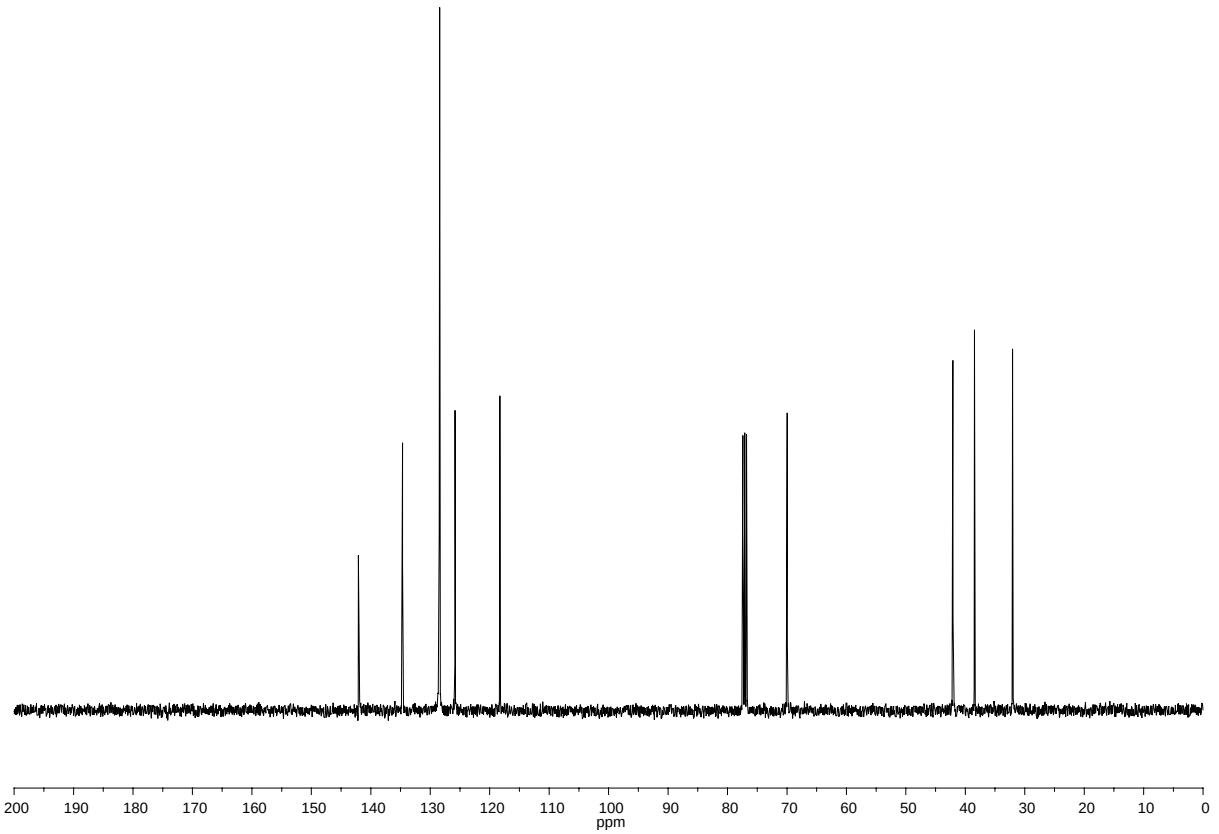

2. Crystallographic Data

3,3'-(5-hydroxy-1,3-phenylene)bis(methylene)bis(1-mesityl-1H-imidazol-3-ium) bromide (98):

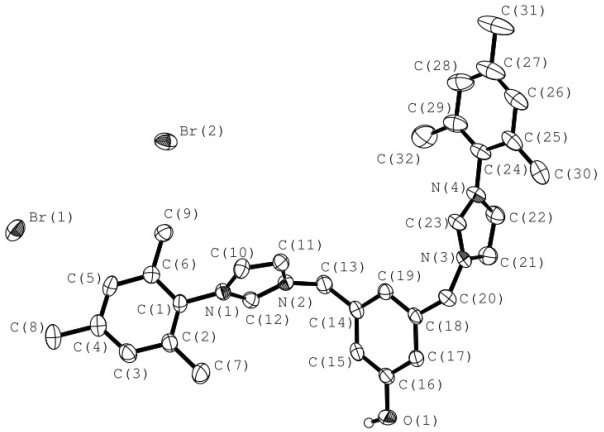

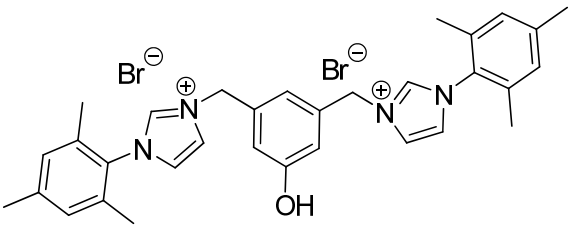

Table 1: Crystal data and structure refinement for 98.

Empirical formula	$C_{32}H_{36}Br_2N_4O$
Formula weight	652.45
Temperature/K	396.15
Crystal system	monoclinic
Space group	$P2_1/c$
a/Å	13.0419(4)
b/Å	28.6801(7)
c/Å	8.8610(2)
α/°	90
β/°	97.163(3)
γ/°	90
Volume/Å^3	3288.53(15)
Z	4
ρ_{calc}mg/mm^3	1.318
m/mm^{-1}	3.345
F(000)	1336
Crystal size/mm^3	0.2014 × 0.0167 × 0.0104
2Θ range for data collection	6.16 to 147.28°
Index ranges	-15 ≤ h ≤ 15, -35 ≤ k ≤ 32, -10 ≤ l ≤ 6

Reflections collected	13168
Independent reflections	6454[R(int) = 0.0456]
Data/restraints/parameters	6454/2/358
Goodness-of-fit on F^2	1.050
Final R indexes [I>=2σ (I)]	R_1 = 0.0540, wR_2 = 0.1430
Final R indexes [all data]	R_1 = 0.0679, wR_2 = 0.1527
Largest diff. peak/hole / e $Å^{-3}$	1.238/-0.962
Flack Parameter	.

Table 2: Fractional Atomic Coordinates ($\times 10^4$) and Equivalent Isotropic Displacement Parameters ($Å^2 \times 10^3$) for 98. U_{eq} is defined as 1/3 of of the trace of the orthogonalised U_{IJ} tensor.

Atom	*x*	*y*	*z*	U(eq)
O1	-882(2)	5305.2(10)	-4373(3)	40.1(9)
N1	1462(2)	3281.0(11)	-2051(3)	28.8(8)
N2	-20(2)	3582.3(10)	-1810(3)	27.7(8)
N3	-2451(2)	4971.8(11)	1582(3)	28.4(9)
N4	-3251(2)	4551.2(12)	3090(3)	33.0(9)
C1	2294(3)	3050.8(13)	-2697(4)	30.1(10)
C2	2962(3)	3321.4(14)	-3443(5)	36.6(11)
C3	3753(3)	3087.9(15)	-4051(5)	40.2(12)
C4	3890(3)	2612.0(15)	-3909(5)	37.2(12)
C5	3209(3)	2356.3(13)	-3135(4)	33.7(11)
C6	2390(3)	2569.5(13)	-2540(4)	29.6(10)
C7	2867(4)	3844.6(16)	-3563(7)	59.2(18)
C8	4765(3)	2365.8(17)	-4551(5)	47.4(16)
C9	1632(3)	2283.6(13)	-1790(4)	35.9(11)
C10	1465(3)	3392.1(13)	-542(4)	33.4(11)
C11	535(3)	3578.5(13)	-383(4)	33.7(11)
C12	547(3)	3402.9(13)	-2797(4)	30.7(10)
C13	-1082(3)	3762.6(13)	-2175(5)	35.1(11)
C14	-1131(3)	4283.6(13)	-2006(4)	29(1)
C15	-957(3)	4559.6(13)	-3230(4)	29.6(10)
C16	-1008(3)	5042.2(14)	-3122(4)	30.3(10)
C17	-1246(3)	5251.0(13)	-1788(4)	28.5(10)
C18	-1398(2)	4969.4(13)	-546(4)	27.2(10)
C19	-1343(3)	4486.6(13)	-652(4)	28.7(10)
C20	-1633(3)	5208.3(14)	888(4)	31.7(11)
C21	-3468(3)	4955.9(15)	964(5)	38.2(12)
C22	-3970(3)	4687.9(15)	1902(4)	36.7(11)
C23	-2337(3)	4728.4(14)	2858(4)	32.3(10)
C24	-3471(3)	4317.7(15)	4452(4)	35.6(11)
C25	-3642(3)	4603.3(18)	5692(4)	41.5(13)
C26	-3852(3)	4378(2)	7004(5)	51.8(16)

C27	-3884(4)	3898(2)	7085(6)	63(2)
C28	-3719(4)	3634(2)	5834(6)	56.7(17)
C29	-3519(4)	3842.2(18)	4479(5)	47.5(14)
C30	-3613(3)	5122.3(18)	5597(5)	47.3(14)
C31	-4099(6)	3663(3)	8554(7)	95(3)
C32	-3404(5)	3556.9(19)	3082(7)	62.6(17)
Br1	3688.0(4)	1017.9(1)	-3773.9(6)	46.7(2)
Br2	-400.8(4)	1234.9(2)	-1630.8(5)	44.6(2)

Table 3: Anisotropic Displacement Parameters ($Å^2×10^3$) for 98. The Anisotropic displacement factor exponent takes the form: $-2π^2[h^2a^{*2}U_{11}+...+2hka×b×U_{12}]$

Atom	U_{11}	U_{22}	U_{33}	U_{23}	U_{13}	U_{12}
O1	57.6(18)	39.0(15)	26.4(13)	6.4(11)	15.9(12)	9.2(13)
N1	28.1(15)	31.1(15)	27.6(14)	-1.2(12)	5.0(11)	3.4(12)
N2	27.6(15)	26.1(14)	29.6(14)	0.2(11)	4.9(11)	-0.1(12)
N3	26.1(15)	33.9(16)	27.0(14)	-3.1(12)	10.3(11)	1.3(12)
N4	29.5(16)	43.6(18)	27.0(15)	1.1(13)	7.4(12)	-6.7(14)
C1	27.3(18)	27.4(17)	36.0(18)	-4.8(14)	6.0(14)	3.8(14)
C2	32.5(19)	31.4(19)	48(2)	-2.4(16)	13.2(16)	0.9(15)
C3	34(2)	39(2)	50(2)	-3.0(18)	14.5(17)	-3.3(16)
C4	31(2)	39(2)	41(2)	-9.8(16)	2.3(15)	3.7(16)
C5	30.0(18)	24.5(17)	45(2)	-5.9(15)	-1.8(15)	5.2(14)
C6	30.0(18)	31.2(18)	26.9(16)	-2.4(13)	1.3(13)	0.4(14)
C7	56(3)	32(2)	96(4)	5(2)	35(3)	5(2)
C8	33(2)	51(3)	58(3)	-11(2)	5.4(19)	11.6(19)
C9	40(2)	30.1(19)	37.8(19)	1.6(15)	6.2(16)	-1.1(16)
C10	37(2)	33.6(19)	28.1(17)	-5.6(14)	-2.1(14)	8.1(15)
C11	44(2)	33.1(19)	25.2(16)	-2.7(14)	8.9(15)	6.2(16)
C12	31.2(18)	33.0(18)	28.2(17)	0.7(14)	5.0(14)	1.9(14)
C13	31.8(19)	33(2)	42(2)	-3.9(16)	10.4(15)	0.3(15)
C14	20.5(16)	35.2(19)	32.1(17)	-3.3(14)	6.9(13)	1.9(14)
C15	23.7(16)	36.6(19)	29.6(17)	-3.9(14)	7.3(13)	6.0(14)
C16	26.4(17)	37.5(19)	28.2(17)	2.9(14)	7.7(13)	3.4(14)
C17	27.0(17)	29.1(17)	30.1(17)	-2.2(14)	6.5(13)	2.2(14)
C18	17.7(15)	34.9(19)	29.9(17)	0.0(14)	6.3(12)	1.7(13)
C19	22.8(16)	33.0(18)	30.5(17)	2.8(14)	4.7(13)	2.8(14)
C20	30.0(18)	37(2)	29.3(17)	-2.8(14)	8.8(14)	-4.8(15)
C21	30(2)	46(2)	38(2)	5.5(17)	1.4(15)	-0.3(16)
C22	24.6(18)	48(2)	37.1(19)	2.3(17)	2.2(14)	-4.1(16)
C23	25.2(17)	46(2)	26.7(17)	1.8(15)	7.0(13)	-3.5(15)
C24	27.8(18)	52(2)	27.8(18)	2.6(16)	6.9(14)	-9.6(16)
C25	25.8(18)	69(3)	30.5(19)	-1.7(18)	6.9(14)	-5.5(18)
C26	36(2)	89(4)	32(2)	2(2)	10.7(17)	-7(2)
C27	40(3)	108(5)	42(3)	20(3)	7.0(19)	-20(3)
C28	45(3)	63(3)	61(3)	22(2)	2(2)	-18(2)
C29	40(2)	55(3)	48(2)	7(2)	7.9(18)	-18(2)

C30	34(2)	64(3)	45(2)	-13(2)	9.0(18)	1(2)
C31	83(5)	145(7)	59(4)	36(4)	22(3)	-36(5)
C32	68(3)	48(3)	72(3)	-7(3)	10(3)	-17(3)
Br1	39.2(3)	30.8(2)	68.4(3)	3.2(2)	-0.2(2)	1.0(2)
Br2	62.1(3)	42.3(3)	30.9(2)	-0.8(2)	12.2(2)	-9.2(2)

Table 4: Bond Lengths for 98.

Atom	Atom	Length/Å	Atom	Atom	Length/Å
O1	C16	1.368(5)	C6	C9	1.502(5)
N1	C1	1.448(5)	C10	C11	1.349(6)
N1	C10	1.374(4)	C13	C14	1.504(5)
N1	C12	1.337(5)	C14	C15	1.384(5)
N2	C11	1.377(4)	C14	C19	1.392(5)
N2	C12	1.318(5)	C15	C16	1.390(5)
N2	C13	1.476(5)	C16	C17	1.394(5)
N3	C20	1.463(5)	C17	C18	1.399(5)
N3	C21	1.371(5)	C18	C19	1.390(5)
N3	C23	1.321(5)	C18	C20	1.508(5)
N4	C22	1.377(5)	C21	C22	1.359(6)
N4	C23	1.335(5)	C24	C25	1.410(6)
N4	C24	1.440(5)	C24	C29	1.366(7)
C1	C2	1.394(6)	C25	C26	1.387(6)
C1	C6	1.391(5)	C25	C30	1.492(7)
C2	C3	1.393(6)	C26	C27	1.379(8)
C2	C7	1.508(6)	C27	C28	1.381(8)
C3	C4	1.380(6)	C27	C31	1.523(9)
C4	C5	1.396(6)	C28	C29	1.394(7)
C4	C8	1.512(6)	C29	C32	1.507(8)
C5	C6	1.390(5)			

Table 5: Bond Angles for 98.

Atom	Atom	Atom	Angle/˚	Atom	Atom	Atom	Angle/˚
C1	N1	C10	125.4(3)	C13	C14	C15	118.5(3)
C1	N1	C12	126.2(3)	C13	C14	C19	121.1(3)
C10	N1	C12	108.3(3)	C15	C14	C19	120.4(3)
C11	N2	C12	109.4(3)	C14	C15	C16	120.1(3)
C11	N2	C13	125.2(3)	O1	C16	C15	118.8(3)
C12	N2	C13	125.5(3)	O1	C16	C17	120.8(3)
C20	N3	C21	124.6(3)	C15	C16	C17	120.3(3)
C20	N3	C23	126.5(3)	C16	C17	C18	119.2(3)
C21	N3	C23	108.9(3)	C17	C18	C19	120.6(3)
C22	N4	C23	108.1(3)	C17	C18	C20	117.7(3)
C22	N4	C24	125.8(3)	C19	C18	C20	121.8(3)
C23	N4	C24	125.5(3)	C14	C19	C18	119.5(3)

N1	C1	C2	118.5(3)	N3	C20	C18	112.3(3)
N1	C1	C6	118.4(3)	N3	C21	C22	106.9(4)
C2	C1	C6	123.1(4)	N4	C22	C21	107.1(3)
C1	C2	C3	116.9(4)	N3	C23	N4	109.0(3)
C1	C2	C7	122.5(4)	N4	C24	C25	116.8(4)
C3	C2	C7	120.6(4)	N4	C24	C29	119.6(4)
C2	C3	C4	122.3(4)	C25	C24	C29	123.7(4)
C3	C4	C5	118.8(4)	C24	C25	C26	116.7(5)
C3	C4	C8	121.5(4)	C24	C25	C30	121.9(4)
C5	C4	C8	119.7(4)	C26	C25	C30	121.4(4)
C4	C5	C6	121.4(4)	C25	C26	C27	121.3(5)
C1	C6	C5	117.5(3)	C26	C27	C28	119.8(5)
C1	C6	C9	122.0(3)	C26	C27	C31	119.8(5)
C5	C6	C9	120.5(3)	C28	C27	C31	120.5(6)
N1	C10	C11	107.5(3)	C27	C28	C29	121.4(5)
N2	C11	C10	106.5(3)	C24	C29	C28	117.2(4)
N1	C12	N2	108.3(3)	C24	C29	C32	121.2(4)
N2	C13	C14	112.1(3)	C28	C29	C32	121.6(5)

Table 6: Hydrogen Bonds for 98.

D	H	A	d(D-H)/Å	d(H-A)/Å	d(D-A)/Å	D-H-A/°
C10	H10	Br1[1]	0.9500	28.900	3.548(4)	128.00
C11	H11	Br2[1]	0.9500	27.900	3.721(4)	166.00
C12	H12	Br2[2]	0.94(3)	2.75(3)	3.619(4)	153(4)
C21	H21	Br1[3]	0.9500	28.600	3.604(4)	136.00
C22	H22	Br1[4]	0.9500	27.800	3.651(4)	153.00
C30	H30C	Br1[5]	0.9800	29.200	3.821(5)	153.00

[1]+X,1/2-Y,1/2+Z; 2+X,1/2-Y,-1/2+Z; 3-X,1/2+Y,-1/2-Z; 4-1+X,1/2-Y,1/2+Z; 5-X,1/2+Y,1/2-Z

Table 7: Torsion Angles for 98.

A	B	C	D	Angle/°
O1	C16	C17	C18	178.2(3)
N1	C1	C2	C3	-180.0(3)
N1	C1	C2	C7	1.7(6)
N1	C1	C6	C5	-178.4(3)
N1	C1	C6	C9	2.9(5)
N1	C10	C11	N2	-0.6(4)
N2	C13	C14	C15	86.6(4)
N2	C13	C14	C19	-93.2(4)
N3	C21	C22	N4	0.9(5)
N4	C24	C25	C26	-179.9(3)
N4	C24	C25	C30	0.9(5)
N4	C24	C29	C28	179.1(4)
N4	C24	C29	C32	-3.4(7)
C1	N1	C10	C11	-176.7(3)

C1	N1	C12	N2	176.9(3)
C1	C2	C3	C4	-1.1(6)
C2	C1	C6	C5	1.4(6)
C2	C1	C6	C9	-177.3(4)
C2	C3	C4	C5	0.3(6)
C2	C3	C4	C8	-178.8(4)
C3	C4	C5	C6	1.4(6)
C4	C5	C6	C1	-2.2(5)
C4	C5	C6	C9	176.5(4)
C6	C1	C2	C3	0.2(6)
C6	C1	C2	C7	-178.1(4)
C7	C2	C3	C4	177.3(4)
C8	C4	C5	C6	-179.4(4)
C10	N1	C1	C2	-100.5(4)
C10	N1	C1	C6	79.4(5)
C10	N1	C12	N2	-0.4(4)
C11	N2	C12	N1	0.0(4)
C11	N2	C13	C14	68.6(5)
C12	N1	C1	C2	82.7(5)
C12	N1	C1	C6	-97.4(4)
C12	N1	C10	C11	0.6(4)
C12	N2	C11	C10	0.4(4)
C12	N2	C13	C14	-110.9(4)
C13	N2	C11	C10	-179.3(3)
C13	N2	C12	N1	179.6(3)
C13	C14	C15	C16	179.2(4)
C13	C14	C19	C18	-179.0(3)
C14	C15	C16	O1	-176.9(3)
C14	C15	C16	C17	-0.7(6)
C15	C14	C19	C18	1.2(6)
C15	C16	C17	C18	2.1(6)
C16	C17	C18	C19	-1.9(5)
C16	C17	C18	C20	178.8(3)
C17	C18	C19	C14	0.2(5)
C17	C18	C20	N3	137.6(3)
C19	C14	C15	C16	-1.0(6)
C19	C18	C20	N3	-41.8(4)
C20	N3	C21	C22	177.2(3)
C20	N3	C23	N4	-177.6(3)
C20	C18	C19	C14	179.5(3)
C21	N3	C20	C18	-68.6(5)
C21	N3	C23	N4	0.3(4)
C22	N4	C23	N3	0.3(4)
C22	N4	C24	C25	-90.6(5)
C22	N4	C24	C29	88.4(5)
C23	N3	C20	C18	109.0(4)
C23	N3	C21	C22	-0.8(5)

C23	N4	C22	C21	-0.8(4)
C23	N4	C24	C25	79.6(5)
C23	N4	C24	C29	-101.4(5)
C24	N4	C22	C21	170.8(4)
C24	N4	C23	N3	-171.4(3)
C24	C25	C26	C27	0.4(6)
C25	C24	C29	C28	-2.0(7)
C25	C24	C29	C32	175.6(5)
C25	C26	C27	C28	-0.9(7)
C25	C26	C27	C31	179.0(5)
C26	C27	C28	C29	0.0(8)
C27	C28	C29	C24	1.4(8)
C27	C28	C29	C32	-176.2(5)
C29	C24	C25	C26	1.1(6)
C29	C24	C25	C30	-178.1(4)
C30	C25	C26	C27	179.6(4)
C31	C27	C28	C29	-179.9(5)

Table 8: Hydrogen Atom Coordinates (Å×10^4) and Isotropic Displacement Parameters (Å^2×10^3) for 98.

Atom	*x*	*y*	*z*	U(eq)
H1	-789	5129	-5100	48
H3	4213	3262	-4583	48
H5	3308	2030	-3012	40
H7A	2972	3982	-2542	71
H7B	2177	3927	-4060	71
H7C	3391	3965	-4164	71
H8A	5426	2492	-4082	57
H8B	4699	2414	-5654	57
H8C	4735	2031	-4335	57
H9A	938	2324	-2340	43
H9B	1636	2386	-734	43
H9C	1828	1954	-1806	43
H10	2020	3346	246	40
H11	307	3686	533	41
H12	230(30)	3388(16)	-3810(30)	37
H13A	-1532	3615	-1491	42
H13B	-1348	3676	-3233	42
H15	-803	4419	-4146	36
H17	-1303	5580	-1723	34
H19	-1449	4297	193	34
H20A	-998	5218	1627	38
H20B	-1846	5534	647	38
H21	-3766	5104	55	46

H22	-4683	4609	1763	44
H23	-1730(20)	4704(16)	3510(40)	39
H26	-3977	4557	7864	62
H28	-3741	3303	5898	68
H30A	-4147	5230	4795	57
H30B	-2933	5222	5362	57
H30C	-3742	5256	6574	57
H31A	-4769	3768	8818	113
H31B	-3555	3746	9374	113
H31C	-4112	3324	8415	113
H32A	-2742	3630	2722	75
H32B	-3970	3630	2284	75
H32C	-3424	3225	3334	75

Crystal Data. $C_{32}H_{36}Br_2N_4O$, M =652.45, monoclinic, a = 13.0419(4) Å, b = 28.6801(7) Å, c = 8.8610(2) Å, β = 97.163(3)°, U = 3288.53(15) Å^3, T = 396.15, space group $P2_1/c$ (no. 14), Z = 4, μ(CuKα) = 3.345, 13168 reflections measured, 6454 unique (R_{int} = 0.0456) which were used in all calculations. The final $wR(F_2)$ was 0.1527 (all data).

3. List of publications

1) S. Wittmann, A. Schätz, R. N. Grass, W. J. Stark, O. Reiser, *Angew. Chem.* 2010, *122*, 1911-1914; *Angew. Chem. Int. Ed.* 2010, *49*, 1867-1870:
   A Recyclable Nanoparticle-Supported Palladium Catalyst for the Hydroxycarbonylation of Aryl Halides in Water.
   Web-Edition: http://dx.doi.org/10.1002/anie.200906166

2) M. Hager, S. Wittmann, A. Schätz, F. Pein, P. Kreitmeier, O. Reiser, *Tetrahedron:Asymmetry* 2010, *21*, 1194-1198:
   The importance of 1:1 and 1:2 metal-ligand species in chiral copper(II)-bis(oxazoline) complexes for catalytic activity.
   Web-Edition: http://dx.doi.org/10.1016/j.tetasy.2010.03.030

3) A. Karmakar, T. Maji, S. Wittmann, O. Reiser, *Chem. J. Eur.* 2011, ASAP:
   L-Proline/$CoCl_2$ Catalyzed Highly Diastereo- and Enantioselective Direct Aldol Reactions.
   Web-Edition: http://dx.doi.org/10.1002/chem.201101299

4. Congresses an scientific meetings

1) Heidelberg Forum of Molecular Catalysis, Heidelberg, Germany, 2009.
   Poster presentation: Noncovalent immobilization of a NHC palladium catalyst on magnetic nanoparticles.

2) 12th Belgian Organic Synthesis Symposium, Namur, Belgium, 2010.
   Poster presentation: A Recyclable Nanoparticle-Supported Palladium Catalyst for the Hydroxycarbonylation of Aryl Halides in Water.

3) Heidelberg Forum of Molecular Catalysis, Heidelberg, Germany, 2011.
   Poster presentation: Noncovalent immobilization of catalysts on magnetic nanoparticles.

5. Curriculum vitae

Personal information

Name	Sebastian Wittmann
Date of birth	09/28/1983
Place of birth	Landshut (Germany)
Marital status	unmarried
Nationality	german

Education

Since 10/2008- current	University of Regensburg / TU München Ph.D. thesis within the Elite Network of Bavaria (ENB) under chairmanship of Prof. Dr. W. A. Herrmann, TU München and supervision of Prof. Dr. O. Reiser, University of Regensburg (part of the international doctorate program NANOCAT - Nanodesign of high performance catalysts)
01/2011- 05/2011	University of Texas at Austin Research project in the group of Prof. Dr. M. Krische
10/2003- 09/2008	University of Regensburg Graduation: Diplom-Chemiker (diploma in chemistry)
01/2008- 09/2008	Diploma thesis in the research group of Prof. Dr. O. Reiser: “Towards the asymmetric total synthesis of Norrisolide”
10/2006- 09/2008	Advanced studies in organic chemistry

2003 & 2004	E.on Nuclear Power, Internship in the field of analytical and radiochemistry
10/2003- 09/2006	University of Regensburg, studies in Chemistry
1994- 2003	Burkhart-Gymnasium Mallersdorf-Pfaffenberg (secondary school) Allgemeine Hochschulreife (High school certificate equivalent)

Languages

German (native)
English (fluently)

Professional References:

Prof. Dr. Oliver Reiser
Institut für Organische Chemie
Universität Regensburg, Universitätsstr. 31
93053 Regensburg, Germany
Phone: +49-941-9434631
Email: oliver.reiser@chemie.uni-regensburg.de

Prof. Michael Krische
The Department of Chemistry and Biochemistry
The University of Texas at Austin
Welch Hall Room 5.146
Austin, TX 78751
Email: mkrische@mail.utexas.edu
Phone: +01 -512-2325892

F. Acknowledgment

Universität Regensburg:
Bei Prof. Oliver Reiser möchte ich mich für die Überlassung des interessanten Themas sowie die Ermöglichung meines Auslandsaufenthaltes bedanken.

Bei Priv. Doz. Dr. Kristen Zeitler, Prof. Henri Brunner und Prof. Manfred Scheer bedanke ich mich herzlich für die schnelle und problemlose Begutachtung der Arbeit sowie die Bereitschaft im Prüfungskomitee mitzuwirken.

Meinen Laborkollegen Andreas Kreuzer, Dr. Mohd Tajudin Mohd Ali sowie Dr. Hana Seo danke ich für die stets angenehme Atmosphäre im Labor.

Meinen Freunden am Arbeitskreis Andreas Kreuzer, Dr. Klaus Harrar, Ka(th)rin Ulbrich und Ludwig Pilsl sowie allen aktuellen Mitarbeitern des Lehrstuhls Reiser danke ich für diverse Grillabende, Feierabendbiere und sonstige Freizeitaktivitäten. Quirin Kainz und Matthias Knorn gilt weiterhin mein Dank für das Korrekturlesen dieser Arbeit.

Dr. Peter Kreitmeier und Priv. Doz. Dr. Kirsten Zeitler gilt mein Dank für die fachkundige Hilfe bei theoretischen sowie praktischen Problemen.

Bei Helena Konkel, Andrea Roithmeier, Robert Tomahogh, Klaus Döring, Georg Adolin, Young Rotermund und Hedwig Ohli möchte ich für diverse größere und kleinere Arbeiten bedanken.

Bei den ehemaligen Mitarbeitern des Lehrstuhls, insbesondere Dr. Markus Hager, Dr. Alexander Schätz, Dr. Alexander Tereshchenko, Dr. Florian Sahr sowie Dr. Michael Kuhn bedanke ich mich für die Unterstützung während der Arbeit und die gemeinsamen Unternehmungen.

Dank gilt auch meinen Bachelors & F-Praktikanten: Viktor Kais, Matthias Knorn, Romulus Lutsch, Michael Hammer, Corina Eichenseer sowie Sandra Pohl.

Meinen Freunden Dr. Roland Geyer und Marco Lorenz danke ich für etliche zu lang geratene Mittagspausen. Ulrike Wenge, Christoph Schwarzmaier, Kilian Wörmann, Simon Ochs, Christian Grassl, Christoph Stock und Melanie Kaske gilt mein Dank für die Freundschaft während des Studiums und der Promotion.

Allen Mitarbeitern der analytischen Abteilungen der Universität Regensburg gilt ebenso mein Dank. Im Besonderen Hans Söllner (Masse), Fritz Kastner (NMR), Joachim Rewitzer (ICP) und Heiko-Ingo Siegmund (TEM) für diverse Messungen.

Florian Pein danke ich für die Hilfe bei der Herleitung der Formel für den Ligandenvergleich.

ETH Zürich:
Prof. W. J. Stark, Dr. Alexander Schätz sowie Martin Zeltner danke ich für die großzügige Versorgung mit Nanopartikeln.

CNRS Toulouse:
Prof. Jean-Pierre Majoral, Prof. Anne-Marie Caminade, Laurie Travers und Michel Keller gilt mein Dank für die schönen Aufenthalte in Toulouse sowie die fruchtbare Zusammenarbeit.

University of Texas at Austin:
Bei Prof. Michael Krische, Dr. Joseph Moran, Dr. Esa Kumpulainen, Dr. Laina Geary, David del Valle und Jane Evans bedanke ich mich für den herzlichen Empfang in Austin.

TU München:
Für die großzügige Finanzierung während der Arbeit danke ich NANOCAT mit den Koordinatoren Dr. Markus Drees, Prof. Fritz Kühn sowie Prof. Wolfgang A. Herrmann.

Ganz besonderen Dank schulde ich meinen Eltern, meiner Oma und meiner Freundin Pia. Ohne Eure anhaltende Unterstützung wären weder mein Studium noch diese Arbeit in dieser Form möglich gewesen.

Herewith I declare that I have made this existing work single-handed. I have only used the stated utilities.

Regensburg, 23th January 2012

Sebastian Wittmann